PROCESSING OF MINING WASTE CONTAINING PHOSPHOGYPSUM AND SODIUM SULPHATE FOR THE RECOVERY OF CALCIUM CARBONATE, SODIUM CARBONATE AND RARE EARTH METALS

by

CONNY PUTSANE MOKGOHLOA

Submitted in partial fulfilment of the requirements for the degree,

DOCTOR OF PHILISOPHY

in

CHEMISTRY

in the

FACULTY OF SCIENCE AND AGRICULTURE

SCHOOL OF PHYSICAL AND MINERAL SCIENCES

at the

UNIVERSITY OF LIMPOPO

Supervisor: Prof. JP Maree

Co-Supervisors: Prof M Mokhonoana

Dr M Mujuru

2024

DECLARATION BY CANDIDATE

“I declare that the thesis hereby submitted to the University of Limpopo, for the degree Doctor of philosophy in Chemistry has not previously been submitted by me for a degree at this or any other university; that is my work in design and in execution, and that all material contained herein has been duly acknowledged.

MOKGOHLOA CP (Ms) **02 September 2024**

DEDICATION

In loving memory of my mother, Ntopa Mmashela Mokgohloa (1952 - 2003).

ACKNOWLEDGEMENTS

This study has been carried out at the Department of Chemistry, University of Limpopo Turfloop Campus. This work is based on research supported the Department of Trade and Industry under the Technology & Human Resources for Industry Programme (THRIP), ROC Water Technologies, TIA Seed Fund, F'SAGRI and NIPMO, who sponsored the grant for the innovation award of 2021 NSTF-South32, that was received by ROC Water. The financial support from these organisations is highly appreciated and acknowledged. Dr Fritz Carlsson provided proof-reading and extensive editorial advice.

First and most importantly, I would like to acknowledge the presence of God in this study. Thank you, God.

Secondly, I would like to acknowledge with thanks and sincere gratitude to the greatest supervisor, Prof JP Maree for his constant support, patience, guidance, regular availability, and accessibility throughout this study. Thanks is extended to my co-supervisors Dr M Mujuru and Prof MP Mokhoanana who made laboratory a friendly place to work in.

I express my appreciation to Dr Mogashane Tumelo Monty, Dr Neville Nyamutswa, Dr Ntumba Nsaka and Dr Malwela Thomas. This study wouldn't have been a success without their assistance in the laboratory.

I am grateful to my kids (Lesedi and Mothupi) for being so understanding and patient with me. Thanks to my sister Mamabolo Irene, my brother Mokgohloa Clement and family for their emotional support towards the completion of this study.

Lastly, a special thanks to numerous people not mentioned here who in some way, no matter how big or small, contributed to this study.

1 Samuel 7:12

ABSTRACT

Waste gypsum from the fertilizer industry, sodium sulphate and magnesium sulphate rich brines from the mining industry and power stations can be utilized for the recovery of valuable products, as an alternative to stockpiling as waste dumps, or stored in brine ponds respectively. Waste gypsum can be used for the recovery of nano calcium carbonate, sulphur, and rare earth elements (REEs) (cerium, praseodymium, lanthanum, neodymium, and samarium). Sodium sulphate can be processed into sodium carbonate, sulphur, and sodium bisulphide. Magnesium sulphate can be processed to magnesium hydroxide, and in combination with sodium sulphide, sodium bisulphide and sodium sulphate can be produced. The proposed project allowed the generation of profits from waste as sodium carbonate has a value of R7 000/t, nano calcium carbonate a value of R14 000/t, magnesium hydroxide a value of R7 000/t and the global REEs market of R139.4 billion in 2023. Rare earth elements are used for magnets and due to its use in the electronic industry, and due to limited resources, it is of strategic value to the Western Word. Rare earth elements in phosphogypsum amounted to 4.48 mg/g gypsum and were collected with the crude $CaCO_3$. Rare earth elements were present in lower concentrations in AMD, ranging from were 0.7 to 9.1 mg/L.

The Mintek Pyrosim software model was used to predict the products formed under the conditions that were studied experimentally. A muffle furnace was used to thermally reduce $CaSO_4$ to CaS and $BaSO_4$ to BaS. OLI and beaker studies were used to determine which compound will precipitate out and which compounds/elements will stay in solution. The pyrosim studies and the muffle furnace studies both showed that $CaSO_4$ and $BaSO_4$ can be converted to CaS and BaS, respectively, through reduction with coal at 1000 °C. Less energy was needed for the conversion of $BaSO_4$ into BaS (1 480 MJ/t coal) than for the conversion of $CaSO_4 \cdot 2H_2O$ into CaS (3 657 MJ/t coal). Furthermore, it was showed that CaS can be used to produce Na_2CO_3, $CaCO_3$ and nano $CaCO_3$.

Acid mine drainage (AMD), a notorious kind of pollution associated with both active and abandoned mining sites, needs to be treated with the aim of achieving net zero waste. The ROC (Reverse Osmosis/Cooling) process can be used for the treatment of AMD though neutralization with Na_2CO_3 for the removal of metals, desalination with

reverse osmosis (RO), freeze-crystallization for recovering Na_2SO_4 from the RO brine, and processing of Na_2SO_4 via Na_2S to its raw material, Na_2CO_3. The conditions needed for the processing of Na_2S to Na_2CO_3 were investigated. It was found that: (i) Na_2S can be reacted with CO_2 to form $NaHCO_3$(*aq*) and NaHS(*aq*), (ii) the latter two compounds can be separated though freeze-crystallization as $NaHCO_3$ has a lower solubility at 0°C, and (iii) $NaHCO_3$ can be converted into Na_2CO_3 though heat-treatment. OLI simulations also confirmed that $NaHCO_3$ and NaHS were formed when Na_2S was reacted with CO_2.

It was showed that $Mg(OH)_2$ can be produced as a single solid compound when reacted with Na_2S, as the other product, Na_2SO_4, has a high solubility. $Mg(OH)_2$ will also form when reacted with CaS or BaS, but this approach will have the disadvantage that the solid, $Mg(OH)_2$ is mixed with other solids, namely $CaSO_4 \cdot 2H_2O$ or $BaSO_4$. The formation of $Mg(OH)_2$ was also predicted by OLI simulations. Magnesium oxide can be formed from $Mg(OH)_2$ through heating. These developments will contribute to achieve zero waste generation during solid waste treatment.

Hydrogen sulphide can be converted to S by using the Claus process. In this study, H_2S gas was produced when CaS or Na_2S was contacted with CO_2. This H_2S was converted to S by contacting it with Fe^{3+} through OLI software. The effect of Fe^{3+} concentration was shown by stepwise by increment of the $Fe_2(SO_4)_3$ dosage from 0 to 3000 mmol/L. It was noted that FeS_2 formed when $Fe_2(SO_4)_3/H_2S$ mole ratio was 0.5 with further dosing of $Fe_2(SO_4)_3$, the formed FeS_2 was converted to mainly S_8. H_2S was also oxidized with O_2. OLI software showed that 50 mmol O_2 was needed for oxidation of H_2S to S_8.

The study also focused on the formation of $CaSO_4 \cdot ½H_2O$ from $CaSO_4 \cdot 2H_2O$. It was noted that $CaSO_4 \cdot ½H_2O$ formed at temperatures of 240 °C and 180 °C when 60 min and 120 min reaction time was allowed, respectively. In the same section, gypsum and the reductant were determined if they should be processed as a powder or as a solid in the form of a brick or a tile. It was noted that hard gypsum formed when anhydrite was contacted with water in the presence of activated carbon.

RESEARCH OUTPUT

Conference presentations

Mokgohloa, C.P., Maree, J.P., van Vuuren, D.S., Mokhonoana, M.P. Recovery of $CaCO_3$, Na_2CO_3 AND $Mg(OH)_2$ from alkali earth metals, The 14th Southern African-Nordic Centre (SANORD 2022) International Conference, The Ranch Hotel, Polokwane, 3-5 December 2022, Oral presentation.

Mokgohloa, C.P., Maree, J.P., Motaung, M.P., Mokhonoana, M.P. Processing of Na_2S to Na_2CO_3 and NaHS, The 35th International Institute of Biological Chemical and Environmental Engineering (IICBEE 2022), Johannesburg, South Africa, 28-29 November 2022, Oral presentation.

Mokgohloa, C.P., Maree, J.P., van Vuuren, D.S., Mokhonoana, M.P. Recovery of $CaCO_3$, Na_2CO_3 and $Mg(OH)_2$ from alkali earth metals, Water institute of Southern Africa (WISA 2022) Biennial Conference, Sandton Convention Centre, South Africa, 28-30 September 2022, Oral presentation.

Mokgohloa, C.P., Maree, J.P., Mujuru, M., Mokhonoana, M.P. Recovery of Na_2CO_3 and nano $CaCO_3$ from Na_2SO_4 and $CaSO_4$ wastes, 11th Postgraduate Research Day, Faculty of Science and Agriculture (FSA 2021), University of Limpopo. 06-08 October 2021, Bolivia Lodge, Polokwane, South Africa. Oral presentation.

Publication

Conny P Mokgohloa, Johannes P Maree, M P Motaung, Malose P Mokhonoana (2022) *Processing of Na_2S to Na_2CO_3 and NaHS*, International Institute of Biological Chemical and Environmental Engineering (IICBEE), Johannesburg, South Africa, Nov 28-29. *Editors*: S.K. Ntwampe, E Fosso, B. Topcuoğlu, ISBN: 978-989-9121-14-0, 30-40.

Book Chapter

Conny P Mokgohloa, Johannes P Maree, David S van Vuuren, Kwena D Modibane, Munyaradzi Mujuru, Malose P Mokhonoana, “Recovery of Na_2CO_3 and nano $CaCO_3$ from Na_2SO_4 and $CaSO_4$ wastes,” in *Application of Nanotechnology in Mining Processes: Beneficiation and Sustainability. Editors*: Elvis Fosso-Kankeu, Martin

Mkandawire and Bhekie Mamba, New York, Wiley Scrivener, 2022, pp. 197 - 235, ISBN:9781119865360, doi: https://doi.org/10.1002/9781119865360.ch6.

Conny P Mokgohloa, Johannes P Maree, Mary P Motaung, Malose P Mokhonoana. 2023. Recovery of $CaCO_3$, Na_2CO_3 and $Mg(OH)_2$ from alkali earth metals, in Customized technologies for sustainable management of industrial wastewater: Circular economy approach, Editors: Elvis Fosso-Kankeu, Bhekie Mamba and Johannes Maree, New York, Wiley Scrivener, In press.

CONTENTS

LIST OF TABLES

LIST OF FIGURES

ABBREVIATIONS AND ACRONYMS

ABC Alkali Barium Carbonate

AMD Acid mine drainage

CSIR Council for Scientific and Industrial Research

EDS Energy-dispersive X-ray spectroscopy

FGD flue gas desulphurization

FC Freeze Crystallization

HR-FESEM High Resolution Field Emission Scanning Electron Microscope

ICP-OES Inductively coupled plasma ICP) - optical emission spectrometry

ICP-MS Inductively coupled plasma mass spectrometry

OECD Organization for Economic Co-operation and Development

PHEs Potentially harmful metallic elements

REEs Rare-earth elements

SEM Scanning technique on microscopy

RO Reverse Osmosis

TGA Thermal gravimetric analysis

SSA Specific surface area

KSA Kingdom of Saudi Arabia

USA United states of America

XRD X-ray diffraction

CHAPTER 1: BACKGROUND

1.1 BACKGROUND

1.1.1 Occurrence of solid waste

Solid waste refers to the range of undesirable and futile garbage materials from a wastewater treatment plant, water supply treatment plant, or air contamination control facility and other discarded material, coming from industrial, commercial, mining, and agricultural operations, as well as from community activities. Solid waste generated from industrial, residential, and commercial activities may be handled in a variety of ways. Regardless of the origin, content, or hazardous potential, solid waste must be managed systematically to ensure environmental best practices (Ferronato & Torretta, 2019) .

Mining activities have considerably increased due to notable population growth and worldwide demand for mineral resources (Reichl, *et al*., 2016).This increase coincides with a new awareness in which environmental concerns have become a growing challenge for all stakeholders within the sector (Dold, 2008). In South Africa, mining and metallurgical wastes comprise one of the biggest challenges to the environment (Matinde, *et al*., 2018). An expanding rate of population growth and increasing per capita income have resulted in the generation of an enormous volume of solid waste, which poses a serious threat to environmental quality and human wellbeing (Snigdha & Sarkhel, 2003). Inappropriate waste disposal by one mining industry affects the entire populace. The South African nation has entrusted every individual, establishment, or institution to contribute significantly to the process of keeping their communities and environment clean (Fobil, 2000; Palczynski, 2002). However, the management of solid waste continues to be a significant challenge in urban areas throughout the world especially in the rapidly growing cities of the developing world (Foo, 1997).

The world produces 2.01 billion tons of municipal solid waste a year, of which at least 33% is managed in a non-environmentally friendly manner (Razzaq, *et al*., 2021). The world produces an average of 0.74 kg of waste per person per day, but this value varies considerably, from 0.11 to 4.54 kg (Karak, et al., 2012). Though they make up

just 16% of the world's population, high-income countries produce about 34%, or 683 million tons, of the world's waste. It has been estimated that for every ton of metal ore mined, at least a ton of waste is generated (Lottermoser, 2010). According to Hudson-Edward et al. the global production of mining waste (several billion tons per year) is in line with the number of terrestrial materials moved by global geological processes (Hudson-Edwards, *et al*., 2011). A report by Jakubick *et al*. illustrates that each day tailings manufacturing has extended through one order of significance in the last 50 years (tens of thousands vs. hundreds of thousands of tons/day) (Jakubick, *et al*., 2003). The Republic of South African gold mining trade created 7.4×10^5 t of gold tailings within the decade from 1997 to 2006, which amounts to 7.4×10^4 t/a (Hilson & Monhemius, 2006). All gold mining waste produced in the past century in South Africa amounts to 6×10^9 t, that covers a complete space of 400 - 500 km^2 and contains 4.30×10^5 t of metal and 3.0×10^4 of sulphur, each of which and particularly the sulphur, have high pollution potential waste (Fashola, *et al*., 2016). In 1995, the world's iron, copper, gold, lead, and mineral mines along generated 35×10^9 t of waste (Singer, 1995). According to incomplete statistics, for example, China disposes quite 0.5 billion tons tailings each year, and therefore the rate of comprehensive utilization of tailings is a lower than 7% at the present (Lu & Cai, 2012).

1.1.2 Effect of solid waste

Mining itself affects relatively small areas, and this does not pose severe environmental problems. The environmental impact arises when ores are mined, processed, roasted, and refined, which results in the generation of huge amounts of solid waste material. This includes rock dumps, gangue, slags, tailings, metallurgical roasting, ash, dust, particulate matter, and other solid waste. These wastes comprise by-products such as carbonates, sulphates oxides and clays. They also contain different amounts of potentially harmful metallic elements (PHEs) as As, Cd, Cr, Cu, Ni, Pb, Zn (Bini & Wahsha, 2014). With the development of the mining industry, mining activities produce more and more solid waste and cause increasingly serious environmental destruction. Nowadays, due to the different mining techniques and the lack of environmental management measures, abandoned mining areas have a great impact on the landscape and the environment related to large amounts of various wastes covering large areas (Abreu, *et al*., 2012; Vallero, 2005; Da Silva, *et al*., 2005).

The impact of some types of waste on the environment depends on its chemical composition and how it is managed. While there are no empirical studies linking waste to the deterioration of human health, it is implicitly known that waste has a direct effect on societies and their well-being. Poor waste management can contaminate both drinking water and air quality, which are further known to exert significant impacts on human health and the environment. Improper disposal can lead to negative consequences for health, for example due to water, soil, and air pollution. Hazardous waste or unsafe waste handling methods such as open burning can directly harm waste workers or other people involved in waste incineration and nearby communities. Vulnerable groups such as children are at increased risk of developing health problems. Improper waste collection leads to environmental and marine pollution and can block water drains. The resulting flooding and other standing water in the waste promotes cholera and other vector-borne diseases such as malaria and dengue fever.

1.1.3 Potential value of solid waste

The value of waste materials varies from one fraction to another and is related to attributes such as the value of virgin materials, the material's recyclability, its quality and purity, and demand for materials. This study focused on the identification of opportunities where sulphate-rich wastes can be beneficiated by conversion into produce valuable products in the form of carbonates, such as Na_2CO_3 and $CaCO_3$ from Na_2SO_4 and $CaSO_4$, respectively. In the process, H_2S, S and/or NaHS will also be recovered. Hydrogen sulphide (H_2S) can be used to produce sulphuric acid and sulphur. It can also be used to produce a variety of inorganic sulphides that are useful in pesticides, dyes, and pharmaceuticals (Zhang, *et al*., 2016). Processing $CaSO_4$ to CaS yield valuable products such as sulphur (S) and $CaCO_3$ which would greatly lessen the sludge disposal problem. Calcium sulphide is used as an additive to lubricants and as a flotation reagent in ore extraction. It can be used to produce elemental sulphur (Hiligsmann, *et al*., 1996; Maree, *et al*., 2005).

Waste gypsum from the fertilizer industry typically contains 0.6% REEs *(Binnemans, et al*., 2015). Rare earth elements are of strategic value as they are needed in the manufacturing of magnets and electronic components. The REE market is dominated by China.

Circular economy, recyclability, recycling, and reuse have been identified as some of the emerging paradigms that can drive the multi-dimensional aspects of sustainability in the mining and metal extraction industries. In this context, a sustainable circular economy is characterized as a change in which the value of products, materials and resources is preserved for as long as possible in the economy and the production of waste is minimized (European, 2015). The storage, collection, transportation and final treatment/disposal of wastes are reported to have become a major problem in urban centres (ADB, 2002; Kaseva & Mbuligwe, 2005; Okot-Okumu & Nyenje, 2011; Rotich, *et al*., 2006). It is an effective way of solving the problem of waste discharge, land occupation and protecting environment if the mine solid wastes can be treated in new ways such as waste reuse, processing waste to recover saleable products, waste rock reduction and waste rock and tailings backfill.

1.2 WATER ISSUES

1.2.1 Background

Aquaculture, household, industrial, animal, water system, mining, public supply, thermoelectric power, and hydroelectric power use all rely on water, which is useful and essential (Hutson, *et al*., 2004). There is a lack of clean, safe water. One of the nations with a lack of water is South Africa (Muller, *et al*., 2009). This is because of the climate and the growing need for water. Utilizing techniques for water harvesting, groundwater preservation, and water re-use is essential for maximizing water use and minimizing surface water runoff. Groundwater from springs and wells is consistently the key sources of water supply particularly in towns and residential areas (Hay, *et al*., 2012). Just 2.5% of the water is fresh water and practically 0.3% of all fresh water is tracked down in streams, lakes and in the atmosphere (Gleick, 1996). Currently, more than 60% of South Africa's rivers are being overexploited. The Organisation for Economic Co-operation and Development (OECD) reported that only a third of the country's main rivers are in good condition and a quarter of the river ecosystems are in critical danger of extinction (OECD, 2015). Around 71% of the worldwide populace inhabit least 1 month of the year in states of moderate to serious water shortage (Mekonnen & Hoekstra, 2016).

Solid waste from mining operations and treatment of wastewater impacts on water quality through the release of leachate from landfills into water sources. As water meets decomposing solid waste, the solid will dissolve together with soluble inorganic and organic wastes producing polluted liquid known as leachate or waste juice. It has a high polluting potential impact due to its high concentrations of organic contaminants and high ammoniacal nitrogen. Once leachate is discharged into water bodies or/and aquatic environment, it will have an acute and chronic impact. If toxic metals are present, this can lead to chronic toxin accumulation in organisms that depend on such water bodies and may consequently affect humans if they consume on these organisms. **Figure 1.1** shows an example of a landfill leachate that brings about the deterioration in underground and surface water quality.

Figure 1.1 Gypsum dump near Phalaborwa, South Africa (Maree & Du Plessis, 1990)

1.2.2 Mine waters

Acid mine drainage is one of mining's most serious threats to water quality. Most streams affected by AMD have pH values in the range 2.5 to 6.0 (Vallero, 2006), with high iron and sulphate concentrations. The environmental, social, and economic problems associated with AMD are significant worldwide. Mining exploration of metal

ore deposits results in large amounts of sulphides exposed to weathering processes (oxygen, water, and bacteria) that create acidic environments and promote metalloid *i.e*, elements with properties (intermediate between those of metals and nonmetals) solubilization and form AMD. Mine waters can be divided into three groups according to their acid-alkaline properties: (i) AMD with pH 6 or lower, (ii) neutral mine waters with pH 6 or higher and (iii) saline mine waters with pH 6 containing more than 1000 mg/l carbonates (Wolkersdorfer, 2008). Metals such as silver (Ag), gold (Au), copper (Cu), Zinc (Zn), and lead (Pb) are normally found in an intimate association with sulphates, therefore their extraction will cause AMD. The formation of AMD starts with the iron pyrite (FeS_2) undergoing reaction in a two-stage process, the primary manufacturing sulphuric acid and ferric sulphate (**Eq.1.1**) and therefore the second orange-red ferric hydroxide and additional sulphuric acid (**Eq.1.2**).

$$2FeS_2 + 7O_2 + 2H_2O \rightarrow 4SO_4^{2-} + 2Fe^{2+} + 4H^+ \quad (1.1)$$

$$Fe^{2+} + \frac{1}{4}O_2 + H^+ \rightarrow Fe^{3+} + \frac{1}{2}H_2O \quad (1.2)$$

The third equation (**Eq.1.3**) involves hydrolysis of ferric iron to produce the solid ferric hydroxide and the release of additional acidity. This step pH dependent. With pH less 3.5, the solid mineral does not form, and ferric iron remains in solution. At pH above 3.5, a precipitate of $Fe(OH)_3$ forms which is commonly referred to as 'yellow boy' (Nicholson, 1994; Jambo & Blowes, 1998).

$$Fe^{3+} + 3H_2O \rightarrow Fe(OH)_3 + 3H^+ \quad (1.3)$$

The overall sequence of reactions (**Eq.1.4**) is acid producing:

$$4FeS_2 + 15O_2 + 14H_2O \rightarrow 4Fe(OH)_3 + 8H_2SO_4 \quad (1.4)$$

Acid mine drainage formation is also accelerated by naturally occurring bacteria that assist in the breakdown of the sulphide-containing rock (Akcil & Koldas, 2006). The rate and degree at which acid-mine drainage proceeds can be significantly increased by the action of these bacteria.

1.2.3 Treatment of mine water

Desalination is a separation process used to reduce the dissolved salinity of the brine to a level suitable for use. All desalination processes involve three liquid flows: saline

feedwater (brine or seawater), water produced with low salinity and salinity concentrate (brine or wastewater). Reverse osmosis desalination is the most common use of membranes in water treatment (Schrotter, *et al*., 2010). It can remove virtually all colloids and dissolved solids from aqueous solutions, providing brine concentrates and near-pure water permeability. Freezing desalination, which includes three stages of ice formation, ice washing and thawing of fresh water to remove contaminants, is an alternative physical process that can be used for desalination based on the various freezing points of fresh water and brine. Comparatively speaking RO is an extremely efficient process that allows the simultaneous concentration, fractionation and purification of products and the ability to perform multiple operations in a single operation (Lazarides & Katsanidis, 2003). Reverse osmosis systems require much less floor space and equipment than evaporative systems because they do not require steam, evaporators, and condensers.

Reverse Osmosis/Cooling deals with treatment of brines from RO (**Figure 1.2**). The aim is to recover valuable products such as $CaCO_3$, $Mg(OH)_2$ and Na_2SO_4 to reduce sludge and brine disposal. ROC also aims to increase the water recovery from 85% to 99%. The ROC process can be described as follows:

- Pre-treatment stage - brine is treated with Na_2CO_3 to allow selective precipitation of metals, *e.g* $Fe(OH)_3$ at pH 3.5, $Al(OH)_3$ at pH 4.5, and $CaCO_3$ at pH 8.0.
- After pre-treatment - the Na-rich water is treated with RO to produce drinking water and brine.
- The resulting brine has a concentration high enough to allow Na_2SO_4 crystallization upon cooling.

These stages have resulted in the following improvements or advantages to current technologies: (i) reduced RO membrane scaling; (ii) increased water recovery – no brine generation; (iii) elimination of mixed sludge generation – no sludge disposal costs, and (iv) production of valuable products from polluted water. Disadvantages associated with the ROC process are: (i) high chemical cost if Na_2CO_3 is used as the alkali and (ii) recovery of pigment would be difficult when $CaCO_3$ or $Ca(OH)_2$ is used for neutralization.

Pigment can be manufactured in the initial steps of treating mine water with the ROC process (**Figure 1.3** and Figure **1.4**). Pre-treatment with ultrafiltration and desalination with reverse osmosis are proven technologies which have been previously implemented (**Figure 1.4**). The first commercial plant, using the Freeze Crystallisation (FC) process, has been constructed for treatment of brine at A-Thermal Retort Technologies (**Figure 1.5**).

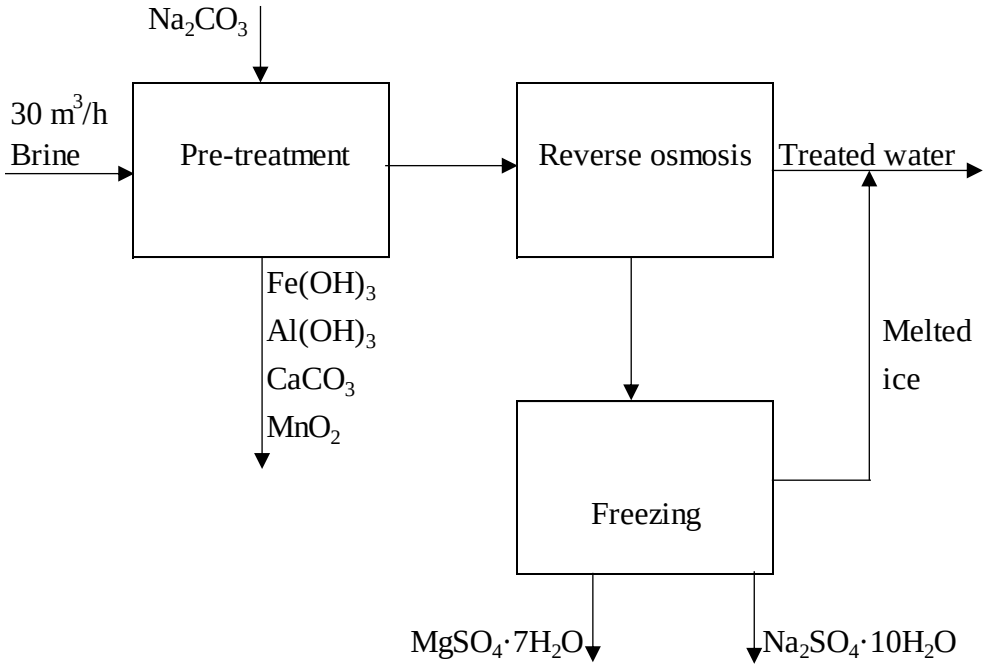

Figure 1.2 Process configuration of the ROC process (Letjiane, *et al*., 2019)

Figure 1.3 Pigments produced from iron-rich mine water (Letjiane, *et al*., 2019)

Figure 1.4 2.4 m^3/h RO stage of the R&D plant at the University of Limpopo (Commissioned in 2018)

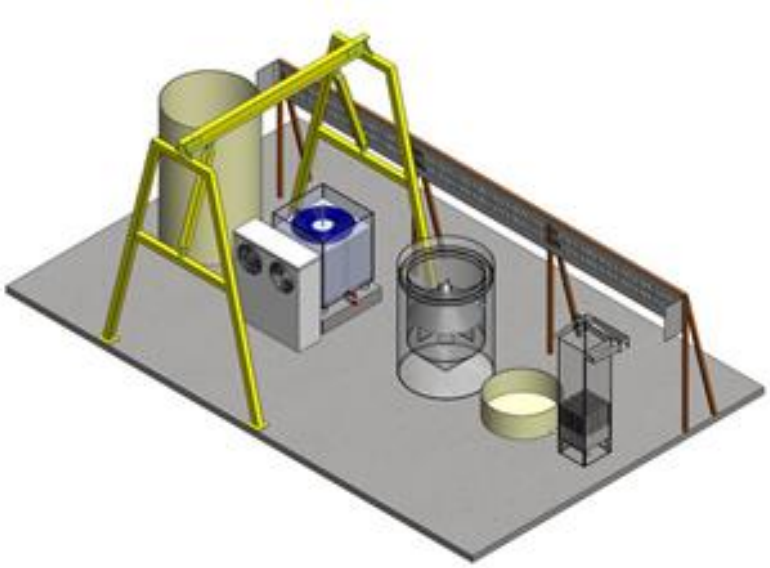

Figure 1.5 Integrated process schematic for brine treatment (Location, A-Thermal Retort Technologies)

1.2.4 Regulatory aspects

The South African mining, environmental and water legislation and associated regulations have been completely rewritten following the democratic transformation in

South Africa in 1994. The most recently introduced legislative measures is the National Environmental Management: Waste Act 59 of 2008. Basically, this regulation is of universal importance, and revolve around environmental protection, protection of local communities, and promotion of business ethics (Phuntsho, *et al*., 2014; Ndlovu, *et al*., 2017).

The Constitution of the Republic of South Africa under Chapter 2 the Bill of Rights stipulates that; everyone has the constitutional right to have an environment that is not harmful to his or her health and to have the environment protected for the benefit of present and future generations through reasonable legislative and other measures that:

i. prevent pollution and ecological degradation.
ii. promote conservation: and
iii. secure ecologically sustainable development and use of natural resources while promoting justifiable economic and social development.

Waste in South Africa is currently governed by means of several pieces of legislation, including but not limited to:

i. The South African Constitution (Act 108 Of 1996)
ii. Environment Conservation Act (Act 73 of 1989)
iii. The National Environmental Management Act (Act 107 of 1998)
iv. Air Quality Act (Act 39 of 2004)
v. National Environmental Management: Waste Act, 2008 (Act 59 of 2008)
vi. National Waste Management Strategy

The legislation regulatory agencies are becoming concerned with the huge amount of solid waste either being disposed of into water bodies or on the land. For instance, the Richards Bay Foskor phosphoric acid plant dispose gypsum effluent consisting of about 10 000 tonnes/day of waste gypsum, containing 70% water by pumping into the sea. There are many different sludge disposal processes used ranging from off-site transport to disposal in mine dumps (Aube, 2004). According to recent Environmental legislation contained in Government Notice 636, Regulation 5 (2013), the hazardous

wastes that are discarded on landfill sites should not contain more than 40 % water. This provides another incentive for why waste streams at mines and other industries need to be processed to saleable products to minimize the need for waste disposal at toxic waste dumps.

1.3 MOTIVATION FOR THE STUDY

South Africa is rich in a variety of minerals. Notwithstanding diamonds and gold, the country additionally has large reserves of iron, platinum, manganese, chromium, copper, silver, beryllium, and titanium. Many of these mineral resources are mined using surface mining operations, which have led to the production of wastes (DWAF, 2008). This study can be utilized to prevent the high disposal costs when zero waste disposal is applied. This means that solid waste needs to be transported and disposed of at solid waste disposal sites such as Holfontein EnviroServ, at Breswol (Msiza, 2013). The cost of waste disposal is high, as the transport cost amounts typically to about R1000/t and the disposal cost to about R1 500/t. Managing solid waste has proved to be expensive to the mining industry, which adds significantly to the production costs (Nengovhela, *et al*., 2007). It is therefore of interest that wastes rather be processed with the aim to recover saleable products.

Several processes have been developed, based on the use of precipitated $CaCO_3$ for neutralisation of AMD and partial desalination (Maree, *et al*., 2013; Maree & du Plessis, 1994; Maree, *et a*l., 2004; Maree, *et al*., 1992; Maree, 1996; Maree, *et al*., 1996). These processes mainly rely on the use of raw limestone and lime for mine water treatment (Bologo, et al., 2012; Maree & Theron, 2005). This technology has been proven to be successful and is commonly used in mining industries. The Alkali Barium Carbonate (ABC) water treatment process that was developed by the Council for Scientific and Industrial Research (CSIR) can be used for neutralisation as well as metal and sulphate removal from AMD by using readily available and affordable chemicals (de Beer, et al., 2010.; Maree, 2013; Maree, et al., 2013; Masukume, et al., 2013; Hlabela, et al., 2007). A reverse osmosis process is used by several mining companies to treat AMD (Hutton, *et al*., 2009), achieving high water recovery levels of between 93 and 99 % (Greenlee, *et al*., 2009). South Africa has advanced significantly in terms of mine water treatment. The ROC process can be used for the treatment of

AMD through neutralisation with Na_2CO_3 for the removal of metals, desalination with RO, freeze crystallisation for recovering Na_2SO_4 from brine. In this work, the brine derived Na_2SO_4 is converted via Na_2S to its raw form, Na_2CO_3. Sodium carbonate is mainly used to manufacture glass, paper, detergents, and soaps.

Gypsum waste can be converted into nano $CaCO_3$, which has a value of R14 000/t. This will generate profit from waste. Due to its frequent application in polymers, paints, plastics, and rubbers, nano calcium carbonate has drawn a lot of interest. The recovery of REEs from waste products has advantages, both environmentally and economically. Environmentally, the recovery of REEs will assist in removing them from waste, which will minimize environmental pollution. Economically, the recovered REEs will assist in the manufacturing of magnets and electrical components.

1.4 PROBLEM STATEMENT

Without water, survival of plants, animals and human beings is not possible. In South Africa, the already scarce fresh water is decreasing in quality because of an increase in pollution. Sodium sulphate waste and gypsum waste are rich in sulphates. Poor waste management ranging from non-existing collection systems to ineffective disposal causes air pollution, and soil contamination. This also contribute to contamination of drinking water and can cause infection and transmit diseases. The presence of sulphates in water increases corrosion, prompts scaling in boilers and heat exchangers, and serves as substrate for microorganisms implicated in bio-corrosion (Trusler, *et al*., 1988). High concentrations of sulphate in the drinking water can have a laxative effect when combined with calcium (Ca^{2+}) and magnesium (Mg^{2+}) ions, which are the two most common constituents of water hardness. Despite the serious environmental, health and socio-economic implications of the sulphates, very little has been done to tackle these problems (Benamor, *et al*., 2005). The presence of REEs in water causes bioaccumulation, environmental degradation, and ultimately human health hazards (Tong, *et al*., 2004). All rare-earth ores contain radioactive elements of the actinide family, such as uranium and thorium, which can contaminate air, surface water, soil, and groundwater. Moreover, the refinement process for REEs uses toxic acids and results in polluted solid waste that must be properly disposed of

(Weber & Reisman, 2012). With current legislation that drives towards zero waste discharge, waste gypsum containing REEs should be treated to recover them.

Because most treatment technologies are either inadequate or too expensive when the cost of waste disposal is included, a significant amount of solid waste is left untreated (Diz, 1997). Evidently, there are huge tracts of land in South Africa, which are unusable because they are already impacted by solid waste, with examples having been reported in the Johannesburg (Serge-Kubanza & Simatele, 2020). Therefore, there is a need to process solid wastes to recover valuable products, which will simultaneously do justice to the environment.

1.5 HYPOTHESIS

Sodium and calcium sulphates can be converted to sodium and calcium carbonates respectively, by a thermal process for the recovery of valuable products such as Na_2S, S, NaHS and CaS and REEs.

1.6 AIMS AND OBJECTIVES

The aim of the study is to process $CaSO_4$ and Na_2SO_4 to recover valuable products such as such as $CaCO_3$, Na_2CO_3, $Mg(OH)_2$, NaHS, CaS and REEs.

The objectives of this study are to investigate the following:

i. Conversion of $CaSO_4 \cdot 2H_2O$ to $CaCO_3$ and $Ca(HS)_2$
ii. Conversion of $BaSO_4$ to BaS
iii. Conversion of $MgSO_4$ to $Mg(OH)_2$
iv. Conversion of Na_2SO_4 to Na_2CO_3, NaHS
v. Conversion of $Ca(HS)_2$ to $CaCO_3$ and H_2S
vi. Conversion of Na_2S to Na_2CO_3 and H_2S
vii. Conversion of Fe^{2+} to Fe^{3+}
viii. Conversion of H_2S to S
ix. Conversion of $CaSO_4 \cdot 2H_2O$ to $CaSO_4.½H_2O$
x. Investigation of hardness on gypsum tiles

xi. Recovery of REEs from $CaSO_4 \cdot 2H_2O$ and AMD

xii. Recovery of REEs from $CaCO_3$

Objectives i and vi were studied in Chapters 4 and 5. In Chapter 4 the focus was on the reduction of $CaSO_4$ and in Chapter 5 on the reduction of $BaSO_4$.

Objectives vii to xii were studied in Chapter 6.

1.7 NOVELTY

The investigation resulted in the following novel findings:

i. Pyrolysis software predictions on product yields corresponded with experimental results.

ii. Na_2SO_4 cannot be converted directly to Na_2S due to the melting of Na_2SO_4 in the same temperature range where the reduction takes place.

iii. Na_2SO_4 can be converted to Na_2S by reacting it first with CaS or BaS.

iv. Nano $CaCO_3$ can be recovered from gypsum.

1.8 STRUCTURE OF THE THESIS

This thesis consists of the following chapters:

Chapter 1: Introduction

This chapter entails of the background of the solid waste problems together with the regulatory solutions to the problem. The occurrence and the potential value of solid waste are also discussed. This chapter also discusses the aim, objectives, hypothesis, and significance of the study.

Chapter 2: Literature review

This chapter reviews the challenges faced by South African' s waste management. The waste management hierarchy, the classification and disposal methods of solid waste are also discussed. This chapter also reviews the applications and processes that have been used to treat solid wastes to recover valuable products.

Chapter 3: Materials and methods

In this chapter, the description of the sampling area, chemicals, feedstock, apparatus, and instruments used throughout the study are discussed. It also includes the approach followed in this work such as sample preparation and sample analysis.

Chapter 4: Recovery of Na_2CO_3 and nano $CaCO_3$ from Na_2SO_4 and $CaSO_4$ wastes via CaS.

The purpose of this chapter was to evaluate the two new technologies to produce Na_2CO_3 from Na_2SO_4. The one technology based on carbothermal reduction of Na_2SO_4 to produce Na_2S as intermediate. This was inconvenient due to the melting of mixtures of Na_2SO_4 at the reaction temperature. As a result of this complication an alternative technology coined the Sulphide/Carbonate process was proposed. The second purpose was to evaluate the process needed to recover $CaCO_3$ and nano $CaCO_3$ from PG. This chapter was published (Mokgohloa, *et al*., 2022).

Chapter 5: Recovery of Na_2CO_3 AND MgO from alkali earth metal sulphates.

The purpose of this investigation was to identify the process steps needed for the processing of Na_2SO_4 to Na_2CO_3 and NaHS. The new process developed by Van Vuuren and Maree was used for the indirect processing of Na_2SO_4 to Na_2S, where Na_2SO_4 was reacted with BaS. This was further used as a reactant to produce Na_2CO_3 and $Mg(OH)_2$. The chapter also focused was on how BaS, produced from $BaSO_4$, can be used to improve the processes where $NaSO_4$, $MgSO_4$ and $CaSO_4$ are processed to produce high-value products. A section of this chapter was published as an article “The processing of Na_2SO_4 to Na_2CO_3 and NaHS, (Mokgohloa, *et al*., 2022). The full chapter is in press.

Chapter 6: Recovery of rare earth metals from waste streams.

The purpose of this chapter was to quantify REEs in waste streams namely, AMD and PG. PG and AMD are a secondary raw material of interest for REEs because they are abundant and contains significant amounts of REEs . The study also focused on the formation of $CaSO_4{\cdot}½H_2O$ from $CaSO_4{\cdot}2H_2O$ and the hydration of $CaSO_4{\cdot}½H_2O$ leading to the crystallization of $CaSO_4{\cdot}2H_2O$.

.**Chapter 7: Conclusions and recommendations.**

In this last chapter of the thesis, summary of the findings and discussions of the results of this study are given. It also outlines recommendations for further research that could be addressed in future.

This thesis (**Chapter 4-6**) has been structured as separate articles which have either been published or to be submitted for publication, duplication in terms of specific types of information (*e.g*., background, methodologies, etc.) was inevitable.

CHAPTER 2: LITERATURE REVIEW

2.1 WASTE MANAGEMENT

2.1.1 Classification of industrial solid waste

2.1.1.1 Introduction

Industrial waste includes sludges, product residues, kiln dust, slags, and ashes from a variety of manufacturing processes. The three main types of industries produce most of the industrial waste: industries of metallurgy, non-metallurgy, and food processing. The raw materials used, the manufacturing processes, and the product outlets all play a role in determining how waste is generated, but there are three main types of waste: gases, liquids, and solids. The wastes are not alike; They might be recyclable, contain inorganic or organic fractions, biodegradable or nonbiodegradable fractions, or both. In general, industrial waste can be divided into two categories: hazardous and non-hazardous.

2.1.1.2 Non-hazardous and hazardous industrial wastes

Carton, plastic, metals, glass, rock, and organic waste are examples of non-hazardous industrial waste, which does not pose a threat to public health or the environment. **Table 2.1** depicts the characteristics of the waste produced by various industries. Even though each nation has its own distinct classification of hazardous waste, the amount of typically non-hazardous waste is significantly higher than that of hazardous waste (Wahlström, *et al*., 2016). In Europe (EU-28), it was reported that only 3.8% of all industrial waste was considered hazardous (Skårman, *et al*., 2019). This is also in line with what has been observed in other significant nations like the United States (less than 10%) (Chen, *et al*., 2021), China (1.1%) (Liang, *et al*., 2020), and India (1.5%) (Kumar, *et al*., 2017). Hazardous waste is toxic, ignitable, corrosive, reactive, or radioactive, and it may pollute water sources in the soil and air (Kushwaha, *et al*., 2018; Kushwaha, *et al*., 2016; Rizvi, *et al*., 2020; Sathe, *et al*., 2020). This has the potential to harm public health or the environment and needs to be mitigated.

Table 2.1 The characteristics of the waste produced by various industries (Taherzadeh, *et al*., 2019).

Industrial sector	**Description**	**Typical waste**
Mining and quarrying	Extraction, beneficiation, and processing of minerals	Solid rock, slag, PG, muds, tailings
Energy	Electricity, gas, steam, and air-conditioning supply	Fly ash, bottom ash, boiler slag, particulates, used oils, sludge
Manufacturing	Chemical	Spent catalyst, chemical solvents, reactive waste, acid alkali, used oils, particulate waste, ash, sludge
	Food	Plastic, packaging, carton
	Textile	Textile waste, pigments, peroxide, organic stabilizer, alkali, chemical solvents, sludge, heavy metals
	Paper	Wood waste, alkali, chemical solvents, sludge
Construction	Construction, demolition activity	Concrete, cinder blocks, gypsum, masonry, asphalt, wood shingles, slate, metals, glass, and plaster
Waste/Water services	Water collection, treatment, and supply	Spent adsorbent, sludge

2.1.2 Disposal methods

2.1.2.1 Introduction

Industrial waste has the same issues with disposal as domestic waste, but it also contains hazardous waste, making disposal more difficult (Wang, *et al*., 2006). Industrial waste disposal has historically been poorly regulated. In fact, it has only been in the last ten years that even developed nations have enacted legislation to curb the widespread uncontrolled and environmentally unacceptable practices. In the absence of such legislation, disposal almost always occurs in an unregulated landfill at locations that frequently pose a risk of water pollution from leachates.

There are numerous chemicals in industrial solid waste, some of which are harmful. If the concentration of the element is higher than a certain threshold, the waste is deemed toxic (Thai, 2009). Even though some waste may occasionally have levels that are higher than what is allowed, the waste itself is only toxic if the average value of the element is higher than the toxicity level. To determine a substance's toxicity, various agencies have developed a variety of criteria and tests. To regulate whether uncontrolled waste release would have toxic effects on humans or other ecosystem organisms, it is necessary to know the waste's properties.

2.1.2.2 Landfilling

The disposal, compression, and embankment fill of waste at appropriate locations is referred to as landfilling. For the time being, landfill is the only all-encompassing waste material disposal method and is simple, adaptable, and less expensive than the other options (Read, *et al*., 1997). Even though the amount of solid waste that is disposed of in landfills has decreased, landfills are likely to continue to play a significant role in integrated systems for managing solid waste all over the world. In addition to its financial benefits, disposing of waste in a landfill minimizes environmental harm and other problems and allows waste to decompose under controlled conditions until it becomes a relatively inert, stable material. All over the world, solid waste was disposed of in landfills. In the United States, for instance, 52.6% of solid waste was disposed of in landfills (Sisinno, *et al*., 2000), in Brazil 59.1% (Billard, 2001), in The Kingdom of Saudi Arabia (KSA) 85 % (Lema, *et al*., 1988), in Malaysia 94.5% (Baig, *et al*., 1999),

in China 79% (Welander, *et al*., 1997), in Venezuela: landfills 32%, controlled disposal 43% and non-controlled disposals or open dumps 24% (Wang, *et al*., 2003), in Mexico: sanitary landfills 65%, in uncontrolled and open dumps 30% (Harmsen, 1983) and in Thailand 27% (Chian & DeWalle, 1976). Waste can only be disposed of in landfills for a limited amount of time, and landfill reclamation can take hundreds of years. (Białowiec, 2011). **Figure 2.1** shows a typical landfill used for solid disposal.

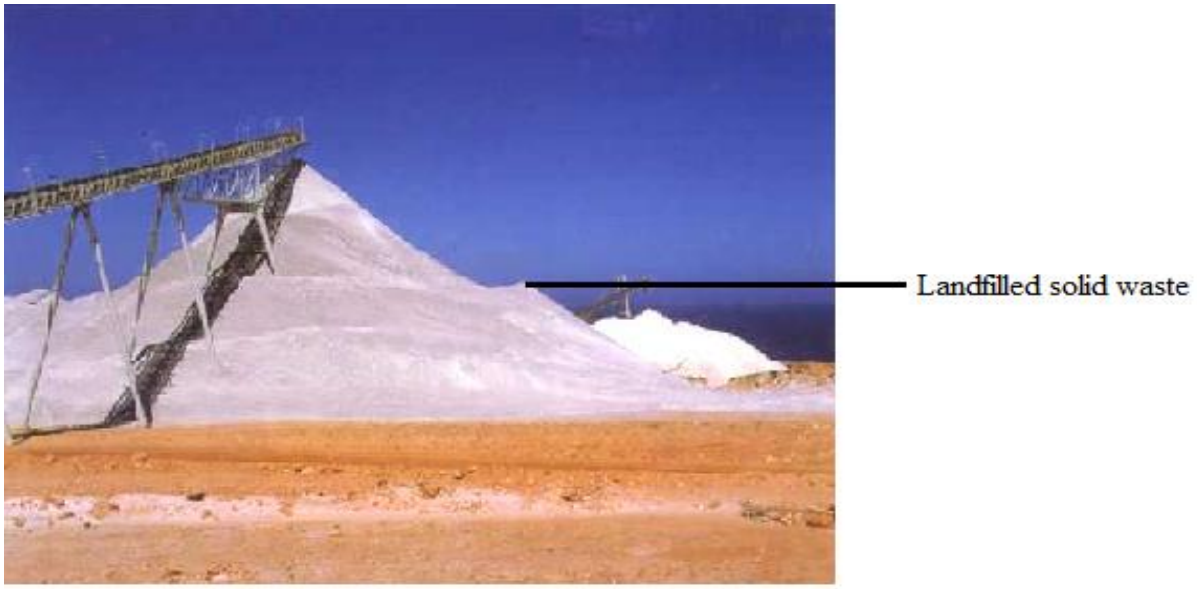

Figure 2.1 Waste disposed in a landfill (from www.epa.gov 29 March 2023)

2.1.2.3 *Incineration*

A waste treatment technique called incineration involves the combustion of organic waste materials (Lam, 2011). There is a widespread misconception that when something is burned, it simply vanishes. Matter simply takes on new forms and cannot be destroyed. Heavy metals that were in the original solid waste are emitted as stack gases from the incinerator stack following incineration, along with tiny particles, and they are also present in the remaining ashes and other residues (Wang, *et al*., 2019). So, incinerators don't take care of the issues of poisonous materials present in waste. As a matter of fact, they basically convert these poisonous materials to different structures, some of which might be more harmful than the first materials. These made synthetics can then re-emerge in the climate as toxins in stack gases, leftover cinders,

and different deposits. A portion of the radiated synthetic substances are cancer-causing (disease causing) and some are endocrine disruptors. Others like sulphur dioxide (SO_2) and nitrogen dioxide (NO_2) (Chang, *et al*., 2004) as well as fine particulate matter, have been associated with adverse impacts on respiratory health.

2.1.2.4 *Onsite burial*

On-site burial entails burying waste in the ground at the accident site. When appropriate environmental controls to safeguard groundwater, surface water, air, and soil are in place and the site's characteristics (such as the depth to the water table) permit it, this disposal option should only be utilized. The most prevalent method of onshore disposal for drilling waste (mud and cuttings) is burial. After the liquid is allowed to evaporate, the solids are typically buried in the reserve pit, which is also used for temporary storage and collection of waste mud and cuttings. Pit burial is a low-tech method that attracts a lot of operators because it doesn't require waste to be moved away from the well site. Waste that contains high concentrations of oil, salt, biologically available metals, industrial chemicals, and other materials with harmful components that could migrate from the pit and contaminate usable water resources may not be a good candidate for on-site pit burial (Onwukwe & Nwakaudu, 2012).

2.1.2.5 *Composting*

Composting, a biological process in which the organic portion of waste is allowed to decompose under carefully controlled conditions, is another method for treating solid waste. The organic waste is reduced by up to 50% because of microbes metabolizing it. Compost or humus are the names given to the stabilized product. It can be used as mulch or a soil conditioner and has a texture and smell that are like those of potting soil. Composting provides a means of simultaneously processing and recycling garbage and sewage sludge. Composting is likely to become more popular as landfill and solid-waste incineration options are restricted by more stringent environmental regulations and location restrictions. (Slater & Frederickson, 2001). The steps involved in the process include sorting and separating, size reduction, and digestion of the refuse. **Figure 2.2** shows a picture of waste gypsum compost.

Figure 2.2 Gypsum compost (Abdel-Fattah, 2012).

2.1.2.6 *Challenges*

South Africa is currently hindered from achieving a cleaner and greener future by numerous waste management issues. Of these, mismanagement and non-compliance are the most common, and pose harmful to the environment and society (Viljoen, *et al*., 2021). As a result of a lack of resources and an ever-increasing population, waste is becoming increasingly difficult to collect and properly dispose of. Municipal solid waste has increased, particularly in densely populated cities, because of the ongoing economic expansion and industrialization trends. It is a problem that is only going to get worse, with recent statistics estimating that cities alone produce 1.5 billion tons of waste annually and that this number will rise to 2.3 billion tons by 2025 (Gutberlet, 2015).

The growing amount of waste has a negative impact on every aspect of society, making the concern is serious. Long-term environmental and public health catastrophes that have a devastating impact on national economies are the result of failing to address the waste issue strategically and sustainably (Kumar, *et al*., 2021). However, to address the issue, developing nations with less developed infrastructure have a long way to go. In many developing nations, the management of solid waste is becoming a major public health and environmental issue as urbanization is on the rise.

To put it another way, planning and carrying out solid waste management are typically hindered by a lack of skilled human resources in developing nations. This frequently occurs in conjunction with inadequate or poorly managed funds allocated to resolving waste issues, ineffective legislation, and a lack of coordination among the primary institutions in charge of waste issues. All these factors contribute to a lack of public education and awareness about waste and its devastating effects.

Reducing solid waste is not as simple as recycling or reducing the number of sources. Unfortunately, these strategies for reducing solid waste are faced with challenges. Recycling is beneficial for reducing solid waste, but it is expensive (Hopewell, *et al*., 2009). It requires more production, transportation, and labour, which cost cities and waste management companies money. Consequently, recycled goods frequently cost more to consumers.

The potential rise in pollution brought about by recycling is yet another area of concern in relation to the reduction of solid waste. Recycling causes pollution because more vehicles are required to collect and transport recyclables. The factories that turn trash into raw materials can then add even more pollution. Obviously, landfills, where trash might otherwise go, can also cause pollution.

The main costs associated with reduction at the source are incurred from research, collection of data, management of waste systems, product design, passage of relevant legislation, education/raising awareness, and advocacy (Debrah, *et al*., 2021). These are much lower, however, compared to the costs of treating waste after it is generated. It is difficult to define and quantify something that has not yet been produced. Therefore, it is difficult to show the results of reduction at the source.

2.1.3 Hierarchy

Throughout the waste life cycle, the waste management hierarchy provides a methodical and all-encompassing approach to waste management that addresses reduction, avoidance, reuse, recovery, treatment, recycling, and safe disposal as the final option (Zhang, *et al*., 2022; Moshtaghian, *et al*., 2021). It lists the most and least preferred waste management practices in that order. The waste hierarchy's goal is to maximize the practical benefits of products, while minimizing waste production. There are numerous benefits to using the waste hierarchy correctly. It can assist in lowering

levels of pollution, greenhouse gas emissions, energy consumption, resource preservation, job creation, and green technology development (Pires & Martinho, 2019). The general approach that guides waste management in South Africa is the waste management hierarchy, which is the basis for the Waste Act's objectives (Karani & Jewasikiewitz, 2007). **Figure 2.3** below is an illustration of the waste management hierarchy as described above.

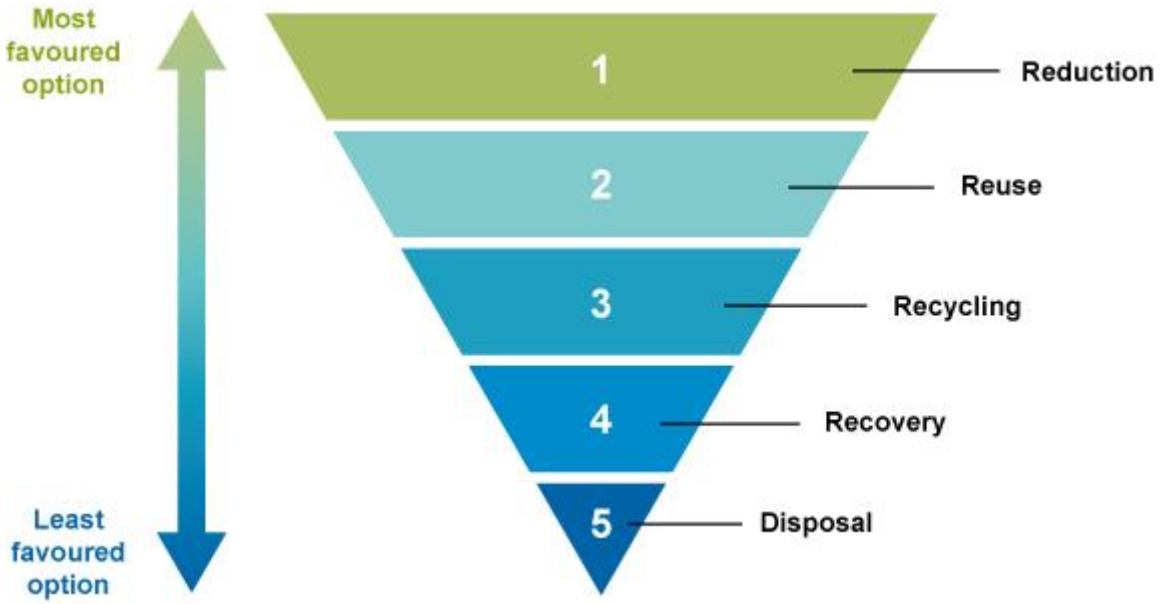

Figure 2.3 Waste management hierarchy (Karani & Jewasikiewitz, 2007).

Where the amount of waste can't be diminished during creation, the reason for executing the waste management hierarchy is to involve waste as an asset and redirect these expected resources from landfill. Although landfill is generally viewed as the most reasonable method for overseeing waste, this view doesn't consider elements such as the ecological effects of landfills; the expenses of creating and keeping up with extra landfill ability to oblige the rising pace of garbage removal; and the expense of shutting and remediating the landfill *(Njoku, et al*., 2019). The stages of waste management hierarchy are described in the next five sections.

2.1.3.1 *Reduce*

Reducing or preventing as much waste production as possible is a top priority in the waste management hierarchy. At this stage, businesses, communities, and

governments are encouraged to use fewer virgin raw materials to make goods and services. The goal is to reduce resource waste and maximize efficiency by following procedures like:

i. Choosing raw materials with the least amount of packaging or refinement resources
ii. Disposable or single-use products should be avoided.
iii. Getting materials that can be repaired, recycled, or reused.
iv. Optimizing inventory to avoid wasting food or other perishable goods.

2.1.3.2 *Reuse*

The second-best waste management hierarchy is to prepare materials for reuse in their original state. Reusing waste not only reduces the amount of waste that ends up in landfills, but it also reduces costs of getting new products or raw materials.

2.1.3.3 *Recycling*

Reusing includes handling materials that would somehow be shipped off landfills and transforming them into new items, *i.e.,* an aspect of circular economy. It's the third step of the waste management hierarchy because of the additional energy and assets that go into making another item. Reusing has numerous ecological advantages since it both forestalls landfilling and takes into consideration asset effectiveness.

2.1.3.4 *Recovery*

Recovery means any operation the principal result of which is waste serving a useful purpose by replacing other materials which would otherwise have been used to fulfil a particular function, or waste being prepared to fulfil that function, in the plant or in the wider economy.

2.1.3.5 *Disposal*

When all else fails, materials that cannot be reused, recycled, or recovered for energy will be landfilled and incinerated (without energy recovery). Because waste that remains in landfills may continue to have a negative impact on the environment, this

approach to waste management is unsustainable. One tonne of food waste disposed of in a landfill, for instance, is estimated to emit 450 kg of CO_2, which is a notorious greenhouse gas associated with global warming. Chemicals and hazardous liquids that can contaminate the groundwater and soil beneath landfills can also leak.

2.2 WASTE APPLICATIONS AND PROCESSING OF GYPSUM TO VALUABLE PRODUCTS

2.2.1 Applications

2.2.1.1 Introduction

Waste gypsum has been utilized by farmers for centuries, but in recent years, it has received renewed attention. Gypsum's resurgence is largely attributable to ongoing research and practical insights from leading experts highlighting its numerous advantages (Zoca & Penn, 2017). In the United States, gypsum was one of the first kinds of fertilizer used. It has been used for more than 250 years to treat agricultural soils (Watts & Dick, 2014). Additionally, the building industry uses it.

2.2.1.2 Agricultural use

Gypsum has a wide range of potential applications in the fields of agriculture and horticulture. It can boost overall plant growth because it is a soluble source of calcium and sulphur, two essential plant nutrients (Rashmi, *et al., 2018)*. Some soils, particularly those with a lot of heavy clay content, can benefit from gypsum amendments as well. Soil aggregation can be facilitated by these amendments, which can (i) aid in preventing soil particle dispersion (ii) reduce surface crust formation, (iii) promote seedling emergence, and (iv) increase the rate of water movement through the soil profile and infiltration (Awadhwal & Thierstein, 1985). It can also lower the concentration of soluble phosphorus in surface water runoff and reduce soil and nutrient losses due to erosion. Gypsum's application improves chemical properties by reducing subsoil acidity and aluminium toxicity (Shamshuddin, *et al*., 2010). This makes it easier for plants to get deep roots and to absorb enough water and nutrients during droughts. Gypsum is likewise the most utilized amendment for sodic soil

recovery and for diminishing the unsafe impacts of high-sodium waters on account of its solubility, minimal expense, and accessibility (Amezketa, *et al*., 2005).

2.2.1.3 The building industry

It has been discovered that gypsum waste is extensively used in the production of building materials (**Figure 2.4**) and components like hollow bricks, structural concretes, and bricks (Singh & Garg, 2020; Singh, 2002). Gypsum is used in construction to prevent fires, keep moisture out, absorb sound, and resist heat. It is extensively utilized in ceiling and partitioning projects as a building decorative material. Concrete, high-strength gypsum sticky powder, whitewashing gypsum, and all kinds of gypsum plates (such as thistle boards and decorative gypsum boards, *etc*.) can all be made from building gypsum, pillar ornaments, gypsum curlicues, and other things. Projects like finishing mortar, wall-surface putty, model making, anaglyphic products, plasterboard partitions and ceilings, and so on, all make use of building gypsum and its products.

Figure 2.4 Gypsum plaster in construction (Mansour, *et al*., 2013)

2.2.1.4 Other applications of gypsum

Gypsum can be used for a variety of other purposes (or historical uses) besides the most common ones for construction and food preparation. Burns, abscesses, and eczema all benefit from the use of gypsum for treatment. It is present in numerous hair

products, including foot creams and shampoos. Gypsum might be able to get rid of toxic heavy metals like lead and arsenic from water, according to some tests (Liu, *et al*., 2018). Historically, medieval scribes made gesso out of gypsum and lead carbonate to apply to illuminated letters and gild illuminated manuscripts with gold.

The CSIR in South Africa has been doing extensive research on the utilization of waste gypsum to recover valuable products. The CSIR built a demonstration plant aimed at the recovery of valuable products from waste gypsum (Maree, *et al*., 2004).

2.2.2 Processing of gypsum

Heating gypsum to a temperature of between 100 ºC and 200 ºC drives off three-quarters of the water of hydration, creating plaster of Paris (Engbrecht & Hirschfeld, 2016). At temperatures above 200 °C, gypsum loses anhydrous $CaSO_4$, and all the moisture forms the basis of ordinary gypsum. The $CaSO_4$ thus obtained is systematically referred to as 'soluble' $CaSO_4$ because, although relatively insoluble, continuous heating at high temperatures turns the salt into an almost insoluble salt. The latter is called "insoluble" $CaSO_4$. Most industrial gypsum waste cannot be used beforehand, for example in the production of gypsum board. These stockpiles cause environmental problems, such as dust in the atmosphere and the low water solubility (2000 mg/l) of gypsum (Nengovhela, *et al*., 2007). Therefore, there is a need to develop methods to convert poor-quality gypsum into a valuable product, namely, CaS, $CaCO_3$, Na_2CO_3 and REES.

The commercial methods for manufacturing sulphur from $CaSO_4$ are through (i) the reduction of $CaSO_4$ to CaS and (ii) the conversion of CaS to sulphur (Sliger & The M, 1986; Rice, *et al*., 1990). Calcium sulphate can be reduced to CaS using reducing agents, such as coal, coke, CH_4, CO, and H_2, but temperatures over 850 °C are required to obtain near-stoichiometric conversions (Argyle & Bartholomew, 2015). Ragin and Brooks studied PG reduction to CaS and discovered that PG can be reduced to CaS at 850 - 1000 °C by using either coal or CO as a reductant and that the required temperature can be lowered to 750 °C with Fe_2O_3 as catalysts (Ragin & Brooks D, 1990). Trikkel and Kuusik also discovered that some additives, especially a semi-coke of coal that contain > 20% volatiles in dry matter in a mixture with ferric oxide (Fe_2O_3) can intensify the CaS recovery process and raise the CaS yield (Trikkel

& Kuusik, 1994). The advantage of reduction using fixed carbon is that cheap reducing agents such as coal and heavy oil ash can be used, and the reducing agents are easy to handle. Despite the fact that many studies on carbon reduction of gypsum at temperatures above 1000 °C have been described in detail,(Turkdogan & Vinters J, 1976; Kutsovskaya M, *et al*., 1996; Strydom, *et al*., 1997; Tao, *et al*., 2001). Few research has been done on the low temperature conversion properties of gypsum to CaO. **Figure 2.5** shows a process flow diagram for reduction of gypsum.

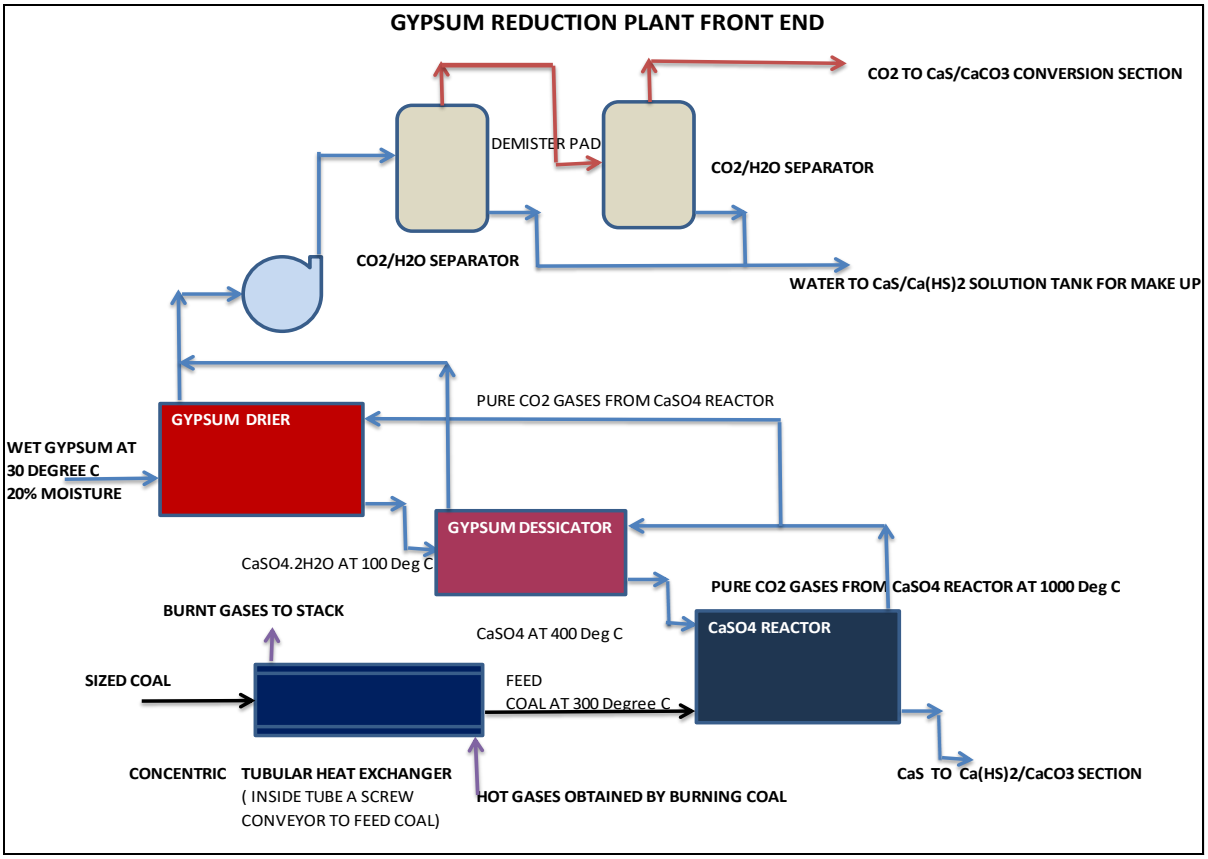

Figure 2.5 Process flow diagram for reduction of gypsum reduction (Nengovhela, *et al*., 2007).

2.2.3 Saleable products

2.2.3.1 $CaCO_3$

2.2.3.1.1 Introduction

Calcium carbonate is one of the most abundant materials found in earth's crust and forms the rock types like limestone and chalk (Pidwirny, 2012). It is also the most

common chemical deposit in oceans, accounting for about 10% of sediment (Department of Geology, 2015). Almost all the $CaCO_3$ that makes up the carbonate platform comes from marine life. It is also an important component of biological systems, such as shells of marine organisms, pearls, and eggshells (Beruto & Giordan, 1993).

2.2.3.1.2 Applications

Calcium carbonate is a dietary supplement used when the amount of calcium absorbed in the diet is not enough. Calcium carbonate is also used as an antacid to relieve heartburn, gastric acid reflux, and indigestion (Wang, *et al*., 2014). It is very important for the construction industry as a separate building material (*e.g.,* marble) and as a component of cement. It helps in the manufacture of mortars used for gluing bricks, concrete blocks, roofs, rubber joints and tiles (Saracho, *et al*., 2021). In fact, $CaCO_3$ has many industrial applications due to its physical and chemical properties such as particle size, shape, density, colour, transparency and other properties and it is known that these properties are mainly determined by the polymorphic $CaCO_3$ (Hathorne, *et al*., 2008).

Use of $CaCO_3$ has been touched by a variety of researchers (Brahaita, *et al*., 2017; Watten, *et al*., 2005; Maree, 1996). These researchers noted that $CaCO_3$ has unique benefits for treating AMD. For example, there are marginal problems associated with low raw material costs, low availability of hazardous substances for treatment, accidental overtreatment, and low-volume, dense sludge production. The main disadvantage was that the $CaCO_3$ could not create a pH above 7 for a fast and efficient oxidation of the iron. The second disadvantage is the low efficiency of use, which leads to excessive use of $CaCO_3$. Another disadvantage is that $CaCO_3$ chemicals must be administered precisely to avoid overdose. The pH-controlled dosing systems are often unsafe, probably due to fluctuations in water flow and poor maintenance. As a result, low pH water (3-10 each) is pumped through the vertical water pipes of the mine, causing corrosion due to low pH or delamination (plaster) due to high calcium concentrations.

A common by-product of $CaCO_3$ neutralization is gypsum (**Figure 2.6**). Gypsum precipitation often occurs because AMD is rich in sulphates and makes the solubility of lime much higher than its saturated product.

Figure 2.6 Typical limestone neutralization plant (courtesy J P Maree)

Another common by-product of lime neutralization is $CaCO_3$. Inorganic carbon for this reaction may be from the AMD itself or may be the result of dissolved CO_2 in the air during aeration. Due to its high pH, this CO_2 is converted to bicarbonate and then partially converted to carbonate. The carbonate fraction precipitates with large amounts of calcium in suspension to form $CaCO_3$. This $CaCO_3$ can play an important role in the stability of the final sludge product, providing neutralizing energy during sludge storage. It is also an indicator of the effectiveness of the lime process. A more efficient neutralization process produces less calcite (**Eq. 2.1**).

$$Ca(OH)_2 + CO_2 \rightarrow CaCO_3 + H_2O \qquad (2.1)$$

2.2.3.2 $CaCO_3$ formation

Calcium carbonate is chemically stable up to 800 °C and decomposes into CaO and CO_2 at high temperatures. Due to its antacid properties, $CaCO_3$ is used in industrial conditions to neutralize acidic conditions in soil and water. Implanted $CaCO_3$ has three polymorphic forms: calcite, aragonite, and vaterite. The formation of each polymorph

depends on synthetic factors, including pH, temperature, concentration and ratio of carbonate and calcium ions, impurities, mixing, reaction time, *etc*. became known. (Zhao, *et al*., 2013; Chang, *et al*., 2017). Calcium carbonate precipitation (**Eq. 2.2**) occurs when calcium ion is combined with either carbonate or bicarbonate ions as follows,

$$Ca^{2+} + CO_3^{2-} \rightarrow CaCO_3 \quad (2.2)$$

$$Ca^{2+} + 2(HCO_3^{-}) \rightarrow CaCO_3 + CO_2 + H_2O \quad (2.3)$$

The above equation (**Eq. 2.3**) shows that the presence of CO_2 increases the solubility of $CaCO_3$ in saline. Increasing CO_2 acidifies the water and lowers the pH. Precipitation of $CaCO_3$ is usually accompanied by a decrease in pressure. This lowers the partial pressure of CO_2, increases the pH and decreases the solubility of $CaCO_3$. The solubility of $CaCO_3$ decreases with increasing temperature. Suwanthai *et al*. 2016 showed that the water solubility of CaS can be improved by synthesizing high purity $CaCO_3$ (mainly calcite) from gypsum residues using acid gas (H_2S) (Suwanthai, *et al*., 2016). High purity $CaCO_3$ (mainly amorphous) could also be produced from medium and low-grade $CaCO_3$ using strongly acidic cation exchange resin (Huang & Wang, 2007). Pure $CaCO_3$ can be obtained from marble or by preparing CO_2 from a solution of $Ca(OH)_2$. In the latter case, $CaCO_3$ is obtained from the mixture, forming a type of product called 'precipitated $CaCO_3$ (PCC)'. The PCC has a very small and controllable particle size of 2 μm, which makes it especially useful for paper production. Another major type of industrial product is "ground calcium carbonate" or GCC. As the name suggests, GCC involves the grinding and processing of lime to form powder shapes classified by size and other characteristics for a variety of industrial and pharmaceutical applications. The most common method of crystallization to obtain $CaCO_3$ is to prepare a 0.5 M solution of $(NH_4)_2CO_3$ and calcium acetate $Ca(CH_3COO)_2$ and then mix them (Weiss, *et al*., 2014). Ammonium carbonate $(NH_4)_2CO_3$ solution is tightly sealed with parafilm to minimize the loss of NH_3 and the introduction of CO_2 from the atmosphere.

Calcium carbonate can only be made from natural mineral sources if it is to be used commercially. Specific properties can be improved, and the size of the material's particles reduced using manufacturing processes. Calcium carbonate is mined from open pits or underground, then, at that point, drilled, impacted, and squashed *(Teir, et*

al., 2005). After this, the crushed stone is sized and washed to remove most of the material's-colored impurities. From there, $CaCO_3$ goes through either wet or dry processing. Carbon dioxide is used in the chemical synthesis of the wet process, which typically follows dry processing to improve purity (Dragan & Ozunu, 2012). This strategy additionally works backward, as when $CaCO_3$ responds with acids, it produces CO_2. Because of this, geologists can test a mineral with confidence to see if it contains $CaCO_3$.

2.2.3.2.1 Dry Calcium Carbonate Processing

Dry processing necessitates a series of reduction procedures that involve physically grinding and reducing material into ever-smaller particles. Commonly, the ground material is then grouped by continued screening for coarse particles - coming about in a "screen grade" material - or through air characterizing to isolate out better particles. The average screen grade material is between 400 and 3360 μm (Jeong, *et al*., 2009). When marble is used to make $CaCO_3$, the processing makes the mineral form even more pure (Chen, *et al*., 2009). Nevertheless, $CaCO_3$ is typically utilized due to its lower price. After that, the ground $CaCO_3$ is graded according to its properties, used for a variety of applications, or further processed through wet processing.

2.2.3.2.2 Processing of Precipitated Calcium Carbonate

Normally, $CaCO_3$ goes through an interaction by which it is precipitated synthetically into a cleaner structure, so the mineral is held inside a suspended arrangement. Wet processing usually results in material that is purer and has finer particles (Chen, *et al*., 2009). The manufacturing of precipitated $CaCO_3$, which is derived from lime, involves hydrating quicklime (CaO) to start a chemical reaction with water to produce a $Ca(OH)_2$ slurry (Jimoh, *et al*., 2018). This basically results in a water-based suspension, half or more of which may be solid matter.

This process involves involving CO_2 and intensity in a cycle called calcination, which brings about what is designated "milk-of-lime" because of its outrageous whiteness (Silakhori, *et al*., 2021). The precipitated $CaCO_3$ can be made with gems of different shapes and sizes, which are acclimated to cause the subsequent material to perform ideally for explicit applications. The paper, plastic, healthcare, and cosmetics and skin

care industries all make use of this refined form of calcium carbonate (Atchudan, *et al*., 2022).

2.2.3.3 *Nano $CaCO_3$*

2.2.3.3.1 Introduction

The nano calcium carbonate (nano $CaCO_3$) refers to an ultra-fine precipitated $CaCO_3$ with an average particle diameter less than 100 nm which can be used as additives in various products (Thammakarn, *et al*., 2014). The nano $CaCO_3$ is widely applied in plastic, paints, and rubber industries because of its unique properties (Khan & Bhat, 2013).

2.2.3.3.2 Applications

Calcium carbonate nanoparticles have received a lot of attention due to their widespread use in polymers, paints, plastics, and rubbers *etc* (Sonawane, *et al*., 2009). Calcium carbonate nanoparticles (<100 nm) have shown many unique properties compared to regular $CaCO_3$ particles (>3 μm) (Pai and Pillai 2008). Thus, fine particles of $CaCO_3$ with distinct morphology are used for specific applications (Liu 2005). Nano- or micro-sized particles offer a much larger surface area and volume for better mass and energy transfer, as well as the potential to limit materials that promote controlled chemical reactions.

Concrete has recently been made with nano-CaCO3 (Shaikh F & Supit, 2014). Additionally, some studies have suggested that the development of cementitious systems may benefit from the physical properties of nano-CaCO3. (Shaikh & Supit, 2015; Camiletti, *et al*., 2013; Kawashima, *et al*., 2013; Makar, *et al*., 2012). Nonetheless, it is trusted that the main test in the nanocomposite research is to disperse the nanomaterials into the network (Korayem, *et al*., 2017; Meng, *et al*., 2017). Nano-$CaCO_3$ is easy to agglomerate form larger secondary particles which tends to reduce the properties of cementitious materials because of its high surface energy. It is believed that the formation of nano-micron composite particle can provide a solution for this question (Yang, *et al*., 2016). As compared to several others, nano $CaCO_3$ is relatively cheaper (Poudyal & Adhikari, 2021). Further studies have shown that nano $CaCO_3$ has the potential to be produced within the cement plant while

utilizing the waste CO_2 from cement production (Poudyal & Adhikari, 2021; Batuecas, *et al*., 2021). A recent study has shown that doping of cement by 2% nano $CaCO_3$ helps reduce the CO_2 emission from cement plants by 69% (Batuecas, *et al*., 2021).

Figure 2.7 depicts the properties and applications of nano $CaCO_3$ particles. In a review paper (Boyoo, *et al*., 2014), the applications of micro and nano sized-$CaCO_3$ are summarized. The following categories of applications are also discussed:

i. Filler material: Coatings, paints and pigments, paper, lubricants, and plastics can all benefit greatly from the addition of $CaCO_3$ as a filler material.

ii. Biomedical - The similarity and non-poisonousness of $CaCO_3$ towards the body makes it an appealing medication conveyance vehicle bringing about various examinations being done on this impact.

iii. Food industry: $CaCO_3$ particles have been designed for a variety of applications in the food industry, including enzyme supports, biosensors, and catalysis.

iv. Environmental - $CaCO_3$ particles' high porosity, large surface area, and low mass transport barrier make them a promising candidate for the development of simple, cost-effective, and dependable biosensors and other environmental applications.

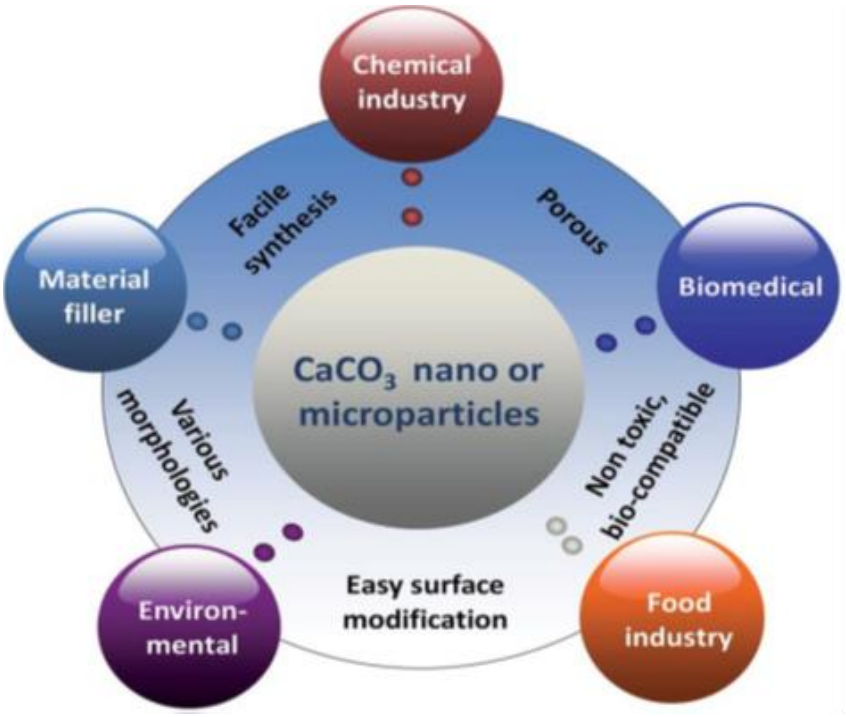

Figure 2.7 Properties and applications of nano $CaCO_3$ particles (Boyjoo, *et al*., 2014)

2.2.3.4 Nano $CaCO_3$ formation

There are several ways to produce nano/micro-calcium carbonate. Some useful synthetic methods include mechanical deposition, microemulsion, hydrothermal, sol-gel, aerosols, pyrolysis, and chemical precipitation (Tavakoli, *et al*., 2007). The classical synthesis of nano $CaCO_3$ by the interaction of $CaCl_2$ with Na_2CO_3 using the method of chemical precipitation of water is very simple and gives different crystalline structures and morphologies in large-scale production. On the other hand, mechanical-chemical treatment using solid-state chemical reaction produces nanoparticles with an average particle size in the range of 4 nm and a homogeneous size and shape with a low agglomeration rate (Tsuzuki & McCormick, 2004). Nano $CaCO_3$ can also be synthesized as an amorphous phase by a hydrophobic agent incorporated into a nanoparticle matrix by a sol-gel method that can produce a uniform particle size. In this method, calcium ethoxide was initially used as a precursor and synthesis of CO_2 sequestration to obtain very small $CaCO_3$ calcite nanoparticles that form the soil, followed by the formation of a gel in the reaction medium. (Palmqvist, *et al*., 2017). Reverse micellar, polymerization exfoliation, biomimetic synthesis and ultrasonic cavitation are other approaches also used to synthesize $CaCO_3$ nanoparticles. Nano $CaCO_3$ in the form of calcite can be synthesized by spray drying of nano $CaCO_3$. This method is advantageous as it avoids the use of surfactants or other chemicals to stabilize the reaction mixture. (Vergaro, *et al*., 2015). In addition, nano $CaCO_3$ self-assembly can use surfactants to obtain spheroidal spheres in water and hydrophobic solvents, or surfactants can be used to transfer spherical nanoparticles. (Bodnarchuk, *et al*., 2014; Wang, *et al*., 2006; Shimpi, *et al*., 2015).

Current techniques to produce fine $CaCO_3$ particles include:

i. Intensive milling of high-grade $CaCO_3$ such as seashells (Gbadeyan, *et al*., 2020).

ii. Carbonation of a suspension of slaked lime (Yu & Wang, 2010)

iii. Reaction between a solution of a calcium salt and a solution of a carbonate salt (Wray & Daniels, 1957; Babou-Kammoe, *et al*., 2012)

iv. Carbonation of a solution of $Ca(HS)_2$ (de Beer, *et al*., 2015)

2.3 WASTE APPLICATIONS AND PROCESSING OF Na_2SO_4 TO VALUABLE PRODUCTS CONVERSION

2.3.1 Applications

2.3.1.1 Introduction

Several industrial activities produce metal sulphates, which are regulated by strict limitations for wastewater concentrations of sulphate. Therefor sulphate recovery methods that reduce the sulphate concentration of purified wastewaters in a commercially-viable and efficient way have recently become a point of interest of several studies (Chen & Dutrizac, 2005; Li, *et al*., 2019; Rögener, *et al*., 2012). The promising methods include precipitation of sulphate as sparingly soluble compounds, such as $CaSO_4 \cdot 2H_2O$, ettringite ($Ca_6Al_2(SO_4)_3)(OH)_{12} \cdot 26H_2O$), or $BaSO_4$ and Na_2SO_4 with either chemical or electrochemical coagulation, or by separating the sulphate via membranes or ion exchange methods (Ghyselbrecht, *et al*., 2013; Mamelkina, *et al*., 2017; Tun & Groth, 2011). A complementary possibility is to reuse a portion of the side stream sulphate solution in other processes, rather than as a waste, increasing circular economy and atom efficiency.

2.3.1.2 Waste sodium sulphate

Sodium sulphate is one such industrial waste needing management. It is produced as a by-product of the desulfurization process when NaOH, Na_2CO_3, or $Na(HCO)_3$ are reacted with SO_2 waste streams (*e.g*., FGD process, acid/base neutralization reactions, *etc*.) It can be managed using the Glaserite process to convert it into high-value potassium sulphate (K_2SO_4) (Ogedengbe, *et al*., 2020). Tuovinen *et al* 2021 utilised waste Na_2SO_4 from battery chemical production in neutral electrolytic pickling (Tuovinen, *et al*., 2021). A process for the utilization (valorisation) of waste Na_2SO_4 by reaction with potassium chloride (KCl) and water to give K_2SO_4 has been reported in a patent (Scherzbert, *et al*., 1991).

2.3.2 Processing of Na_2SO_4

Sodium sulphate is a white crystalline solid or powder employed in the manufacture of kraft paper, paperboard, glass, and detergents and as a raw material to produce

various chemicals. There are two types of sodium sulphate natural and by product, also known as synthetic (Gawaad, *et al*., 2011):

i. Natural Na_2SO_4 is produced from naturally occurring brines and crystalline deposits found in California and Texas.

ii. It is also found as a constituent of saline lakes, such as the Great Salt Lake in Utah. Synthetic Na_2SO_4 is recovered as a by-product of various manufacturing processes.

iii. Both types of Na_2SO_4 have several important and useful applications in various consumer products.

It is now well known that heating Na_2SO_4 up to the point of its softening by way of a carbon-containing reducing medium, produces Na_2S with the simultaneous formation of carbon monoxide (CO). Studies of the reactions between Na_2SO_4 and carbon or CO began as early as 1801 (Clement & Desormes, 1801). Berzelius, Berthier, and Regnault all made partial studies of the reaction, but Unger seems to have been the first to propose an actual equation for the reaction (Berzelius, 1822; Berthier, 1823; Regnault, 1836; Unger, 1847). He concluded that the primary reaction (**Eq. 2.4**) was:

$$Na_2SO_4 + 2C \rightarrow Na_2S + 2CO_2 \qquad (2.4)$$

Further work on the reaction was done by d' Heureuse, (Heureuse, 1848). In 1858 Stromayer reported finding polysulfides and carbonates among the reaction products (Stromayer, 1858). In 1890, the reaction began to assume industrial importance. Berthelot made a study at 1000 °C but experienced challenges due to the reaction of materials with SiO_2-derived at that temperature (Berthelot, 1890). The only study in which the reduction of the Na_2SO_4 was accomplished solely by CO was made by Okuno, Masumi, and Fukuyama (Okuno, *et al*., 1933). They used a static system to place sodium sulphate in a reaction tube boat heated by an electric tube furnace. The system was designed to introduce a specific mixture of CO and CO_2 and to measure the change in pressure as the reaction progressed. When a white colour formed, they changed the method of converting Na_2SO_4 to Na_2S by adding CaO to a mixture of Na_2SO_4 and CO_2 (White, 1955). Budnikov and Ulakhovich reported that the rate of reduction was affected by the source of carbon used (Budnikov & Ulakhovich, 1980). Sodium sulphate has also been reduced to sodium sulphide in relatively poor yields

by reducing gases such as hydrogen, methane, and hydrogen sulphide (Vadapalli, *et al*., 2013; Ranjit, *et al*., 1995).

Equation 2.5 has been investigated at temperatures ranging from 500 ºC to 900 ºC, without catalysts and in the presence of such catalysts as iron nickel, sodium sulphide and sodium hydroxide with conflicting results (Naranjo, 2006).

$$Na_2SO_4 + 4H_2 \rightarrow Na_2S + 4H_2O \qquad (2.5)$$

Mashigwana *et al* discovered that Na_2SO_4 is not reduced directly with carbon. The reason why Na_2SO_4 is not reduced directly with carbon is because Na_2SO_4 has a relatively low melting point of 890 °C. It forms a eutectic mixture with Na_2S that has a melting point of only 745 °C at a concentration of 72 mol% Na_2SO_4 whereas the temperatures that are typically required for carbothermal reduction reactions are typically more than 800 °C (Mashigwana, *et al*., 2022). Therefore, when Na_2SO_4 is directly reduced with carbon at elevated temperatures, an intermediate molten phase (**Figure 2.8)** is formed that is difficult to contain and which is very corrosive. Nevertheless, Leblanc set up the first Leblanc process plant in 1791 to reduce Na_2SO_4 in the presence of $CaCO_3$ to form Na_2CO_3 and calcium sulphate and this process was later also commercialised in England (Leblanc, 1791). The process led to severe environmental problems and was later replaced with the Solvay process in which Na_2CO_3 is produced by the reaction of sodium chloride (NaCl) and ammonium carbonate $(NH_4)_2CO_3$ to form Na_2CO_3 and ammonium chloride (NH_4Cl).

Today there are plants in China and India that produce Na_2S from Na_2CO_3 (Xiong, *et a*l., 2020). However, the purpose of these plants is to produce Na_2S, which is a niche product. It is unclear what material of construction is used in these plants, but it is suspected that the construction material is viewed as a consumable.

Figure 2.8 Photo of melted Na_2SO_4 when heated to 1000 °C (Mashigwana, *et al*., 2022).

2.3.3 Saleable products

2.3.3.1 *Na_2CO_3*

2.3.3.1.1 Introduction

All the world's Na_2CO_3 was manufactured synthetically prior to 1965. The discovery of natural resources (trona mineral and brine) led to the intervention of natural Na_2CO_3. The synthetic manufacturing method is once again gaining popularity because of the depletion of natural resources and the rising demand for Na_2CO_3 (Wu, *et al*., 2019).

Currently, all South Africa's Na_2CO_3 is imported. Sodium carbonate is consumed off in enormous amounts by significant industries in South Africa. It is a critical part in the glass producing, cleanser fabricating, and different synthetics, which is all presently being brought at excessive costs into South Africa (Masindi, 2017).

Purchasers of Na_2CO_3 locally and globally are working in our current reality where they should depend on imports of restricted neighbourhood supply to run their cycles. The Roskill Report, which details the outlook for Na_2CO_3, and the supporting data was purchased by IDC. According to the report, the continent of Africa used approximately 1 Mt of Na_2CO_3 in 2009, while South Africa used approximately 357 000 t/pa.

Based on 2009 consumption, the estimated Rand value of import replacement is: 357 000 tpa x $400 per ton x R10 per dollar = R1, 5 billion. Bots Ash and Ansac are two

examples of the many countries from which South Africa imports (Tathavadkar, *et al*., 2003).

2.3.3.1.2 Uses

Sodium carbonate is widely used in industrial applications (**Figure 2.9)** such as the manufacture of chemicals (20%), soap and detergents (12%), glass (50%), water treatment (5%), metallurgy (10%), and other applications (3%) (Örgül, 2003).

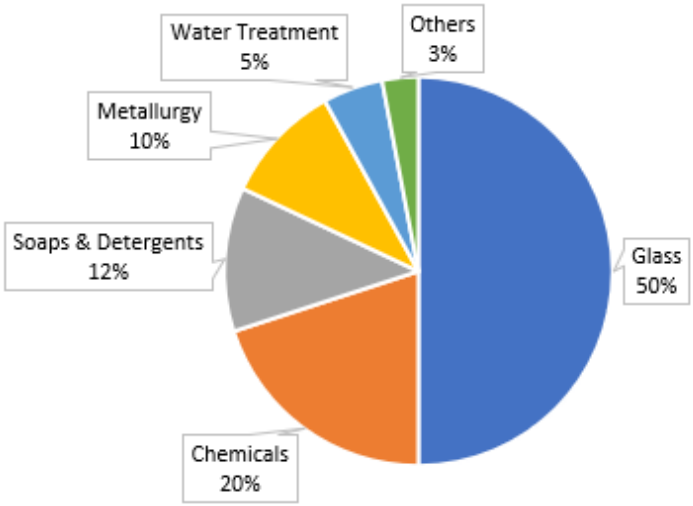

Figure 2.9 Uses for Na_2CO_3 (Örgül, 2003)

i. Glass industry- Sodium carbonate of about 50% is used in the glass manufacturing as shown in **Figure 2.9**. This includes flat glass, bottles, jars, insulation, television tubes, lighting, glassware and labware. In the production of glass, the soda ash goes about as a fluxing agent which reduces the melting temperature of the silica and lowers the energy consumption.

ii. Chemical industry - Approximately 20% of Na_2CO_3 is utilized in chemical industry. It is utilized in reactions to create natural and inorganic compounds that are used in several applications, including the production of sodium silicate (Na_2SiO_3), sodium thiosulphate ($Na_2S_2O_3$), $Na(HCO)_3$, sodium hydrosulphite ($Na_2S_2O_4$), sodium nitrite ($NaNO_2$) and sodium sulphite (Na_2SO_3).

iii. Soaps and detergents – About 12% of Na_2CO_3 is used to produce soaps and detergents. This is due to its smaller particle size which gives a free-flowing material and enhances the reactivity (Backus, 2007).

iv. Metallurgy- Approximately 10% is utilized in treatment of uranium minerals, oxidizing calcination of chrome metal, lead reusing from disposed of batteries, and reusing of aluminium and zinc.

v. Water treatment – Sodium carbonate is normally used to increase the pH of acidic water in water treatment and to precipitate calcium and magnesium compounds that render water hard.

vi. Others- Only about 3% of Na_2CO_3 is used for the manufacturing of various chemical fertilizers, artificial sodium bentonites, synthetic detergents, organic and in the inorganic colouring industry, in the petroleum industry and in natural gas refining, the enamelling industry and in the glue, fats and gelatine industries, *etc*. (Örgül, 2003; Backus, 2007; Council, 2003).

Sodium carbonate has been used to modify pH and remove heavy metals from AMD water as precipitates (Kaur, *et al*., 2018). Sodium carbonate has the disadvantage that they require accurate dosing to prevent under or over application. Silva *et al* studied manganese removal in AMD using $CaCO_3$ mixed with Na_2CO_3. They discovered Na_2CO_3 provided carbonate ions to precipitate high-manganese contents in mine water and industrial effluents, whereas powdered limestone induced the heterogeneous nucleation of manganese carbonate ($MnCO_3$) (Silva, *et al*., 2012). Sodium carbonate is used in the pre-treatment stage for formation of pigment and precipitation of other metals in the ROC process (Mogashane, *et al*., 2023). In the past, the production of soda ash was done by aqueous extraction of the ashes of certain plants, such as Spanish Barilla (Curlin, *et al*., 1991).

2.3.3.1.3 Formation of Na_2CO_3

Globally, 25% of soda ash is mined from natural deposits and the remaining 75% is produced by engineered measures. The natural deposits of Na_2CO_3 are reported to be in abundance in the United states of America (USA) (DSI, 1995) followed by parts of Africa *e.g*. Botswana and Lake Magadi in Kenya (Jacob, *et al*., 2016). Natural soda ash sources are lacking in Asia, Europe, the Middle East, and South America. These locations produce soda ash synthetically by means of the Solvay process.

Solvay Process

Ernest Solvay, (1838-1932) was the inventor of the Solvay Process which produces synthetic Na_2CO_3 that is used in many industrial applications as a major commodity and important raw material (Steinhauser, 2008). Hence, the Solvay process is one of the most important inorganic chemical processes.

The starting materials, *viz*., brine (NaCl), and $CaCO_3$, are promptly accessible at minimal price, and a large portion of the alkali used in the process can be recovered. Ammonia is firstly absorbed in a saturated and purified NaCl-brine solution. Sodium bicarbonate is then precipitated *via* carbonization utilizing CO_2 that is acquired by simmering of $CaCO_3$. The by-product is aqueous ammonium chloride solution illustrated in a result (**Eq. 2.6**). Upon calcination, $NaHCO_3$ disintegrates and Na_2CO_3, H_2O, and CO_2 are formed (**Eq. 2.7**). Heating of $CaCO_3$ produces calcium oxide (**Eq. 2.8**). It is utilized as milk of lime (**Eq. 2.9**), a suspension of calcium hydroxide, to recover NH_3 in the so-called ammonia distillation. (**Eq. 2.10**) (Kasikowski, *et al*., 2004)(Gao, *et al*., 2007); (Steinhauser, 2008) forming $CaCl_2$ as a by-product that must be sold or disposed, (**Eq. 2.11**). The chemical reactions are given below:

$$2NH_3 + 2NaCl_{(aq)} + 2CO_2 + 2H_2O \rightarrow 2NaHCO_3 \downarrow + 2NH_4Cl_{(aq)} \quad (2.6)$$

$$2NaHCO_{3(s)} \rightarrow Na_2CO_{3(s)} + CO_2 \uparrow + H_2O \uparrow \quad (2.7)$$

$$CaCO_{3(s)} \rightarrow CaO_{(s)} + CO_2 \uparrow \quad (2.8)$$

$$CaO_{(s)} + H_2O \rightarrow Ca(OH)_{2(s)} \quad (2.9)$$

$$2NH_4Cl_{(aq)} + Ca(OH)_{2(s)} \rightarrow 2NH_3 \uparrow + CaCl_{2(aq)} + 2H_2O \quad (2.10)$$

The overall reaction is:

$$2NaCl + CaCO_3 \rightarrow Na_2CO_3 + CaCl_2 \quad (2.11)$$

Conventional production of soda ash by the Solvay Process results in undesirable solid and liquid wastes (Trypuć & Łyjak, 2001). These wastes are regularly released to rivers, lakes, and/or the sea, because the large waste volumes created by a single soda ash plant cannot be discarded in ordinary disposal sites. The Solvay Process configuration is shown in **Figure 2.10.**

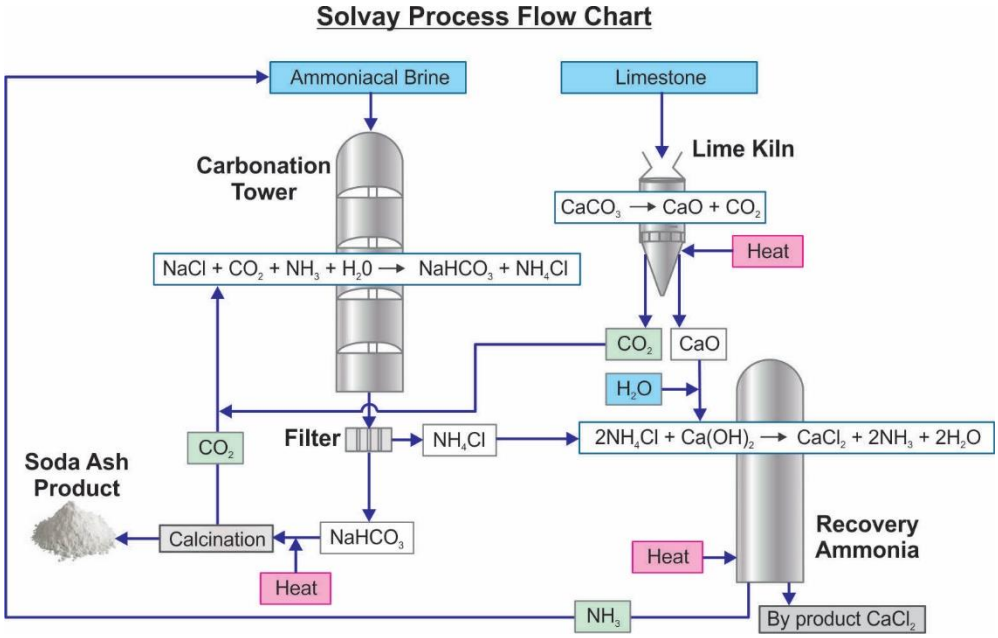

Figure 2.10 Process configuration of Solvay Process (Steinhauser, 2008; de Carvalho Pinto, *et al*., 2015)

Modified Solvay Process

The development and operation of the Modified Solvay Process plants were carried out in Japan. It is also known as the DUAL Process because several modifications were introduced. Its first commercial application was in 1980. The cycle is accomplished through a mix of the production of ammonium chloride and the production of soda ash. $Mg(OH)_2$ is removed as a contaminant. In contrast to the Solvay process, the ammonium chloride formed is precipitated by cooling and through the expansion of strong sodium chloride solutions. The significance of the DUAL application in Japan was driven by of the high cost of imported rock salt and also the use of the ammonium chloride as a plant food, particularly in rice cultivation (Örgül, 2003). Most of the plants that use the Modified Solvay process are found in Japan and China. The main raw materials used are carbon dioxide, sodium chloride and ammonia. Limestone is not required in this process.

The following chemical reaction (**Eq. 2.12**) illustrates the formation of ammonium chloride:

$$NaCl + NH_3 + CO_2 + H_2O \rightarrow NaHCO_3 + NH_4Cl \qquad (2.12)$$

In this step, ammonium chloride is solidified out and isolated by adding sodium chloride. The following instantaneous reaction (**Eq. 2.13**) takes place in the presence of NaCl:

$$NH_4^+ + HCO_3^- + NaCl_{(aq)} \rightarrow NaHCO_{3(s)} + NH_4Cl_{(aq)} \quad (2.13)$$

In this step, sodium bicarbonate precipitates leaving ammonium chloride in partially desalinated water. The final product is sodium carbonate. This is achieved by heating to 160 ˚C – 230 ˚C, producing water and carbon dioxide as by-products. A configuration of the Modified Solvay Process is given in **Figure 2.11**.

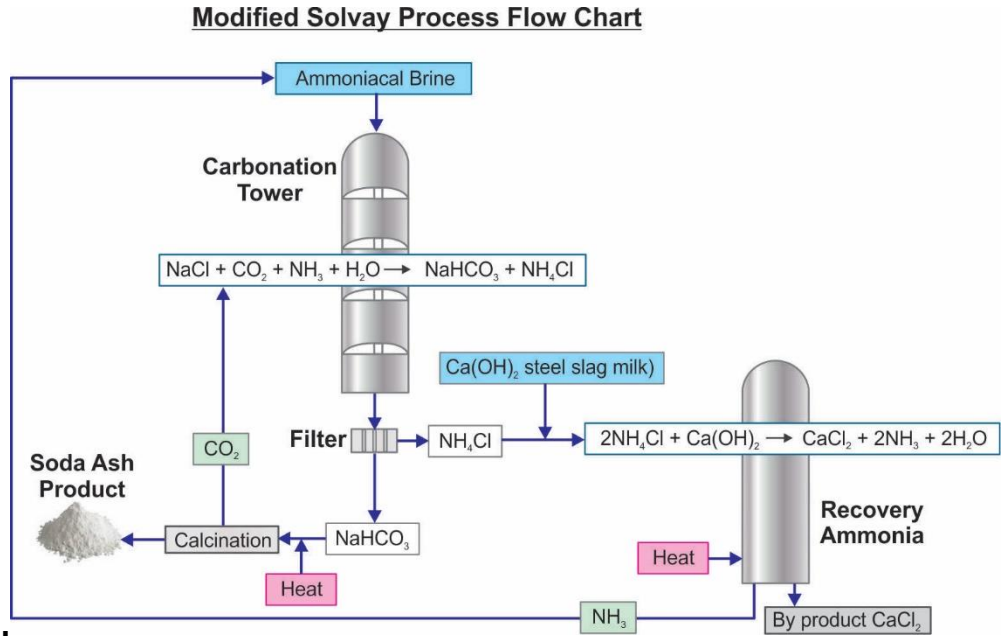

Figure 2.11 Flow configuration of the Modified Solvay process (Abdel-Aal, *et al*., 2016; de Carvalho Pinto, *et al*., 2015)

The conventional way to produce sodium carbonate from sodium sulphate as in the LeBlanc Process, sodium sulphate is carbo-thermally reduced in the presence of calcium carbonate to form a solid mixture of sodium carbonate and calcium sulphide. The sodium carbonate is then leached with water from the mixture.

2.3.3.1.4 World soda ash market

The creation of regular soda ash is to a great extent reliant upon the mineral stores. The biggest trona reserve is in Wyoming, USA and is draining at a pace of 8.5 million tons for every annum (Gorakhki & Bareither, 2015). Natural soda ash is not as good

as synthetic soda ash, which is why synthetic soda ash is preferred. However, compared to synthetic methods, the natural soda ash beneficiation process is 30-40% less expensive (Benalia, *et al*., 2022). Both normal and synthetic anyway exchange at comparable edges on the lookout. The benefits for a South African assembling plant include:

i. Being close to local customers.

ii. The potential for BEE partners to support local consumers' BEE procurement policies.

iii. Imports save money on transportation costs; also,

iv. Decreased wastage on imports and compromised quality.

The world soda production in the year 2000 was 34.7 x 10^6 t. This corresponds to the use of an efficient production capacity of 83%. World consumption was estimated at 34.5 x 10^6 t per annum and was expected to reach 38.1 x 10^6 t in 2005, growing at an average annual rate of 2% over the next five years. The countries that consumed the most sodium carbonate was mainly developed countries. However, the growth rates of consumer goods in these countries were also lower than in developing countries. Although production and consumption vary from country to country, end-use patterns are largely the same. Glass, chemicals, and detergents were the main sectors. Estimates of world sodium carbon production are provided in **The global** Na2CO3 production is about 55 million t/a. Of this, China produces about 20 million t/a and Botswana 770 x 103 t/a .

Currently, Botswana Soda Ash supplied to South Africa is principally used by the glass industry. The three main glass manufacturers in the country are Consol Glass, Nampak Wiegand and PFG.

The size of the total South African Na2CO3 market is about 357 000 t/a . However, the research on treatment of AMD discovered that if a dosage of 2g/ℓ of Na2CO3 is used to remove calcium before treating the water with RO, it will create a Na2CO3 demand of 255 000 t/a . At R4000/t, the value that can be derived from the supply of the Na2CO3 is about R1 billion per year.

Table 2.2.

The global Na_2CO_3 production is about 55 million t/a. Of this, China produces about 20 million t/a and Botswana 770 x 10^3 t/a (Gabasiane, *et al*., 2021).

Currently, Botswana Soda Ash supplied to South Africa is principally used by the glass industry. The three main glass manufacturers in the country are Consol Glass, Nampak Wiegand and PFG.

The size of the total South African Na_2CO_3 market is about 357 000 t/a (Masindi, *et al*., 2017). However, the research on treatment of AMD discovered that if a dosage of 2g/ℓ of Na_2CO_3 is used to remove calcium before treating the water with RO, it will create a Na_2CO_3 demand of 255 000 t/a (Mogashane, *et al*., 2020). At R4000/t, the value that can be derived from the supply of the Na_2CO_3 is about R1 billion per year.

Table 2.2 World soda ash production, reserves, and reserve base (USGS, 2009).

	Production		Reserves	Reserve Base
Natural	**2001**	**2002**		
United States	10 300	10 300	23 000 000	39 000 000
Botswana	270	270	400 000	NA
Kenya	260	300	7 000	NA
Mexico	-	-	200 000	450 000
Turkey	-	-	200 000	240 000
Uganda	NA	NA	20 000	NA
Other Countries	-	-	260 000	220 000
World Total, natural	10 800	10 900	24 000 000	40 000 000
World Total, synthetic	24 300	22 100		
World Total	35 100	33 000		

2.4 WASTE APPLICATIONS AND PROCESSING OF $BaSO_4$ TO VALUABLE PRODUCTS CONVERSION

2.4.1 Applications of $BaSO_4$

2.4.1.1 Introduction

Barium sulphate is very inert, insoluble, and stable to light and heat. Barium is one of the alkaline earth metals. It occurs in nature as a free metal and as salts. It is also produced for various industrial uses. The barium salt most found in the earth's crust is $BaSO_4$, which is found in limestone (barite), shales, and rocky sediments (Bonny & Jones, 2008). In a crushed form, it is the source for several other Ba compounds.

2.4.1.2 Applications

The major use of $BaSO_4$ is in the oil and gas industry to make lubricant muds for drilling. Barium salts are excellent to be used in the removal of sulphates in AMD. The commonly used barium salts for removal of sulphates by precipitation include barium carbonate, barium hydroxide and barium sulphide (Adlem, *et al*., 1991). Barium sulphate is a contrast agent. It starts functioning by coating the inside of oesophagus, stomach, or intestines which allows them to be seen more clearly on a CT scan or other radiologic (X-ray) examination (Katsanoulas, *et al*., 2007). It can be taken into use to help diagnose certain disorders of the oesophagus, stomach, or intestines. About 80% of the world's barium sulphate production, mostly purified mineral, is

consumed as a component of oil well drilling fluid (Sakorn, *et al*., 2002). It increases the density of the fluid, increasing the hydrostatic pressure in the well and reducing the chance of a blow-out. It is used in the casting of copper anode plates as a coating material. Barium sulphate is used to increase the density of the polymer by acting as a filler for plastics. It is also used to test the pH of the soil.

2.4.2 Processing of $BaSO_4$

In 1603, Vincenzo Cascariolo used barite, found at the bottom of Mount Paterno near Bologna, in one of his non-fruitful attempts to produce gold (Harvey, 1957). After grinding and heating the mineral with charcoal under reducing conditions, he obtained a persistent luminescent material rapidly, called Lapis Boloniensis, or Bolognian stone (Smet, *et al*., 2010).

Barium sulphide production is based on a process called “black ash”, which reduces the crude barite in coal in a rotary kiln heated to a temperature of 1100 °C. The “black ash” method can be expressed as an equation (**Eq. 2.14**) (MacWilliams, 1978; Lung, *et al*., 1991; Bafghi, *et al*., 2011).

$$BaSO_{4(s)} + 2C_{(s)} \rightarrow BaS_{(s)} + 2CO_{2(g)} \quad (2.14)$$

Whereas the chemical reactions taking place between the two solid reactants are exceptionally complex, it is by and large acknowledged that the real reducing agent is CO (**Eq. 2.15**) which is regenerated by CO_2 (**Eq 2.16**). CO_2 is produced from the gaseous reduction (**Eq. 2.16**) (Bafghi, *et al*., 2011; Jagtap, *et al*., 1990).

$$BaSO_{4(s)} + 4CO_{(g)} \rightarrow BaS_{(s)} + 4CO_{2(g)} \quad (2.15)$$

$$C_{(s)} + CO_{2(g)} \rightarrow 2CO_{(g)} \quad (2.16)$$

Be that as it may, the coal reduction process for $BaSO_4$ decomposition is energy consuming process, in which two particles of carbon are spent to change over one particle of $BaSO_4$ resulting in an incredible amount of CO_2 emission. Barite reduction can be performed by utilizing distinctive reducing agents, such as methane, natural gas, and carbon monoxide (Shakhtakhtinskii, *et al*., 1972; Jamshidi & Ebrahim, 2008). Another interesting process (**Eq.2.17**) is the hydrogen reduction of $BaSO_4$ to BaS:

$$BaSO_{4(s)} + 4H_{2(g)} \rightarrow BaS_{(s)} + 4H_2O_{(g)} \quad (2.17)$$

Equation 1.28 has been proposed as part of a cyclic reaction to reduce $BaSO_4$ to BaS, which has been reused as a reducing agent to convert sulphur dioxide gas to elemental sulphur (Sohn, *et al*., 2006). The advantage of this reduction scheme is that the gaseous product is only water vapor, which is effective in some industries to address the environmental issues associated with desulphurization plants (Sohn, *et al*., 2006; Sohn, 2003). However, this may not be beneficial concerning the energy savings and emission reduction in the production of barium sulphide from barite, since using hydrogen as a reductant to replace carbon may spend more energy thus emitting more CO_2, as comparing **Eq. 2.15** with **Eq. 2.17**.

China has been the world's largest producer of barite since the 1980s, and barite deposits are widespread (Sun, *et al*., 1998; Clark, *et al*., 2004; Yang, *et al*., 2008). Meanwhile, the natural sulphur deposit is also huge in China (Fu & Sheng, 1999; Peng & Guizhi, 2010; Zhang, *et al*., 1998). Based on the principle of correlating the use of resources, these authors proposed a new scheme for the elementary reduction of barium sulphur for the combined production of barium sulphur and sulphuric acid (**Eq. 2.18**). The essential reaction can be expressed as:

$$BaSO_{4(s)} + S_{2(g)} \rightarrow BaS_{(s)} + 2SO_{2(g)} \qquad (2.18)$$

Barium sulphide can also be used to distort X-rays and to see soft tissues clearly. The use of soluble barium compounds gives better results in the precipitation of sulphate compared to other neutralization processes (Jones, *et al*., 2002). However, barium salts are expensive and to make this technology viable, barium sulphate sludge can be recycled, in turn, into barium sulphide and then into barium carbonate (Hu, *et al*., 2000). This reduces costs and allows additional revenue from the production of sulphur from the H_2S elements developed.

2.4.3 Saleable products

2.4.3.1 *Barium sulphide*

2.4.3.1.1 Introduction

For this study the focus is only BaS as it is needed to produce Na_2S. Barium sulphide is an important precursor to other barium compounds with applications from ceramics

and flame retardants to luminous paints and additives, and recent research shows potential technological applications in electrical and optical devices (Kuzminchuk, *et al*., 2023). Barium sulphide has different characters, so it is used in a variety of ways.

2.4.3.1.2 Applications

i. Reduces the clear or transparent appearance of cosmetics and personal care products and may be used in skin makeup for hiding blemishes.
ii. Surface coating materials as pigment extender and in glass, rubber industries.
iii. An important precursor to other barium compounds including ZnS/BaSO and $BaCO_3$
iv. Luminous paints
v. Flame retardant and acts as a reducing agent
vi. Hair removing formulations and in the manufacture of Lithopone.
vii. To reduce the Ferric Sulphate in the Alum solution to Ferrous Sulphate (O'Brien, 2002)
viii. Barium sulphide was chemically processed into barium carbonate and elemental sulphur (Masukume, *et al*., 2013). In the process barium sulphide was reacted with carbon dioxide at ambient temperature and atmospheric pressure to produce $BaCO_3$ and H_2S.

2.4.3.1.3 Properties

Barium sulphide is a sulphide of barium found naturally as the mineral barite. It is colourless, although like many sulphides, it is commonly obtained in impure coloured forms. Barium is a metallic alkaline earth metal with the symbol Ba, and atomic number 56. It never occurs in nature in its pure form due to its reactivity with air but combines with other chemicals such as sulphur or carbon and oxygen to form barium compounds that may be found as minerals (Turner & Filella, 2020). The properties of BaS are summarised in

Table 2.3.

Table 2.3 Properties of BaS

Compound formula	BaS
Molecular weight (g/mol)	169.39
Appearance	Powder
Melting point (ºC)	1200
Boiling point	Decomposes
Density (g/cm^3)	4.25
Solubility	N/A
Exact mass (g/mol)	169.88
Monoisotopic mass (g/mol)	169.88

2.5 WASTE APPLICATIONS AND PROCESSING OF $MgSO_4$ TO VALUABLE PRODUCTS CONVERSION

2.5.1 Applications of $MgSO_4$

2.5.1.1 Introduction

Magnesium is the second most abundant intracellular cation and the fourth when the extracellular medium is also considered (Telci, *et al*., 2002). As a cofactor, it is involved in more than 300 known reactions, such as: hormone binding to receptors, flow of transmembrane ions, regulation of the adenylate kinase system, muscle contraction, neuronal activity, vasomotor tone, cardiac excitability, release of neurotransmitters, and calcium binding to calcium channels (Schulz-Stübner, *et al*., 2001).

2.5.1.2 Applications

Magnesium sulphate is a magnesium salt having sulphate as the counterion. It has a role as an anticonvulsant, a cardiovascular drug, a calcium channel blocker, an anaesthetic, a tocolytic agent, an anti-arrhythmia drug, an analgesic, and a fertilizer.

It is used to increase and compensate for magnesium and sulphur oxide deficiencies. Magnesium is one of the essential elements in the structural units of chlorophyll molecules found in the green parts of the plant, which convert sunlight into chemical energy during the photosynthesis. The advantage of magnesium sulphate compared to other magnesium salts, such as dolomite, is its high solubility which allows the farmer to splash the fertilizer directly onto the leaves, thus helping the plant to absorb through the leaves easily. Magnesium deficiency, seizures, and anaesthesia in diabetic women can be treated by using magnesium sulphate (Barbosa, *et al*., 2010). In organic synthesis, it is used as a drying agent. It is also used a soaking solution to relieve pain in the leg, to relieve minor sprains, bruises, muscle aches or discomfort, joint stiffness or soreness, and tired feet. Used in marine aquariums for calcification process. Magnesium sulphate is used for short-term relief of constipation as a laxative. Magnesium sulphate and its nanoparticles have been applied to enhance lipid production by mixotrophic cultivation of algae using biodiesel waste (Sarma, *et al*., 2014). It was founded that unlike $MgSO_4$, its nanoparticles were found to enhance the lipid production.

2.5.2 Saleable products

2.5.2.1 *$Mg(OH)_2$*

2.5.2.1.1 Introduction

Bine after freeze crystallization is rich in Na_2SO_4 and $MgSO_4$. Na_2SO_4 is removed through cooling due to the low solubility of Na_2SO_4. The separated Na_2SO_4 and $MgSO_4$ can be treated with BaS to form Na_2S and $Mg(OH)_2$, respectively.

2.5.2.1.2 Uses of $Mg(OH)_2$

An attractive alternative to neutralizing mine water is magnesium hydroxide. Due to the high solubility of $MgSO_4$ (260 g/L) only metal hydroxides are precipitated. $Mg(OH)_2$ also can raise the pH to 10, which is enough to do something to iron metals such as manganese and zinc because the pH does not rise enough. Two mechanisms work to neutralize AMD with $Mg(OH)_2$. The first mechanism is the precipitation of metal hydroxide metals. The second mechanism is the absorption of the metal on the surface

of $Mg(OH)_2$ particles. Teringo found that with $Mg(OH)_2$, metals can be removed from solution at one pH unit lower than when NaOH is used (Teringo, 1987). Magnesium hydroxide produces a faster settling rate for metal hydroxide flocs as well as a denser sludge (Marshall & St. Armand, 1992), compared to lime and NaOH. This is because the low solubility of $Mg(OH)_2$ causes the slow release of OH^- ions from the solution, resulting in a gradual increase in pH. This results in the formation of larger metal hydroxide particles and smaller or denser deposits. A study on the application of magnesium hydroxide and barium hydroxide for the removal of metals and sulphate ions from mine water and discovered that sulphate removal was stoichiometrically equivalent to the $Ba(OH)_2$ dosage (Bologo, *et al*., 2012) .

One of the biggest benefits of using MgO is that it effectively removes phosphorus and has no harmful by-products during use, thereby minimizing the impact on the environment. When MgO is applied to the wastewater, it reacts with the solution to form $Mg(OH)_2$. The natural properties of $Mg(OH)_2$ suspensions give them the best performance in wastewater treatment (Schiller, *et al*., 1984). Below is the list of benefits that it possesses:

i. Due to the high alkalinity, the pH level can be easily monitored without the risk of exceeding the maximum allowed limit of 9.

ii. The addition of the suspension to the wastewater rapidly increases the pH, while maintaining optimal conditions for the growth of bacteria for biological treatment.

iii. If heavy metals are present in the effluent, the suspension will deposit the sediment well and remove it from the water.

iv. Suspension is also more effective at removing phosphorus than sodium hydroxide and calcium hydroxide. This feature is useful for dairy farms or dairies.

v. Safe and non-corrosive, easy to handle and safe.

vi. Does not cause scaling problems.

vii. Non-toxic (when used correctly), safe for the environment.

The magnesium hydroxide slurry has been widely utilized for heavy metal precipitation and acid neutralization of industrial wastewater. Many industrial and municipal wastewater facilities are now converting over to magnesium hydroxide for utilization in aerobic and anaerobic biological treatment systems. Other uses of magnesium hydroxide:

i. Antibacterial agent
ii. Paper preservative
iii. Component of membranes
iv. Chemical sensor for ethanol
v. Additive for mechanical reinforcement of starch-based bio nanocomposite

2.5.2.1.3 Properties of $Mg(OH)_2$

Magnesium hydroxide has different properties depending on the source used for production and the combustion conditions. The main parameters used to evaluate the properties of $Mg(OH)_2$ are reactivity, specific surface area (SSA), crystallite size, crystal structure, density, cohesion coefficient (*i.e.,* the ratio of initial particle size to crystal size) and porous structure, total porosity, and morphology (Aphane, *et al*., 2009; Alvarado, *et al*., 2000; Birchal, *et al*., 2000; Liu, *et al*., 2007). It decomposes when heated to 360 °C and forms the oxide, MgO. It is very slightly soluble in water at 0.00122 g/100 mL and has a solubility product of 5.61×10^{-12}. It is a white to off-white crystalline powder with a specific gravity of 2.4 and a Mohs hardness of around 3.0. It loses 30.9% of its mass as water vapor on heating above 450 °C.

2.5.2.1.4 $Mg(OH)_2$ formation

Magnesium Hydroxide, chemically named $Mg(OH)_2$, is an inorganic compound most often distributed in powdered or slurry form. It can be produced using three key methodologies: its natural occurrence as the mineral brucite, through the hydration of magnesium oxide, and through precipitation of seawater or brine.

Brucite as a Natural Source of Magnesium Hydroxide

In 1824, a blue/green-coloured tabular crystal of brucite was discovered in New Jersey (Finch, 1824). Because it is a naturally occurring compound, it needs to be found and

mined, which can be a disincentive something compared to less expensive and more convenient synthetic alternatives. The largest known deposits of brucite ore are located in China and eastern Russia, according to current mineral maps (Zhao, *et al*., 2022). Natural brucite (**Figure 2.12**) is the most uncommon form of magnesium hydroxide. However, brucite ore has numerous advantages over other readily available raw materials, including a lower manufacturing time, zero carbon dioxide content, which can contribute to climate change when released during mineral processing, and a high magnesium content percentage.

Figure 2.12 Brucite (Frost & Kloprogge, 1999)

Synthetic Manufacturing of $Mg(OH)_2$ through Brine or Seawater Precipitation

Precipitating the sample from seawater or brine and lime is a more common method, accounting for approximately 60% of the global supply of $Mg(OH)_2$ (Cipollina, *et al*., 2015). The largest synthetic producers in the world have since perfected this method, which was first used in France in the 19th century: China, Israel, and the US - explicitly California, Michigan, Delaware, and Utah (Wolfe, 1984).

Both seawater and brine must be manually collected, typically in a constructed sump cavern. Seawater can shift in consistency, containing different natural mixtures that can confound the precipitation stage. The chemistry of the rocks and other

geographical formations around a well or lake can also have an impact on the brine's appearance. Before mixing, these initial materials must be purified to ensure the best possible composition.

In addition, the temperature, time, and pressure requirements of this process, which is carried out in a series of agitating reactors and is complemented by washing and filtration, have a significant impact on the quality of the $Mg(OH)_2$ that is produced. In view of these factors, the result requires critical testing to guarantee meeting quality and purity standards (Ashok, *et al*., 2018).

Hydration of MgO to Create $Mg(OH)_2$

The hydration of MgO is the final method for producing $Mg(OH)_2$. This is typically done in an agitation tank to speed up the exothermic (heat-producing) reaction, which must be cooled before continuing (Hornsby & Watson, 1990). Although this is the preferred method for producing the $Mg(OH)_2$ slurry, the final product must be carefully monitored for viscosity, solids content, and particle size. Magnesium oxide is produced when magnesium carbonate ($MgCO_3$) is calcined at high temperatures and loses more than half of its weight to CO_2 (Frontera, *et al*., 2017).

CHAPTER 3: MATERIAL AND METHODS

3.1 INTRODUCTION

In this chapter, the description of study areas, origin of samples and the analytical procedures used for sample preparation and analysis are described. Equipment and instrumentation as well as instrumental parameters, used during thermal studies are included. The full details of all experimental procedures, feedstock and sample preparation are described separately in each of Chapters 4, 5, and 6.

3.2 DESCRIPTION OF SAMPLING AREA

South Africa's coal-energy producers are burdened with a major water quality concern: acid mine drainage (AMD). After a coal mine is abandoned, it often leaches highly acidic water, which then flows into surrounding ecosystems. Coal mining in South Africa is historically mainly centred in the Mpumalanga province, east of the city of Johannesburg. eMalahleni, formerly Witbank, is a coal-rich area located in the Mpumalanga Province, South Africa. It is at the centre of a coal-mining area in which more than 20 collieries operate. The eMalahleni Water Treatment Plant was designed and built to recover potable water from acid mine drainage from several mines in the eMalahleni (Witbank) area.

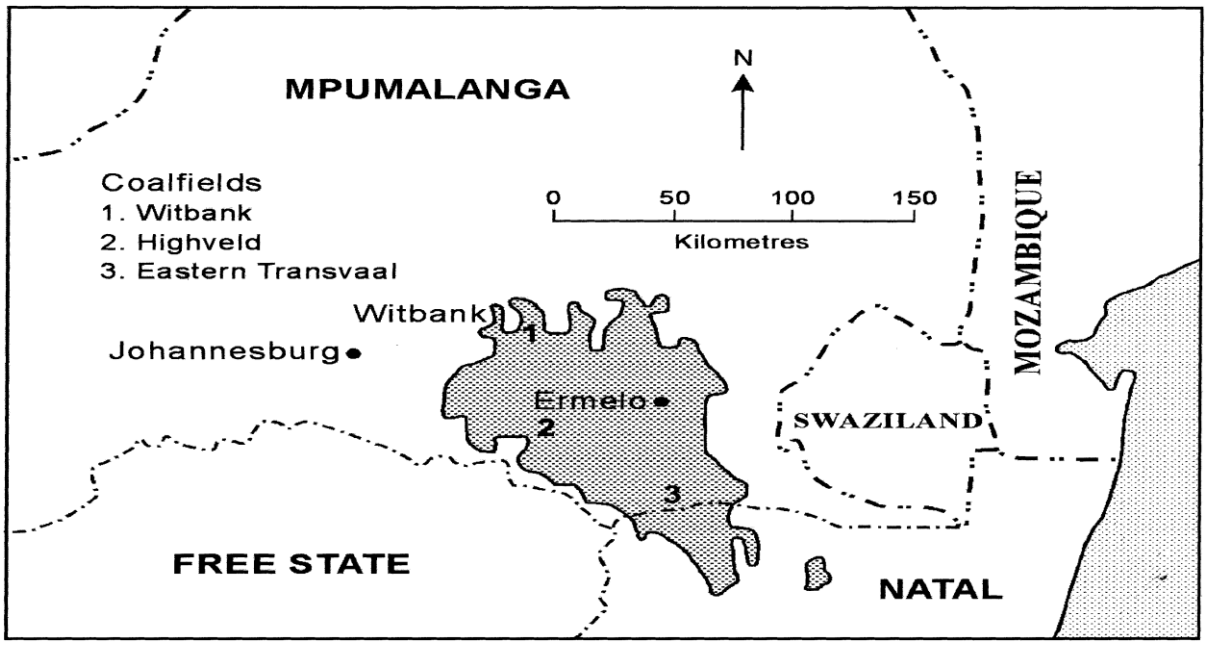

Figure 3.1 Location of the Witbank coal field (Bell *et al*., 2001)

Figure 3.2 shows gypsum at FOSKOR Phalaborwa, which contains REEs and can be converted to $CaCO_3$ via CaS. It is an open cast calcium phosphate rock, located near Phalaborwa. Phalaborwa is a mining town, east of the Drakensberg mountains and north of the Olifants River near Kruger National Park in Limpopo province, South Africa. It is built on top of an old black African mining centre of iron and copper ore; traces of their workings and clay smelting ovens have been found in the nearby granite hills.

Figure 3.2 Gypsum dump near Phalaborwa (Courtesy of JP Maree)

3.3 SAMPLE COLLECTION

PG was collected from a waste gypsum dump of the fertilizer industry (FOSKOR) in Phalaborwa. The AMD samples were collected from a coal mine in Mpumalanga Province, South Africa. Pre-cleaned bottles were used to gather the AMD samples. Before samples were taken, the bottles were carefully cleaned and twice rinsed with

the sample water at the location. Prior to being utilized in REEs recovery experiments, the samples were kept in storage in the lab. Before use, the AMD samples were filtered (Whatman No 1) to eliminate suspended solids.

3.4 FEEDSTOCK

High purity reagents were used throughout this work for preparation of samples. Ultrapure water was used as a for all solutions and dilutions. The glassware used was kept in 10% HNO_3 overnight and subsequently washed several times with deionized water before using.

3.5 APPARATUS AND INSTRUMENTATION

3.5.1 Thermal Studies

A muffle furnace (Carbolite, type s3 fitted with 2AU ESF Eurotherm, England (**Figure 3.3**) was used to thermally reduce $CaSO_4{\cdot}2H_2O$ to CaS and $BaSO_4$ to BaS. After processing the mixture, three samples of the product were be taken for sulphide analysis.

Figure 3.3 Laboratory muffle furnace used in this study (courtesy C P Mokgohloa)

3.5.2 $Na(HCO)_3$ and NaHS formation

The following laboratory set-up was used for monitoring the precipitation of $NaHCO_3$ when Na_2S was reacted with CO_2.

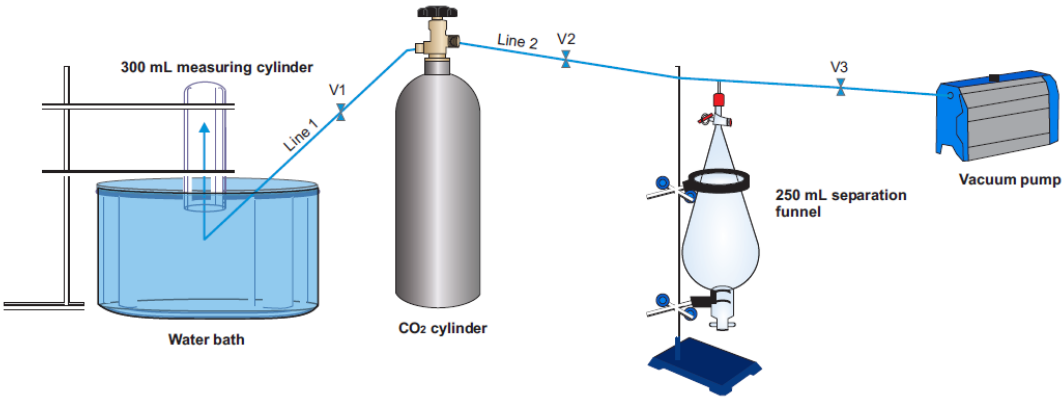

Figure 3.4 Schematic diagram of a laboratory set-up used for monitoring the precipitation of $NaHCO_3$ when Na_2S is reacted with CO_2.

3.5.3 Separation of Na_2SO_4 and NaHS via Freeze crystallization

Batch studies were performed in 1000 mL beakers as a water bath for freeze crystallization. The temperature of the sample was measured using a thermometer (red spirits filled -10 ºC to 150 ºC (1.0 ºC), 300 mm – OMSONS. The freeze crystallization experimental set up is shown in **Figure 3.5**. A portable pH/Electrical Conductivity (EC) meter (HACH HQ4OD, Aqualytic, South Africa) was used to measure pH readings of the samples during the experiments.

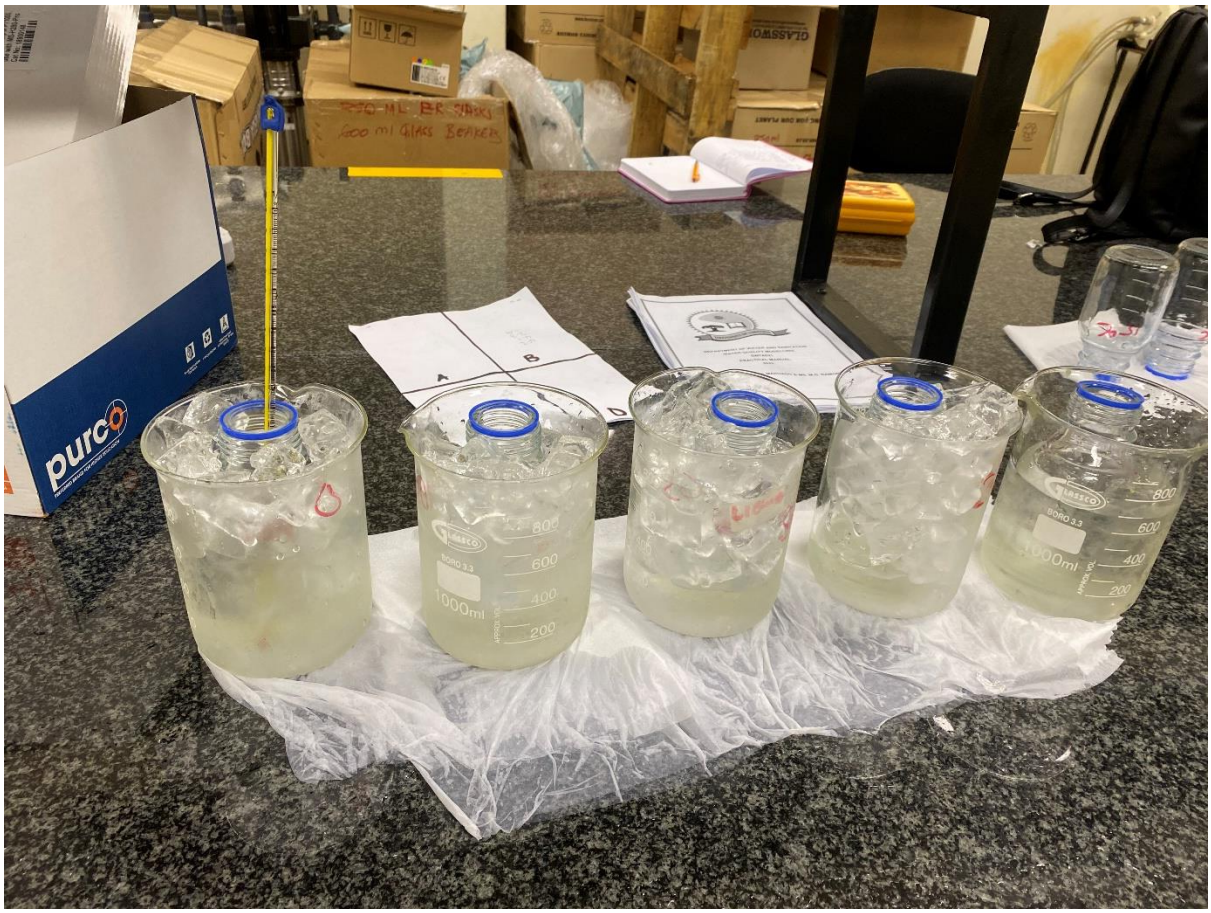

Figure 3.5 Experimental set up for separation of Na_2SO_4 and NaHS (Courtesy C P Mokgohloa)

3.5.4 Leaching agent of REEs in PG

The leaching agent that was used for REEs was 5N HNO_3 due to the following factors:

i. Strong oxidizing agent - Nitric acid is a powerful oxidizing agent. It can readily donate oxygen to react with various minerals and compounds containing REEs. This oxidation reaction helps in breaking down the mineral ores and dissolving the rare earth metals into solution.

ii. Acidic nature - Nitric acid is a strong acid, which means it has a high concentration of hydrogen ions (H^+). The acidic nature of HNO_3 helps in dissolving and solubilizing the rare earth metals by protonating them, forming soluble metal ions. This facilitates the extraction of REEs from the ore.

iii. Formation of soluble nitrates - Nitric acid reacts with rare earth metals to form soluble nitrates. These nitrates can easily dissolve in water and be separated from the insoluble impurities present in the ore. The resulting nitrate solutions can then undergo further processing to isolate and purify the rare earth elements.

iv. Selective leaching - Nitric acid has the advantage of selectively leaching rare earth metals while leaving behind other unwanted minerals and impurities. This selectivity is beneficial in the separation and purification of REEs from complex mineral ores.

3.5.5 Analytical procedure for CaS and BaS

The analysis of the CaS and BaS product from the conversion of gypsum were conducted by iodometry following a method reported by Snell & Hilton. Three representative product samples were taken and each mixed well with Titrisol standard solution. A small portion of each was milled fine with a mortar-and-pestle. Samples (0.5 g) of each were weighed (to 0.1 mg) into three conical flasks. Standard iodine (0.1 M) solution (10 mL) were added by pipette followed by H_2O (100 mL). The mixtures were acidified with 1:1 HCl (2 mL) and swirled to mix and titrated with standard (0.1 M) NaS_2O_3 (starch indicator) to a colourless endpoint. The mean value was calculated from the three results. The CaS and BaS content will be calculated as follows:

$$\%CaS = \frac{[(CV)_{I2} - (CV)_{S2O3}]\ X\ 36}{Sample\ mass\ (mg)} \times 100 \qquad (3.1)$$

v = titration volume (mL) of 0.1 M NaS_2O_3; 10 = 10 mL volume of added 0.1 M Iodine. The finely milled products were also be subjected to SEM for analysis.

3.5.6 Pyrosim Mintek Model

The outcome of the gypsum conversion to CaS was demonstrated by Pyrosim Mintek model which will be linked to the Thermo model. Thermo models were used to predict various properties such as the change of entropy, change of Gibbs free energy and the change in enthalpy. Conditions such as operating temperature, operating pressure, energy losses, were specified with Pyrosim.

3.5.7 OLI simulations and Beaker studies

OLI simulations (OLI ESP software program from OLI Systems, Inc) and beaker studies were used to determine which compound will precipitate out and which compounds/elements will stay in solution.

OLI is an aqueous equilibrium chemistry estimator with an interactive and self-instructive interface for clarifying reactions. It can work with all kinds of common equilibrium reactions, it has a strong solution algorithm, and expressive and easily understandable displays of results, and the ability to produce results in multiple formats according to different uses. The OLI System Chemical Analyser was used to perform single point equilibrium calculations and multiple point survey calculations. The concentration of the various species in solutions or solids were calculated as a function of temperature, pressure, pH, and initial concentrations. The calculations provide liquid- and solid-phase separations for a specialised model.

The OLI Analyser 9.0 System was used to simulate the reactions by running a simulated sample with assumed values of temperature, pressure, and pH. The effect of temperature on the solubility of sodium compounds were determined. Once the input values are used in a calculation by the OLI Systems Chem Analyzer, a calculated summary of the simulated results appears. This could be used to predict the actual reactions that will take place under specific conditions and the final concentration of the various chemical species.

3.6 ANALYTICAL METHODS

3.6.1 Scanning Electron Microscopy

Scanning electron microscopy (SEM) (**Figure 3.6**) has been used worldwide in many disciplines. It can be regarded as an effective method in analysis of organic and inorganic materials on a nanometre (nm) to micrometre (μm) scale. SEM works at a high magnification reaches to 300,000x and even 1000000 (in some modern models) in producing images very precisely of wide range of materials. High Resolution Field Emission Scanning Electron Microscope (HR-FESEM) that can perform Energy-dispersive X-ray spectroscopy (EDS) (the Auriga Cobra FIB-FESEM (Model: Sigma

VP FE-SEM with Oxford EDS Sputtering System, Carl Zeiss, USA) was used to analyse the morphology and elemental properties of samples.

Figure 3.6 Scanning electron microscopy ((Courtesy of C P Mokgohloa)

3.6.2 Inductively coupled plasma ICP) - optical emission spectrometry (OES)

In optical emission spectrometry, the sample is subjected to temperatures high enough to cause not only dissociation into atoms but to cause significant amounts of collisional excitation (and ionization) of the sample atoms to take place. Once the atoms or ions are in their excited states, they can decay to lower states through thermal or radiative (emission) energy transitions. In OES, the intensity of the light emitted at specific wavelength is measured and used to determine the concentrations of the elements of interest. In this current, (ICP OES) (iCAP 7000 Series, ANATECH, South Africa) (**Figure 3.7**) was used to analyse the concentration of Na^+ from freeze crystallization experiments. It was also used to determine the concentration of REEs in AMD, PG, $CaCO_3$ and $Ca(HS)_2$.

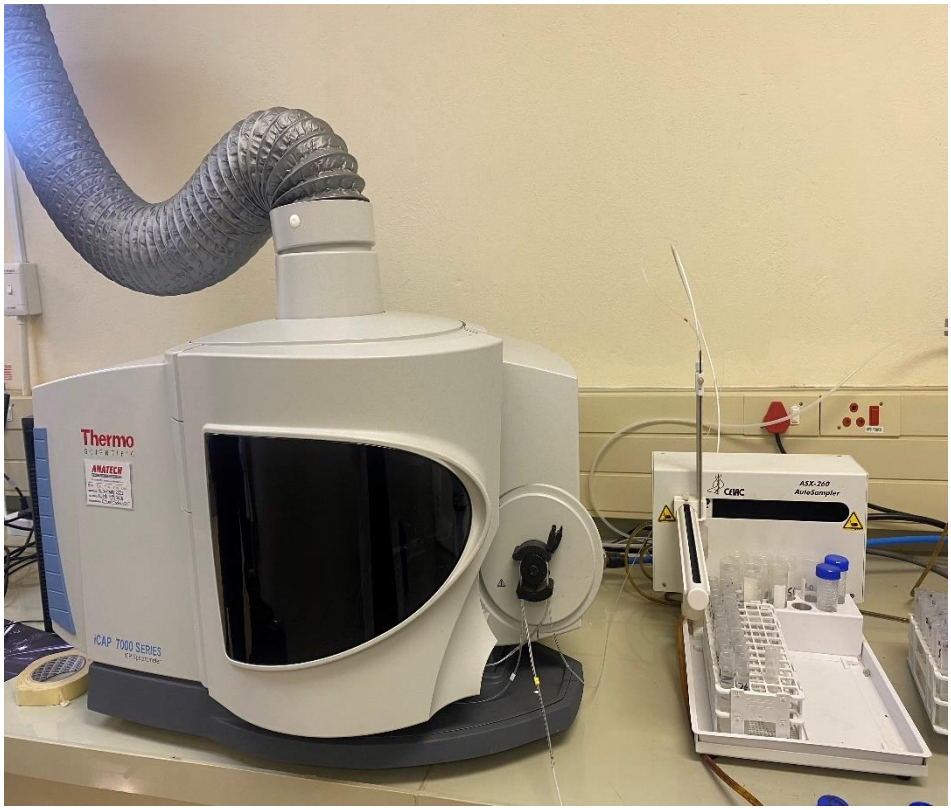

Figure 3.7 Inductively coupled plasma optical emission spectrometry (Courtesy of C P Mokgohloa)

3.6.3 Ion chromatography.

Ion chromatography, also known as ion-exchange chromatography, separates ions and polar compounds according to their affinity for the ion exchanger. Large proteins, tiny nucleotides, and amino acids are all examples of charged molecules that it can function on. In this study, IC (**Figure 3.8**) was used to determine the concentration of SO_4^{2-} in freeze crystallization samples.

Figure 3.8 Ion chromatography (Courtesy of C P Mokgohloa)

3.6.4 Thermal gravimetric analysis

Thermogravimetric Analysis is a method in which the weight of a substance is measured over time or temperature as the sample specimen is exposed to a temperature-controlled atmosphere. TGA is often used to identify specific properties of materials that exhibit either mass loss or gain due to oxidation, decomposition, or volatilization. It was used in this study to show the effect of oxygen on the products, CaS and BaS.

See also Chapters 4,5,and 6 for further information on Materials and Methods

CHAPTER 4: RECOVERY OF Na_2CO_3 AND NANO $CaCO_3$ FROM Na_2SO_4 AND $CaSO_4$ WASTES VIA CaS

Conny P Mokgohloa[1,2], Johannes P Maree[1,3], David S van Vuuren[4], Kwena D Modibane[2], Munyaradzi Mujuru[1], Malose Mokhonoana[2]

Email addresses: connyputjie@gmail.com; johannes.maree@ul.ac.za; dawie.vanvuuren@up.ac.za; kwena.modibane@ul.ac.za; munyaradzi.mujuru@ul.ac.za; malose.mokhonoana@ul.ac.za

[1]Department of Water and Sanitation, University of Limpopo, Private Bag X1106, Sovenga, 0727, South Africa.

[2]Department of Chemistry, University of Limpopo, Private Bag X1106, Sovenga, 0727, South Africa.

[3]ROC Water Technologies, P O Box 70075, Die Wilgers, Pretoria, 0041, South Africa.

[4]Department of Chemical Engineering, Faculty of Engineering, Built Environment and Information Technology, University of Pretoria, Private Bag X20, Hatfield, 0028, South Africa.

Abstract

Sodium sulphate (Na_2SO_4) and/or calcium sulphate are often produced as waste materials by the mining and fertilizer industries. However, valuable products such as Na_2CO_3, nano $CaCO_3$ and NaHS can be recovered from these salts. Sodium carbonate is used for mine water treatment and glass manufacturing with a current price of R4 500/t (US$345/t). $CaCO_3$ is used, among other uses, as a filler in the paper and pharmaceutical industries.

Two new technologies were evaluated to produce Na_2CO_3 from Na_2SO_4. The one technology based on carbothermal reduction of Na_2SO_4 to produce Na_2S as intermediate is inconvenient due to the melting of mixtures of Na_2SO_4 at the reaction temperature. As a result of this complication an alternative technology coined the Sulphide/Carbonate process was proposed. In this process, CaS produced through thermal reduction of gypsum with coal at 1000 °C was used as an intermediate reactant and evaluated to produce Na_2S from Na_2SO_4. Furthermore, it was also

proposed to use CaS to produce nano $CaCO_3$. The Freeze Crystallization process (University of Limpopo) was used for the conversion of Na_2S to $NaHCO_3$ and NaHS.

These developments have completed the search for technological solutions that will result in zero waste during mine water treatment.

4.1 INTRODUCTION

Mine water legislation in South Africa requires the industry to aim for zero effluent to protect surface and groundwater from possible contamination by leachate from solid waste dumps or brine evaporation ponds. According to recent environmental legislation contained in Government Notice 636, Regulation 5 (2013), the hazardous wastes that are discarded on landfill sites should not contain more than 40% water. In South Africa the disposal costs for brine typically amounts to ca R2 500/t; R1 500/t for transportation from the mining site to the waste disposal site and R1 000/t for disposal. These high costs are generally unaffordable for many struggling mines. An attractive solution to offset costs would be the recovery of saleable products from the waste.
The South African fertilizer industry produces approximately 5 000 t/d of waste PG. In addition to the $CaSO_4$, PG from the fertilizer industry contains REEs. Rare earth elements are of strategic value as they are used in applications from battery cells to catalytic converters. Phosphate rock contains up to 1% rare earth oxides present in isomorphous substitutions for Ca^{2+} (Habashi, 1985). A large gypsum-rich waste dump (4 800 000 t) found at Zincor contains lead-silver, iron, and plant effluent residues.

Sulphur dioxide (SO_2) is a significant contributor to smog and acid rain. It originates from the burning of coal, representing about half of yearly worldwide emissions. A further 25-30% of SO_2 comes from the burning of oil. The majority of SO_2 emissions come from South Africa's coal fired electric power generation plants. Emanations must be diminished considering legislative controls. Additionally, sulfur-rich gases such as SO_2 and H_2S are formed in pyro-metallurgical cycles where pyrite, a sulfur containing mineral present in many mined minerals, is oxidized to SO_2 when exposed to higher temperatures under oxidizing conditions and to H_2S when heated in reducing conditions. Numerous smelters in Africa produce extreme emissions of SO_2 which impact on the climate as well as on the country's legal acceptability as exporter of

minerals to Europe and North America. In order to reduce SO_2 emissions, it is typically absorbed and reacted with lime to form gypsum.

In the case of the ROC process, Na_2CO_3 can be recovered from Na_2SO_4. Na_2CO_3 is imported from Botswana at a cost of R6 000/t and South Africa imports about 200 000 t/a. This amounts to R1.2 billion pa. Gypsum can be converted to $CaCO_3$, with a value of R2 000-R4 000/t. If nano $CaCO_3$ is produced, the value can increase to R14 000/t. From both $CaSO_4$ and Na_2SO_4, products such as sulphur, sulphuric acid and sodium bisulphide can be made from the sulphate components.

ROC Water Technologies received financial support from the WRC (Water Research Commission) and the dtic (The Department of Trade, Industry and Competition) for the development of technologies to process the wastes to saleable products. The work is being done in collaboration with the University of Limpopo, University of Pretoria, and Tshwane University of Technology.

Malutsa (Pty) Ltd was responsible for the construction of the so-called Wader demonstration plant. In the Wader Programme, a one m^3/h demonstration plant was constructed to recover drinking water and pigments from iron rich AMD. In the pre-treatment stage, Na_2CO_3 is employed for selective recovery of metals by stepwise raising of the pH. At pH 3.2, only $Fe(OH)_3$ precipitates while the other metal ions, e.g. Al^{3+}, Mg^{2+}, Ca^{2+}, Mg^{2+} K^+, Na^+, remain in solution. At pH 8.5, Mn^{2+} and Ca^{2+} will be precipitated whilst Mg^{2+}, K^+ and Na^+ remain in solution. Removing metals with Na_2CO_3 in the pre-treatment stage, offers the benefit that no gypsum scaling takes place in the following RO stage where clean water of drinking quality is produced and brine with a TDS (total dissolved solids) concentration of 80 g/L results as a waste. This is significantly higher than the 30 g/L that is achieved when lime is used for pre-treatment. The brine from the RO stage is further processed by Freeze Crystallization where $Na_2SO_4.10H_2O$ is recovered through cooling. Na_2SO_4 has a high solubility of 300 g/L at room temperature but only 45 g/L at 0 °C. Through ice crystallization, more water and Na_2SO_4 can be recovered.

The dtic project funding provides support for the processing of the Na_2SO_4 recovered after freeze crystallization, to Na_2CO_3. Much work has been done on the processing of $CaSO_4$ to $CaCO_3$ and $BaSO_4$ to $BaCO_3$ as indicated in Section 2: Literature review. In the case of Na_2SO_4, the conversion to Na_2CO_3 is difficult as the Na_2SO_4, melts in

the same temperature range where the reduction takes place. Another problem is the high reactivity of Na_2S. It adheres to the surface of the material of the crucible. An innovative solution was proposed by Van Vuuren and Maree (2020) to convert Na_2SO_4 to Na_2CO_3 (van Vuuren & Maree, 2020).

In this innovation, Na_2SO_4 was reacted with, $Ca(HS)_2$, or CaS, for the production of NaHS (**Eq. 4.1**). The resultant NaHS was reacted with CO_2 to produce Na_2CO_3 (**Eq. 4.2**). It was also suggested that nano $CaCO_3$ can be produced in a similar way by reacting $Ca(HS)_2$ with Na_2CO_3 (**Eq. 4.3**).

$$Ca(HS)_{2(aq)} + Na_2SO_{4(aq)} \rightarrow CaSO_4 \cdot 2H_2O_{(s)} + 2NaHS_{(aq)} \quad (4.1)$$

$$2NaHS_{(aq)} + H_2O + CO_{2(g)} \rightarrow Na_2CO_{3(aq)} + 2H_2S_{(g)} \quad (4.2)$$

$$Ca(HS)_{2(aq)} + Na_2CO_{3(aq)} \rightarrow CaCO_{3(S)} + 2NaHS_{(aq)} \quad (4.3)$$

The purposes of this present investigation were to demonstrate the technical feasibility of how CaS can be used in the processing of wastes (solid or liquid) to saleable products. Specific objectives included the following:

Processing of:

i. $CaSO_4$ to CaS;
ii. CaS to $Ca(HS)_2$ with CO_2 or H_2S;
iii. Na_2SO_4 to Na_2CO_3, and
iv. $CaSO_4$ to nano $CaCO_3$

4.2 LITERATURE SURVEY

4.2.1 Gypsum

Gypsum is a naturally occurring rock-like mineral used in different industrial applications. Huge amounts of industrial waste gypsum are formed as a by-product when H_2SO_4 rich effluents are neutralized with $Ca(OH)_2$ or $CaCO_3$: *e.g.*, effluents from zinc refineries, copper, coal and gold mines. Another source of by-product gypsum is coal-fired electric power plants with an integrated flue gas desulphurization (FGD) unit. Gypsum is used as a supplement source of Ca and S for plant growth *(Shainberg, et al*., 1989). Gypsum is likewise the most utilized amendment for sodic soil recovery and

for diminishing the unsafe impacts of high-sodium waters on account of its solubility, minimal expense and accessibility (Amezketa, *et al*., 2005). It can also be utilized to lessen run-off rate, increase water infiltration and loss of nutrients (Watts & Dick, 2014).

The concept of zero waste discharge aims to reduce the environmental burden and enhance economic benefit and thus, converting waste gypsum into valuable products such as sulphur and calcium carbonate partially achieves this aim (Nengovhela, *et al*., 2007). However, the large tonnages of waste gypsum create environmental concerns and ultimately health hazards. The main environmental concerns associated with waste gypsum dumps and disposal sites are the releasing of water rich in sulphate into surface and underground water and the generation of airborne dust (Mbhele, et al., 2009).Consequently, it is important to develop methods to process waste gypsum to saleable products such as sulphur and calcium carbonate.

Sulphur can be recovered from waste gypsum by a biological process (Maree, *et al*., 2004) and by catalytic and thermal processes (Rameshni & Santo, 2005). However, these processes are costly, not easy to operate, consume high amounts of fuel and suffer from limited ability to control temperature and the occurrence of side reactions. Calcium sulphate reacts with carbon if it is heated above about 1000 ºC (Arai, 1975) and involves reactions between gases and solids (Lucko, 2003). The basic steps of the sulphur-recovery process from gypsum are:

- Dehydration (**Eq. 4.4**) followed by reduction of calcium sulphate to calcium sulphide using reducing agents such as activated carbon or coal (**Eq. 4.5**), carbon disulphide (**Eq. 4.6**), carbon monoxide (**Eq. 4.7**) or hydrogen (**Eq. 4.8**)

$$CaSO_4 \cdot 2H_2O_{(s)} \rightarrow CaSO_4 \cdot \frac{1}{2}H_2O_{(s)} + 1\frac{1}{2}H_2O_{(g)} \rightarrow CaSO_{4(s)} + 2H_2O_{(g)} \quad (4.4)$$

$$CaSO_{4(s)} + 2C_{(s)} \rightarrow CaS_{(S)} + 2CO_{2(g)} \quad (4.5)$$

$$3CaSO_{4(s)} + 2CO_{2(g)} \rightarrow 3CaS_{(s)} + 2CO_{2(s)} + 4SO_{2(g)} \quad (4.6)$$

$$CaSO_{4(s)} + 4CO_{(g)} \rightarrow CaS_{(s)} + 4CO_{2(g)} \quad (4.7)$$

$$CaSO_{4(s)} + 4H_{2(g)} \rightarrow CaS_{(s)} + 4H_2O_{(g)} \quad (4.8)$$

- CaS, obtained as in **Eqs. 4.4 – 4.8**, suspended in water forms a CaS slurry. From this slurry, the H_2S can be stripped off by passing CO_2 (**Eq. 4.9**) through the suspension followed by conversion of the H_2S to elemental sulphur by reacting it with an aqueous solution of Fe^{3+} at low pH (**Eq. 4.10**).

$$CaS_{(s)} + H_2O_{(l)} + CO_{2(g)} \rightarrow CaCO_{3(s)} + H_2S_{(g)} \quad (4.9)$$

$$H_2S_{(g)} + 2Fe^{3+}_{(aq)} \rightarrow S_{(s)} + 2Fe^{2+}_{(aq)} + H_2 \quad (4.10)$$

4.2.2 Nano $CaCO_3$

Calcium carbonate nanoparticles have attracted interest among recent researchers especially for therapeutic applications. An enormous variety of nano/microparticles has featured and streamlined to expand viability and upgrade the focusing of malignant growth cells. Calcium carbonate is a critical biomaterial controlled by certain properties, *e.g*., morphology, structure, size, explicit surface area and compound purity (Vergaro, *et al*., 2015).

The pH sensitive $CaCO_3$ nanoparticles are believed to be useful as drug delivery systems especially for anti-tumour agents. This is because tumour growth is accompanied by approximately 5-fold elevation in extracellular hydrogen ion concentration and a subsequent pH decrease (Neri & Supuran, 2011).

Other potential biomedical uses of $CaCO_3$ nano-particles include: aragonite-based material with coordinated gentamicin for replacement of bone and counteraction or treatment of osteomyelitis (Lucas-Girot, *et al*., 2005), and for $CaCO_3$ based toothpastes to accomplish the right measure of abrasiveness to tooth-enamel or dentine (Pickles, 2005). In addition, to the transdermal conveyance of insulin into the bloodstream of diabetics.

Nanoparticles of calcium carbonate typically crystallize very rapidly in aqueous solution without any additives. The size of nanoscale calcium carbonate particles is typically 10 - 80 nm. The specific surface areas are in the range 30 - 60 m2/g range with an average particle diameter of <100 nm which can be used as additives to various products.

4.2.2.1 Composition and particle size of $CaCO_3$

Calcium carbonate is a critical material, in industry. It has been utilized as filler material for paints, colours, coatings, paper, and plastics. $CaCO_3$ can be formed by organisms into complex shapes as in bones, shells, teeth, and a cycle known as biomineralization. There are four polymorphs of $CaCO_3$ namely, vaterite, calcite, aragonite, and amorphous calcium carbonate, of which calcite is the most thermodynamically stable form.

Calcite has a high stability index and is being studied in various sizes, shapes and structures (Zhang, *et al*., 2010) and (Guo, *et al*., 2019) and occurs naturally in trigonal crystalline form. The other two polymorphs existing in metastable forms, are vaterite, usually colourless with an hexagonal crystal structure (Xu, *et al*., 2008) and aragonite, also naturally occurring (Zhao, *et al*., 2011).

4.2.3 Na_2CO_3

Sodium carbonate is the third largest mineral product by mass produced in the inorganic chemicals industry. Sodium carbonate occurs as a crystalline decahydrate ($Na_2CO_3 \cdot 10H_2O$), which readily forms the monohydrate ($Na_2CO_3 \cdot H_2O$). It is produced in four types namely, light, medium, granular, and dense, soda ash. This is due to the bulk density, size, and shape of the particles to fit different industrial requirements (DSI, 1995). The light form is more promptly dissolved while the granular form is simpler to deal with mechanical conveying on plants and will in general be favoured. The bulk density of dense soda ash varies from 0.95 t/m^3 to 1.1 t/m^3 and that of light soda ash varies from 0.52 t/m^3 to 0.60 t/m^3 (Wagialla, *et al*., 1992). The glass industry prefers the dense soda ash due to its size of the particle that is amounts equally to that of silica and this results in a homogeneous mixing of raw materials and produces a high-quality product (Backus, 2007).

4.2.3.1 Properties of Na_2CO_3

Sodium carbonate is a stable solid that is hygroscopic. It rapidly dissolves in water to produce weakly acidic carbonic acid, and the strong base, sodium hydroxide. In this manner, a fluid solution of Na_2CO_3 is a strong base. Sodium carbonate reacts intensely with numerous acids. It decomposes to form poisonous disodium oxide (Na_2O) when

exposed to high temperature. In air at 96% relative humidity its mass can increase by 1.5% within 30 min. If Na_2CO_3 is put away under moist conditions, its alkalinity reduces because of absorption of moisture and carbon dioxide from the air. The reaction of water vapour with sodium carbonate above 400 °C produces sodium hydroxide and carbon dioxide. At 25 °C the pH of 1, 5 and 10 wt % solutions are 11.37, 11.58 and 11.70, separately (Eggman, 2001). Above 150 °C, sodium carbonate reacts exothermically with chlorine to form NaCl, CO_2, O_2 and $NaClO_4$.

Notwithstanding the anhydrous sodium carbonate, Na_2CO_3, there are three known hydrates that exist, namely:

i. Sodium carbonate monohydrate, $Na_2CO_3 \cdot H_2O$ has a slightly lower density than the anhydrous sodium carbonate.

ii. Sodium carbonate heptahydrate, $Na_2CO_3 \cdot 7H_2O$ results when seven water molecules per molecule of sodium carbonate are absorbed.

iii. Sodium carbonate decahydrate, $Na_2CO_3 \cdot 10H_2O$ occurs as transparent crystals which readily effloresce when exposed to air.

The physical properties of Na_2CO_3 are summarised in **Table 4.1.**

Table 4.1 Physical properties of Na_2CO_3 (Lewis, 2012)

Chemical formula	**Na_2CO_3**
Molecular mass (g/mol)	105.99
Density at 20ºC (g/cm^3)	2.533
Melting point ºC	851
Heat of formation (J/g)	10.676
Structure	Monoclinic
Heat of solution (J/g)	-222
Specific heat capacity (J/gK)	1.043
Heat of fusion (J/g)	316
Colour	White

4.3 MATERIALS AND METHODS

4.3.1 Chemicals, feedstock, and reagents

The following chemicals were used: Na_2SO_4 (Protea Chemicals), $CaSO_4 \cdot 2H_2O$ (Foskor), activated carbon (MCL), CO_2 gas (Air Liquide, South Africa), 1 M HCl, 0.1 N I_2, 0.1 N $Na_2S_3O_4$, 1M NaOH, 0.1 M Iodine solution and starch solution. All chemicals were of analytical reagent grade. Deionized water was utilised to prepare all solutions.

4.3.2 Equipment

The following equipment was used: A muffle furnace for reduction of $CaSO_4$ to CaS, 500 mL beakers for reaction studies, *BirCraft* agitator, pH and conductivity meter, CO_2 gas supplied at a pressure of 50 kPa.

4.3.3 Experimental and Procedure

4.3.3.1 *Thermal treatment*

Calcium sulphide was produced through the thermal processing of a mixture of $CaSO_4$ and coal at elevated temperatures (1 000 to 1 110 ˚C) in the muffle furnace. The weighed, dry calcium sulphate (20 g) and powdered coal (5 g) were mixed thoroughly, placed in ceramic crucibles for all the reduction experimental trials. Solid samples were collected and analyzed for sulphide content, mass loss, and alkalinity. The retention times for all the reduction experiments were 30 – 60 minutes.

4.3.3.2 *OLI simulations and Beaker studies*

OLI simulations (OLI ESP software program from OLI Systems, Inc) and beaker studies were used to determine which compound will precipitate out and which compounds/elements will stay in solution.

4.3.3.3 *Na_2S formation*

OLI simulations were caried out to determine whether an aqueous solution of Na_2S can be formed by contacting a $Ca(HS)_2$ solution with Na_2SO_4.

4.3.3.4 $Ca(HS)_2$ formation

A 25 g CaS was mixed with 500 mL water and contacted with CO_2 to drop the pH to 9 to form $CaCO_3$(s) and dissolved $Ca(HS)_2$. Samples (10 mL) were collected with a syringe at various pH levels. The solid and liquid fraction of the 10 mL sample were separated by forcing the liquid through a filter attached to the syringe. Both the liquid and solid fractions were analysed for pH, sulphide, and alkalinity.

4.3.3.5 Nano $CaCO_3$ formation

A 100 mL $Ca(HS)_2$ solution was contacted with various dosages of Na_2CO_3. Samples (10 mL) were collected with a syringe at various pH levels. The solid and liquid fraction of the 10 mL sample were separated by forcing the liquid through a filter attached to the syringe. Both the liquid and solid fractions were analysed for pH, sulphide, and alkalinity.

4.3.4 Analysis

Sulphide was determined by standard iodometry (APHA, 2012) as follows: A weighed sample of CaS, mass 50 mg was mixed with 100 mL of deionized water. Standard iodine (0.1 N) solution (10 mL) was added to the mixture. The mixture was acidified with 1 N HCl (2 mL) and titrated with standard (0.1 N) sodium thiosulphate using starch indicator to a colourless endpoint. The % CaS in the reduction mixture was calculated as follows:

$$\%CaS = \frac{[(CV)_{I2} - (CV)_{S2O3}]\ X\ 36}{Sample\ mass\ (mg)} \times 100 \qquad (4.11)$$

4.3.5 OLI software simulations

The OLI System Chemical Analyser program was utilized to predict the behaviour of metals dissolved in water when treated with salts. (OLI, 2015).

4.4 RESULTS AND DISCUSSION

4.4.1 Direct conversion of Na_2SO_4 to Na_2S

Sodium sulphate is not reduced directly with carbon because sodium sulphate has a nearly low melting point of 890 °C and it forms a eutectic mixture with sodium sulphide

that melts at 745 °C at a concentration of 72 mol% sodium sulphate. Mashgwana found that the temperatures that are required for carbothermal reduction reactions are typically in excess of 800 °C (Mashigwana, *et al*., 2022). Therefore, when sodium sulphate is directly reduced with carbon at elevated temperatures, an intermediate molten phase is formed that is difficult to contain and which is very corrosive (Nyman & O'Brien, 1947). A maximum operating temperature of 630 °C was recommended. Roberts studied the reduction of Na_2SO_4 with carbon monoxide at 900 °C (Roberts, 1947). He found that the Na_2S formed, adhered strongly to both ceramic and platinum boats (Roberts, 1947). It will be difficult to find a suitable material of construction for Na_2SO_4 reduction boats or crucibles at elevated temperatures. Feldbaumer *et al*. (1980) have developed an apparatus to reduce sodium sulphate to sodium sulphide including a device that feeds sodium sulphate into the reduction chamber in which the sodium sulphate is exposed to a reducing atmosphere while simultaneously being exposed to high temperature above its melting point (Feldbaumer, *et al*., 1980). This system needed a special procedure to deal with the off gas. The problem of containment of a compound to be reduced was not experienced in the thermal processing of $CaSO_4$ to CaS and $BaSO_4$ to BaS (Tewo, *et al*., 2017; Tewo, 2014; Tewo, *et al*., 2014). The researchers therefore looked at a way to combine the process of $CaSO_4$ reduction with Na_2S production.

4.4.2 $CaSO_4$ reduction

4.4.2.1 *CaS formation*

Tewo *et al*. (2017) studied the reduction of $CaSO_4$ with coal as the reductant and focussed on the following areas: (i) gypsum reduction using coal as reductant (laboratory tube furnace plus Pyrosim modelling studies); (ii) solubilization of calcium sulphide using hydrogen sulphide to form calcium bi-sulphide ($Ca(HS)_2$), and (iii) conversion of $Ca(HS)_2$ to calcium carbonate and hydrogen sulphide (Tewo, *et al*., 2017).

The gypsum reduction experiments focused on the effects of the following process parameters: (i) temperature; (ii) gypsum to coal ratio, and (iii) reaction time.

It was found that 75% - 85% conversions were obtained in the temperature range of 900 – 1200 °C and using a fixed carbon to S ratio of 2.1:1.

Validation of the reduction studies involved the use of the Mintek Pyrosim simulation model using the process parameters derived in the reduction experiments. The validation studies focussed on the effects of temperature and gypsum to coal ratio in the reduction of gypsum to calcium sulphide. Chemical thermodynamic parameters such as variations in entropy, Gibbs free energy and enthalpy were also simulated to provide a better understanding of the nature of the reactions involved. The simulation proved that the process is an endothermic reaction and the following process conditions were found to be required for satisfactory conversions: temperature range, 1 000 – 1 100 °C, and fixed carbon to S mol ratio, 4:1, in agreement with the experimental findings.

The last experimental studies were aimed at establishing suitable process conditions for the chemical processing of CaS to $CaCO_3$ and H_2S. Calcium sulphide was converted under batch conditions to soluble $Ca(HS)_2$ by contacting it with H_2O and H_2S. In the following step, the ($Ca(HS)_2$) was contacted with CO_2 gas to precipitate $CaCO_3$ and to liberate hydrogen sulphide. The following findings were made: (i) CaS has a low solubility of <100 mg/L as CaS; (ii) $Ca(HS)_2$ has a high solubility of >100 g/L as CaS; (iii) $CaCO_3$ with a purity of 60% was produced when the $Ca(HS)_2$ solution was unfiltered and 98% when filtered. The following process conditions were found to be necessary for $CaCO_3$ precipitation: (i) CaS concentrations in the range 100 - 300 g/L; (ii) agitation speed of 125 – 500 rpm. The H_2S feed flowrate had no detectable effect on the dissolution of CaS.

The procedure as described by Tewo *et al*. was used to produce CaS from PG (Tewo, 2014; Tewo, *et al*., 2014; Tewo, *et al*., 2017).

Table 4.2 shows the results when CaS was produced from $CaSO_4.2H_2O$ in triplicate. Two methods were used to determine the conversion: (i) sulphide and (ii) alkalinity. The sulphide value increased to the formation of CaS. Alkalinity can also be measured as $Alk = 2[CO_3^{2-}] + [HCO_3^-] + [OH^-] - [H^+] + 2[S^{2-}] + [HS^-]$. The equation for Alkalinity was modified to make provision for HS^- and S^{2-}. The percentage conversion, X, was calculated as 72.2% by the sulphide method and 77.5% using the alkalinity method, using the following data/approach:

Table 4.2 Determination of $CaSO_4 \cdot 2H_2O$ conversion to CaS via sulphide and alkalinity measurements

Parameter	**Exp No**		
	1.00	2.00	3.00
Reaction time (h)	1.00	1.00	1.00
Furnace	Muffle	Muffle	Muffle
Crucible	25 mL crucible	25 mL crucible	25 mL crucible
Material	Porcelain	Porcelain	Porcelain
Lid	With lid	With lid	With lid
Gypsum (g)	20.00	20.00	20.00
Gypsum ($CaSO_4.2H_2O$) purity (%)	95.00	95.00	95.00
Act carbon (g)	5.58	5.58	5.58
C/$CaSO_4$ ratio	3.79	3.79	3.79
Carbon dioxide blanket	No	No	No
Nitrogen blanket	No	No	No
Coal (% C)	90.00	90.00	90.00
Mol mass $CaSO_4.2H_2O$ g/mol	172.00	172.00	172.00
Mol mass Product, CaS g/mol	72.00	72.00	72.00
$CaSO_4$ + Coal (g)	25.58	25.58	25.58
Temp (°C)	1,100.00	1,100.00	1,100.00
Time (min)	60.00	60.00	60.00
Method 1: Mass loss			
Mass of Reactants to boat (g)	25.58	25.58	25.58
Mass loss (g)	16.93	17.25	16.07
Mass product (g)	8.64	8.20	9.52
CaSO4.2H2O (g)	19.00	19.00	19.00
Carbon Ash (g)	0.56	0.56	0.56
CaS (g)	7.50	9.25	7.66
CaSO4 not reacted (g)	0.10	-3.10	-0.20
Gypsum ash	1.00	1.00	1.00
Carbon reacted (g)	2.50	3.08	2.55
Unreacted carbon (g)	2.52	1.94	2.47
Product measured (g)	8.64	8.20	9.52
Product calc (g)	11.68	6.70	8.02
Converion (%)	94.30	116.28	96.36
Average (%)	101.23		
Standard deviation	4.72		
Method 1: Sulphide			
Mass used for sulphide (g)	0.05	0.05	0.05

CaS in titration (g in 50 mg)	0.0342	0.0353	0.0338
Mass of Product (g)	8.64	8.20	9.52
CaS in product (g)	5.91	5.79	6.44
CaSO4 used (g)	20.00	20.00	20.00
Conversion (%)	70.59	69.11	76.96
Average (%)	72.22		
Standard deviation	3.41		
Method 2: Alkalinity			
Sample from furnace (g)	0.50	0.50	0.50
CaS in 0.5 (g)	0.35	0.37	0.37
Product (g)	8.64	8.20	9.52
CaS in Product (g)	6.10	6.14	6.99
$CaSO_4.2H_2O$ originally (g)	20.00	20.00	20.00
Conversion (%)	72.82	73.34	83.51
Average (%)	76.56		
Standard deviation	4.92		

4.4.2.2 $Ca(HS)_2$ formation

CaS can be partially converted to $Ca(HS)_2$ by contacting it with CO_2 or fully converted by contacting it with H_2S (**Eq. 4.12** and **Eq. 4.13**).

$$2CaS + CO_2 + H_2O \rightarrow CaCO_3 + Ca(HS)_2 \quad (4.12)$$

$$CaS + H_2S \rightarrow Ca(HS)_2 \quad (4.13)$$

See Sections 4.4.1 and 4.4.2.

4.4.3 Na_2CO_3 production

4.4.3.1 Indirect conversion of Na_2SO_4 to Na_2S

The problems associated with the direct conversion of Na_2SO_4 to Na_2S were overcome by reacting Na_2SO_4 with CaS or $Ca(HS)_2$, as proposed by van Vuuren and Maree (van Vuuren & Maree, 2020) and simulated by Mashigwana *et al.* using OLI software (Mashigwana, *et al*., 2022). The production of CaS was achieved through thermal reduction of gypsum mixed with coal at 1000 °C as discussed in Section 4.2.

Table 4.3 and

Table 4.4 showed that Na_2SO_4 can be reacted with either CaS or $Ca(HS)_2$ to form $CaSO_4.2H_2O$ and Na_2S and/or NaHS (**Eq. 4.14** and **Eq. 4.15**) (OLI, 2015).

$$Na_2so_{4(aq)} + CaS + 2H_2O \rightarrow CaSO_4 \cdot 2H_2O_{(s)} + Na_2S_{(aq)} \quad (4.14)$$

$$Na_2so_{4(aq)} + Ca(HS)_{2(aq)} + 2H_2O \rightarrow CaSO_4 \cdot 2H_2O_{(s)} + 2NaHS_{(aq)} \quad (4.15)$$

The reaction with $Ca(HS)_2$ was the preferred option for the following reasons:

- More gypsum was produced when 700 mmol CaS (50.4 g) was reacted with 700 mmol of Na_2SO_4 (74.2 g) in 1 L - 644.2 g/L in the case of $Ca(HS)_2$ versus 519.0 g/L in the case of CaS. This was due to the high pH of above 12 in the case of Na_2S where a portion of the CaS was converted to $Ca(OH)_2$ and $Ca(HS)_2$ (**Eq. 4.16**).
- Sulphide was mainly in the HS^- form while in the case of CaS both HS^- and S^{2-} species were present at pH 12.

$$2CaS + 2H_2O \rightarrow Ca(HS)_2 + Ca(OH)_2 \quad (4.16)$$

This finding as predicted through OLI simulations need to be confirmed through laboratory studies.

Table 4.3 Chemical compositions resulting from Na_2SO_4 being reacted with CaS (OLI, 2015; Mashigwana, *et al*., 2022)

H_2O [mmol] (Y2)	Na_2SO_4 [mmol]	CaS [mmol] (Y2)	$S^{(-2)}$ (aq) [mmol] (Y2)	$Ca(HS)_2$ [mmol] (Y2)	pH	$CaSO_4 \cdot 2H_2O$ (Gypsum)	$Ca(OH)_2$ (Portlandite) -	$Ca^{(+2)}$ (aq) [mmol] (Y2)	$S^{(+6)}$ (aq) [mmol] (Y2)	$Na^{(+1)}$ (aq) [mmol] (Y2)	S^{-2} [mmol] (Y2)	HS^{-1} [mmol] (Y2)	OH^{-1} [mmol] (Y2)	H_2S^{-} (aq) [mmol] (Y2)
55508.2	0	700	700	0	11.9	0.0	152.6	547.4	0.0	0	363.6	336.4	16.0	0.0
55508.2	100	700	700	0	12.0	85.8	161.2	453.0	14.2	200	347.4	352.6	16.1	0.0
55508.2	200	700	700	0	12.0	182.4	169.6	348.0	17.6	400	331.6	368.4	16.5	0.0
55508.2	300	700	700	0	12.1	276.2	173.7	250.2	23.8	600	324.0	376.0	17.7	0.0
55508.2	400	700	700	0	12.1	363.1	170.2	166.7	36.9	800	330.3	369.7	20.2	0.0
55508.2	500	700	700	0	12.2	435.4	157.4	107.2	64.6	1000	353.5	346.5	24.6	0.0
55508.2	600	700	700	0	12.3	486.3	140.0	73.7	113.7	1200	384.3	315.7	30.0	0.0
55508.2	700	700	700	0	12.4	519.0	124.5	56.6	181.0	1400	411.1	288.9	35.2	0.0

Table 4.4 Chemical compositions resulting when Na_2SO_4 was reacted with $Ca(HS)_2$ (OLI, 2015)

H_2O [mmol] (Y2)	Na_2SO_4 [mmol]	CaS [mmol] (Y2)	$S^{(-2)}$ (aq) [mmol] (Y2)	$Ca(HS)_2$ [mmol] (Y2)	Ph	$CaSO_4.2H_2O$ (Gypsum)	$Ca(OH)_2$ (Portlandite)	$Ca^{(+2)}$ (aq) [mmol] (Y2)	$S^{(+6)}$ (aq) [mmol] (Y2)	$Na^{(+1)}$ (aq) [mmol] (Y2)	S^{-2} [mmol] (Y2)	HS^{-1} [mmol] (Y2)	OH^{-1} [mmol] (Y2)	H_2S - (aq) [mmol] (Y2)
55508.2	0	0	1400	700	9.3	0.0	0.0	700.0	0.0	0	4.2	1391.6	0.0	4.3
55508.2	100	0	1400	700	9.3	93.4	0.0	606.6	6.6	200	3.7	1392.4	0.0	3.9
55508.2	200	0	1400	700	9.4	192.5	0.0	507.5	7.5	400	3.4	1393.2	0.0	3.5
55508.2	300	0	1400	700	9.4	291.2	0.0	408.8	8.8	600	3.0	1393.9	0.0	3.1
55508.2	400	0	1400	700	9.4	389.0	0.0	311.0	11.0	800	2.7	1394.5	0.0	2.8
55508.2	500	0	1400	700	9.5	485.1	0.0	214.9	14.9	1000	2.4	1395.1	0.0	2.5
55508.2	600	0	1400	700	9.5	575.5	0.0	124.5	24.5	1200	2.1	1395.7	0.0	2.2
55508.2	700	0	1400	700	9.5	644.2	0.0	55.8	55.8	1400	1.9	1396.1	0.0	2.0

Equations **4.14** and **4.15** were possible due to the high solubility of Na_2SO_4 compared to that of $CaSO_4$ (**Table 4.5**).

Table 4.5 Solubility of chemicals (OLI, 2015)

Compound	**Solubility**		**Temp**
	mmol/L	**g/L**	**°C**
$CaSO_4.2H_2O$	15	2.64	25.0
CaS	186	13	25.0
$NaHCO_3$	1 300	109	25.0
$CaCl_2$	901	100	30.0
$Ca(NO_3)_2$	732	120	30.0
Na_2S	2 540	198	25.0
Na_2SO_4	2 873	408	25.0
$Ca(HS)_2$	A strong function of H_2S partial pressure		
NaHS	88 200	4 939	25.0

Laboratory studies were used to confirm that Na_2SO_4 can be converted to Na_2S by reacting it with CaS (**Eq. 4.14**) or $Ca(HS)_2$ (**Eq. 4.15**). $Ca(HS)_2$ it was produced by reacting CaS with CO_2 according to **Eq 4.12**. CO_2 was added during the course of the experiment to control the pH at 7.9. This resulted in the removal of 50% of the alkalinity due to the precipitation of $CaCO_3$.

As CaS has a limited solubility, as shown in **Table 4.5**, the effect of CaS concentration was investigated. The CaS section in **Table 4.6** shows that the soluble fraction of sulphide decreased from 97.8% to 52.3% as the CaS concentration increase from 25 g/L to 100 g/L. It is concluded that CaS can be used for Na_2S formation provided that the concentration is kept below 25 g/L. The Alkalinity in solution (expressed as CaS) was much lower than that of sulphide. In Run 1.1, for example, the Alk in solution after 180 min was 990 mg/L (as CaS), compared to 2 610 mg/L sulphide (as CaS). This difference can be ascribed to the formation of $Ca(OH)_2$(s) as shown with OLI (**Table 4.4**). **Equation 4.17** shows a possible reaction to produce the products in the ratio as predicted by OLI.

$$24CaS + 24Na_2SO_4 + 10H_2O \rightarrow 18CaSO_{4(s)} + 4Ca(OH)_{2(s)} + 6Na_2SO_{4(aq)} + Ca(OH)_{2(aq)} + Ca(HS)_{2(aq)} + 14Na_2S_{(aq)} + 8NaHS_{(aq)} \quad (4.17)$$

The following approach was followed with **Table 4.6**:

- 125 mL solution containing 3.1, 6.3 and 12.5 g 92% CaS
- The equivalent dosage of Na_2SO_4 was added to precipitate Ca^{2+} as $CaSO_4 \cdot 2H_2O$ after 20,60, and180 min reaction time.
- pH and sulphide (as CaS) were measured on filtered samples.
- At a low concentration of 25 g/L CaS, 100% of the initial CaS was in solution, compared to 74% for 50 g/L CaS and 56% for 100 g/L.

Table 4.6 Effect of CaS concentration on the soluble sulphide fraction

Parameter	**CaS**			**$Ca(HS)_2$**		
Run	**1.1**	**1.2**	**1.3**	**2.1**	**2.2**	**2.3**
CaS 92% (g/L)	25.0	50.0	100.0	25.0	50.0	100.0
CO_2 to pH 7.9	No	No	No	Yes	Yes	Yes
Conditions						
H_2O (mL)	125.0	125.0	125.0	125.0	125.0	125.0
CaS (92%) (g)	3.1	6.3	12.5	3.1	6.3	12.5
CaS in 125 mL (92%) (mg)	3 125	6 250	12 500	3 125	6 250	12 500
CaS (%)	92.0	92.0	92.0	92.0	92.0	92.0
				initially	Initially	Every time
Na_2SO_4/CaS mole ratio	1.0	1.0	1.0	1.0	1.0	1.0
Na_2SO_4 (g)	5.7	11.3	22.7	5.7	11.3	22.7
Results						
Time (min)	Ph			Ph		
0.0	11.4	11.9	12.2	7.9	7.9	7.9
20.0	11.7	12.1	12.2	11.6	11.1	7.9
60.0	12.2	12.4	12.5	12.1	11.6	7.9
180.0	12.4	12.5	12.6	12.3	11.9	7.9
Time (min)	CaS (mg in 125 mL)			CaS (mg in 125 mL)		
0.0	2 880	4 590	6 150	2 790	5 580	8 400
20.0	3 060	4 320	6 300	2 610	5 220	8 100
60.0	2 700	4 230	5 925	2 700	4 950	7 650
180.0	2 610	4 050	5 700	2 520	5 040	7 800
Average	2 813	4 298	6 019	2 655	5 198	7 988
%	97.8	74.7	52.3	92.3	90.4	69.5

Time (min)	Alkalinity (mg CaS in 125 mL)			Alkalinity (mg CaS in 125 mL)		
0.0	540	360	1 080	1 710	2 880	2 340
20.0	720	675	1 215	2 070	3 240	2 610
60.0	810	720	1 350	2 430	3 510	2 520
180.0	990	900	1 620	2 790	3 690	3 150

A second experiment was carried out where Na_2SO_4 was reacted with $Ca(HS)_2$ **(Eq. 4.14)** and not with CaS (**Eq. 4.15**). **Table 4.6** shows that the soluble fraction of sulphide was significantly higher when compared with the corresponding concentrations of the CaS section, which can be ascribed to the high solubility of $Ca(HS)_2$. The Alkalinity in solution (expressed as CaS) was lower than that of sulphide. This was due to the way in which $Ca(HS)_2$ was prepared as described above. $CaCO_3$ precipitated when CaS was reacted with CO_2 (**Eq. 4.12**).

4.4.3.2 $NaHCO_3$ formation

$NaHCO_3$ can be formed by reacting Na_2S, or NaHS, with water and CO_2.

$$Na_2S + H_2O + CO_2 \rightarrow NaHCO_3 + NaHS \quad (4.18)$$

$$NaHS + CO_2 + H_2O \rightarrow NaHCO_3 + H_2S \quad (4.19)$$

NaHS is a valuable product that is used in the tanning industry for hair removal and by the metallurgical industry as a flotation agent. H_2S can be used as raw material for sulphuric acid production.

4.4.3.3 $NaHCO_3$ and NaHS separation

Mashigwana showed that $NaHCO_3$ and NaHS can be separated due to the low solubility of $NaHCO_3$ (109.6 g/L, 20ºC) compared to the high solubility of NaHS (4 939 g/L, 20ºC) (**Table 4.7**) (Mashigwana, *et al*., 2022). He showed the effect when 12 000 mmol CO_2 was added in increments to a solution of 1 000 mL water containing 3 000 mmol Na_2S. The following observations were made:

- With a CO_2 dosage of 0 to 1 500 mmol, the pH dropped from 14 down to 10 as 3 000 mmol Na_2S dissolved to produce 3000 mmol $S^{2-}(aq)$ and 6000 $Na^{+}(aq)$ (Phase 1) (**Eq. 4.20**)

- A further CO_2 dosage from 1 500 to 3 000 mmol resulted in the precipitation of 2 663 mmol $NaHCO_3$ (Phase 2), S^{2-} remained constant at 3 000 mmol as all the S^{2-} dissolved during Phase 2 **(Eq. 4.21)**.
- A further CO_2 dosage from 3000 to 6000 mmol (Phase 3) resulted in the precipitation of more $NaHCO_3$ (up to 4 884 and the stripping of 2 390 mmol H_2S due to excess CO_2 (**Eq. 4.22**).
- Further dosage of CO_2 resulted in dilution of the H_2S in the vapour with less H_2S remaining in the solution.

$$Na_2S_{(S)} + CO_2 + H_2O \rightarrow NaHCO_{3(aq)} + NaHS_{(aq)} \quad (4.20)$$

$$Na_2S_{(aq)} + CO_2 + H_2O \rightarrow NaHCO_{3(s)} + NaHS_{(aq)} \quad (4.21)$$

$$NaHS_{(aq)} + CO_2 + H_2O \rightarrow NaHCO_{3(s)} + H_2S_{(g)} \quad (4.22)$$

4.4.3.4 *Na_2CO_3 formation*

Sodium hydrogen carbonate decomposes to sodium carbonate, carbon dioxide and water (**Eq 4.23**) when heated in a rotating drum oven at 450 ºK.

$$2\mathrm{NaHCO_3} \rightarrow \mathrm{Na_2CO_3} + \mathrm{CO_2} + \mathrm{H_2O} \quad (4.23)$$

4.4.3.5 *Up-concentration of NaHS (Freeze Crystallization)*

After removal of $NaHCO_3$ as a solid, NaHS remained in solution (Mashigwana, *et al*., 2022). After removal of $NaHCO_3$ with CO_2 addition, the NaSH had a concentration of 188 g/L (3.37 mol/L). This solution can be concentrated to be sold as a commercial product. NaHS should not be concentrated beyond 188 g/L (as NaHS), to avoid the decomposition of the NaHS into H_2S.

Figure 4.1 shows that when 1 000 mL of water (55 508 mmol) was reduced down to 150 mL (8 117 mmol) by freeze crystallization, the NaHS concentration in solution increased from 188 g/L to 1 180 g/L (21 100 mmol/L). The $NaHCO_3$ concentration would have increased to the same extent if the $NaHCO_3$ was not removed as a solid prior to water removal through freeze crystallization.

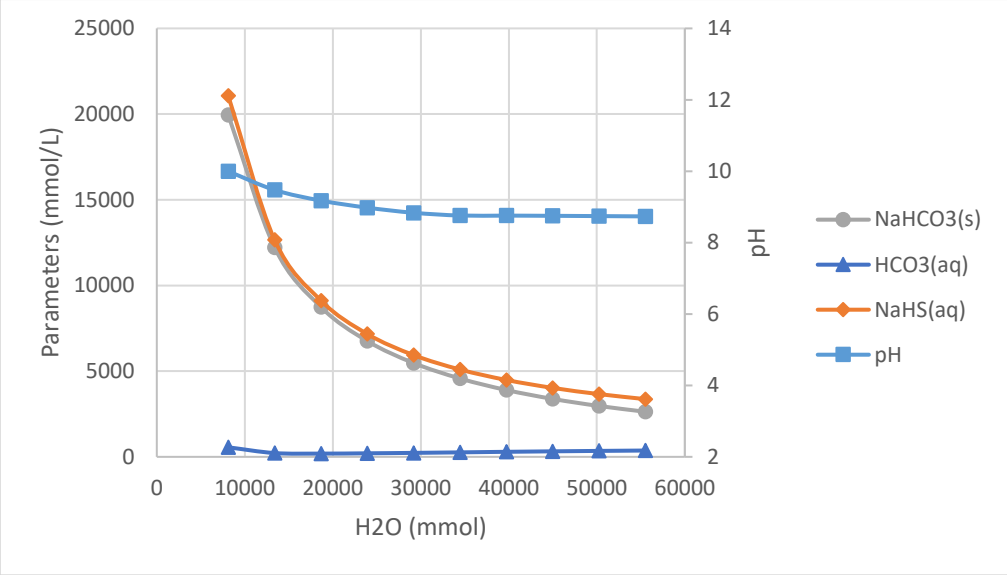

Figure 4.1 Concentration of NaHS by freeze crystallization (Mashigwana, *et al*., 2022)

4.4.4 $CaCO_3$ formation

4.4.4.1 Crude and pure $CaCO_3$ and $Ca(HS)_2$ formation

CaS can be converted to $Ca(HS)_2$ by contacting it with either CO_2 or H_2S (**Eq. 4.24** and **Eq. 4.25**).

$$2CaS + CO_2 + H_2O \rightarrow CaCO_{3(s)} + Ca(HS)_{2(aq)} \quad (4.24)$$

$$CaS + H_2S + \rightarrow Ca(HS)_{2(aq)} \quad (4.25)$$

$$Ca(HS)_2 + 2CO_2 + 2H_2O \rightarrow Ca(HCO_3)_2 + 2H_2S \quad (4.26)$$

$$Ca(HCO_3)_2 + air \rightarrow CaCO_3 + CO_2 + H_2O \quad (4.27)$$

De Beer *at al.* showed that low-grade carbonate products (i.e. <90% by mass as $CaCO_3$) can be recovered from waste gypsum through thermal reduction to calcium sulphide, followed by direct aqueous carbonation (**Eq. 4.24**) (de Beer, et al., 2014; de Beer, 2014).

After studying the production of low grade $CaCO_3$, de Beer *et al*. did a follow-up study where they developed an indirect aqueous CaS carbonation process for the production of high-grade $CaCO_3$ (i.e. >99% by mass, as $CaCO_3$) or precipitated calcium carbonate (PCC) (de Beer, *et al*., 2015; de Beer, 2014; de Beer, *et al*., 2014). The process used an acid gas (H_2S) to form soluble $Ca(HS)_2$ (**Eq. 4.25**). After filtration,

pure $CaCO_3$ can be allowed to precipitate from $Ca(HS)_2$ after dosing of CO_2 that results in removal of H_2S (**Eq. 4.26**). After CO_2 stripping with air, pure $CaCO_3$ crystallize (**Eq. 4.27**). Calcite was the only $CaCO_3$ polymorph obtained; no vaterite or aragonite were detected. The carbonate product was primarily calcite (99.5%) with traces of quartz (0.5%). The product was made up of micron-size particles, which were further characterised by XRD, TGA, SEM, BET and true density. Results showed that about 0.37 ton of high-grade PCC could be produced from 1.0 ton of waste gypsum whilst generating ca 0.19 ton of residue, representing a reduction of 80 % by mass of the original waste gypsum. The residue needs to be discarded.

- **Table 4.8** and **Table 4.9** show the calculated chemical compositions when CO_2 and H_2S were added respectively to 350 mmol/L (25.2 g/L) CaS to lower the pH stepwise (OLI, 2015). In Table 4.8, 350 mmol CO_2 was added to 350 mol CaS and 1 L water (55 508 mmol). In Table 4.9, 350 mmol H_2S was added to 350 mol CaS and 1 L water. The columns S^{-2} Aq (**Table 4.8 and Table 4.9**) are the sums of the next three columns showing the sulphur species in solution: S^{2-}, HS^- and H_2S, respectively.

The Tables showed the following:

- Total S^{2-} remained at 350 mmol **Table 4.8** while it increased to 700 mmol when 350 mmol H_2S was added (**Table 4.9**).
- When 175 mmol CO_2 was added, the pH dropped to about 9.5 and about 50% of the calcium precipitated as $CaCO_3$. When 350 mmol was added the pH dropped to 6.45 and 95% of the calcium precipitated as $CaCO_3$
- In the case of H_2S, Ca^{2+} remained in solution because of the production of soluble $Ca(HS)_2$.
- H_2S was only stripped off at the end of the CO_2 addition. All H_2S remained in solution as $Ca(HS)_2$. This offered the benefit that the solution could be purified by a filtration step. When CO_2 is added subsequently, ultra-pure $CaCO_3$ will be precipitated.
- The concentrations of the remaining species had relatively low values.

Table 4.7 Behaviour of various parameters when CO_2 is added stepwise to Na_2S(aq) (OLI, 2015)

CO_2 [mmol]	pH	Na_2S [mmol]	H_2O [mmol]	Temperature [°C]	$S(^{-2})$ Aq [mmol]	$NaHCO_3$ (Nahcolite) - Sol [mmol]	Na_2S·9H2O - sol [mmol]	$Na(^{+1})$ Aq [mmol]	H_2S - Vap [mmol]	H_2O - Vap [mmol]	H_2O [mmol]	CO_2 - Vap [mmol]
-	14.10	3 000	55 508	0	904	-	2 096	1 809	-	-	36 564	-
600	12.86	3 000	55 508	0	1 761	-	1 239	2 665	-	-	39 471	-
1 200	12.50	3 000	55 508	0	2 790	-	210	3 617	-	-	42 601	-
1 800	9.73	3 000	55 508	0	3 000	384	0	3 753	-	-	44 395	-
2 400	9.71	3 000	55 508	0	3 000	1 535	0	3 849	-	-	50 025	-
3 000	8.74	3 000	55 508	0	3 000	2 663	0	3 337	-	-	52 508	-
3 600	8.36	3 000	55 508	0	2 467	3 236	0	2 764	532.96	3	51 913	7
4 200	8.23	3 000	55 508	0	1 903	3 771	0	2 229	1 096.78	6	51 327	25
4 800	8.07	3 000	55 508	0	1 371	4 260	0	1 740	1 629.45	10	50 773	73
5 400	7.90	3 000	55 508	0	918	4 649	0	1 351	2 081.68	14	50 305	205
6 000	7.73	3 000	55 508	0	612	4 884	0	1 116	2 387.54	17	49 994	493
6 600	7.61	3000	55 508	0	440	4 999	0	1001	2 559.82	21	49 825	922
7 200	7.53	3000	55 508	0	341	5 056	0	944	2 658.62	25	49 732	1 427
7 800	7.48	3000	55 508	0	279	5 088	0	912	2 720.88	28	49 675	1 969
8 400	7.44	3000	55 508	0	236	5 109	0	891	2 763.51	32	49 637	2 531
9 000	7.41	3000	55 508	0	205	5 122	0	878	2 794.57	36	49 608	3 103
9 600	7.39	3000	55 508	0	182	5 132	0	868	2 818.25	39	49 587	3 683
10 200	7.37	3000	55 508	0	163	5 140	0	860	2 836.92	43	49 569	4 267
10 800	7.35	3000	55 508	0	148	5 146	0	854	2 852.04	47	49 555	4 854
11 400	7.34	3000	55 508	0	135	5 150	0	850	2 864.55	50	49 543	5 444
12 000	7.33	3000	55 508	0	125	5 154	0	846	2 875.08	54	49 532	6 035

Table 4.8 Chemical compositions when **CO_2** was added stepwise to 350 mmol/L (25.2 g/L) CaS (OLI, 2015)

H2S [mmol]	CO2 [mmol] (Y2)	CaS [mmol] (Y2)	S(-2) Total [mmol] (Y2)	H2O [mmol] (Y2)	H2O [mmol] (Y2)	Temperature [°C] (Y2)	pH	Ca(+2) Aq [mmol] (Y2)	CaCO3 (Calcite) - Sol [mmol] (Y2)	Ca(OH)2 (Portlandite) - Sol [mmol] (Y2)	S(-2) Aq [mmol] (Y2)	S-2 [mmol] (Y2)	HS-1 [mmol] (Y2)	H2S - Aq [mmol] (Y2)	S(-2) Vap [mmol] (Y2)	OH-1 [mmol] (Y2)	HCO3-1 [mmol] (Y2)	Ca(HS)2 [mmol] (Y2)	CO3-2 [mmol] (Y2)	C(+4) Vap [mmol] (Y2)	C(+4) Aq [mmol] (Y2)
-	-	350.00	350.00	55 508.25	55 318.06	25.00	12.01	269.27	-	80.73	350.00	159.82	190.18	0.00	-	17.52	-	-	-	-	-
-	35.00	350.00	350.00	55 508.25	55 353.05	25.00	12.01	269.29	34.98	45.73	350.00	159.80	190.20	0.00	-	17.53	0.00	-	0.00	-	0.02
-	70.00	350.00	350.00	55 508.25	55 388.04	25.00	12.01	269.29	69.98	10.73	350.00	159.79	190.21	0.00	-	17.54	0.00	-	0.00	-	0.02
-	105.00	350.00	350.00	55 508.25	55 384.30	25.00	11.83	245.02	104.98	-	350.00	121.06	228.94	0.00	-	11.50	0.00	-	0.00	-	0.02
-	140.00	350.00	350.00	55 508.25	55 359.96	25.00	11.48	210.02	139.98	-	350.00	61.72	288.28	0.01	-	4.98	0.00	-	0.00	-	0.02
-	175.00	350.00	350.00	55 508.25	55 333.16	25.00	9.50	175.02	174.98	-	350.00	0.69	348.54	0.77	-	0.05	0.00	-	0.00	-	0.02
-	210.00	350.00	350.00	55 508.25	55 298.25	25.00	7.45	140.14	209.86	-	350.00	0.00	280.11	69.88	-	0.00	0.08	-	0.00	-	0.14
-	245.00	350.00	350.00	55 508.25	55 261.81	25.00	7.21	105.28	244.72	-	304.70	0.00	210.30	94.40	45.30	0.00	0.18	-	0.00	0.02	0.26
-	280.00	350.00	350.00	55 508.25	55 224.74	25.00	7.03	70.64	279.36	-	236.47	0.00	140.83	95.65	113.53	0.00	0.33	-	0.00	0.17	0.47
-	315.00	350.00	350.00	55 508.25	55 188.94	25.00	6.77	37.64	312.36	-	170.59	0.00	74.24	96.35	179.41	0.00	0.88	-	0.00	1.37	1.27
-	350.00	350.00	350.00	55 508.25	55 165.28	25.00	6.45	17.97	332.03	-	125.26	0.00	32.78	92.47	224.74	0.00	2.86	-	0.00	13.06	4.91

Table 4.9 Chemical composition when **H_2S** was added stepwise to 350 mmol/L (25.2 g/L) CaS (OLI, 2015)

H2S [mmol]	CO2 [mmol] (Y2)	CaS [mmol] (Y2)	S(-2) Total [mmol] (Y2)	H2O [mmol] (Y2)	H2O [mmol] (Y2)	Temperature [°C] (Y2)	pH	Ca(+2) Aq [mmol] (Y2)	CaCO3 (Calcite) - Sol [mmol] (Y2)	Ca(OH)2 (Portlandite) - Sol [mmol] (Y2)	S(-2) Aq [mmol] (Y2)	S-2 [mmol] (Y2)	HS-1 [mmol] (Y2)	H2S - Aq [mmol] (Y2)	S(-2) Vap [mmol] (Y2)	OH-1 [mmol] (Y2)	HCO3-1 [mmol] (Y2)	Ca(HS)2 [mmol] (Y2)	CO3-2 [mmol] (Y2)	C(+4) Vap [mmol] (Y2)	C(+4) Aq [mmol] (Y2)
-	-	350.00	350.00	55 508.25	55 318	25.00	12.01	269.27	-	80.73	350.00	159.82	190.18	0.00	-	17.52	-	-	-	-	-
35.00	-	350.00	385.00	55 508.25	55 371	25.00	12.00	296.06	-	53.94	385.00	178.13	206.87	0.00	-	17.30	-	-	-	-	-
70.00	-	350.00	420.00	55 508.25	55 425	25.00	11.99	323.07	-	26.93	420.00	196.86	223.14	0.00	-	17.10	-	-	-	-	-
105.00	-	350.00	455.00	55 508.25	55 479	25.00	11.97	350.00	-	-	455.00	215.54	239.46	0.00	-	16.87	-	-	-	-	-
140.00	-	350.00	490.00	55 508.25	55 487	25.00	11.82	350.00	-	-	490.00	188.81	301.19	0.00	-	11.79	-	-	-	-	-
175.00	-	350.00	525.00	55 508.25	55 493	25.00	11.67	350.00	-	-	525.00	159.70	365.30	0.01	-	8.26	-	-	-	-	-
210.00	-	350.00	560.00	55 508.25	55 497	25.00	11.51	350.00	-	-	560.00	129.11	430.88	0.01	-	5.70	-	-	-	-	-
245.00	-	350.00	595.00	55 508.25	55 501	25.00	11.33	350.00	-	-	595.00	97.59	497.40	0.02	-	3.75	-	-	-	-	-
280.00	-	350.00	630.00	55 508.25	55 504	25.00	11.11	350.00	-	-	630.00	65.45	564.52	0.03	-	2.23	-	-	-	-	-
315.00	-	350.00	665.00	55 508.25	55 506	25.00	10.76	350.00	-	-	665.00	32.92	632.01	0.07	-	1.01	-	-	-	-	-
350.00	-	350.00	700.00	55 508.25	55 508	25.00	9.43	350.00	-	-	700.00	1.65	696.60	1.75	-	0.05	-	-	-	-	-

The results reported in **Table 4.8,** where OLI software was used to predict the behaviour when CaS is reacted with CO_2. The results reported in **Table 4.10,** where OLI software was used to predict the behaviour when CaS is reacted with H_2S. It showed that $CaCO_3$ precipitated while $Ca(HS)_2$ remained in solution. This behaviour was confirmed experimentally (**Table 4.10**). The formation of $CaCO_3$ and $Ca(HS)_2$ were monitored experimentally by adding CO_2 stepwise to a 25 g CaS in 500 mL H_2O mixture. The liquid fraction was separated from the solid fraction using a syringe equipped with a filter. It showed that the Total Sulphide remained in the liquid fraction (96.5%) while $CaCO_3$ was in the solid fraction (96.4%).

Table 4.10 Separation of $Ca(HS)_2$ and $CaCO_3$ separation by CO_2 addition

	Original	Liquid		Solid	
Ph		Sulphide	Alkalinity*	Sulphide	Alkali
	mg CaS	mg CaS	mg CaS	mg CaS	As mg CaS
	17 775.0				
10.1		18 000	1 469	180	16 157
9.1		16 920	1 322	360	17 332
8.1		16 560	1 102	432	17 919
		%	%	%	%
10.1	17 775.0	101.3	8.3	1.0	90.9
9.1		95.2	7.4	2.0	97.5
8.1		93.2	6.2	2.4	100.8
Average		96.5	7.3	1.8	96.4

25 g CaS, 71.1% = 17 755 mg 100% CaS

pH was adjusted with CO_2 to reported pH values

*Alkalinity is normally expressed as mg/L $CaCO_3$. In this case it was expressed as CaS in order to make a direct comparison between Sulphide concentration and Alkalinity concentration.

4.4.4.2 *Nano $CaCO_3$ formation*

$$Ca(HS)_2 + Na_2CO_3 \rightarrow nano\ CaCO_3 \qquad 4.28$$

Nano $CaCO_3$ is normally produced by reacting a concentrated solution of $CaCl_2$ or $Ca(NO_3)_2$ with a concentrated solution of Na_2CO_3. Since relatively concentrated aqueous solutions of

$Ca(HS)_2$ can be produced from CaS produced from waste gypsum, the latter will be an attractive alternative raw material.

The aim with this Section is to identify conditions needed to produce nano $CaCO_3$. In Section 4.3 it was shown that $CaCO_3$ is produced when CO_2 was added to CaS. The $CaCO_3$ produced this way would form at a much slower rate than when highly soluble Na_2CO_3 is mixed with CaS or $Ca(HS)_2$. **Table 4.11** shows that the pH rised from 10.6 to 11.5 when Na_2CO_3 was added to CaS. It showed that 87.1% of the sulphide remained in the liquid fraction. The alkali concentration in the liquid was only 14.7% of the original CaS mass. This finding was confirmed by the high $CaCO_3$ mass in the solid fraction. This $CaCO_3$ will meet nano $CaCO_3$ standards and will be subjected to particle size analyses.

Table 4.11 Recovery of $CaCO_3$ from $Ca(HS)_2$ and Na_2CO_3 with syringe filter

	Original		Liquid fraction			Solid fraction	
pH			Sulphide	Alkali	Alk precipitated	Sulphide	Alkali
	mg CaS in 100 mL	Na_2CO_3 added (mg as CaS)	mg CaS in 100 mL	mg as CaS in solution	$CaCO_3$ (as CaS)	mg CaS	mg CaS
10.6	3 555	0.0	3096	497.0		14.4000	-1 102
11.0	3 555	679.0	3073	507.0	172.0	3.6000	1 836
11.5	3 555	2717	3125	566.0	2151	-3.6000	3 305
			%	%		%	%
10.6			**87.10**	14.0		0.4100	
11.0			86.40	14.3		0.1000	
11.5			87.90	15.9		-0.1000	
Average			87.10	14.7		0.1000	

4.4.5 Morphological characteristics of products

4.4.5.1 $CaCO_3$

Figure 4.2 shows the SEM micrographs of $CaCO_3$ produced from contacting CaS with CO_2 at an initial pH 12.4 down to 7.0 at a stirring of 500 min^{-1} (CaS slurry containing 50 g/ℓ). It reveals that the detailed morphology of $CaCO_3$ products is a well-defined large particle of a flower-like calcite with diameters in the range of 0.2 µm to 0.6 µm. A close-up view of the flower-like nanostructures in **Figure 4.2c** demonstrates the “petals” are about 3.1 µm in

length (**Figure 4.3**), and they regularly contacted with each other into flower-like structures. The flower “petals” grow out of opposite sides to show a small hole feature of 1.4 µm in diameter. There was also an appearance of irregular morphology surrounding the flower where some crystal planes had smooth surfaces, while other planes had a rough structure. This may be due to the disadvantage of CO_2 bubbling process, *i.e.*, is the limited controlling on the supersaturation and Ca^{2+}/CO_3^{2-} ratio (Kralj, *et al.*, 2008). The complexity of the raw materials has significant impacts on the crystal morphology and microstructure of carbonated materials. For example, the presence of impurities, *i.e.*, $CaSO_4$ and C in the raw materials of CaS may impact the crystallization of $CaCO_3$ during carbonation.

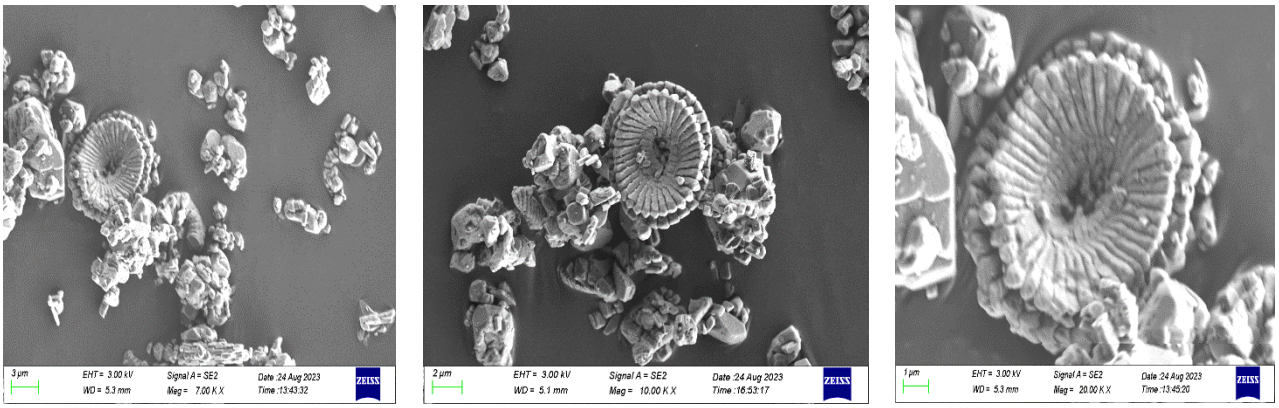

a. 7 k times magnification b. 10 k times magnification c. 20 k times magnification

Figure 4.2 SEM micrographs of $CaCO_3$

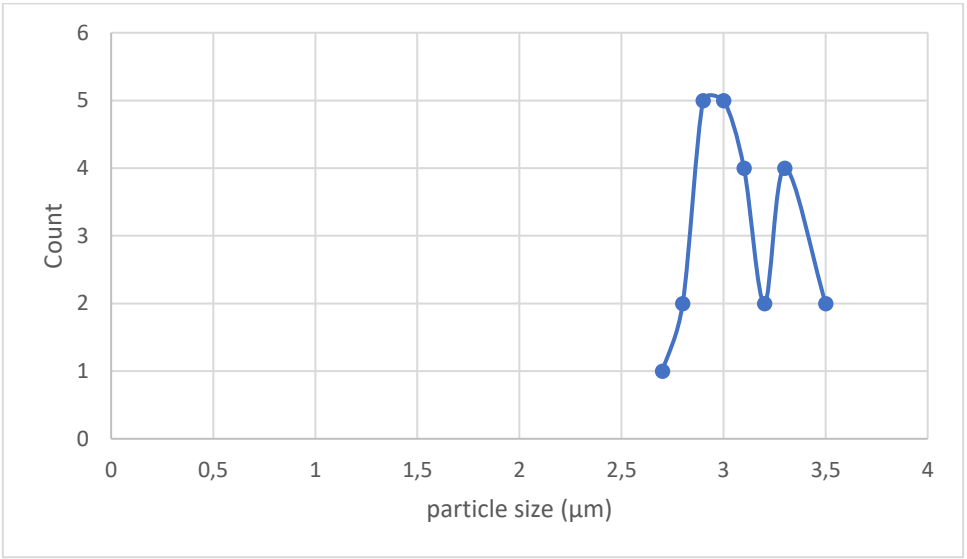

Figure 4.3 Particle size distribution of $CaCO_3$

4.4.5.2 Nano $CaCO_3$

Figure 4.4 shows the SEM images revealing the morphological properties of the synthesized material from lower to higher magnification, *i.e*., 40 to 50 times. **Figure 4.4a** shows the scale for 1 µm, while **Figure 4.4b** and **Figure 4.4c** shows the scale for 200 nm. Figure reveals two morphologies, (i) nanosized spherical $CaCO_3$ (vaterite) with particle size of 93.6 nm (**Figure 4.5**), (ii) the micro sized cubic-like particles (0.8 µm) embedded together.

The addition of $Ca(HS)_2$ into 20% Na_2CO_3 solution was crucial to obtain nano $CaCO_3$ at 25°C and at the solution injecting flow rate of 20 ml/min. The $Ca(HS)_2$ used was produced by CO_2 bubbling process in CaS slurry. The CO_2 bubbling process is very efficient at producing nano-sized particles, which are the most sought-after size in industry (George, 2000). Because of the simplicity of liquid-liquid reaction, solution mixing is the most frequently explored process of preparing nano $CaCO_3$ in laboratory research. In this process, the mixing ways of the solutions influenced the size and the appearance of nano $CaCO_3$ (Wang, *et al*., 2016). Many morphologies could be obtained from solution mixing process with different operating variables, such as rhombohedral (Njegi, *et al*., 2009), cubic, spherical, rod-like (Huang, *et al*., 2019)], dendrite-shaped, wheatgrass-like, needle-like, whiskers, double-taper-like (Lei, *et al*., 2006), hollow micro spheric (Ji, *et al*., 2008), sponge-like (Park & Meldrum, 2002), and super hierarchical (Lei, *et al*., 2006) morphology. In many cases, the product in solution mixing process comprises of two or more polymorphs and morphologies, either due to their simultaneous nucleation or due to transformation of a metastable polymorph (Rodriguez-Blanco, *et al*., 2011).

It is concluded that $CaCO_3$ with a smaller particle size of $CaCO_3$ (93.6 nm) was produced when $Ca(HS)_2$ was reacted with Na_2CO_3, compared to 1 µm when CaS was reacted with CO_2. The requirement for nano $CaCO_3$ is a particle size of <40 nm. It will be possible to reduce the 93.6 nm particles size to <40 nm by applying more effective rapid mixing (Yuan, *et al*., 2022).

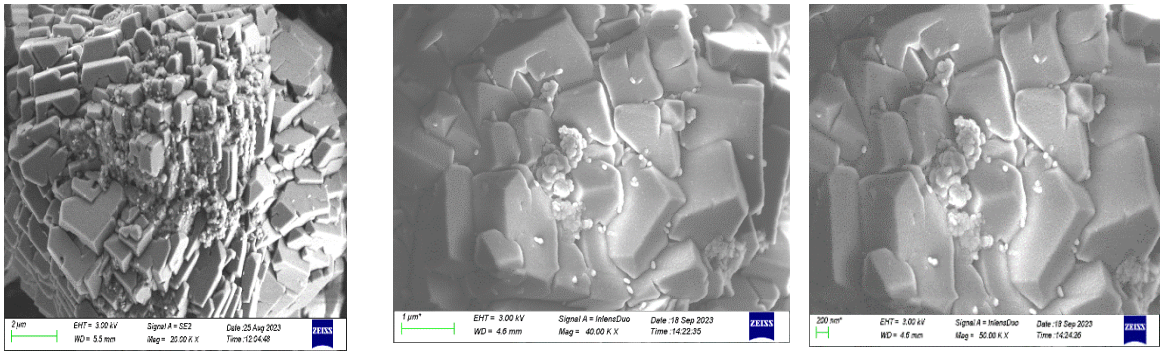

a. 40 k times magnification b. 50 k times magnification c. 50 k times magnification

Figure 4.4 SEM images of nano $CaCO_3$

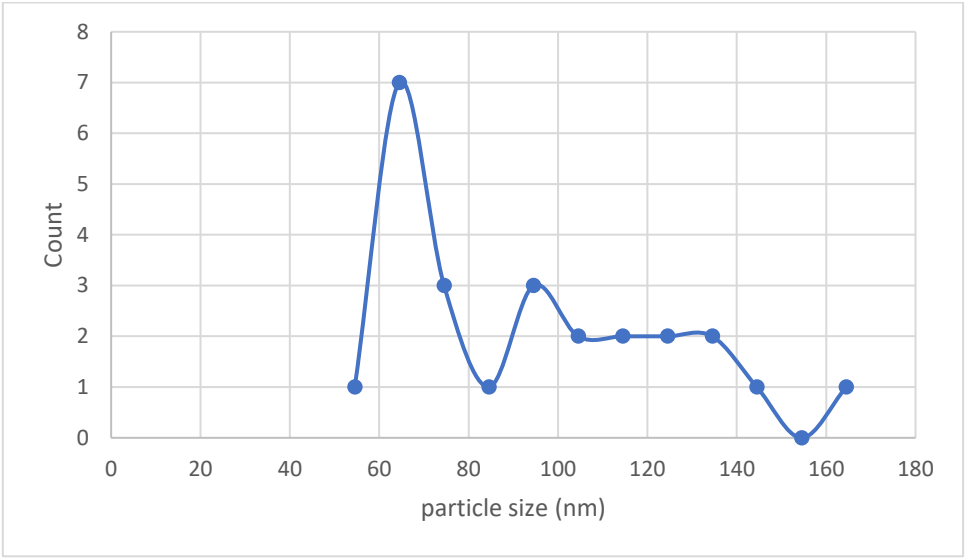

Figure 4.5 Particle size distribution of nano $CaCO_3$

4.5 CONCLUSIONS

i. CaS can be produced through reduction of $CaSO_4$ with carbon at 1000 °C.

ii. Na_2SO_4 can be converted to Na_2S by reacting it with CaS.

iii. $Ca(HS)_2$ can be produced by reacting CaS with CO_2.

iv. $NaHCO_3$(s) and NaHS(aq) can be produced by reacting Na_2S with CO_2.

v. Freeze crystallization can be used to separate $NaHCO_3$(s) and NaHS(aq).

vi. Na_2CO_3 can be produced from $NaHCO_3$ through heating.

vii. Crude $CaCO_3$ can be produced by reacting CaS with CO_2.

viii. High-grade precipitated $CaCO_3$ can be produced by reacting CO_2 with a solution of $Ca(HS)_2$.

ix. Nano $CaCO_3$ can be produced by reacting a solution of $Ca(HS)_2$ with a solution of Na_2CO_3.

CHAPTER 5: RECOVERY OF Na_2CO_3 AND $Mg(OH)_2$ FROM ALKALI EARTH METAL SULPHATES

Conny P Mokgohloa[1,2], Johannes P Maree[1,3], Malose P Mokhonoana[2], Mary P Motaung[4]

Email addresses: connyputjie@gmail.com; johannes.maree@ul.ac.za; malose.mokhonoana@ul.ac.za, motaungneo35@gmail.com

[1]Department of Water and Sanitation, University of Limpopo, Private Bag X1106, Sovenga, 0727, South Africa.

[2]Department of Chemistry, University of Limpopo, Private Bag X1106, Sovenga, 0727, South Africa.

[3]Institute for Nanotechnology and Water Sustainability (iNanoWS), College of Science, Engineering and Technology, University of South Africa, Private Bag X6, Florida Science Campus, Johannesburg 1709, South Africa.

[4]DepartmentsChemical, Metallurgical and Materials Engineering, Tshwane University of Technology, Private Bag X680 Pretoria, 0001, South Africa.

Abstract

Acid mine drainage is one of mining's most serious threats to water scarcity. It is highly acidic, rich source of sulphate and heavy metals. High sulphate content has a negative impact on humans. The presence of sulphate in AMD also contributes to corrosion and gypsum scale-formation, as well as corrosion of equipment. However, valuable products such as sodium carbonate (Na_2CO_3) can be recovered from the sulphates namely, calcium sulphate ($CaSO_4$) and barium sulphate ($BaSO_4$). Na_2CO_3 is used for mine water treatment and glass manufacturing with a current price of R4 500/t (US$345/t). In the Reverse Osmosis-Cooling (ROC) process, Na_2CO_3 is used in the pre-treatment stage for the formation of pigment and precipitation of other metals. Calcium carbonate ($CaCO_3$) is used to remove acidity and achieve only partial sulphate and metal removal. Magnesium hydroxide ($Mg(OH)_2$) is used to filter out suspended solids and to precipitate dissolved heavy metals. The Mintek Pyrosim software model was used to predict the products formed under the conditions that were studied experimentally. Pyrosim studies showed that $CaSO_4$ can be converted to CaS, and $BaSO_4$ can be converted to BaS through reduction with coal at 1000 °C. This correlates with the muffle furnace studies which showed that $CaSO_4$ and $BaSO_4$ can be converted to calcium sulphide (CaS) and barium sulphide (BaS), respectively. CaS was used for the production of $CaCO_3$. The new process developed by Van Vuuren and Maree was used for the indirect

processing of sodium sulphate (Na_2SO_4) to sodium sulphide (Na_2S), where Na_2SO_4 was reacted with BaS. This was further used as a reactant to produce sodium carbonate (Na_2CO_3) and $Mg(OH)_2$. The reduction of alkalinity from 136 500 mg/L (as Na_2S) at a CO_2/Na_2S mole ratio of 1, to 113 100 (as Na_2S) at a CO_2/Na_2S mole ratio of 4 confirmed the precipitation of $NaHCO_3$. Na_2CO_3 can be recovered by heating sodium bicarbonate ($NaHCO_3$). The OLI simulations and beaker studies revealed that $Mg(OH)_2$ formed when magnesium sulphate ($MgSO_4$) was contacted with Na_2S. The Fe^{2+} can be back oxidised to Fe^{3+} through chemical or biological oxidation. H_2S can be converted to S by contacting it with Fe^{3+}.

5.1 INTRODUCTION

Acid mine drainage (AMD) is the most significant environmental pollution problem associated with the mining industry. The high concentration of toxic metals and high levels of acidity in AMD are harmful to the vegetation, aquatic life, terrestrial wildlife and human beings. Pyrite (FeS_2) is a major constituent of the strata being mined and large rock surfaces become exposed to air and water during mining activities (Sasowsky, *et al*., 2000). Pyrite is oxidized to soluble iron complexes and sulphuric acid, catalysed by sulphur-oxidizing bacteria (Sawyer, *et al*., 1994), according to the reaction shown in **Eq. 5.1.**

$$2FeS_{2(s)} + 7O_{2(aq)} + 2H_2O \rightarrow 2Fe^{2+} + 4SO_{4(aq)}^{2-} + 4H_{(aq)}^{+} \quad (5.1)$$

Because of its detrimental effects on the environment and public health, it is mandatory to treat acid mine drainage (AMD) with the aim to achieve zero waste. AMD can be treated by two methods: *viz*., active treatment and passive treatment. Active treatment includes the use of chemical agents such as limestone ($CaCO_3$), hydrated lime ($Ca(OH)_2$), caustic soda (NaOH), soda ash (Na_2CO_3), calcium oxide (CaO), anhydrous ammonia (NH_3), magnesium hydroxide ($Mg(OH)_2$), and magnesium oxide (MgO) (RoyChowdhury, *et al*., 2015). Passive treatment can be further classified into two types: conventional and emerging. Examples of conventional passive treatment are constructed wetlands and anaerobic sulphate-reducing bioreactors, while an example of an emerging passive treatment is phytoremediation (RoyChowdhury, *et al*., 2015).

The Reverse osmosis cooling (ROC) process can be used for the treatment of AMD through neutralization with Na_2CO_3 for the removal of metals, desalination with reverse osmosis (RO), freeze-crystallization for the recovery of Na_2SO_4 from the RO brine and processing of Na_2SO_4 to Na_2S. In the ROC process, Na_2CO_3 is used for selective recovery of metals through a

stepwise increase of the pH, resulting in the formation of Na_2SO_4, which can be recovered from the brine after the reverse osmosis and freeze-crystallization stages. It would be beneficial if the raw material, Na_2CO_3, can be recovered from the product, Na_2SO_4. Since Na_2CO_3 has a high price of 263.3 US$/t, it would be economically beneficial if it can be processed from the product, Na_2SO_4.

Studies by Mashigwana (2022), on the direct conversion of Na_2SO_4 into Na_2CO_3 under thermal conditions found that it was not possible, as Na_2SO_4 melted in the same temperature range where the reduction took place, *i.e*., 860 to 920 °C (Mashigwana, et al., 2022). Van Vuuren and Maree proposed that Na_2CO_3 can be produced indirectly from CaS or BaS (van Vuuren & Maree, 2020). Various researchers have studied the reduction of $CaSO_4$ and $BaSO_4$ in depth without experiencing the melting problem of one of the reactants (Masukume, *et al*., 2013; Ruto, *et al*., 2011; Ruto, *et al*., 2012; Ruto, *et al*., 2011). Recently, Mokgohloa *et al*. studied the reduction of $CaSO_4$ and found that, Na_2CO_3 can be produced from Na_2SO_4 *via* CaS (Mokgohloa, *et al*., 2022). In the indirect method, $CaSO_4$ precipitates, due to its relatively low solubility, while Na_2S or NaHS remain in solution and are converted into Na_2CO_3 or $NaHCO_3$ by contacting them with CO_2. A limitation of the CaS route is, however, the partial solubility of $CaSO_4{\cdot}2H_2O$ (2 440 mg/L). The Na_2S formed, is therefore contaminated with Ca^{2+}. $BaSO_4$ offers the benefit that Na_2S will be pure due to the low solubility of $BaSO_4$ (2.44 mg/L) compared to the 2 640 mg/L in the case of $CaSO_4{\cdot}2H_2O$. More energy is also needed for the conversion of $BaSO_4$ into BaS (226.12 kJ/mol) than for the conversion of $CaSO_4$ into CaS (155.8 kJ/mol).

The purpose of this investigation was to identify the process steps needed for the processing of Na_2SO_4 to Na_2CO_3 and NaHS.

In the previous chapter, the focus was on $CaSO_4$ to $CaCO_3$ and Na_2SO_4 to Na_2CO_3. The focus in this chapter is on how BaS, produced from $BaSO_4$, can be used to improve the processes where $NaSO_4$, $MgSO_4$ and $CaSO_4$ are processed to produce high-value products.

The objectives of this investigation are as follows:

i. Thermal conversion of $BaSO_4$ and $CaSO_4$ to BaS and CaS, respectively.
ii. Conversion of Na_2SO_4 to Na_2S using BaS.
iii. Processing of Na_2S into $NaHCO_3$ and NaHS.
iv. Processing of $NaHCO_3$ into Na_2CO_3.

v. Processing of $MgSO_4$ to $Mg(OH)_2$, Na_2SO_4 and NaHS.

5.2 LITERATURE

This chapter deals with processing of solids, liquids and gases as well as the reactions that take place from a temperature of 0 °C to 1000 °C. This section therefore covers the thermodynamic and kinetic principles of various reactions. It further describes the Freeze crystallization by the ROC process and the types of freeze crystallization.

5.2.1 Solids, liquids, gases

Solids are one of the three basic states of matter, the others being liquids and gases. Because the solid form of a liquid or gas has relatively ordered atoms, the energy of the atoms decrease as they adopt a three-dimensional structure (Ayyıldız & Tarhan, 2013). Solids have certain properties that distinguish them from liquids and gases. For example, all solids can withstand a force acting normally or parallel to a surface (perpendicular or shear load, respectively). These properties depend on the characteristics of the atoms that form the solid, and the arrangement of the atoms as well as the forces between the atoms. Solids are generally divided into three major classes: crystalline, non-crystalline (amorphous) and semi-crystalline (Goodstein, 2002).

The liquid state is sometimes described as a state between the solid and gaseous states, and for simple molecules, the distinction is unclear. However, the clear distinction between liquid, gaseous and solid states apply only to substances whose molecules are composed of a small number of atoms (Dalarsson, *et al*., 2011). In a liquid, the attraction between the particles keeps the volume of the liquid constant. Due to the movement of particles, liquids take different forms. The liquid flows and fills the bottom of the container and takes on the shape of the container, but the volume does not change. Liquids have a very limited compressibility because the space between the particles is limited.

A gas is a state of matter that does not have a definite shape or volume. Gases have their own behaviour depending on various variables such as temperature, pressure, and volume (San Marchi, *et al*., 2007). While each gas is different, all gases act in a similar manner. The particles that make up a gas can range from individual atoms to complex molecules.

5.2.2 Kinetics

Chemical kinetics is the branch of physical chemistry that deals with the understanding of the speed at which chemical reactions take place. Chemical kinetics has a significant impact, as it encompasses many aspects of cosmology, geology, biology, engineering and even psychology (Zhang, 2021). The principles of chemical kinetics apply to purely physical processes as well as to chemical reactions.

The kinetic behaviour of a general chemical reaction is usually studied to determine the effect of certain external factors, such as reactant concentrations, temperature, and pressure, on the reaction rate (Robinson, 2015). In the case of a reaction in which two substances A and B react with each other, the reaction rate is sometimes proportional to their concentrations of A, denoted by [A], and [B]. In that case, the reaction is said to be a second-order reaction; it is first order in both [A] and [B]. In such a case the reaction rate (v) can be expressed as shown in **Eq. 5.2.**

$$v = k[A][B] \tag{5.2}$$

where k is a constant, known as the rate constant for the reaction.

The transformation of substance A into another substance may be the subject of an equation of motion of the form v = k [A], which is a first-order reaction. The kinetics of a reaction simply does not correspond to the coefficients in the balanced chemical equation of the reaction. Therefore, the reaction shown in **Eq. 5.3** is not necessarily second order in both directions.

$$A + B \rightleftharpoons Y + Z \tag{5.3}$$

5.2.3 Thermodynamics

Thermodynamics is the science of studying the relationship between heat, work, temperature, and energy. In broad terms, thermodynamics deals with the transfer of energy from one place to another, and transformation from one form to another. The laws of thermodynamics are:

- Zeroth law of thermodynamics: When two systems are each in thermal equilibrium with a third system, the first two systems are in thermal equilibrium with each other. If a = b and b = c, then a = c.
- The first law of thermodynamics or the law of conservation of energy: The change of the internal energy of a system is equal to the sum of the heat added to the system by the environment and the work done to the environment of the system. **Eq. 5.4**

describes the first law of thermodynamics in terms of internal energy, work and heat transfer mechanisms.

$$\Delta U = q + W \tag{5.4}$$

where, ΔU is the change in internal energy of the system, q is the algebraic sum of heat transfer between system and surroundings, W is the work interaction of the system with its surroundings.

- The second law of thermodynamics: Heat does not flow spontaneously from a colder area to a warmer area, and heat at a given temperature is not completely converted into work. As a result, the entropy or thermal energy per unit temperature of a closed system increases to its maximum value over time. Therefore, any closed system tends to be in balance with maximum entropy and without energy to do useful work as shown in **Eq. 5.5**.

$$\Delta S_{uni} = \Delta S_{sys} + \Delta S_{surr} \geq 0 \tag{5.5}$$

where ΔS_{uni} is the entropy of the universe, ΔS_{sys} is the entropy of the system, ΔS_{surr} is the entropy of the surrounding.

- The third law of thermodynamics: As the temperature approaches absolute zero, the entropy of a perfect crystal of an element in its most stable form tends to zero. It defines the absolute measure of entropy that statistically defines the degree of randomness or disorder in a system as described in **Eq. 5.6.**

$$S = k \log \Omega \tag{5.6}$$

where S = entropy, k = Boltzmann constant and Ω = number of microstates.

5.2.4 Gibbs free energy

The Gibbs free energy is a quantity used to measure the maximum amount of work performed in a thermodynamic system when temperature and pressure are kept constant. The Gibbs free energy of a system at any moment in time is defined as the enthalpy of the system minus the product of the temperature times the entropy of the system as shown in **Eq. 5.7.**

$$G = H - TS \tag{5.7}$$

Thus, the change in the Gibbs free energy of a system that takes place during a reaction is equal to the change in the enthalpy of the system minus the change in the product of the temperature multiplied by the entropy of the system as shown in **Eq. 5.8.**

$$\Delta G = \Delta H - \Delta(TS) \quad (5.8)$$

If the reaction is run at constant temperature, **Eq. 5.8** can be written as shown in **Eq. 5.9.**

$$\Delta G = \Delta H - T\Delta S \quad (5.9)$$

The change in free energy of a system that occurs during a reaction can be measured in all cases. When data is collected under standard-state conditions, the result is the reaction energy under standard state ΔG^o as shown in **Eq. 5.10**.

$$\Delta G^o = \Delta H^o - T\Delta S^o \quad (5.10)$$

5.2.5 Enthalpy and heat of reaction

Heat of reaction, or enthalpy of reaction, is an important parameter for the safe and successful scaling of chemical processes. Heat of reaction is the energy released or absorbed when a chemical substance is transformed in a chemical reaction. It describes the change in energy content when reactants are transformed into products. A reaction can be exothermic (heat-releasing) or endothermic (heat-absorbing) (Desai, *et al*., 2021). The heat of reaction or reaction enthalpy is typically expressed as molar enthalpy in kJ/mol, or as specific enthalpy in kJ/kg or kJ/L. The enthalpy can be calculated using **Eq. 5.11**.

$$H = U + PV \quad (5.11)$$

where U is internal energy, P is pressure and V is volume. In the case of a change in enthalpy (ΔH), **Eq. 5.11** changes to **Eq. 5.12.**

$$\Delta H = \Delta U + P\Delta V + V\Delta P \quad (5.12)$$

In practice, the pressure is held constant, and **Eq. 5.12** changes to **Eq. 5.13.**

$$\Delta H = \Delta U + P\Delta V \quad (5.13)$$

However, for a constant pressure system, the change in enthalpy is simply the heat (q) transferred as shown in **Eq. 5.14**.

$$\Delta H = q \quad (5.14)$$

5.2.6 Freeze-crystallization by the ROC process.

Freeze crystallization can be used to separate compounds with different solubilities by removing water from the solution through freezing of ice. This method was used in this chapter to separate $NaHCO_3$, which has a lower solubility at 0 °C from NaHS, which has a high solubility. This section provides background information on freeze-crystallization.

5.2.6.1 *Introduction*

The ROC process was developed for the treatment of brines from desalination processes, such as reverse osmosis (Mtombeni & Maree, 2014; Mtombeni, *et al*., 2014; Mtombeni, *et al*., 2016). In the ROC process, the brine is treated with chemicals such as Na_2CO_3 and/or NaOH in the pre-treatment stage to allow selective precipitation of metals ($CaCO_3$, MnO_2 and $Mg(OH)_2$). After pre-treatment, the Na-rich and Mg-rich water is passed through a membrane stage to produce drinking water and brine. The brine has a Na_2SO_4 concentration which is high enough to allow Na_2SO_4 crystallizations upon cooling/freeze desalination.

5.2.6.2 *Types of freeze crystallization*

Freezing crystallization (FC) is used to separate fresh water from a salt solution in the form of ice crystals and then thawed to purify the water. The process was discovered by Thomas Bartolinus (1680), who said that fresh water can be obtained by melting ice from sea water (Kucera, 2014). Its first commercial market was in the 1950s (Hendrickson & Moulton, 1956). Karnofsky and Steinhoff and Weigandt *et al*. proposed the first direct freezing process using butane as a coolant for seawater desalination (Karnofsky & Steinhoff, 1960; Wiegandt, *et al*., 1968). The freezing method uses the transition of water from liquid to solid. In addition to crystallization, this involves separating ice crystals from brine, washing them to remove salt from the crystal surface, and thawing the ice to obtain the final fresh water (Lu & Xu, 2010). The literature mentions different freezing-crystallization methods through four main methods: direct, indirect, vacuum, and eutectic freezing-crystallization (Kucera, 2014). Recent advances in freezing crystallization have introduced two new methods of ice crystallization that are subject to indirect contact crystallization: suspension crystallization and surface crystallization at low temperature (Randall, *et al*., 2011; Kucera, 2014; Williams, *et al*., 2015; Wang & Chung, 2012). According to the literatures (Rich, *et al*., 2011; Rahman, *et al*., 2006), the energy cost of the freezing desalination process is theoretically equal to the cost of the reverse osmosis (RO) membrane unit. However, the investment and operating costs of the

freezing technology are high due to the significant reduction in biological contamination using lower temperatures than the installation of RO membranes.

5.2.6.3 *Direct contact freeze-crystallization*

Direct contact freezing uses a refrigerant in direct contact with the freezing solution. This method mainly has an operating temperature of -5 °C, which is characterized as a low energy process (Kucera, 2014). The main advantages of this method are the efficient design with high production speed, small size, and low driving force. On the other hand, freezing crystallization requires a specific coolant. The refrigerant must have a normal boiling point of -4 °C or less, water-resistant, non-toxic, non-flammable, chemically stable, inexpensive, and commercially available (Kucera, 2014). In addition to all these requirements, it is important to mix the refrigerant solution correctly to obtain ice crystals with minimal impurities.

5.2.6.4 *Indirect contact freeze-crystallization*

In indirect contact freeze-crystallization, the refrigerant is used without direct contact with the crystallization solution by indirect contact with the frozen crystal, and the energy of the refrigerant passes through the wall of the heat exchanger (Randall, *et al*., 2009). Generally, indirect freezing can be classified into two main classes: (i) suspension freezing and (ii) freezing on a cold plate (Randall, *et al*., 2011; Amran, *et al*., 2016). When the suspension crystallizes, many fine ice particles form in two stages from the mother liquor suspension. The crystals first form in the ice core and then smaller crystals are recrystallized by the Ostwald maturation mechanism (Amran, *et al*., 2016). However, crystallization in suspension is commonly used in the food concentration industry (Randall, *et al*., 2009). This technique has many cons such as cost, complexity, difficult nucleation, and crystal growth control (Miyawaki, *et al*., 2012; Liu, *et al*., 1997). Alternatively, freezing on a cold surface forms a single crystal layer on a cooled surface.

5.2.6.5 *Vacuum freeze-crystallization*

Crystallization by vacuum freezing is a specialized freeze-crystallization technique that provides a cooling effect by using a high vacuum to evaporate a little water and then lowering the temperature of the solution to produce ice crystallization. (Kucera, 2014). Crystallization by vacuum-freezing is especially used in the food, chemical, and pharmaceutical industries to separate and purify solids from liquids. Ice crystals are created in a solution under low

temperature and pressure conditions in this approach. The solution is first frozen to form a solid mass in the process (Roos, *et al*., 2003). The frozen solid mass is then placed in a vacuum chamber under reduced temperature and pressure, hence, causing the ice to change from solid to vapor without melting. A concentrated solution containing the needed solid is left behind as the sublimation process occurs. This process provides several significant advantages, including the preservation of crystal structure and shape, as well as the production of high-purity solids. However, some of the constraints of this technique include its slow nature and high cost required at its development (Rahman, *et al*., 2006)

5.2.6.6 *Eutectic freeze crystallization*

Eutectic freeze-crystallization (EFC) dates to the 1950s, when Nelson and Thompson attempted to determine the salt crystallization sequence. However, the use of EFC as a separation technique was introduced by Stepakoff *et al*. in the 1970s. In 1974, EFC techniques was improved by adding coolant directly to the solution (Stepakoff, *et al*., 1974). Eutectic freeze-crystallization is a new water purification technology that allows the recovery of ice and salty products from a concentrated brine stream. There are several benefits to using EFC as part of overall water treatment process. Crystallization is a physical process of separation, so no chemicals are required (Lorain, *et al*., 2001). Freeze crystallization is thermodynamically more efficient than evaporative crystallization, as the heat of fusion of water is six times lower than the heat of evaporation of water (Van der Ham, 1999). The principle of the EFC process is that when a saturated solution cools slowly below the solidification line, ice crystals begin to form and rise to the surface, and the salt concentrates in the rest of the solution and finally crystallizes at the eutectic temperature (Genceli, *et al*., 2005). Under the conditions of the eutectic process, ice and salt crystallize simultaneously and can be separated depending on the difference in density (Genceli, 2008). Crystallization of both products occurs in pure form, eliminating the need for a secondary separation process (Halde, 1980). A significant part of the energy spent to achieve lower operating temperatures can be stored and recovered in the ice product. Lower operating temperatures further reduce the corrosion potential of mechanical equipment, allowing the use of cheaper building materials (Johnson, 1976). Disadvantages of EFC include high capital costs (Randall, *et al*., 2009) and the formation of an insulating ice scale layer on cooled crystallizer surfaces (Pronk, 2006). Reddy *et al*. (2010) reported that EFC can be utilized to treat a reverse osmosis retentate stream containing 4 wt.% sodium sulphate and several impurities (F^-, Cl^-, K^+, Li^+,

Mg^{2+}, Ca^{2+}, NO_3^- and NH_3^+) producing pure water and sodium sulphate decahydrate (Reddy, *et al*., 2010). Theoretically, high performance (100% binary system) and purity can be achieved in EFC and this method results in the recovery of salt with residual solubility at final operating temperatures over crystallization limited to cooling (Van der Ham, 1999; Seckler, *et al*., 2002). In addition, the growth process that produces high purity crystals can be closely monitored to avoid the formation of solid solutions and impurities (Van der Ham, 1999). Cheaper materials of construction are required due to minimal corrosion at low temperatures characteristic of EFC processes (Huige, 1972; Stepakoff, *et al*., 1974). For aqueous solutions with very low process temperatures, EFCs can be economically inefficient due to the large surface area required for heat transfer. A major limitation of EFC is the contamination of the surface of the heat exchanger due to the formation of an ice sheet, which significantly reduces the heat transfer coefficient and, consequently, reduces the heat flow, thus reducing the crystallization rate. Layers of ice can also damage the mechanical equipment of the crystallizer. The cost of EFC equipment is still high, but it is expected to decrease over time as better projects develop.

5.3 MATERIALS AND METHODS

5.3.1 Feedstock, chemicals and reagents

High purity reagents were used in this work for the preparation of samples. Deionised water was used for all solutions and dilutions. The following chemicals were used: $BaSO_4$, Na_2SO_4, (Protea Chemicals), $CaSO_4 \cdot 2H_2O$ (Foskor), activated carbon (MCL), CO_2 gas (Air Liquide, South Africa), 1 N HCl, 0.1 N I_2, 0.1 N $Na_2S_3O_4$, 1 M NaOH, and starch solution.

5.3.2 Equipment

A muffle furnace was used for reduction of $CaSO_4$ to CaS and $BaSO_4$ to BaS. 500 mL beakers for reaction studies, *BirCraft* agitator, pH and conductivity meter, CO_2 gas supplied at a pressure of 50 kPa.

5.3.3 Experimental and Procedure

5.3.3.1 *Thermal treatment*

Thermal studies were carried out by reacting mixtures of $CaSO_4$/$BaSO_4$ and coal at elevated temperatures (1 000 to 1 110 ºC) in the muffle furnace to produce CaS. The weighed, dry

$CaSO_4/BaSO_4$ (20 g) and powdered coal (5 g) were mixed thoroughly, placed in ceramic crucibles for all the reduction experimental trials. Solid samples were collected and analyzed for mass loss, sulphide content, and alkalinity. The retention times for all the reduction experiments were 30 – 60 minutes.

5.3.3.2 *Na_2S formation*

OLI simulations (OLI ESP software program from OLI Systems, Inc) and beaker studies were used to determine which compound will precipitate out and which compounds/elements will stay in solution.

- The conversion of Na_2SO_4 to Na_2S by reacting it with BaS was carried out in the laboratory using the BaS, produced from $BaSO_4$. A BaS solution (10.00 g BaS in 100 mL H_2O) was mixed with a Na_2SO_4 solution (8.40 g Na_2SO_4 in 100 mL).
- OLI simulations were caried out to determine whether an aqueous solution of Na_2S can be formed by contacting a $Ca(HS)_2$ solution with Na_2SO_4.

5.3.3.3 *Na_2S processing*

Beaker studies were carried out to convert Na_2S into $NaHCO_3$ and NaHS by reacting it with CO_2. The following procedure was followed in the experiment by using the laboratory set-up shown in **Figure 3.4**.

- CO_2 was put in a 300 mL measuring cylinder, with the open end on top of a water bath *via* Line 1.
- Na_2S (0.88 g Na_2S + 4.38 g H_2O; 200 g Na_2S/L H_2O) was put in a 250 mL separation funnel.
- Air was removed from the separation funnel with a vacuum pump *via* Line 3 and replaced with CO_2 stored in the 300 mL measuring cylinder *via* Line 2.
- The Na_2S and CO_2 in the separation funnel were allowed to react by shaking it for 15 min. CO_2 additions were repeated 1, 2 and 4 times to determine the effect of CO_2/Na_2S mole ratio on the completion of the reaction.
- The CO_2 in the measuring cylinder was replaced with air.
- The volume of CO_2 reacted with the Na_2S was determined by allowing the air in the measuring cylinder to flow into the 250 mL separation funnel *via* Line 2, which was

partially under vacuum due to the CO_2 reaction with Na_2S. The volume of CO_2 reacted was determined by reading the volume of water that was sucked into the 300 mL measuring cylinder.

- Sulphide and alkalinity analyses were carried out on the filtered liquid samples collected from the separation funnel. Filtered samples were collected by using a 25 mL syringe with a filter tip.

5.3.4 Analysis

Sulphide was determined by standard iodometry (APHA, 2012)as follows: A 50 mg sample of the reduced product was weighed, dissolved, and made up to 100 mL with deionized water. Then 10 mL of standard iodine solution (0.1 N) was added, followed by 50 mL of deionized water. The resulting mixture was acidified using 2 mL of 1 N HCl solution and subsequently titrated with standard (0.1 N) sodium thiosulphate using starch as indicator to a colourless endpoint as shown in **Eq. 5.15.**

$$\%CaS = \frac{[(CV)_{I2} - (CV)_{S2O3}]\,X\,36}{Sample\ mass\ (mg)} \times 100 \qquad (5.15)$$

5.3.5 Pyrosim Mintek Simulation

The prediction of $CaSO_4$/$BaSO_4$ was done using the Pyrosim Mintek model. **Figure 5.1** (a) shows the thermo page and (b) the Pyrosim page of Pyrosim Mintek model. The Pyrosim Mintek model is a computer simulation program for steady-state simulation of pyrometallurgical and other high temperature processes. It has a built-in capacity to evaluate multi-phase equilibria, with the potential of predicting high temperature processes more accurately. It also gives proficiency of steady state mass and energy calculations for high temperature processes (Abdellatif & Freeman, 2011).

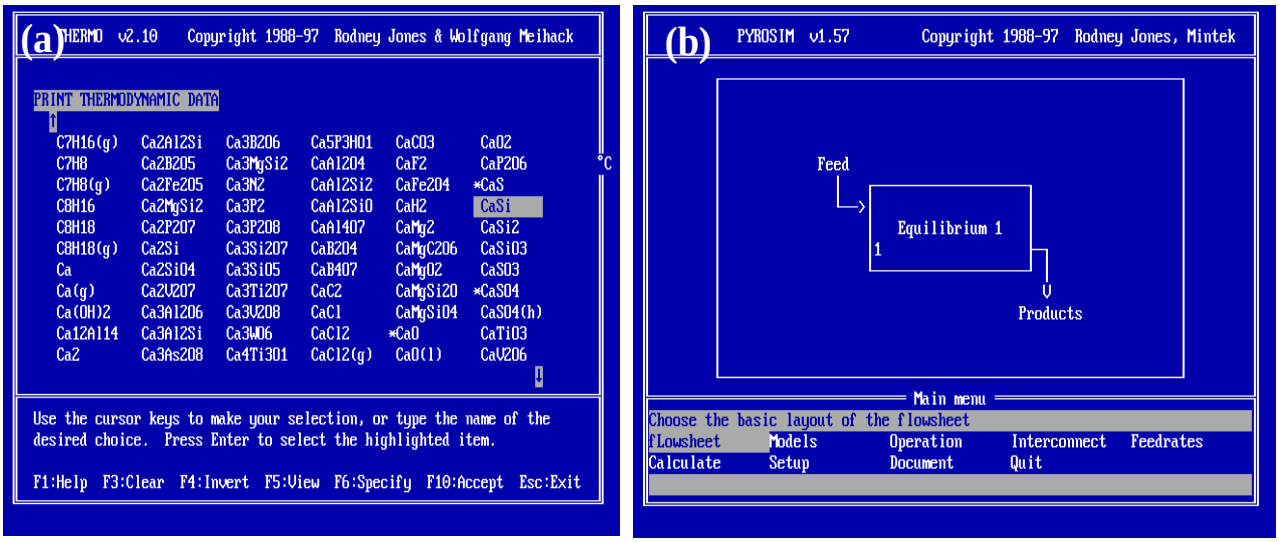

Figure 5.1 (a) Screen layout during the specification of the chemical species present in the slag phase; and (b) Screen layout showing the Pyrosim Mintek operation page.

5.3.6 OLI software simulations

The OLI System Chemical Analyser software program was used to predict the behaviour of metals dissolved in water when treated with alkalis such as $MgSO_4$ and Na_2SO_4 (OLI, 2015). OLI is an aqueous equilibrium chemistry estimator with an interactive and self-instructive interface for clarifying reactions. It can work with all kinds of common equilibrium reactions, it has a strong solution algorithm, and expressive and easily understandable displays of results, and the ability to produce results in multiple formats according to different uses. The OLI System Chemical Analyser was used to perform single point equilibrium calculations and multiple point survey calculations. The concentration of the various species in solutions or solids were calculated as a function of temperature, pressure, pH and initial concentrations. The calculations provide liquid- and solid-phase separations for a specialised model.

5.4 RESULTS AND DISCUSSION

For the processing of Na_2SO_4 to Na_2S it was learned that direct conversion is difficult due to the melting of Na_2SO_4 in the same temperature range where the reduction takes place. Na_2S can be formed by reacting it with either CaS or BaS. Thermodynamic calculations were used to determine the carbon (coal) needed for the reduction of the various compounds. Further attention was given to the processing of Na_2S to Na_2CO_3 and how to utilize it for processing $MgSO_4$ to $Mg(OH)_2$.

5.4.1 Thermodynamic values for $CaSO_4$, $BaSO_4$ and Na_2SO_4

Table 5.1, Table 5.2 and

Table 5.3 show the values for heat of formation, Standard Gibbs free energy of formation and standard entropy values for the various reactants and products respectively.

- The heat of formation, also known as enthalpy of formation, is a measure of the energy released or consumed when one mole of a substance is created from its pure elements under standard conditions. It is given by the **Eq. 5.16.**

$$\Delta H^{o}_{reaction} = \sum H^{o}_{f(Products)} - \sum H^{o}_{f(Reactants)} \quad (5.16)$$

- Enthalpy is the sum of the internal energy and the product of the pressure and volume of a thermodynamic system as shown in **Eq. 5.17.**

$$H = U + PV \quad (5.17)$$

where U is internal energy, P is pressure and V is volume.

- Standard Gibbs free energy of formation is the change in Gibbs free energy for the formation of one mole of the compound in its standard state from its constituent elements in their standard states. It is given by the **Eq. 5.18.**

$$\Delta G^{o}_{f} = \Delta H^{o}_{f} - T\Delta S^{o} \quad (5.18)$$

where ΔH^{o}_{f} is standard enthalpy of formation, T is standard temperature, ΔS^{o} is standard entropy and subscript f indicates that the substance is formed from its elements.

- Standard entropy is the entropy of 1 mole of a substance in its standard state, at 1 atm of pressure and temperature of 298 K. It can be calculated from the difference in standard entropy between the products and the reactants as shown in **Eq. 5.19.**

$$\Delta S^{o} = \sum S^{o}_{(\text{Products})} - \sum S^{o}_{(\text{Reactants})} \quad (5.19)$$

- Specific heat capacity, c, is defined as the quantity of heat absorbed per unit mass of the material when its temperature increases as shown in **Eq. 5.20**.

$$c = \frac{Q}{m\Delta T} \quad (5.20)$$

where Q is the heat energy, m is the mass and ΔT is change in temperature.

Table 5.5 and **Table 5.4** show the heat of reaction (H_r) (**Eq. 5.16**) and specific heat capacity (C_p) for the various reactions. The following approach was followed to determine how much coal was needed for the processing of $CaSO_4 \cdot 2H_2O$ to CaS and $BaSO_4$ to BaS, respectively.:

(i) The enthalpy (sensible heat) for the various reactants ($CaSO_4 \cdot 2H_2O$, $CaSO_4$, C, H_2O) at the input temperature (30 °C) were calculated by using the mass flow rate and the heat of reaction as shown in **Eq. 5.21.**

$$H(kW) = \dot{m}\left(\frac{kg}{s}\right) \times Hr\left(\frac{kJ}{kg}\right) \quad (5.21)$$

(ii) The enthalpy for the various products ($CaSO_4$, CaS, BaS, CO_2, H_2O) at the output temperature (1 000 °C) were calculated by using the **Eq. 5.21.**

(iii) Activation energy

a. The latent heat of vaporization of H_2O was calculated by using the mass flow rate ($\dot{m}$), latent heat of vaporization (Hv) and the temperature change (ΔT) as shown in **Eq. 5.22**

$$\mathrm{H(kW)} = \dot{m}\left(\frac{\mathrm{kg}}{\mathrm{s}}\right) \times \mathrm{Hv}\left(\frac{\mathrm{kJ}}{\mathrm{K.\,kg}}\right) \times \Delta\mathrm{T} \quad \left(\mathrm{Hv} = \frac{2260\mathrm{kJ}}{\mathrm{kg.\,K}}\right) \tag{5.22}$$

b. The heat of combustion of coal was calculated by using the mass flow rate of coal ($\dot{m}$) and the coal calorific value (H_{CV}) as shown in **Eq. 5.23.**

$$\mathrm{H(kW)} = \dot{\mathrm{m}}\left(\frac{\mathrm{kg}}{\mathrm{s}}\right) \times \mathrm{H_{CV}}\left(\frac{\mathrm{kJ}}{\mathrm{kg}}\right) \quad \left(\mathrm{H_{CV}} = \frac{27\mathrm{MJ}}{\mathrm{kg}}\right) \tag{5.23}$$

c. The enthalpy for reactions 1 to 5 in

d.

e.

f.

g.

h. Table 5.5, were calculated by using **Eq. 5.21**.

(iv) The amounts of coal needed were calculated from the difference in enthalpy-out and enthalpy-in and divided by the calorific value of coal.

5.4.1.1 Standard enthalpy/heat of formation

The standard enthalpy values for the reactants and products during thermal process are given in **Table 5.1**. The standard enthalpy/heat of formation gives the thermodynamic data for reactions that takes place. It shows the measure of the energy released or consumed when one mole of a substance is created under standard conditions *i.e*., constant pressure of 1 atm and at room temperature of 25 °C. As it can be seen in **Table 5.1**, the standard enthalpies of formations are negative. This is an indication that the formation of a compound from its elements is an exothermic reaction.

Table 5.1 Standard enthalpy/heat of formation (Speight, 2017)

Compound	**Heat of formation**		Mol mass
	kJ/mol	**kJ/kg**	**g/mol**
Na_2SO_4	-1 387.1	-9 768	142
$NaHCO_3$	-932.3	-11 099	84
NaHS	-257.7	-4 602	56
Na_2S	-443.3	-5 683	78
$CaSO_4$	-1 425.2	-10 479	136
$CaSO_4 \cdot 2H_2O$	-2 022.6	-11 759	172
$CaSO_4 \cdot ½H_2O$	-1 575.0	-10 862	145
CaS	-482.4	-68 914	72
$BaSO_4$	-1 473.2	-6 323	233
BaS	-460.0	-2 722	169
CO_2	-393.5	-8 943	44
H_2O	-285.8	-15 879	18
C	0.0	0	12

5.4.1.2 Standard Gibbs free energy of formation

The standard Gibbs free energy of formation for the thermal reduction of $NaSO_4$, $CaSO_4.2H_2O$ and $BaSO_4$ are given in **Table 5.2**. The standard Gibbs free energy of formation of a compound is the free energy change that occurs when 1 mole of the compound is synthesized from its constituent elements, each in their standard state. It is defined as a measure of a compound's stability relative to its elements. As it can be seen in **Table 5.2**, the standard Gibbs free energy of formations for all the reactants and products are negative. The negative value indicates that, the reaction is spontaneous, and a positive value indicates that the reaction is non-spontaneous.

Table 5.2 Standard Gibbs free energy of formation (Speight, 2017)

Compound	**Gibbs free energy**		**Mol mass**
	kJ/mol	**kJ/kg**	**g/mol**
Na_2SO_4	-1,270.2	-8,945	142

NaHCO3	-848.7	-10,104	84
NaHS	-249.8	-4,461	56
Na_2S	-438.1	-5,617	78
$CaSO_4$	-1,309.1	-9,626	136.0
$CaSO_4 \cdot 2H_2O$	-1,797.5	-10,451	172.0
$CaSO_4 \cdot ½H_2O$	-1,436.8	-9,909	145.0
CaS	-477.4	-6,631	72.0
$BaSO_4$	-1,362.2	-5,846	233.0
BaS	-456.0	-2,698	169.0
CO_2	-394.4	8,963	44.0
H_2O	-237.1	-13,174.4	18.0
C	0.0	0.0	12.0
Steam	-228.6	-12,700.6	18.0

5.4.1.3 Standard entropy values

Entropy is the physical property that is most associated with a state of disorder, randomness, or uncertainty in a reaction. It is the measure of how the energy of a reaction system energy is spread out or dispersed. As it can be seen in

Table 5.3, the standard entropy of the compounds used in this study are positive indicating that a system is more disordered.

Table 5.3 Standard entropy values (Speight, 2017)

Compound	Standard entropy		Mol mass
	J/mol·K	J/kg·K	g/mol
Na2SO4	149.6	1,053.5	142.0
NaHCO3	150.2	1,788.1	84.0
NaHS	121.8	2,175.0	56.0
Na_2S	103.3	1,324.4	78.0
$CaSO_4$	108.4	797.1	136.0
$CaSO_4 \cdot 2H_2O$	194.1	1,128.5	172.0
$CaSO4 \cdot ½H_2O$	130.5	900.0	145.0
CaS	56.5	784.7	72.0
$BaSO_4$	132.2	567.4	233.0
BaS	78.2	462.7	169.0
CO_2	213.8	4,858.8	44.0
Steam	188.8	10,490.8	18.0
H_2O	70.0	3,886.1	18.0
C	5.7	478.3	12.0

5.4.1.1 Specific heat capacity values for reactant and products

Specific heat capacity is defined as the amount of heat it takes to raise the temperature of 1 kg of a substance by 1 °C with no change in state.

Table 5.4 shows the specific heat capacities of all the compounds used in this study.

Table 5.4 Specific heat capacity values for reactants and products

Compound	**Specific heat capacity**		**Mol mass**	**Reference**
	kJ/K.mol	**kJ/K.kg**	**g/mol**	
Na_2SO_4	0.128	0.901	142	Speight, J G(2017)
$NaHCO_3$	0.088	1.043	84	
NaHS	-	-	56	
Na_2S	0.083	1.062	78	
$CaSO_4 \cdot 2H_2O$	0.186	1.081	172	(Robie, Russell-Robinson, & Hemingway, 1989)
$CaSO_4$	0.099	0.728	136	Speight, J G(2017)
$CaSO_4 \cdot ½H_2O$	0.442	2.570		
C	0.009	0.710	12	
CaS	0.047	0.658	72	

CO_2	0.037	0.848	44	
H_2O	0.075	4.186	18	
Steam	0.035	1.950	18	
$BaSO_4$	0.102	0.436	233	
BaS	0.049	0.292	169	
Coal		1.260		Engineering toolbox

5.4.1.2 Reaction energy values for various reactions

The heat of reaction can be defined as the amount of energy released or absorbed in the reaction. As it can be seen in

Table 5.5, the reactions are endothermic since they require energy from the environment to proceed hence a plus sign is put in front of the amount of energy absorbed from the environment into the reactants for the reaction to occur. The only exothermic reaction in

Table 5.5 was the one of $NaHCO_3$ and NaHS production via Na_2S.

Table 5.5 Reaction energy values for various reactions

No	Reaction	Heat of reaction, Hrxn (Eq. 5.21)	Heat of reaction, Hrxn	Gibbs Free Energy of reaction (Eq 5.18)	Entropy of reaction (Eq 5.19)
		kJ/mol	kJ/kg product	kJ/mol	kJ/mol·K
1	$Na_2SO_4 + 2C \rightarrow Na_2S + 2CO_2$	156.8	1 104.1	43.3	0.387
2	$Na_2S + CO_2 + H2O \rightarrow NaHCO_3 + NaHS$	-67.4	-864.1	-28.9	0.231
3	$CaSO_4{\cdot}2H_2O \rightarrow CaSO_4 + 2H_2O$	25.7	3 501	14.12	0.054
4	$CaSO_4{\cdot}2H_2O \rightarrow CaSO_4{\cdot}½H_2O + 1½H_2O$	18.9	2 734	4.99	0.075
5	$CaSO_4 + 2C \rightarrow CaS + 2CO_2$	155.78	11 216	42.92	0.376
6	$BaSO_4 + 2C \rightarrow BaS + 2CO_2$	226.17	38 223	117.42	0.374

5.4.2 Mass and energy balance models for reduction of Na_2SO_4, $CaSO_4$ and $BaSO_4$

A material and energy balance model can be used to determine the amount of coal needed for the reduction of metal sulphate compounds. The mass and energy were determined using an easy-to-use Excel- balance template which allows easy modification of the plant model. The reference enthalpies of each species were zero at 25 °C. All physical properties and equations used were found in Perry's Handbook of Chemical Engineering (Green & Southard, 2019).

In **Table 5.6** it was calculated that 14.9 t/h coal is needed for converting 50 t/h Na_2SO_4 to Na_2S. In **Table 5.7** it was calculated that 11.7 t/h coal is needed for converting 31.63 t/h $CaSO_4$ to CaS. In **Table 5.8** it was calculated that 9.6 t/h coal is needed for converting 50 t/h $BaSO_4$ to BaS.

Table 5.9 summarizes the previous results and shows that the coal usage per Mmol MSO_4 varies between 42.2 and 50.4 t coal/Mmol compound. It is noted that coal to $BaSO_4$ ratio is less than that for the coal to $CaSO_4$ ratio. This, together with the lower solubility of $BaSO_4$, makes $BaSO_4$ and attractive option for the processing of Na_2SO_4 to Na_2S. In terms of the energy required, it can be concluded that less energy is needed for the conversion of $BaSO_4$ into BaS (1480 MJ/t $BaSO_4$ or 344.9 kJ/mol $BaSO_4$) than for the conversion of $CaSO_4$ into CaS (3 657 MJ/t CaSO4 or 497.4 kJ/mol $CaSO_4$) (**Table 5.9**). The corresponding values for Na_2SO_4 amounted to (1 950 MJ/t Na_2SO_4 or 276.9 kJ/mol Na_2SO_4).

Table 5.6 Calculation of coal needed for the processing of 50 ton/h Na_2SO_4 to Na_2S

	Input (Mass) (t/h)	Output (Mass)(t/h)	T1 (°K)	T2 (°K)	Cp (KJ/kg.K)	H_f (KJ/mol)	Hv (KJ/kg)	Enthalpy (MJ/h)	Hrxn (MJ/mol)
ROUTE A	**Step 1. Reduction ($Na2SO_4$ + 2C → Na2S + 2CO_2)**								
Total Inputs								97 771	**-1.3871**
Input								285	
Na_2SO_4	50.0		298.0	303.0	0.90	-1 387		225	-1.3871
Coal for reduction	11.27		298.0	303.0	1.06	0.00		59.8	0.0000
Coal for combustion	3.61						27 000.0	97 486	
Total outputs								97 771	**-1.2303**
Outputs								42 567	
Na_2S		27.46	303.0	1 073.0	1.06	-443.3		22 449	-0.4433
CO_2		30.99	303.0	1 073.0	0.84	-393.5		20 118	-0.7870
Heat of reaction NaS_2		27.46				156.8		**55 204**	0.1568
Total Energy required for step 1	3.6							**97 486**	
Total coal usage	14.9								
Coal usage (t coal/t wet gypsum)	0.1								
Na_2SO_4 for Route A (MJ/t Na_2SO_4)								1 950	
Coal (MJ/kg)								27.0	
Coal required (kg/t Na_2SO_4)								72.2	
Coal required (kg/h) (equal to cell C9)								3 611	
	Step 2. Carbonation Na2S + CO_2 + H_2O → $NaHCO_3$ + NaHS								
Inputs									-0.0674
Na_2S	27.46		298.0	298.0	1.06	-443.3			-0.4433
H_2O	6.34		298.0	298.0	4.19	-285.8			-0.2858
CO_2	15.49				0.84	-393.5			-0.3935
Outputs									
$NaHCO_3$		29.58	298.0	298.0	1.04	-932.3			-0.9323
NaHS		19.72	298.0	298.0	-	-257.7			-0.2577
Reaction energy								**-23 733**	-0.0674
Total energy for route A								**73 753**	
Note 1. Sensible heat, E= mCpΔT									
Note 2. Carbon content of reductant coal (%)			75						

Table 5.7 Calculation of coal needed for the processing of 50 ton/h $CaSO_4 \cdot 2H_2O$ to CaS

Parameter	Input (Mass) (t/h)	Output (Mass) (t)	T1 (°K)	T2 (°K)	Cp (KJ/kg.K)	H_f (KJ/mol)	Hv (KJ/kg)	Enthalpy (MJ/h)	Hrxn (MJ/mol)

Wet gypsum	**50.00**								
Moisture content (%)	20.0								
	Step 1. Drying H_2O (aq) → H_2O (g)								**0.00**
Total inputs								**29 409**	
Input (Sensible)								426	
$CaSO_4.2H_2O$	**40.00**		298	303.0	1.08	**-2 023**		216	**-2.02**
H_2O	10.00		298	303.0	4.19	-285.8		209	-0.29
Combustion of Coal	1.07						27 000	28 984	
Total output								**29 409**	
Output (Sensible)								6 809	
$CaSO_4.2H_2O$		40.00	298	378.0	1.08			3 460	**-2.02**
H_2O (Free)		10.00	298	378.0	4.19			3 349	**-0.29**
Steam		10.00	378	378.0	1.95	-285.83		0	**-0.24**
H_2O to Steam		10.00					2 260	22 600	
	Step 2. Gypsum to Anhydride $CaSO_4.2H_2O$ → $CaSO_4 + 2H_2O$								**0**
Total inputs								**35 083**	
Input (Sensible)								3 460	
$CaSO_4.2H_2O$	40.00		298	378.0	1.08	-2 023		3 460	**-2.02**
Coal (for drying)	1.17						27 000	31 623	
Total outputs									
Output (Sensible)								**35 083**	**0.00**
$CaSO_4$		31.63	298	673.0	0.73	-1 425		8 634	**-1.43**
H_2O (Free)		8.37	298	373.0	4.19			2 631	
Steam		8.37	373	673.0	1.95			4 898	
Steam		8.37	373	673.0	1.95	-285.8	2 260	18 921	**-0.24**
									0.00
	Step 3. Reduction ($CaSO_4$ + 2C → CaS + $2CO_2$)								
Total Inputs								**63 749**	
Input								8 681	
$CaSO_4$	31.63		298	673.0	0.73	-1 425		8 634	**-1.43**
Coal for reduction	7.44		298	303.0	1.26	0.00		47	
Coal for Step 3	2.04						27 000	55 068	**0.00**
Total outputs								**63 749**	
Outputs (Sensible)								27 521	
CaS		16.74	303	1 273.0	0.66	-482.4		10 687	**-0.48**
CO_2		20.47	303	1 273.0	0.85	-393.5		16 834	**-0.79**
Heat of reaction CaS		16.74				155.8		36 228	**0.16**
Total coal usage (t/h)	**11.7**						27 000	**86 900**	
Total Energy Required	**3.22**							115 675	

Table 5.8 Calculation of coal needed for the processing of 50 ton/h $BaSO_4$ to BaS

	Input (Mass) (t/h)	**Output (Mass) (t/h)**	**T1 (°K)**	**T2 (°K)**	**Cp (KJ/kg.K)**	**H_f (KJ/mol)**	**Hv (KJ/kg)**	**Enthalpy (MJ/h)**	**Heat of formation Hrxn (MJ/mol)**
ROUTE A	**Step 1. Reduction ($BaSO_4$ + 2C → BaS + $2CO_2$)**								
Total Inputs								74 176	**-1.473**
Input								152.2	
$BaSO_4$	50.00		298.0	303.0	0.44	-1 473.2		109.0	-1.473
Coal for reduction	6.87		298.0	303.0	1.26	0.0		43.3	0.000

Coal for combustion	2.74						27 000	74 023	
Total outputs								74 176	**-1.247**
Outputs								25 641	
BaS		36.27	303.0	1 273.0	0.29	-460.0		10 254	-0.460
CO_2		18.88	303.0	1 273.0	0.84	-393.5		15 387	-0.787
Heat of reaction BaS		36.27				226.17		**48 534**	0.226
Total Energy required for step 1								**74 023**	
Total coal usage	9.6								
$BaSO_4$ for Route A (MJ/t $BaSO_4$)								1 480	
Coal (MJ/kg)								27.0	
Coal required (kg/t $BaSO_4$)								54.8	
Coal required (kg/h) (equal to cell C9)								2 742	
Standard Heat of Reaction, $H_{rxns}(BaSO_4 + 2C = BaS + 2CO_2)$(KJ/mol)								226.2	
	Step 2. Carbonation BaS + CO_2 + H_2O → $BaCO_3$ + H_2S)								
Inputs									-0.094
BaS	36.27		298.0	298.0	0.29	-460.0			-0.460
H_2O	3.86		298.0	298.0	4.20	-285.8			-0.286
CO_2	9.44				0.84	-393.5			-0.394
Outputs									
$BaCO_3$		42.35	298.0	298.0	0.44	-1 213.0			-1.213
H_2S		7.30	298.0	298.0	1.01	-20.6			-0.021
Reaction energy								**-20 227**	-0.094
Total energy for route A								**53 796**	

Table 5.9 Comparison of coal and energy needed for the reduction of Na_2SO_4, $CaSO_4$ and $BaSO_4$

Compound	**Mol mass**	**MSO_4**	**Coal**	**Coal / MSO_4 ratio**	**coal / MSO_4**	**Energy needed**		
	g/mol	**t/h**	**t/h**	**t/t**	**t / Mmol**	**MJ/h**	**MJ/t compound**	**kJ/mol compound**
Na_2SO_4	142	50.00	14.88	0.298	42.25	97 486	1 950	276.9
$CaSO_4$	136	31.63	11.73	0.371	50.42	115 675	3 657	497.4
$BaSO_4$	233	50.00	9.61	0.192	44.78	74 023	1 480	344.9

5.4.3 Reduction of $CaSO_4$ and $BaSO_4$

Table 5.10 shows the optimum conditions, as determined **experimentally**, for the reduction of $CaSO_4 \cdot 2H_2O$ to CaS.

Table 5.11 shows the results for the reduction of $BaSO_4$ to BaS. It was found that the optimum temperature for both reactions was 1000 °C, the optimum reaction time for $BaSO_4$ reduction was 20 min versus 60 min for $CaSO_4 \cdot 2H_2O$ and the higher the carbon-metal sulphate ratio, the better was the conversion. From the results in **Table 5.8**, at a C/$CaSO_4$ mol/mol ratio of 2 and higher, and at a temperature of 1000 °C, 100 % of the $CaSO_4$ was converted to CaS. For lower C/$CaSO_4$ mol/mol ratios, the CaS yield was linearly related to the ratio. Unreacted $CaSO_4$ remained with the CaS.

Table 5.12 and **Table 5.13** show the $CaSO_4$ and $BaSO_4$ reduction using coal as a redundant, simulation result via modelling with the Pyrosim Mintek model. From the experimental results obtained through thermal studies in the laboratory (**Table 5.10** and **Table 5.11**), it can be seen that the calculated experimental values corresponded well with the predicted values using the Pyrosim Mintek models (**Table 5.12** and **Table 5.13**).

At lower temperatures (200 °C to 600 °C) the CaS yield dropped from 92,7% to 0% while the $CaCO_3$ yield increased from 3 to 99%. In a previous study it was noted that the kinetics of $CaCO_3$ formation at low temperatures were slow and not feasible for implementation (Mokgohloa, *et al*., 2022). CO was the main gas product from carbon at the higher C/$CaSO_4$ ratios (**Eq. 5.24**), while CO_2 replaced CO as main product, as the ratio decreased (**Eq. 5.25**).

$$CaSO_4 + 4C \rightarrow CaS + 4CO \quad (5.24)$$

$$CaSO_4 + 2C \rightarrow CaS + 2CO_2 \quad (5.25)$$

The reduction of $BaSO_4$ was similar to that of $CaSO_4$, as seen, at a C/$BaSO_4$ mol/mol ratio of 2 and higher, and at a temperature of 1000 °C, more than 98% of the $BaSO_4$ was converted to BaS. As the C/$BaSO_4$ ratio in the experiments was always greater than 2, the $BaCO_3$ did not exceed 2%. It can also be seen that at lower temperatures (200 °C to 600 °C) the BaS yield dropped from 86% to 0% while the $CaCO_3$ and S were formed together with BaS. In addition, CO was the main gas product from carbon at the higher C/$BaSO_4$ ratios (**Eq. 5.26**), while CO_2 replaced CO as main product, as the ratio decreased (**Eq. 5.27**).

$$BaSO_4 + 4C \rightarrow BaS + 4CO \quad (5.26)$$

$$BaSO_4 + 2C \rightarrow BaS + 2CO_2 \quad (5.27)$$

Table 5.10 Effect of various parameters (bold) on the rate of thermal reduction of $CaSO_4 \cdot 2H_2O$

Parameter	**Unit**	**Exp No**											
Exp No		**6.1**	**6.2**	**6.3**	**6.4**	**7.1**	**7.2**	**7.3**	**7.4**	**8.1**	**8.2**	**8.3**	**8.4**
Chemical		$CaSO_4.2H_2O$	$CaSO_4.2H_2O$	$CaSO_4.2H_2O$	$CaSO_4.2H_2O$	$CaSO_4.2H_2O$	$CaSO_4.2H_2O$	$CaSO_4.2H_2O$	$CaSO_4.2H_2O$	$CaSO_4.2H_2O$	$CaSO_4.2H_2O$	$CaSO_4.2H_2O$	$CaSO_4.2H_2O$
mol mass		172	172	172	172	172	172	172	172	172	172	172	172
Product		CaS	CaS	CaS	CaS	CaS	CaS	CaS	CaS	CaS	CaS	CaS	CaS
mol mass		72	72	72	72	72	72	72	72	72	72	72	72
Mass	G	20.00	20.00	20.00	20.00	20.00	20.00	20.00	20.00	20.00	20.00	20.00	20.00
Carbon	G	5.58	5.58	5.58	5.58	5.58	5.58	5.58	5.58	1.40	2.79	4.19	5.58
Ash content	%	8	8	8	8	8	8	8	8	8	8	8	8
Ash	G	0.45	0.45	0.45	0.45	0.45	0.45	0.45	0.45	0.11	0.22	0.33	0.45
Unreacted C	G	4.17	3.46	2.71	3.47	4.76	3.96	2.67	3.51	0.78	1.76	2.44	2.83
C/Chem mole ratio		3.68	3.68	3.68	3.68	3.68	3.68	3.68	3.68	**0.92**	**1.84**	**2.76**	**3.68**
Temperature	°C	**900**	**950**	**1000**	**1100**	1000	1000	1000	1000	1000	1000	1000	1000
Reaction time	Min	60	60	60	60	**15**	**30**	**60**	**120**	60	60	60	60
Conversion	%	35.16	55.03	72.51	57.02	16.78	48.46	70.30	44.68	21.92	32.18	53.93	71.54

$$\text{Mass of Cas in product sample used for titration (mg)} = \frac{(40+32)}{2} \text{x } \frac{[(CV)_{I2} - (CV)_{S2O3}]}{Sample\ mass\ (mg)} \text{ x } 1000$$

Mass of CaS in product after treatment of 20 g of $CaSO_4 \cdot 2H_2O$ (g)

$$= \left(\frac{\text{Mass of CaS in product (g)}}{1000}\right) \text{x} \left(\frac{20}{0.05\text{g}}\right)$$

$$\text{Conversion (\%)} = \left(\frac{\text{Mass of CaS in product (g)}}{72}\right) \div \left(\frac{20}{172}\right) \text{x } 100$$

Table 5.11 Effect of various parameters (bold) on the rate of thermal reduction of $BaSO_4$

Parameter	**Unit**	**Exp No**											
Exp No		**16.1**	**16.2**	**16.3**	**16.4**	**17.1**	**17.2**	**17.3**	**17.4**	**18.1**	**18.2**	**18.3**	**18.4**
Chemical		$BaSO_4$	$BaSO_4$	$BaSO_4$	$BaSO_4$	$BaSO_4$	$BaSO_4$	$BaSO_4$	$BaSO_4$	$BaSO_4$	$BaSO_4$	$BaSO_4$	$BaSO_4$
mol mass		233	234	235	236	237	238	239	240	241	242	243	244
Product		BaS	BaS	BaS	BaS	BaS	BaS	BaS	BaS	BaS	BaS	BaS	BaS
mol mass		169	170	171	172	173	174	175	176	177	178	179	180
Mass	g	20.00	20.00	20.00	20.00	20.00	20.00	20.00	20.00	20.00	20.00	20.00	20.00
Carbon	g	4.11	4.11	4.11	4.11	4.11	4.11	4.11	4.11	1.03	2.06	3.09	4.11
Ash content	%	8	9	10	11	12	13	14	15	16	17	18	19
Ash	g	0.33	0.37	0.41	0.45	0.49	0.53	0.58	0.62	0.16	0.35	0.56	0.78
Unreacted C	g	3.07	2.88	1.99	2.56	3.51	2.92	1.97	2.59	0.33	1.13	1.96	2.25
C/Chem mole ratio		3.67	3.65	3.63	3.60	3.58	3.55	3.52	3.50	**0.87**	**1.72**	**2.56**	**3.39**
Temperature	°C	**900**	**950**	**1000**	**1100**	1000	1000	1000	1000	1000	1000	1000	1000
Reaction time	min	20	20	20	20	**5**	**10**	**20**	**40**	20	20	20	20
Conversion	%	34.74	60.08	86.93	59.67	13.34	42.18	88.17	58.16	18.10	28.80	50.74	82.56

Mass of BaS in product sample used for titration (mg)

$$= \frac{(137 + 32)}{2} \text{ x } \frac{[(CV)_{I2} - (CV)_{S2O3}]}{Sample\ mass\ (mg)}$$

Mass of BaS in product after treatment of 20 g $BaSO_4$(g)

$$= \left(\frac{\text{Mass of CaS in product (g)}}{1000}\right) \text{x} \left(\frac{20}{0.05\text{g}}\right)$$

Conversion (%)

$$= \left(\frac{\text{Mass of CaS in product (g)}}{169}\right)$$

$$\div \left(\frac{20\text{ g}}{233}\right) \text{x } 100$$

Table 5.12 Thermal reduction of $CaSO_4$ (Pyrosim Mintek simulation)

No	Conversion					Input data							Matte						
	$CaCO_3$	S	CaS	$CaSO_4$	C/ $CaSO_4$	Temp	$CaSO_4$	$CaSO_4$	Coal	Coal	H_2O	Volatiles	$CaCO_3$	CaO	CaS	$CaSO_4$	S	C	Total
	%	%	%	%	%	°C	%	kg/h	kg/h	%	%	%	%	%	%	%	%	%	%
	Effect of $C/CaSO_4$ ratio							142.00											
1	0.26	0.00	100.65	0.00	3.40	1000.00	100.00	100.00	40.00	75.00	5.40	19.60	0.35		98.35	0.00		0.41	99.11
2	0.42	0.00	100.45	0.01	2.13	1000.00	100.00	100.00	25.00	75.00	5.40	19.60	0.57		98.65	0.03		0.00	99.25
3	0.35	0.00	84.35	15.99	1.70	1000.00	100.00	100.00	20.00	75.00	5.40	19.60	0.42		72.88	26.09		0.00	99.39
4	0.25	0.00	63.40	36.95	1.28	1000.00	100.00	100.00	15.00	75.00	5.40	19.60	0.26		47.25	52.02		0.00	99.53
	Effect of temperature																		0.00
5	0.42	0.00	100.45	0.01	2.13	1000.00	100.00	100.00	25.00	75.00	5.40	19.60	0.57		98.65	0.03	0.00	0.00	99.25
6	3.17	0.00	92.72	2.11	2.13	600.00	100.00	100.00	25.00	75.00	5.40	19.60	4.46		94.08	4.05	0.00	0.91	103.50
7	22.26	0.00	77.89	0.00	2.13	400.00	100.00	100.00	25.00	75.00	5.40	19.60	27.57		69.44	0.01	0.00	2.85	99.86
8	99.46	0.00	0.78	0.32	2.13	200.00	100.00	100.00	25.00	75.00	5.40	19.60	92.54		0.52	0.41	0.00	6.49	99.96

Matte						Volatiles						Gas						Pyrosim
C	S	CaS	$CaSO_4$	$CaCO_3$	Total	CO	SO_2	H_2S	CO_2	H_2O	S	H_2O	CO	CO_2	H_2S	S	SO_2	MWh/t
kg/h	kg/h	kg/h	kg/h	kg/h	kg/h	%	%	%	%	%	%	%	%	%	%	%	%	
12.00	32.00	78.00	142.00	106.00														
0.42	0.00	53.29	0.00	0.19	53.70	74.97		0.07	16.95	3.40		1.91	65.62	23.31	0.08			1.02
0.00	0.00	53.18	0.01	0.31	53.50	10.92		0.18	81.35	2.94		1.25	7.22	84.53	0.15			1.06
0.00	0.00	44.66	15.99	0.26	60.90	1.97		0.19	90.49	2.73		1.12	1.26	90.84	0.15			0.80
0.00	0.00	33.56	36.95	0.18	70.70	1.50		0.18	91.23	2.45		1.00	0.96	91.27	0.14			0.57
0.00	0.00	53.18	0.01	0.31	53.50	10.92		21.99	81.35	0.18	0.00	1.25	7.22	84.53	0.15	0.00		1.39
0.88	0.00	49.08	2.11	2.33	54.00	6.24		1.49	85.41	2.09		0.14	0.28	86.74	12.85			1.06
2.85	0.00	41.24	0.00	16.37	59.30	2.91		4.11	83.13	0.54	6.74	0.23	0.20	83.94	3.22	4.95		0.87
6.49	0.00	0.41	0.32	73.13	79.00	0.00		5.85	33.72	0.16	53.87	0.08	0.00	38.90	5.24	45.26		0.20

Table 5.13 Thermal reduction of $BaSO_4$ (Pyrosim Mintek simulation)

Yield (% mol/mol $BaSO_4$)						Input data							Matte						
$BaCO_3$	S	BaS	$BaSO_4$	H_2S	C/ BaSO4	Temp	$BaSO_4$	$BaSO_4$	Coal	Coal	H_2O	Vola-tiles	$BaCO_3$	BaO	BaS	$BaSO_4$	S	C	Total
Effect of C/$BaSO_4$ ratio:							%	kg/h	kg/h	%	%	%	%	%	%	%	%	%	%
0.41	0.00	119.97	0.35	-20.32	5.83	1 000	100.00	100.00	40.00	75.00	5.40	19.60	0.35		87.02	0.00	0.00	11.60	83.00
1.02	0.00	99.09	1.18	-0.27	3.64	1 000	100.00	100.00	25.00	75.00	5.40	19.60	1.18		98.09	0.00	0.00	0.36	99.62
1.59	0.00	98.74	1.84	-0.58	2.91	1 000	100.00	100.00	20.00	75.00	5.40	19.60	1.84		97.78	0.00	0.00	0.05	99.68
1.90	0.00	98.17	2.19	-0.36	2.18	1 000	100.00	100.00	15.00	75.00	5.40	19.60	2.19		97.14	0.40	0.00	0.00	99.72
Effect of Temperature:																			
1.02	0.00	99.35	1.18	-0.53	3.64	1 000	100.00	100.00	25.00	75.00	5.40	19.60	1.18	0.01	98.09	0.00		0.36	99.63
						800	100.00	100.00	25.00	75.00	5.40	19.60							
13.16	0.59	86.97	13.63	-1.19	3.64	600	100.00	100.00	25.00	75.00	5.40	19.60	13.63		77.23	0.00	0.10	8.94	99.90
69.96	0.00	29.86	65.06	5.08	3.64	400	100.00	100.00	25.00	75.00	5.40	19.60	65.06		23.82	0.28	0.00	10.81	99.97
68.09	72.93	0.00	63.23	-36.16	3.64	200	100.00	100.00	25.00	75.00	5.40	19.60	63.23		0.00	24.30	11.00	12.39	110.93

Matte					Volatiles								Gas								Pyrosim
S	BaS	$BaSO_4$	$BaCO_3$	Total	CO	SO_2	H_2S	CO_2	H_2O	S	Total	Vol	H_2O	CO	CO_2	H_2S	SO_2	S	Total	Gas	MWh/t product
kg/h	kg/h	kg/h	kg/h	kg/h	%	%	%	%	%	%	%	kg/h	%	%	%	%	%	%	%	kg/h	
0.00	87.02	0.35	0.35	83.00	88.71		0.08	0.89	3.74				3.74	88.71	0.89	0.08					1.16
0.00	71.87	1.18	0.86	73.00	81.62		0.26	10.17	3.30				1.92	73.87	14.46	0.29					1.13
0.00	71.62	1.84	1.35	73.00	57.71		0.51	34.21	2.96	0.00			1.53	46.40	43.22	0.49					0.92
0.00	71.21	2.19	1.60	73.10	16.29		0.80	75.73	2.54	0.00			1.10	10.99	80.24	0.66		0.00			0.69
																			0.00		
0.00	72.06	1.18	0.87	73.20	81.62		0.26	10.17	3.30		95.35		1.92	73.87	14.46	0.29			90.53		1.13
0.08	63.08	13.63	11.13	81.60	18.57		5.42	67.65	0.89		92.52		0.39	12.48	71.42	4.43			88.71		0.53
0.00	21.66	65.06	59.15	90.90	0.51		8.83	53.46	0.11	27.60	90.51		0.05	0.35	56.68	7.25		21.32	85.64		0.45
10.02	0.00	63.23	57.57	101.00	0.00		11.53	32.76	0.28	42.44	87.01		0.13	0.00	35.88	9.78		33.86	79.65		0.11

5.4.4 Oxidation of CaS and BaS

The reduction of $CaSO_4$ and $BaSO_4$ requires reducing conditions during the reaction and even in the cooling stage thereafter. If the product is in contact with air/oxygen, back oxidation may take place (**Eq 5.28** and **Eq 5.29**)

$$CaS + 2O_2 \rightarrow CaSO_4 \quad (5.28)$$

$$BaS + 2O_2 \rightarrow BaSO_4 \quad (5.29)$$

Figure 5.2 and **Figure 5.3** show the effect of oxygen on the products, CaS and BaS, respectively, as determined with TGA studies. In the presence of oxygen, the sulphide is oxidised back to the sulphate compound at temperatures above 600°C, as indicated by the mass increase due to the conversion of sulphides to sulphates. Under reducing condition (N_2 atmosphere), no oxidation was observed. This shows the importance that no oxygen should be in contact with the product, even during the cooling stage.

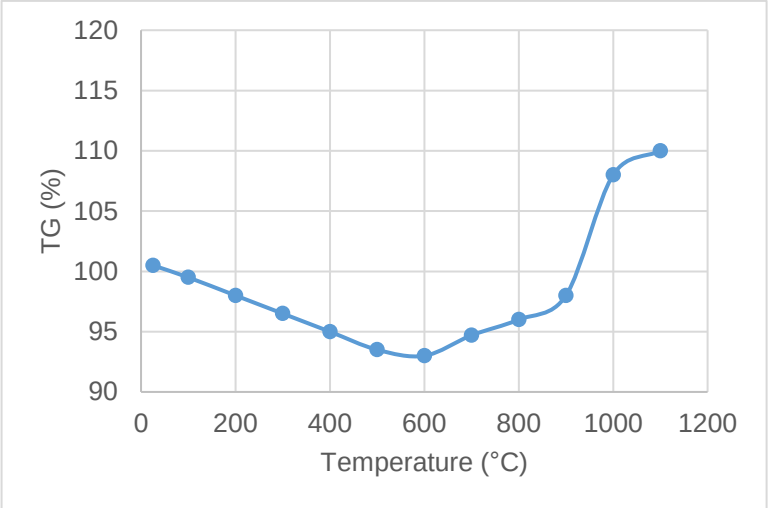

Figure 5.2 Oxidation of CaS when O_2 is present

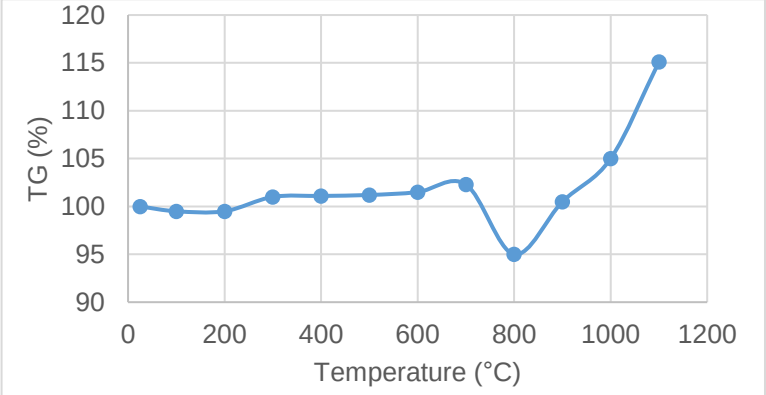

Figure 5.3 Oxidation of BaS when O_2 is present

5.4.5 Conversion of Na_2SO_4 to Na_2S

Unlike $CaSO_4$ and $BaSO_4$ that can be converted easily to their sulphides through thermal reduction, it is not easy in the case of Na_2SO_4, because it melts in the same temperature range (960 °C) where the conversion takes place. This is the reason why it was necessary to study the formation of Na_2S from Na_2SO_4 via reaction with CaS or BaS.

5.4.5.1 Solubility of sulphate, sulphide and bicarbonate compounds

The solubility of alkaline-earth earth is important for many industrial applications and calculations related to the geochemical assessment of natural brine (Voigt, 2015). Except for magnesium sulphate, alkaline-earth sulphate is characterized by a very low solubility. Their low solubility makes a significant difference in the reported solubility of these minerals compared to the solubility of chlorides and alkaline-earth bromides. The sulphate is partially dissolved with the hydrating energy. The solubility of $MgSO_4$ and $CaSO_4$ also depends on whether the salt is hydrated. **Table 5.14** compares the solubility of different alkaline substances and alkaline products. Barium sulphate is present as a white precipitate in solution. Slight formation of a precipitate indicates that barium sulphate is insoluble. Exact solubility is of practical importance for the development of separation methods for a particular pair or group of compounds or for the removal of most of a particular compound, for example from preparation to testing (Stenger, 1996). They may also be useful in connection with theoretical studies of ionic solubility or other possible parameters of the solution. For example, the solubility of barium sulphate is only 0.07% (mole/mole) of that of calcium sulphate (0.0105 / 15 x 100) (**Table 5.14**). However, the solubility of $BaSO_4$ increases the ionic strength of water. Excess sulphate ions tend to coagulate the precipitate, and the excess barium ions tend to disperse the precipitate.

Table 5.14 Solubility of various alkalis and alkali products.

Compound	**Solubility**		**Temp**
	mmol/L	g/L	°C
$CaSO_4 \cdot 2H_2O$	15	2.64	25.0
CaS	186	13	25.0
$NaHCO_3$	1300	109	25.0
$MgSO_4$	2 161.3	260	0.0
$MgSO_4$	2 801.3	337	20.0
$BaSO_4$	0.0105	0.002448	20.0
Na_2S	2540	198	25.0
Na_2SO_4	2873	408	25.0
$Ca(HS)_2$	A strong function of H_2S partial pressure		
NaHS	88 200	4 939	25.0

5.4.5.2 Conversion of Na_2SO_4 to Na_2S via BaS

Na_2S is the raw material in the formation of Na_2CO_3, nano $CaCO_3$ and $Mg(OH)_2$. Since direct conversion of Na_2S from Na_2SO_4 is a problem, it needs to be converted from either CaS or BaS. The reason for the difficulty in the direct conversion is that Na_2SO_4 melts in the same temperature range, 800 °C to 900 °C, where Na_2SO_4 is converted to Na_2S.

The purpose of this section was to identify which one of CaS or BaS would be the most suitable for the production of Na_2S. It is of industrial interest to convert alkali and alkaline earth metal sulphates into their carbonates. The sulphate compounds are generally produced as waste that needs to be stockpiled, while the carbonates are important raw material in industrial processes. Barium sulphate is mined as a raw material and converted to $BaCO_3$ to be used for glass manufacturing, brick manufacturing, oil-drilling, ceramics, photographic and chemical industries. $CaSO_4$ is produced in the fertilizer industry when sulphuric acid (H_2SO_4) is used for leaching phosphoric acid (H_3PO_4) from phosphate rock ($Ca_5(PO_4)_3F$) and when sulphate (SO_4^{2-})-rich acidic effluents are neutralized with $Ca(OH)_2$ or $CaCO_3$. Na_2SO_4 is produced when SO_4^{2-}-rich acidic effluents are neutralized with Na_2CO_3 or NaOH.

If Na_2S is produced using the CaS route, it will contain more $CaSO_4$ than when produced via the BaS route, due to the higher solubility of $CaSO_4$. The purpose of this section was to study the formation of Na_2S from both BaS and CaS. **Table 5.15** shows, through OLI simulations, that Na_2S formed stoichiometrically when BaS was reacted with Na_2SO_4, as indicated by the

reduction of sulphate from 1 000 mmol/L to 0.3 mmol/L. This finding was also **experimentally** confirmed (

Table 5.16). This experiment was repeated, using OLI simulations, with CaS to determine how effective SO_4^{2-} was removed from solution when precipitated as $CaSO_4$, instead of $BaSO_4$. **Table 5.17** shows that in the case of CaS, sulphate was decreased from only 1000 mmol/L to only 254.8 mmol/L. The difference in sulphate concentrations were due to the difference in the solubilities of $BaSO_4$ (0.0285 mg/L) and $CaSO_4 \cdot 2H_2O$ (2 640 mg/L).

The above finding showed that the BaS route will be the preferred route for Na_2S production for applications where the presence of sulphate is a problem. Therefore, from the results obtained in **Table 5.15** and

Table 5.16, It is thus clear that the BaS-route is the preferred on for processing Na_2SO_4 to Na_2S and the downstream products.

Table 5.15 Conversion of Na_2SO_4 to Na_2S via BaS (OLI simulation)

BaS [mmol]	Na_2SO_4 [mmol]	$BaSO_4$ (Barite) - Sol [mmol] (Y2)	$S^{(+6)}$ (aq) [mmol] (Y2)	$Ba^{(+2)}$ (aq) [mmol] (Y2)	$S^{(-2)}$ (aq) [mmol] (Y2)	$Na^{(+1)}$ (aq) [mmol] (Y2)	pH
0	1 000	0	1 000.0	0	0	2 000	7.4
100	1 000	100	900.0	0	100	2 000	12.5
200	1 000	200	800.0	0	200	2 000	12.7
300	1 000	300	700.0	0	300	2 000	12.8
400	1 000	400	600.0	0	400	2 000	12.9
500	1 000	500	500.0	0	500	2 000	12.9
600	1 000	600	400.0	0	600	2 000	13.0
700	1 000	700	300.0	0	700	2 000	13.0
800	1 000	800	200.0	0	800	2 000	13.0
900	1 000	900	100.0	0	900	2 000	13.1
1 000	1 000	1 000	0.3	0	1 000	2 000	13.1

Temp = 25 °C; pH = 12.5 to 13.1

Table 5.16 Conversion of Na_2SO_4 to Na_2S via BaS (Experimental)

Parameter	Value
BaS (g)	10.00
Purity (%)	95.00
BaS (meq)	112.43
Na_2SO_4 (g)	8.40
H_2O (mL)	200.00
Na_2S (q)	4.37
Na_2S (meq)	112.00
NaS production (%)	99.62

Table 5.17 Conversion of Na_2SO_4 to Na_2S via CaS (OLI simulation)

CaS [mmol]	Na_2SO_4 [mmol]	$CaSO_4 \cdot 2H_2O$ (Gypsum) [mmol] (Y2)	$Ca(OH)_2$ (Portlandite) – (s) [mmol] (Y2)	$S^{(+6)}$ (aq) [mmol] (Y2)	$Ca^{(+2)}$ (aq) [mmol] (Y2)	$S^{(-2)}$ (aq) [mmol] (Y2)	$Na^{(+1)}$ (aq) [mmol] (Y2)	Ph
0	1 000	0.0	0.0	1 000.0	0.0	0	2 000	7.4
100	1 000	81.6	0.0	918.4	18.4	100	2 000	12.5
200	1 000	178.9	0.0	821.1	21.1	200	2 000	12.7
300	1 000	269.1	6.7	730.9	24.2	300	2 000	12.7
400	1 000	346.7	26.5	653.3	26.8	400	2 000	12.7
500	1 000	421.9	48.0	578.1	30.1	500	2 000	12.6
600	1 000	494.5	71.5	505.5	34.0	600	2 000	12.6
700	1 000	563.7	97.3	436.3	39.0	700	2 000	12.6
800	1 000	629.1	125.6	370.9	45.3	800	2 000	12.5
900	1 000	689.9	156.9	310.1	53.2	900	2 000	12.5
1 000	1 000	745.2	191.2	254.8	63.5	1 000	2 000	12.4

Temp = 25°C; pH = 12.5 to 12.4

5.4.6 Production of $NaHCO_3$ and NaHS from Na_2S and CO_2

For the processing of Na_2S to valuable products like $NaHCO_3$, NaHS and Na_2CO_3, it needs to be reacted with the CO_2, that is produced in the thermal stage, where coal is used both as energy source and as the reductant.

5.4.6.1 Solubilities of sodium compounds

The production of $NaHCO_3$ and NaHS from the reactants, Na_2S and CO_2 (**Eq. 5.30**) is influenced by the solubility of the reactant, Na_2S and the products, $NaHCO_3$ and NaHS (**Table 5.18**). $NaHCO_3$ and NaHS are produced by reacting with CO_2 and water (**Eq. 5.30**). This reaction occurs at an elevated temperature of 60 – 70 °C and a pressure of 1-2 atm.

$$Na_2S + CO_2 + H_2O \rightarrow NaHS + NaHCO_3 \quad (5.30)$$

Table 5.19 and

Table 5.20 show the behaviour of **Na_2S** added to water in steps of 1 000 mmol/L (78 g/L). As it can be seen in

Table 5.19 and

Table 5.20, Na_2S dissolved completely below the solubility of 2 619.8 mmol/L (*i.e*., 204.3 g/L). At higher dosages a portion of the Na_2S remained as a hydrated solid in suspension, first as $Na_2S \cdot 9H_2O$ and then as $Na_2S \cdot 5H_2O$ as more water is available.

Table 5.18 Solubility of Na_2S, $NaHCO_3$ and NaHS (OLI simulation)

Compound	**Temp**	**Solubility**		**Table No**
	(°C)	**mmol/L**	**g/L**	
Na_2S	25	2 620	204.3	19
Na_2S	80	6 101	475.9	21
$NaHCO_3$	25	1 110	86.5	22
$NaHCO_3$	0	640	49.9	23
NaHS	25	88 203	4 939.4	24

Table 5.19 Solubility of Na_2S (higher concentrations) (OLI simulation)

Na_2S [mmol]	**Na_2S [g/L]**	**pH**	**Temp (°C)**	**$S^{(-2)}$ (aq) [mmol] (Y2)**	**$Na_2S.9H_2O$ [mmol] (Y2)**	**$Na_2S.5H_2O$ [mmol] (Y2)**	**$Na^{(+1)}$ (aq) [mmol] (Y2)**	**H_2O [mmol] (Y2)**
0	0	7.0	25	0	0	0	0	55 508
1 000	78	13.1	25	1 000	0	0	2 000	55 364
2 000	156	13.4	25	2 000	0	0	4 000	55 311

3 000	234	13.6	25	2 393	607	0	4 786	49 841
4 000	312	13.6	25	1 638	2 362	0	3 275	34 106
5 000	390	13.6	25	882	4 118	0	1 764	18 372
6 000	468	13.6	25	127	5 873	0	253	2 637
7 000	546	15.6	25	0	5 127	1 873	0	0
8 000	624	15.6	25	0	3 877	4 123	0	0
9 000	702	15.6	25	0	2 627	6 373	0	0
10 000	780	15.6	25	0	1 377	8 623	0	0

Table 5.20 Solubility of Na_2S (lower concentration (OLI simulation)).

Na_2S [mmol]	**Na_2S [g/L]**	**pH**	**Temp (°C)**	**$S^{(-2)}$ (aq) [mmol] (Y2)**	**$Na_2S.9H_2O$ [mmol] (Y2)**	**$Na_2S.5H_2O$ [mmol] (Y2)**	**$Na^{(+1)}$ (aq) [mmol] (Y2)**	**H_2O [mmol] (Y2)**
0	0	7.0	25	0	0	0	0	55 508
300	23	12.8	25	300	0	0	600	55 425
600	47	12.9	25	600	0	0	1 200	55 393
900	70	13.1	25	900	0	0	1 800	55 371
1 200	94	13.2	25	1 200	0	0	2 400	55 352
1 500	117	13.3	25	1 500	0	0	3 000	55 336
1 800	140	13.4	25	1 800	0	0	3 600	55 321
2 100	164	13.4	25	2 100	0	0	4 200	55 307
2 400	187	13.5	25	2 400	0	0	4 800	55 293
2 700	211	13.6	25	2 620	80	0	5 239	54 562
3 000	234	13.6	25	2 393	607	0	4 786	49 841

Table 5.21 shows the effect of temperature on the solubility of Na_2S. As it can be seen in **Table 5.21**, the solubility of Na_2S increased with an increasing temperature. It can be concluded that more Na_2S dissolved in hot water than in cold water. The increase in solubility of Na_2S as the temperature increases can be due to the fact that the dissolution process of Na_2S in water being an endothermic process. An increase in temperature leads to an increase of input energy hence the energy of the water molecules increases. This makes Na_2S molecules more easily and more effectively, resulting in a higher solubility.

Table 5.21 Effect of temperature on the solubility of Na_2S (OLI simulation)

Temperature [°C]	Na_2S [mmol] (Y2)	Na_2S soluble (g)	NaS_2 solubility (g/L)	$Na_2S.9H_2O$ [mmol] (Y2)	$Na_2S.5H_2O$ [mmol] (Y2)	S^{-2} [mmol] (Y2)	HS^{-1} [mmol] (Y2)	H_2O [mmol] (Y2)	Na^{+1} [mmol] (Y2)	$H_2S \cdot$ (aq) [mmol] (Y2)	pH (Y2)
0	6000	3.7	107	5 952	0	43	4.4	1 934	96	0.0	14.1
10	6000	5.5	143	5 929	0	65	6.1	2 139	142	0.0	13.9
20	6000	8.1	185	5 896	0	95	8.8	2 434	208	0.0	13.7
30	6000	12.2	233	5 844	0	143	13.6	2 903	313	0.0	13.6
40	6000	20.5	296	5 737	0	239	24.5	3 851	526	0.0	13.5
50	6000	301.6	377	0	2 134	3 472	394.4	44 445	7 732	0.0	13.5
60	6000	375.3	425	0	1 189	4 249	561.6	49 002	9 622	0.0	13.4
70	6000	468.0	475	0	0	5 199	801.4	54 707	12 000	0.0	13.3
80	6000	468.0	476	0	0	5 065	934.8	54 573	12 000	0.0	13.1

Note Na_2S solubility (g/L) = Na_2S soluble x 55 500 / mmol H_2O

pH = 14.1 to 13.1

Table 5.22 and**Table 5.23** show the solubility of $NaHCO_3$, as 1 109.5 mmol/L (86.5 g/L) at 25 °C and 640.2 mmol/L (49.9 g/L) at 0 °C respectively. The solubility of $NaHCO_3$ as it can be seen in

Table 5.22 and **Table 5.23**, decreased when the temperature was reduced from 25 °C to 0 °C. This behaviour is the caused by the fact that the dissolution of $NaHCO_3$ involves an acid-base reaction, $NaHCO_3$ form carbonic acid (H_2CO_3) when it reacts with water, thereby dissociating to form water and carbon dioxide gas. The dissolution is an exothermic reaction, as the temperature increases, the equilibrium shifts towards the products side, hence, more carbon dioxide gas is produced as less $NaHCO_3$ is dissolved.

Table 5.22 Solubility of $NaHCO_3$ at 25 °C (OLI simulation)

$NaHCO_3$ [mmol]	$NaHCO_3$ (g/L)	Temp	pH	$NaHCO_3$ (Nahcolite) – (s) [mmol] (Y2)	$Na^{(+1)}$ (aq) [mmol] (Y2)	$C^{(+4)}$ (aq) [mmol] (Y2)
0	0.0	25	7.0	0	0	0
300	25.2	25	7.9	0	300	300
600	50.4	25	7.9	0	600	600
900	75.6	25	7.8	0	900	900
1 200	100.8	25	7.8	0	1 200	1 200
1 500	126.0	25	7.7	196	1 304	1 304
1 800	151.2	25	7.7	496	1 304	1 304
2 100	176.4	25	7.7	796	1 304	1 304
2 400	201.6	25	7.7	1 096	1 304	1 304
2 700	226.8	25	7.7	1 396	1 304	1 304
3 000	252.0	25	7.7	1 696	1 304	1 304

Table 5.23 Solubility of $NaHCO_3$ at 0 °C (OLI simulation)

$NaHCO_3$ [mmol]	$NaHCO_3$ (g/L)	Temp	pH	$NaHCO_3$ (Nahcolite) – (s) [mmol] (Y2)	$Na^{(+1)}$ (aq) [mmol] (Y2)	$C^{(+4)}$ (aq) [mmol] (Y2)
0	0.0	0	7.46	0	0	0
300	25.2	0	8.19	0	300	300
600	50.4	0	8.10	0	600	600
900	75.6	0	8.05	0	900	900
1 200	100.8	0	8.04	280	920	920
1 500	126.0	0	8.04	580	920	920

1 800	151.2	0	8.04	880	920	920
2 100	176.4	0	8.04	1180	920	920
2 400	201.6	0	8.04	1480	920	920
2 700	226.8	0	8.04	1780	920	920
3 000	252.0	0	8.04	2080	920	920

In the dissolution of NaHS in water, NaHS dissolves and the salt forms sodium (Na^+) and hydrosulphide (HS^-) ions. There is an attraction of negative ends of water molecules (oxygen atoms) to the positive Na^+ ions whereas the HS^- ions are attracted to the positive ends of water molecules (hydrogen atoms). Due to H_2S being produced, is important to carry out this experiment in a well-ventilated area.)

Table 5.24 shows that NaHS has a solubility of 88 203 mmol/L or 4 939 g/L NaHS. At higher concentrations NaHS decomposes into Na_2S and H_2S (**Eq. 5.31**).

$$2NaHS \rightarrow Na_2S + H_2S \quad (5.31)$$

Table 5.24 Solubility of NaHS (OLI simulation)

NaHS [mmol]	pH	Na_2S – (s) [mmol] (Y2)	$S^{(2-)}$ (aq) [mmol] (Y2)	H_2S – (vap) [mmol] (Y2)	$HS^{(1-)}$ [mmol] (Y2)	$S^{(2-)}$ [mmol] (Y2)	H_2S - (aq) [mmol] (Y2)	$Na^{(1+)}$ (aq) [mmol] (Y2)	H_2O [mmol] (Y2)
0	7.0	0.0	0	0	0	0.00	0.00	0	55 508
10 000	9.7	0.0	10 000	0	9 994	2.82	2.83	10 000	55 508
20 000	9.9	0.0	20 000	0	19 998	0.75	0.75	20 000	55 508
30 000	10.3	0.0	30 000	0	29 999	0.25	0.08	30 000	55 508
40 000	10.6	0.0	40 000	0	40 000	0.07	0.01	40 000	55 508
50 000	10.9	0.0	50 000	0	50 000	0.01	0.00	50 000	55 508
60 000	11.3	0.0	60 000	0	60 000	0.00	0.00	60 000	55 508
70 000	11.6	0.0	70 000	0	70 000	0.00	0.00	70 000	55 508
80 000	12.1	0.0	80 000	0	80 000	0.00	0.00	80 000	55 508
90 000	12.5	1 796.8	86 406	1 797	86 406	0.00	0.00	86 406	55 508
100 000	12.5	6 796.8	86 406	6 797	86 406	0.00	0.00	86 406	55 508

Temp. = 25 °C

5.4.6.2 *Reaction between Na_2S and CO_2*

Table 5.25 shows the OLI simulated reaction of Na_2S and CO_2 at 25°C. As it can be seen in

Table 5.25**,** 10 000 mmol of Na_2S (780 g Na_2S) reacted with 1 L H_2O to form 1 377 mmol $Na_2S{\cdot}9H_2O$ and 8 622.9 mmol $Na_2S{\cdot}5H_2O$ at pH 12.2, with no free H_2O left. The reason why a portion of the Na_2S was converted to $Na_2S{\cdot}5H_2O$ and not $Na_2S{\cdot}9H_2O$, was due to the

availability of water. Upon addition of 8 000 mmol CO_2 to pH 9.3, 2 656 mmol $Na_2CO_3.NaHCO_3 \cdot 2H_2O$ formed. By increasing the CO_2 dosage to 20 000 mmol, 18 417 mmol $NaHCO_3$ and 8 875 mmol H_2S formed (**Eq. 5.32**). The solid $NaHCO_3$ can be converted to Na_2CO_3 and H_2S to elemental sulphur.

$$Na_2S + 2CO_2 + 2H_2O \rightarrow 2NaHCO_3 + H_2S \quad (5.32)$$

Table 5.26 below shows the same result as in

Table 5.25 except that in the case of a lower Na_2S concentration (2 500 mmol/kg H_2O and less than), no $Na_2S \cdot 9H_2O$ or $Na_2S \cdot 5H_2O$ formed due to the availability of sufficient water.

$NaHCO_3$ has a lower solubility at 0 °C (640.2 mmol/L or 49.9 g/L; **Table 5.23)** than at 25 °C (1 109.5 mmol/L or 86.5 g/L;

Table 5.22). Therefore, it may be beneficial to separate $NaHCO_3$ from NaHS at 0 °C, rather than at room temperature.

Table 5.27 shows that 2 119 mmol $NaHCO_3$ formed at 0°C, which is more than the 1 941 mmol $NaHCO_3$ that formed at 25°C (

Table 5.26). Due to the small benefit associated with cooling to 0°C, it is recommended that the reaction be carried out at room temperature. The optimum concentration needs to be determined for the production of $NaHCO_3$ from Na_2S and CO_2.

Table 5.28 showed that $NaHCO_3$ (nahcolite) formed at concentration up to 10 000 mmol/kg water. At higher dosages the complex $Na_2CO_3 \cdot NaHCO_3$ formed.

Table 5.25 Reaction between 10 000 mmol Na_2S and CO_2 at 25 °C (OLI simulation)

CO_2 [mmol]	Na_2S [mmol] (Y2)	pH	$NaHCO_3$ (Nahcolite) – (s) [mmol] (Y2)	$Na_2CO_3.NaHCO_3.2H_2O$ – (s) [mmol] (Y2)	$NaHCO_3$ - (aq) [mmol] (Y2)	$Na_2S.9H_2O$ [mmol] (Y2)	$Na_2S.5H_2O$ [mmol] (Y2)	H_2S – (vap) [mmol] (Y2)	H_2S - (aq) [mmol] (Y2)	HS^{-1} [mmol] (Y2)	S^{-2} [mmol] (Y2)	HCO_3^{-1} [mmol] (Y2)
0	10 000	15.6	0	0	0.0	1 377	8 623	0	0.00	0	0.0	0.0
2 000	10 000	12.2	0	0	0.2	9	5 873	0	0.00	3 999	119.1	0.6
4 000	10 000	12.2	0	0	0.4	0	1 875	0	0.00	**7 998**	**127.0**	**1.3**
6 000	10 000	11.2	0	2 018	2.7	0	0	0	0.05	**9 973**	**26.5**	**5.2**
8 000	10 000	9.3	2 399	2 656	30.8	0	0	868	4.09	9 128	0.6	41.8
10 000	10 000	9.3	9 691	0	33.8	0	0	225	4.51	9 769	0.7	45.6
12 000	10 000	9.2	11 736	0	46.0	0	0	2 151	6.80	7 842	0.6	55.3
14 000	10 000	9.0	13 747	0	64.6	0	0	4 083	10.66	5 906	0.5	71.9
16 000	10 000	8.7	15 693	0	93.6	0	0	5 999	17.33	3 983	0.4	103.7
18 000	10 000	8.4	17 417	0	135.5	0	0	7 766	27.69	2 206	0.2	172.1
20 000	10 000	8.1	18 417	0	172.0	0	0	8 875	34.80	1 090	0.1	281.1

Temp = 25°C

Table 5.26 Reaction between 2 500 mmol Na_2S and CO_2 at 25 °C (OLI simulation)

CO_2 [mmol]	Na_2S [mmol] (Y2)	pH	$NaHCO_3$ (Nahcolite) - Sol [mmol] (Y2)	$NaHCO_3$ - (aq) [mmol] (Y2)	HCO_3^{-1} [mmol] (Y2)	HS^{-1} [mmol] (Y2)	H_2S^{-} (aq) [mmol] (Y2)	S^{-2} [mmol] (Y2)
0	2 500	13.6	0	0	0	220	0.00	2 280
250	2 500	13.1	0	0	0	571	0.00	1 929
500	2 500	12.7	0	0	0	1 029	0.00	1 471
750	2 500	12.4	0	0	0	1 512	0.00	988
1 000	2 500	12.0	0	1	1	2 002	0.01	498
1 250	2 500	10.8	0	16	24	2 460	0.11	39
1 500	2 500	9.7	77	168	257	2 495	1.47	3
1 750	2 500	9.6	557	179	265	2 495	2.06	3
2 000	2 500	9.4	1 034	190	274	2 495	3.24	2
2 250	2 500	9.1	1 506	203	285	2 492	6.68	1
2 500	2 500	8.3	1 942	216	299	2 458	41.83	0

Temp = 25°C; Pressure = 1 atm

Table 5.27 Reaction between 2 500 mmol Na_2S and CO_2 at 0 °C (OLI simulation)

CO_2 [mmol]	Na_2S [mmol] (Y2)	pH	$NaHCO_3$ (Nahcolite) – (s) [mmol] (Y2)	$NaHCO_3^{\cdot}$ (aq) [mmol] (Y2)	HCO_3^{-1} [mmol] (Y2)	HS^{-1} [mmol] (Y2)	$H_2S^{\cdot}$ (aq) [mmol] (Y2)	S^{-2} [mmol] (Y2)
0	2 500	14.1	0	0	0.0	96	0.0	951.1
250	2 500	13.4	0	0	0.0	510	0.0	841.5
500	2 500	13.0	0	0	0.0	1 004	0.0	725.6
750	2 500	12.8	0	0	0.0	1 502	0.0	627.0
1 000	2 500	12.6	0	0	0.1	2 001	0.0	498.8
1 250	2 500	11.0	0	9	4.1	2 487	0.2	12.8
1 500	2 500	9.7	233	178	86.6	2 496	2.9	0.7
1 750	2 500	9.7	710	192	95.2	2 496	3.1	0.7
2 000	2 500	9.7	1 187	206	104.0	2 496	3.2	0.7
2 250	2 500	9.6	1 665	219	112.2	2 495	4.0	0.6
2 500	2 500	8.7	2 119	230	117.5	2 467	32.8	0.1

Temp = 0°C; Pressure = 1 atm

Table 5.28 Reaction between 0 to 20 000 mmol Na_2S and 0 to 20 000 mmol CO_2 at 25 °C (OLI simulation)

CO_2 [mmol]	Na_2S [mmol] (Y2)	pH	$NaHCO_3$ (Nahcolite) – (s) [mmol] (Y2)	$Na_2CO_3.NaHCO_3.2H_2O$ – (s) [mmol] (Y2)	H_2S – (vap) [mmol] (Y2)	CO_2 – (vap) [mmol] (Y2)	$S^{(-2)}$ (aq) [mmol] (Y2)	$Na^{(+1)}$ (aq) [mmol] (Y2)	$C^{(+4)}$ (aq) [mmol] (Y2)	H_2O [mmol] (Y2)
0	0	7.0	0	0	0	0.00	0	0	0	55 508
2 000	2 000	8.3	1 358	0	0	0.00	2 000	2 642	642	55 508
4 000	4 000	8.6	3 599	0	29	0.48	3 971	4 401	400	55 508
6 000	6 000	8.8	5 697	0	80	0.39	5 920	6 303	303	55 508
8 000	8 000	9.1	7 722	0	142	0.26	7 858	8 278	278	55 508
10 000	10 000	9.3	9 691	0	225	0.17	9 775	10 309	309	55 508
12 000	12 000	9.3	3 210	4 274	4 446	3.31	7 554	7 968	239	55 508
14 000	14 000	9.5	0	6 903	7 059	2.71	6 941	7 290	191	55 508
16 000	16 000	9.8	0	7 896	8 091	0.92	7 909	8 313	208	55 508
18 000	18 000	10.1	0	8 851	9 143	0.36	8 857	9 446	297	55 508
20 000	20 000	10.5	0	9 706	10 291	0.20	9 709	10 881	587	55 508

Temp = 25°C; Pressure = 1 atm

5.4.6.3 *Separation of $NaHCO_3$ and NaHS*

$NaHCO_3$ can be recovered from a $NaHCO_3$/NaHS solution by using the solubility differences (**Table 5.18**). OLI simulations showed that 204.3 g/L Na_2S can dissolve in water at 25°C (**Table 5.18)**. An experiment was planned to confirm that sulphide (S^-) will remain in solution when contacted with CO_2.

Table 5.29 shows the experimental results when a 50 mL Na_2S solution was contacted with 250 mL CO_2 (at STP), where the CO_2/Na_2S mole ratios varied between 5 and 0.5. The

experimental set-up used was shown in, **Figure 3.4 section 3.5.2.** It was noted that the sulphide (S^-) in solution, as measured with the iodine method, corresponded closely with the Na_2S that was prepared, as expected from **Eq. 5.30.**

Table 5.29 Sulphide in solution after Na_2S has reacted with CO_2 (Experimental)

Na_2S prepared	**Na_2S prepared**	**Na_2S**	**CO_2/Na_2S ratio**	**Volume**	**pH**	**Sulphide measured**
mg Na_2S/ 50 mL	**g Na_2S/L**	**meq/50mL**		**Ml**		**mg Na_2S/50mL**
174	3.5	4.5	5.0	50	12.1	166
435	8.7	11.2	2.0	50	12.0	410
871	17.4	22.3	1.0	50	11.5	819
1 741	34.8	44.6	0.5	50	11.4	1 716

CO_2 volume = 250 Ml

The results obtained from OLI simulations (

Table 5.28), and the one done experimentally (

Table 5.29), showed that Na_2S has a high solubility of 204.3 g/L. This can be determined through sulphide analyses (as Na_2S) (**Eq. 5.33**) or Alkalinity analyses (as Na_2S) (**Eq. 5.34**).

$$\mathrm{Na_2S}\left(\frac{\mathrm{mg}}{\mathrm{L}}\right) = \text{eq. mass of } \mathrm{Na_2S} \times \left(\mathrm{V_{I2}} \times \mathrm{N_{I2}} - \mathrm{V_{S_2O_3}} \times \mathrm{N_{S_2O_3}}\right) \times \frac{1000}{\text{Sample Vol}} \quad (5.33)$$

$$= \frac{78}{2} \times (10 \times 0.096 - 4.6 \times 0.1) \times \frac{1000}{0.1}$$

$$\mathrm{Na_2S}\left(\frac{\mathrm{mg}}{\mathrm{L}}\right) = \text{eq. mass of } \mathrm{Na_2S} \times \mathrm{V_{HCl}} \times \mathrm{N_{HCl}} \times \frac{1000}{\text{Sample Vol}} \quad (5.34)$$

$$= \frac{78}{2} \times 5 \times 1 \times \frac{1000}{0.1}$$

Table 5.30 shows that: (i) the Na_2S concentration, determined with both the sulphide and the alkalinity method, as 195 g/L (as Na_2S), corresponded with the prepared concentration of 200 g/L (as Na_2S), (ii) Sulphide remained in solution, as expected from **Eq. 5.30**. It only converted from S^{2-} to HS^-. (iii) $NaHCO_3$ precipitated according to **Eq. 5.30** when Na_2S reacted with CO_2, as indicated by the reduction of alkalinity from 136 500 mg/L (as Na_2S) at a CO_2/Na_2S mole ratio of 1, to 113 100 (as Na_2S) at a CO_2/Na_2S mole ratio of 4. The reason why the alkalinity was not already lower at a ratio of 1 can be ascribed to incomplete mixing between the large volume of CO_2 needed, *i.e*., (250 mL) and the small volume of the concentrated Na_2S solution (4.3 mL of a 200 g/L Na_2S solution). This challenge was overcome by bubbling CO_2 through a 100 mL solution of 200 g/L Na_2S.

Table 5.31 shows how the pH dropped from 13.1 to 8.2 as CO_2 was added, the Na_2S concentration remained constant around 195 975 mg/L Na_2S, as S^{2-} was converted to HS^- and alkalinity decreased by 50% as $NaHCO_3$ precipitated (from 198 900 to 93 600), according to **Eq. 5.34**.

Table 5.30 Effect of CO_2 addition to a Na_2S solution of 200 g/L Na_2S

Reactants	**Mass (g)**	**CO_2/Na_2S mole ratio**

		Feed	**1.00**	**2.00**	4.00
Na_2S (g)	200	0.88	0.88	0.88	0.88
H_2O (g)	1 000	4.38	4.38	4.38	4.38
CO_2 (g)	113	0.49	0.49	0.99	1.97
CO_2 (mL)		251.28	251.3	502.6	1 005.1
Parameters					
pH		13.1	10.6	9.5	8.7
Sulphide (mg/L Na_2S)		195 000	206 700	198 900	187 200
Alkalinity (mg/L Na_2S)		195 000	136 500	120 900	113 100

Tamp = 25°C

Table 5.31 $NaHCO_3$ precipitation when CO_2 is bubbled through a 200 g/L Na_2S solution (100 mL)

Time	**pH**	**S^{2-}**	**Alk**
Min		**mg/L Na_2S**	**mg/L Na_2S**
0	13.1	198 900	198 900
5	12.1	202 800	167 700
10	11.1	191 100	159 900
15	10.0	200 850	140 400
20	9.1	195 000	117 000
21	8.2	187 200	93 600
Average		195 975	

5.4.6.4 *Na_2CO_3 from $NaHCO_3$*

Na_2CO_3 can be produced from $NaHCO_3$ by heating it to 200 °C. In the case of dilute $NaHCO_3$ solutions, it can be concentrated by removing water though freeze crystallization or through evaporation.

Table 5.32 shows the conversion of $NaHCO_3$ to Na_2CO_3 during evaporation at 100 °C. It is noted that the double salt, $Na_2CO_3 \cdot NaHCO_3 \cdot 2H_2O$, formed as described in **Eq. 5.35**. At a

concentration of 500 mmol $NaHCO_3$/20 535 mmol H_2O, it was noted that $NaHCO_3$(aq) start to precipitate as Na_2CO_3/$NaHCO_3$.2H_2O, which corresponds to a concentration of 48.7 g/L $NaHCO_3$.

$$3NaHCO_3 + H_2O \rightarrow Na_2CO_3.NaHCO_3 + CO_2 + 2H_2O \quad (5.35)$$

Table 5.32 Conversion of $NaHCO_3$ to Na_2CO_3

$NaHCO_3$ [mmol] (Y2)	H_2O [mmol]	$NaHCO_3$ (Nahcolite) – (s) [mmol] (Y2)	$Na_2CO_3.NaHCO_3.2H_2O$ – (s) [mmol] (Y2)	$Na^{(+1)}$ (aq) [mmol] (Y2)	H_2O – (vap) [mmol] (Y2)	CO_2 – (vap [mmol] (Y2)
500	55 500	0	0.0	500	29 279	204
500	50 505	0	0.0	500	28 118	206
500	45 510	0	0.0	500	26 750	209
500	40 515	0	0.0	500	25 143	212
500	35 520	0	0.0	500	23 263	214
500	30 525	0	0.0	500	21 082	217
500	25 530	0	0.0	500	18 589	219
500	20 535	0	0.0	500	15 810	221
500	15 540	0	31.5	406	13 006	211
500	10 545	0	163.4	10	10 321	168

Temp = 100 °C; pH = 9.46

5.4.7 Production of $Mg(OH)_2$ from $MgSO_4$ and NaHS

The purpose of this section is to identify a way how only $Mg(OH)_2$(s) will be formed from brine streams rich in $MgSO_4$. During freeze-crystallization, $MgSO_4$ remains in solution due to its high solubility of 260 g/L (**Table 5.14**). The use of Na_2S appeared to be attractive as the products, Na_2SO_4, as shown in **Eq 5.36**, is highly soluble (408 g/L) (**Table 5.14**). The use of BaS is not attractive as $BaSO_4$, would form which has a low solubility (0.0025 g/L) (**Table 5.14)**.

5.4.7.1 Reaction between Na_2S and $MgSO_4$

Table 5.33 shows the OLI simulation for the conversion of $MgSO_4$ to $Mg(OH)_2$ with Na_2S. From Table 5.33, it can be seen that $Mg(OH)_2$ formed when $MgSO_4$ was contacted with Na_2S (**Eq. 5.36**). When 500 mmol Na_2S was contacted stepwise with $MgSO_4$, it was noted that (i)

the pH dropped from 12.9 to 9.3 as $Mg(OH)_2$ formed, (ii) only 250 mmol $Mg(OH)_2$ formed from 500 mmol Na_2S, showing that two Na_2S reacted with one $MgSO_4$, (iii) the remaining 250 mmol Mg^{2+} was linked to SO_4^{2-}, and (iv) the Na^+ from Na_2S was linked to HS^-

$$MgSO_4 + 2Na_2S + 2H_2O \rightarrow Mg(OH)_2 + 2NaHS + Na_2SO_4 \quad (5.36)$$

From **Table 5.33**, OLI simulations further showed that, at concentrations above 2 100 mmol/L $MgSO_4$ and Na_2S, solid $Na_2SO_4.10H_2O$ precipitated together with $Mg(OH)_2$. In the case of $MgSO_4$ and CaS, solid gypsum precipitated together with $Mg(OH)_2$. The reaction shown in **Eq. 5.36** was confirmed experimentally by reacting Na_2S with $MgSO_4$ at $Na_2S/MgSO_4$ mole ratios of 1, 2 and 4 as shown in **Table 5.34**. It was also found that Mg^{2+} was removed as $Mg(OH)_2$ at a mole ration of 1 as indicated by the low alkalinity value of 124 800 and the low Mg^{2+} values where the ratio was 2 and higher. Sulphide remained high at the same concentration of the feed.

$Mg(OH)_2$(s) can be separated from the NaHS and the Na_2SO_4 through settling or filtration with a belt filter. The separation of Na_2SO_4 and NaHS can be done through freeze-crystallization as discussed in the next section.

Table 5.33 Conversion of $MgSO_4$ to $Mg(OH)_2$ with Na_2S (OLI simulation)

$MgSO_4$ [mmol]	Na_2S [mmol] (Y2)	pH	$MgSO_4$ [mmol] (Y2)	$Mg(OH)_2$ (Brucite) - [illegible]	$Mg^{(+2)}$ Aq [mmol] (Y2)	SO_4^{-2} [mmol] (Y2)	HS^{-1} [mmol] (Y2)	S^{-2} [mmol] (Y2)	$S^{(-2)}$ (aq) [mmol] (Y2)	$S^{(+6)}$ (aq) [mmol] (Y2)	$Na^{(+1)}$ (aq) [mmol] (Y2)
0	500	12.9	0	0	0.0	0.0	105.8	394.2	500	0	1 000
50	500	12.6	50	50	0.0	22.8	160.7	339.3	500	50	1 000
100	500	12.4	100	100	0.0	46.4	233.5	266.5	500	100	1 000
150	500	12.1	150	150	0.0	70.6	317.4	182.6	500	150	1 000
200	500	11.7	200	200	0.0	95.3	407.1	92.9	500	200	1 000
250	500	10.1	250	249	1.4	120.5	497.0	2.8	500	250	1 000
300	500	9.4	300	250	49.8	146.7	498.3	0.5	500	300	1 000
350	500	9.2	350	250	99.5	173.7	498.0	0.4	500	350	1 000
400	500	9.2	400	251	149.4	201.5	497.8	0.4	500	400	1 000
450	500	9.1	450	251	199.2	230.1	497.6	0.4	500	450	1 000
500	500	9.1	500	251	249.2	259.5	497.4	0.4	500	500	1 000

Temp = 25°C

Table 5.34 Effect of $Na_2S/MgSO_4$ mole ratio on the conversion of $MgSO_4$ to $Mg(OH)_2$

Parameter	**Feed**	**$Na_2S/MgSO_4$ mole ratio**			
		1	**2**	**4**	**Average**
Temperature (°C)		25	25	25	25
Na_2S (g/L)	400	400	400	400	400
Na_2S stock sol (g/L)	400	400	400	400	400
$MgSO_4$ stock sol (g/L)	616.9	616.9	616.9	616.9	616.9
Na_2S (g/L)		200	200	200	200
$MgSO_4$ (g/L)		308.46	154.23	77.12	
Na_2S stock sol (mL)	100	100	100	100	100
$MgSO_4$ stock sol (mL)	0	100	50	25	
H_2O (mL)		0.00	50.00	75.00	
Total Vol (mL)		200	200	200	200
Ph	13.13	10.68	10.41	10.28	
Sulphide mg/L Na_2S)	191 100	198 900	195 000	189 150	193 538
Alk (mg/L Na_2S)	202 800	124 800	140 400	167 700	
Mg^{2+} (mg/L Na_2S)		3 861.00	3 705.00	3 549.00	

5.4.7.2 *Separation of Na_2SO_4 and NaHS*

Na_2SO_4 can be separated from the NaHS through cooling as Na_2SO_4 has a solubility of only 45 g/L at 0 °C compared to 400 g/L at room temperature. The solubility of Na_2SO_4 was first studied for a pure Na_2SO_4 solution, with both OLI simulation (

Table 5.35) and experimentally (**Table 5.36**). OLI simulation showed that Na_2SO_4 has a solubility of 44.3 g/L at 0 °C. This compared well with the experimentally determined solubility of 53.1 g/L at 0 °C as showed in **Table 5.36**.

Table 5.35 Effect of temperature on the solubility of Na_2SO_4 (OLI simulation)

Temperature [°C]	Na_2SO_4 [mmol]	$Na_2SO_4.10H_2O$ (Mirabilite) [mmol] (Y2)	$S^{(+6)}$ (aq) [mmol] (Y2)	$Na^{(+1)}$ (aq) [mmol] (Y2)	SO_4 (g/L)	Na (g/L)	Na_2SO_4 (g/L)	H_2O [mmol] (Y2)
60	2 500	0.0	2 500.0	5 000.0	240.00	115.00	355.0	55 508
54	2 500	0.0	2 500.0	5 000.0	240.00	115.00	355.0	55 508
48	2 500	0.0	2 500.0	5 000.0	240.00	115.00	355.0	55 508
42	2 500	0.0	2 500.0	5 000.0	240.00	115.00	355.0	55 508
36	2 500	0.0	2 500.0	5 000.0	240.00	115.00	355.0	55 508
30	2 500	0.0	2 500.0	5 000.0	240.00	115.00	355.0	55 508
24	2 500	1 012.8	1 487.1	2 974.3	174.63	83.68	258.3	45 380
18	2 500	1 687.0	813.0	1 625.9	112.12	53.72	165.8	38 637
12	2 500	2 027.0	473.0	946.0	71.53	34.27	105.8	35 238
6	2 500	2 211.8	288.2	576.6	45.99	22.05	68.0	33 391
0	2 500	2 318.5	181.5	363.0	29.92	14.34	44.3	32 323

Table 5.36 Effect of temperature on the solubility of Na_2SO_4 (experimentally determined)

Temp.	pH	$Na_2SO_4.10H_2O$		
°C		g/L SO_4	g/L Na	g/L Na_2SO_4
25	6.76	89.35	46.98	136.33
20	6.98	62.62	33.04	95.66
15	7.08	66.00	34.96	100.96
10	7.26	50.31	25.33	75.64
5	7.34	37.46	18.86	56.32
0	7.73	35.29	17.81	53.10

The results collected with a pure Na_2SO_4 solution was repeated for a solution containing both Na_2SO_4 and NaHS using OLI simulation. **Table 5.37** shows the effect of temperature when 2 000 mmol NaHS (112.0 g) reacted with 1 000 mmol Na_2SO_4 (142 g) (OLI simulation). It was noted that 928.4 mmol $Na_2SO_4 \cdot 10H_2O$ crystallized from the 1 000 mmol Na_2SO_4 due to its decreased solubility at colder temperatures. NaHS remained in solution as it has a high solubility of 88 203 mmol/L at 25 °C (**Table 5.18**). NaHS can be concentrated through removal of water through freeze-crystallization.

The freeze-crystallization technology is essentially a freeze desalination process that separates a liquid phase from a dissolved solid phase. A temperature change of approximately 25 °C to 0 °C is required, which indicates a temperature drop of 25 °C or more. The freeze-crystallization principle shows the potential for economic efficiency in terms of low energy demand, low by-product contamination, process flexibility, simplicity, and the possibility of further use of low-temperature energy as a process by-product. The main advantage of freeze-crystallization over current wastewater treatment technologies such as distillation and evaporation ponds come from the much lower heat of fusion of ice (333 kJ/kg) compared to the heat of vaporization (2500 kJ /kg) of water (Mtombeni, *et al*., 2013).

Table 5.37 Separation of Na_2SO_4 and NaHS through solubility difference during cooling (OLI simulation)

Temperature [°C]	H_2O [mmol] (Y2)	Na_2SO_4 [mmol] (Y2)	$Na_2SO_4.10H_2O$ (Mirabilite) [mmol] (Y2)	NaHS [mmol] (Y2)	$S^{(-2)}$ (aq) [mmol] (Y2)	$SO_42-^{(+6)}$ (aq) [mmol] (Y2)	$Na^{(+1)}$ (aq) [mmol] (Y2)	$S^{(+6)}$ (aq) [mmol] (Y2)
25	55 508	1 000	0.0	2 000	2 000	1 000	4 000	1 000
23	55 508	1 000	0.0	2 000	2 000	1 000	4 000	1 000
20	55 508	1 000	86.6	2 000	2 000	913	3 827	913
18	55 508	1 000	338.6	2 000	2 000	661	3 323	661
15	55 508	1 000	519.2	2 000	2 000	481	2 962	481
13	55 508	1 000	649.7	2 000	2 000	350	2 701	350
10	55 508	1 000	744.6	2 000	2 000	255	2 511	255
8	55 508	1 000	813.8	2 000	2 000	186	2 372	186
5	55 508	1 000	864.4	2 000	2 000	136	2 271	136
3	55 508	1 000	901.4	2 000	2 000	99	2 197	99
0	55 508	1 000	928.4	2 000	2 000	72	2 143	72

Table 5.38 shows that Na^+ decreased from 37.3 g/L to 18.9 g/L as the temperature decreased from 25 °C to 0 °C when 600 mmol/L Na_2SO_4 (85.2 g/L) was mixed with 600 mmol/L NaHS (33.6 g/L). The SO_4^{2-} decreased from 51.8 to a low 0.9 g/L due to the high Na^+ concentration (**Eq 5.37**). The Na^+, SO_4^{2-} and S^{2-} initial concentrations of

the mixed solution amounted to 41.4, 57.6 and 19.2 g/L respectively. The sulphide concentration remained constant at 19.2 g/L. It was calculated that 72.14 g/L $Na_2SO_4 \cdot 10H_2O$ crystallized as indicated by the Na_2SO_4 concentrations. This is in line with what was predicted by OLI (**Table 5.37**).

$$Na_2SO_4 + 10H_2O \rightarrow Na_2SO_4 \cdot 10H_2O \quad (5.37)$$

Table 5.38 Effect of temperature on the removal of Na_2SO_4 in the presence of NaHS

Temp.	Na^+(aq)	SO_4^{2-}(aq)	$S^{2-(aq)}$	Ph	Na_2SO_4(s)
°C	g/L	g/L	g/L		
25	37.25	51.83	19.2	4.52	0.00
20	32.02	43.15	19.2	4.46	12.29
15	29.91	39.95	19.2	4.41	16.82
10	25.79	34.07	19.2	4.39	25.16
5	18.91	24.42	19.2	4.31	38.83
0	15.44	0.90	19.2	4.22	72.14

5.4.7.3 *Up-concentration of NaHS*

After removal of $NaHCO_3$ as a solid, NaHS remained in solution (Mashigwana, et al., 2022). **Figure 5.4** shows that when 1 000 mL of water (55 508 mmol) was reduced down to 150 mL (8 117 mmol) by freeze crystallization, the NaHS concentration in solution increased from 188 g/L to 1 180 g/L (21 100 mmol/L). The $NaHCO_3$ concentration would have increased to the same extent if the $NaHCO_3$ was not removed as a solid prior to water removal through freeze crystallization.

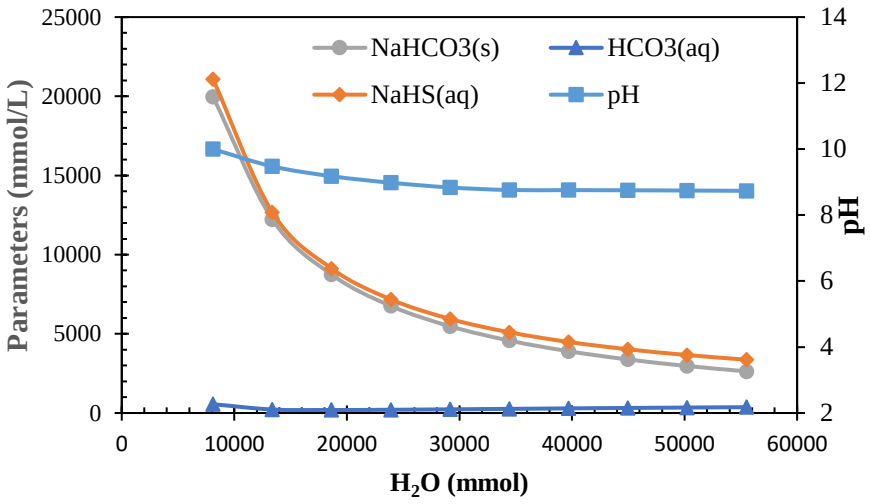

Figure 5.4 Concentration of NaHS by freeze-crystallization (Mashigwana, et al., 2022)

5.4.8 Sulphur from H_2S

5.4.8.1 H_2S oxidation with Fe^{3+}

H_2S gas is produced when BaS, CaS or Na_2S is contacted with CO_2 (**Eq. 5.32**). H_2S can be converted to S by using the Claus process (Elsner, *et al*., 2003).

$$H_2S + 1.5O_2 \rightarrow SO_2 + H_2O \quad (5.38)$$

$$2H_2S + SO_2 \rightarrow 3S + 2H_2O \quad (5.39)$$

$$3H_2S + 1.5O_2 \rightarrow 3S + 3H_2O \quad (5.40)$$

It would be attractive if H_2S can be converted to S by contacting it with a solution. Masukume *et al*. (2013) assumed that S forms when H_2S is contacted with an Fe^{3+} solution (**Eq. 5.41**.) (Masukume, *et al*., 2013). OLI software was used to verify if this assumption was correct. If not correct, the question is which compound was formed? **Table 5.39** showed the oxidation of 600 mmol/L H_2S (20 400 mg/L) with $Fe_2(SO_4)_3$ (Fe^{3+}). The effect of Fe^{3+} concentration was shown by stepwise by increment of the $Fe_2(SO_4)_3$ dosage from 0 to 3 000 mmol/L. It was noted that 300 mmol $Fe_2(SO_4)_3$ (600 mmol Fe^{3+} and 900 mmol SO_4^{2-}) reacted with 600 mmol H_2S to form FeS_2. The 900 mmol S^{+6} (SO_4^{2-}) came from the $Fe_2(SO_4)_3$ that was dosed. FeS_2 formed when the

$Fe_2(SO_4)_3$ / H_2S mole ratio was 0.5 (**Eq 5.41**). Due to the increase in the concentration of $Fe_2(SO_4)_3$ (0 to 3 000 mmol/L) the pH dropped from 4 to negative values.

$$H_2S + Fe_2(SO_4)_3 \rightarrow S + 2FeSO_4 + H_2SO_4 \quad (5.41)$$

Upon further dosing of $Fe_2(SO_4)_3$ to 780 mmol/L, the formed FeS_2 was converted to mainly S_8 (**Eqs. 5.42 & 5.43**) and a smaller portion was converted to SO_4^{2-}.

$$4FeS_2 + 8Fe^{3+} \rightarrow S_8 + 12Fe^{2+} \quad (5.42)$$

$$4FeS_2 + 4Fe_2(SO_4)_3 \rightarrow S_8 + 12FeSO_4 \quad (5.43)$$

With further dosing of $Fe_2(SO_4)_3$, the S_s can be oxidised to H_2SO_4 (**Eqs. 5.44 & 5.45**). A large excess mole ratio is actually needed, namely a Fe^{3+} / S_8 mole ratio of 48.

$$S_8 + 48Fe^{3+} + 32H_2O \rightarrow 8SO_4^{2-} + 48Fe^{2+} + 64H^+ \quad (5.44)$$

$$S_8 + 24Fe_2(SO_4)_3 + 32H_2O \rightarrow 48FeSO_4 + 32H_2SO_4 \quad (5.45)$$

Table 5.39 H_2S oxidation with Fe^{3+} for 600 mg/L H_2S

H_2S [mmol] (Y2)	$Fe_2(SO_4)_3$ [mmol]	pH	$S^{(-2)}$ (aq) [mmol] (Y2)	S_8 (Sulphur) – (s) [mmol] (Y2)	FeS_2 (Pyrite) – (s) [mmol] (Y2)	$S^{(+6)}$ (aq) [mmol] (Y2)	$Fe^{(+2)}$ (aq) [mmol] (Y2)	$Fe^{(+3)}$ (aq) [mmol] (Y2)	$FeSO_4.7H_2O$ (Melanterite) [mmol] (Y2)	H_2O [mmol]
600	0	4.00	99.3	0.0	0.0	0	0	0.0	0.0	55 560
600	300	0.43	0.0	0.0	300.0	900	300	0.0	0.0	55 560
600	600	0.28	0.0	0.0	257.1	1 886	943	0.0	0.0	55 560
600	900	0.27	0.0	62.5	0.0	2 800	1 800	0.0	0.0	55 560
600	1 200	0.04	0.0	50.0	0.0	3 800	2 400	0.0	0.0	55 560
600	1 500	-0.19	0.0	37.5	0.0	4 347	2 547	0.0	453.1	55 560
600	1 800	-0.42	0.0	25.0	0.0	4 796	2 596	0.1	1 004.0	55 560
600	2 100	-0.67	0.0	12.5	0.0	5 171	2 571	0.4	1 628.8	55 560
600	2 400	-0.96	0.0	0.1	0.0	5 536	2 534	2.5	2 263.9	55 560
600	2 700	-1.72	0.0	0.0	0.0	4 507	607	600.0	4 193.4	55 560
600	3 000	-1.77	0.0	0.0	0.0	4 949	149	1 200.0	4 650.5	55 560

The above experiment was repeated for a lower H_2S concentration of 100 mg/L H_2S and the results are shown in

Table 5.40. As it can be seen in **Table 5.41**, FeS_2 formed when 50 mmol/L $Fe_2(SO_4)_3$ was added to 100 mmol/L H_2S (**Eq. 5.41**). Upon further addition of $Fe_2(SO_4)_3$, no S_8 was formed, as in the case of higher concentrations. FeS_2 was oxidised to form $FeSO_4$ and H_2SO_4 (**Eqs. 5.46 & 5.47**). The lower H_2S-concentration can be the reason why no S_8 was formed.

$$FeS_2 + 14Fe^{3+} \rightarrow 2S^{6+} + 15Fe^{2+} \quad (5.46)$$

$$FeS_2 + 7Fe_2(SO_4)_3 + 8H_2O \rightarrow 15FeSO_4 + 8H_2SO_4 \quad (5.47)$$

Table 5.40 H_2S oxidation with Fe^{3+} for 100 mg/L H_2S

H_2S [mmol] (Y2)	$Fe_2(SO_4)_3$ [mmol]	pH	$S^{(-2)}$ (aq) [mmol] (Y2)	S_8 (Sulphur) - Sol [mmol] (Y2)	FeS_2 (Pyrite) - Sol [mmol] (Y2)	$S^{(+6)}$ (aq) [mmol] (Y2)	$Fe^{(+2)}$ (aq) [mmol] (Y2)	$Fe^{(+3)}$ (aq) [mmol] (Y2)	$FeSO_4.7H_2O$ (Melanterite) [mmol] (Y2)	Enthalpy - Total [cal] (Y2)
100	0	4.00	99.3	0.0	0.00	0	0	0	0.0	-3.79E+06
100	50	1.14	0.0	0.0	50.00	150	50	0	0.0	-3.83E+06
100	100	1.06	0.0	0.0	42.86	314	157	0	0.0	-3.86E+06
100	150	0.98	0.0	0.0	35.71	479	264	0	0.0	-3.89E+06
100	200	0.91	0.0	0.0	28.57	643	371	0	0.0	-3.93E+06
100	250	0.84	0.0	0.0	21.43	807	479	0	0.0	-3.96E+06
100	300	0.77	0.0	0.0	14.29	971	586	0	0.0	-3.99E+06
100	350	0.71	0.0	0.0	7.14	1 136	693	0	0.0	-4.03E+06
100	400	0.65	0.0	0.0	0.00	1 300	800	0	0.0	-4.06E+06
100	450	0.69	0.0	0.0	0.00	1 450	800	100	0.0	-4.10E+06
100	500	0.72	0.0	0.0	0.00	1 600	800	200	0.0	-4.13E+06

5.4.8.2 H_2S oxidation with O_2

In the previous sections, $Fe_2(SO_4)_3$ was used for oxidation. In this section O_2 has been used for H_2S oxidation.

Table 5.41 shows the 100 mol O (50 mmol O_2) was used for oxidation of H_2S to S_8 (**Eq. 5.48**). With further addition of O_2, S_8 was oxidized to form H_2SO_4 (**Eqs. 5.47 - 5.49**).

$$8H_2S + 4O_2 \rightarrow S_8 + 8H_2O \quad (5.48)$$

$$S_8 + 12O_2 + 8H_2O \rightarrow 8H_2SO_4 \quad (5.49)$$

$$S + 1½O_2 + H_2O \rightarrow H_2SO_4 \quad (5.50)$$

Table 5.41 H_2S oxidation with O_2

H_2S [mmol] (Y2)	O_2 [mmol]	pH	$S^{(-2)}$ (aq) [mmol] (Y2)	S_8 (Sulfur) - Sol [mmol] (Y2)	$S_{(+6)}$ (aq) [mmol] (Y2)	Enthalpy - Total [cal] (Y2)	O_2 – (vap) [mmol] (Y2)
100	0.0	4.00	99.3	0.0	0.0	-3.79E+06	0.0
100	25.0	4.14	50.0	6.2	0.0	-3.80E+06	0.0
100	50.0	3.56	0.4	12.4	0.1	-3.80E+06	0.0
100	75.0	1.69	0.0	10.4	16.7	-3.80E+06	0.0
100	100.0	1.43	0.0	8.3	33.3	-3.80E+06	0.0
100	125.0	1.28	0.0	6.2	50.0	-3.81E+06	0.0
100	150.0	1.18	0.0	4.2	66.7	-3.81E+06	0.0
100	175.0	1.09	0.0	2.1	83.3	-3.81E+06	0.0
100	200.0	1.02	0.0	0.0	100.0	-3.81E+06	0.0
100	225.0	1.02	0.0	0.0	100.0	-3.81E+06	23.8
100	250.0	1.02	0.0	0.0	100.0	-3.81E+06	48.8

5.4.8.3 Fe^{2+}-oxidation with O_2

In **Section 5.4.8.1,** it was shown that H_2S can be converted to S by contacting it with Fe^{3+}. The products, Fe^{2+}, need to be back oxidised to Fe^{3+}. This could be an alternative to the Claus process for the treatment of H_2S-rich streams. Another application for

Fe^{2+} oxidation is when iron-rich AMD needs to be neutralized. Acid mine water is normally rich in both Fe^{2+} and Fe^{3+}. The neutralization of Fe^{3+} with $CaCO_3$ is a rapid reaction, whereas the neutralization of Fe^{2+} with $CaCO_3$ is slow. The Fe^{2+} first need to be oxidised to Fe^{3+}. It would be beneficial if Fe^{2+} can be oxidised before the neutralization stage, so that all Fe is in the Fe^{3+} state. OLI simulations showed that Fe^{2+} can be oxidised to Fe^{3+} (

Table 5.42) according to **Eq. 5.51**.

$$2Fe^{2+} + ½O_2 + 2H^+ \rightarrow 2Fe^{3+} + H_2O \qquad (5.51)$$

Table 5.42 Fe^{2+}-oxidation with O_2

$FeSO_4$ [mmol]	O_2 [mmol]	pH	$Fe^{(+2)}$ (aq) [mmol] (Y2)	$Fe^{(+3)}$ (aq) [mmol] (Y2)	$S^{(+6)}$ (aq) [mmol] (Y2)
100	0.0	1.54	100	0	150
100	2.5	1.60	90	10	150
100	5.0	1.66	80	20	150
100	7.5	1.73	70	30	150
100	10.0	1.80	60	40	150
100	12.5	1.89	50	50	150
100	15.0	1.98	40	60	150
100	17.5	2.09	30	70	150
100	20.0	2.22	20	80	150
100	22.5	2.37	10	90	150
100	25.0	2.53	0	100	150

The Fe^{2+} can be back oxidised to Fe^{3+} through chemical or biological oxidation (**Eqs. 5.52 – 5.54**). This reaction is important in the pre-treatment of AMD before neutralization. Mogashane *et al*. (2023) from their research findings on ferric hydroxide recovery from iron-rich AMD concluded that that the rate of neutralization with $CaCO_3$ is rapid in the case of mine water rich in Fe^{3+}, but slow in the case of Fe^{2+}-rich water (Mogashane, *et al*., 2023) . The reasons for this are: (i) that Fe^{2+} remains in solution up to pH 8, while Fe^{3+} precipitates as $Fe(OH)_3$ at pH 3.5 and (ii) the rate of Fe^{2+} oxidation increases with increase in pH values. At pH 7.2 and higher the rate of Fe^{2+}-oxidation is fast. The difference in behaviour is that Fe^{2+} first need to be oxidised to Fe^{3+}.

$$H_2S + 2Fe^{3+} \rightarrow S + 2Fe^{2+} + 2H^+ \quad (5.52)$$

$$2Fe^{2+} + ½O_2 + 2H^+ \rightarrow 2Fe^{3+} + H_2O \ (pressure + O_2\ reaction) \quad (5.53)$$

$$H_2S + ½O_2 \rightarrow S + H_2O \quad (5.54)$$

5.4.9 Morphological characteristics of the reactants and products

High resolution scanning electron microscopy (SEM) analysis was performed to evaluate the fine-scaled topological features of the reactants and products.

5.4.9.1 $Ca_2SO_4{\cdot}2H_2O$

Figure 5.5 shows SEM images of $Ca_2SO_4{\cdot}2H_2O$. This $Ca_2SO_4{\cdot}2H_2O$ was thermally reduced to CaS (**Figure 5.7**) and $CaSO_4{\cdot}½H_2O$ (**Figure 6.10**). The images show plate-like particles with well-defined rhombohedral shape with an average particle size 43.9 µm. The smallest particle size was found to be 5.4 µm and the largest 142.5 µm (**Figure 5.6**). At higher magnifications, the plates are made of layers that can be peeled off. This is shown by the cracks in between the layers.

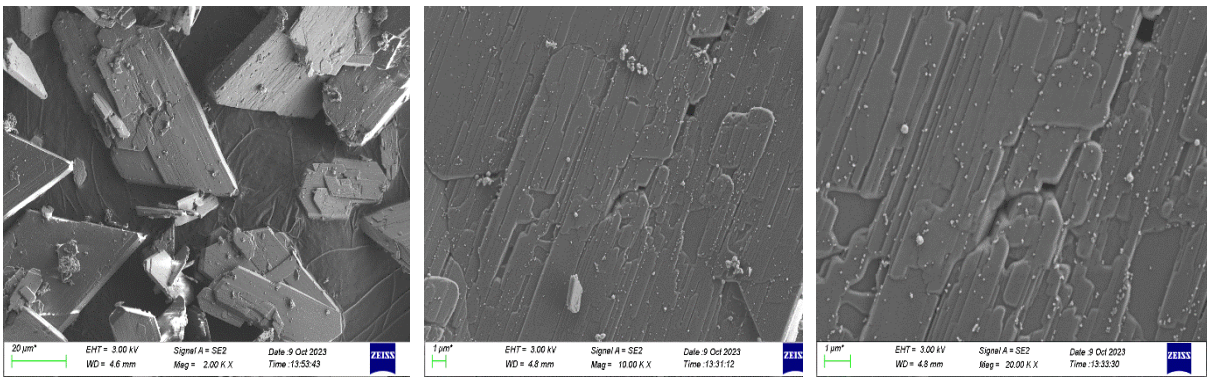

a. 2 k times magnification b. 10 k times magnification c. 20 k times magnification

Figure 5.5 SEM images of $Ca_2SO_4{\cdot}2H_2O$

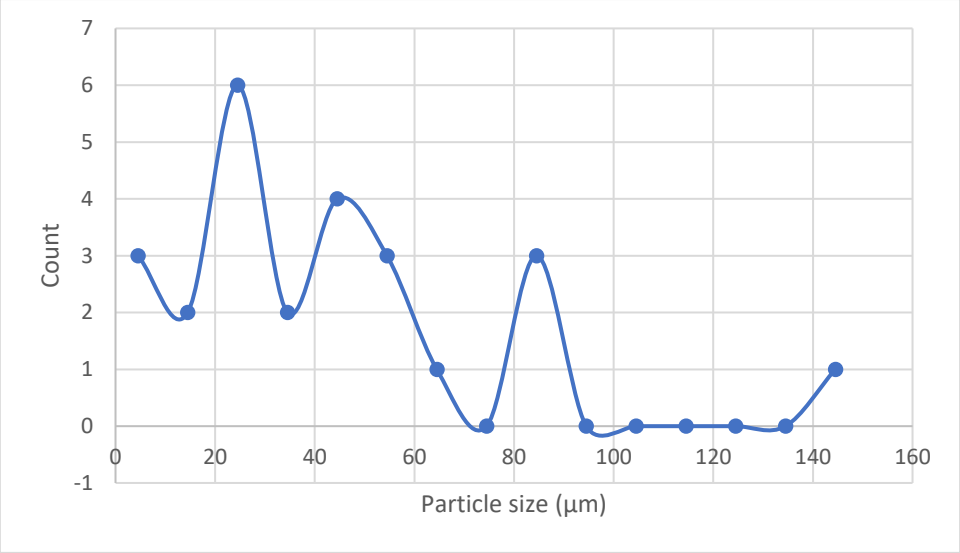

Figure 5.6 Particle size distribution of $CaSO_4.2H_2O$

5.4.9.2 CaS

Figure 5.7 shows the morphologies of CaS crystals obtained after thermal reduction of $Ca_2SO_4 \cdot 2H_2O$ with carbon at a retention time of 60 min and temperature 1000ºC. The figure reveals the SEM images of the CaS at different magnifications. It was observed that the microstructure of CaS has a uniform shape with cubic morphology, slightly different particle sizes ranging from 0.2 µm to 1.2 µm (**Figure 5.8**) and mixed with particles from coal residue. The morphology of $Ca_2SO_4 \cdot 2H_2O$ changed from rhombohedral to cubic of CaS. The average particle sizes decreased from 43.9 µm of $Ca_2SO_4 \cdot 2H_2O$ to 0.4 µm of CaS. As it can be seen if **Figure 5.5** the particles were scattered as compared to **Figure 5.7** where the particles were embedded together.

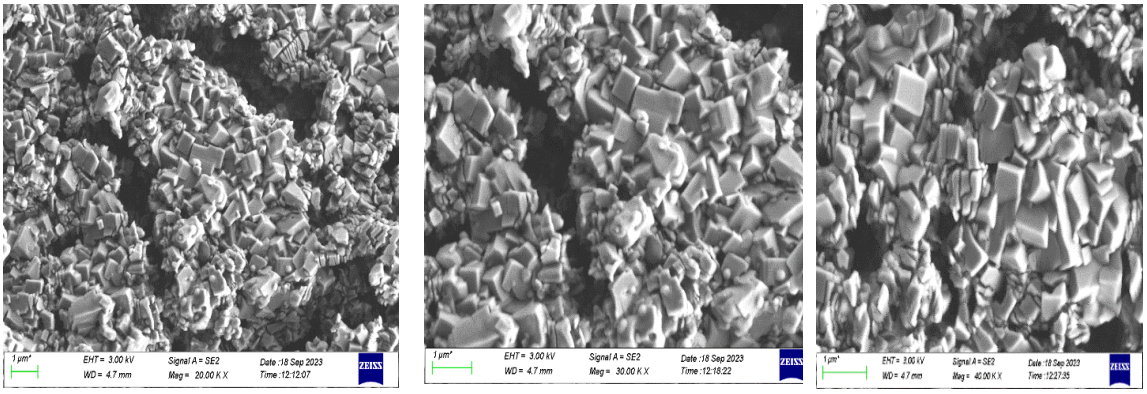

a. 20 k times magnification b. 30 k times magnification c. 40 k times magnification

Figure 5.7 SEM images of the CaS prepared for 60 min in a muffle furnace of 1000 ºC.

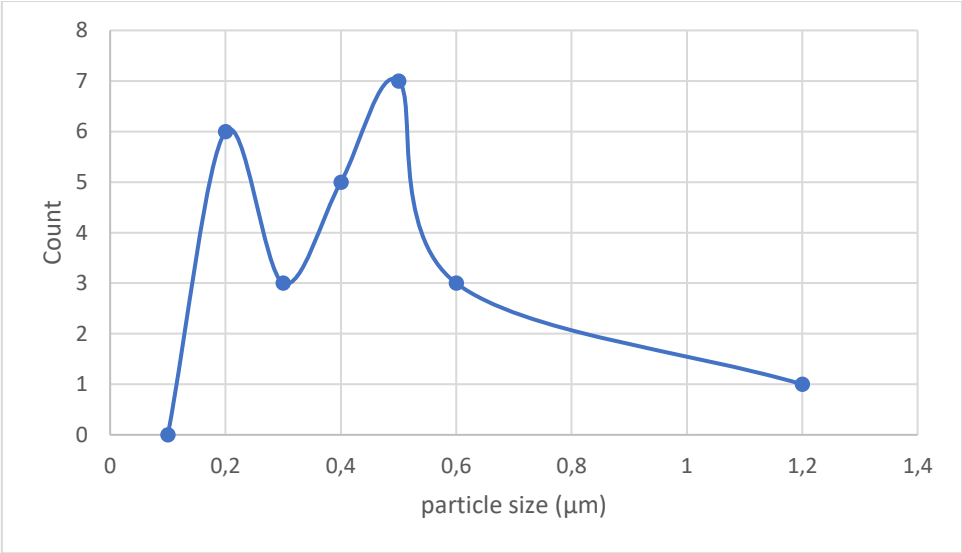

Figure 5.8 Particle size distribution of CaS

5.4.9.3 $BaSO_4$

Figure 5.9 shows the SEM images of $BaSO_4$ which was thermally reduced to BaS (**Figure 5.11)**. This BaS was used an alternative route to produce Na_2S in section 5.4.5.2. The figure depicts the combination of circular small particles and large rice-like shaped particles that have roundish holes on the heads. The particle sizes ranged from 0.2 µm to 2.8 µm with the average particle size of 0.8 µm (**Figure 5.10**). The average diameter of the particle was found to be 0.3 µm.

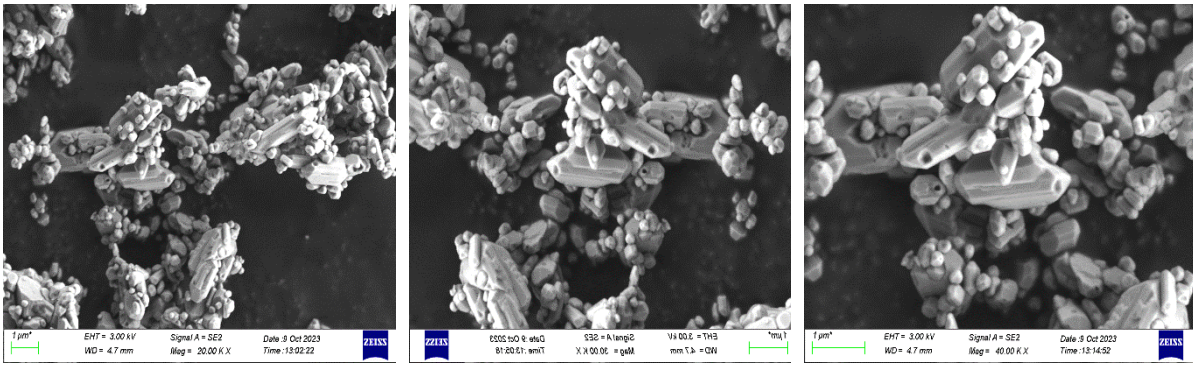

a. 20 k times magnification b. 30 k times magnification c. 40 k times magnification

Figure 5.9 SEM micrographs of $BaSO_4$

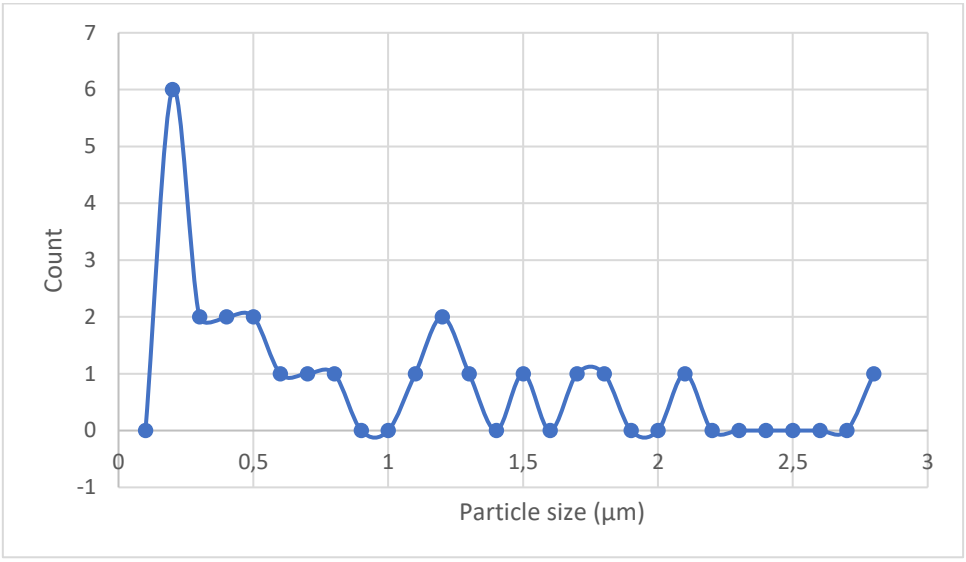

Figure 5.10 Particle size distribution of $BaSO_4$

5.4.9.4 BaS

Figure 5.11 shows the morphologies of BaS crystals obtained after thermal reduction of $BaSO_4$ with carbon at a retention time of 20 min and temperature 1000 ºC. The figure reveals the presence of a cubic morphology with particle size 0.3 µm, which are scattered across the surface of the material. The cubic morphology symbolizes that BaS particles formed. The morphology of $BaSO_4$ changed from circular and rice-like to cubic BaS. The particles of BaS (**Figure 5.11**) are not chained together as compared to the particles of $BaSO_4$ (**Figure 5.9**). The average particle size also changed from 0.8 µm. to 0.3 µm (**Figure 5.12**). The BaS sample contained 86% of BaS (**Table 5.11**)

and 14% unreacted $BaSO_4$ and coal residue, as indicated by the irregular morphologies revealed in the images.

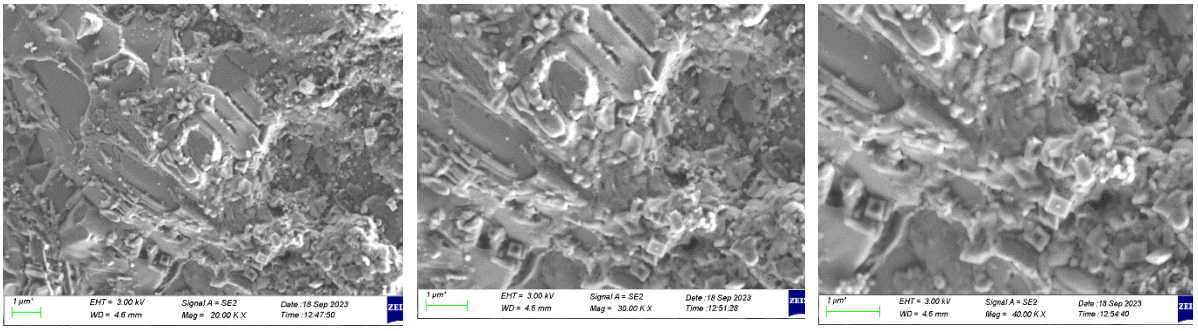

a. 20 k times magnification b. 30 k times magnification c. 40 k times magnification

Figure 5.11 SEM images of the BaS prepared for 20 min in a muffle furnace of 1000 ºC.

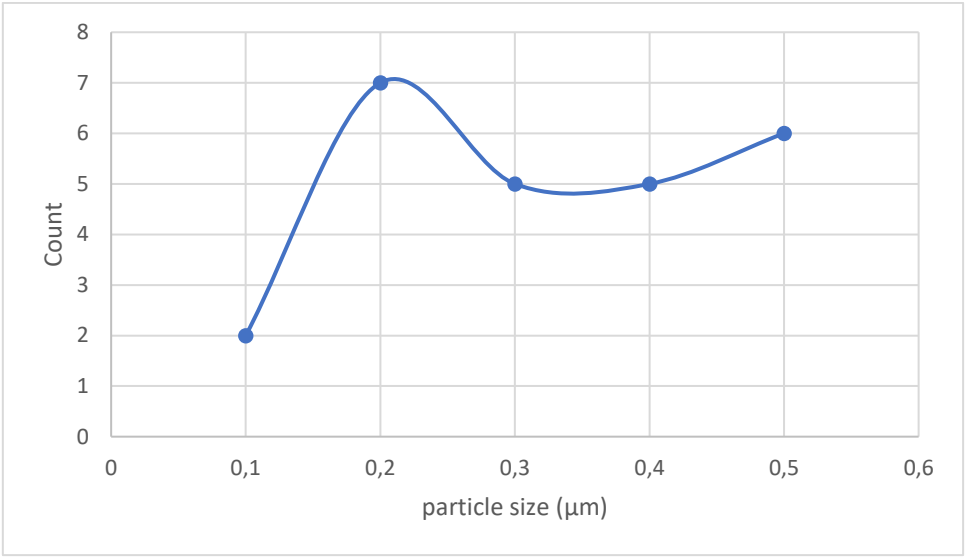

Figure 5.12 Particle size distribution of BaS

5.4.9.5 Na_2CO_3

Figure 5.13 shows the SEM images of Na_2CO_3. The images depict large irregular particles with an average size of 479.6 µm (**Figure 5.14**). These large particles are surrounded by holes with a diameter of 43.3 µm and spherical particles with a diameter of 40.0 µm. The large particles appear to have rough surfaces while the spherical particles are smooth and shiny.

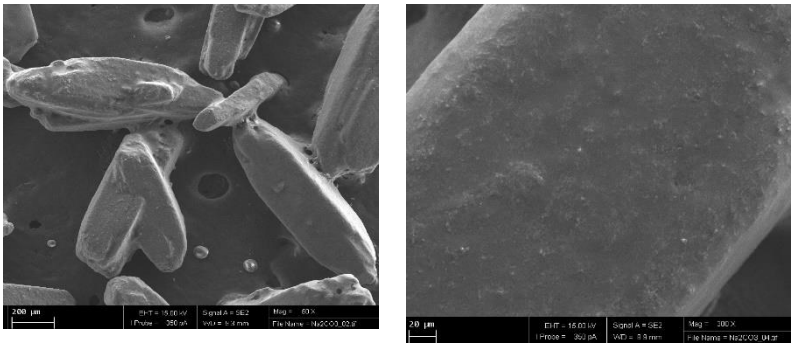

a. 60 times magnification b. 300 times magnification

Figure 5.13 SEM images of Na_2CO_3

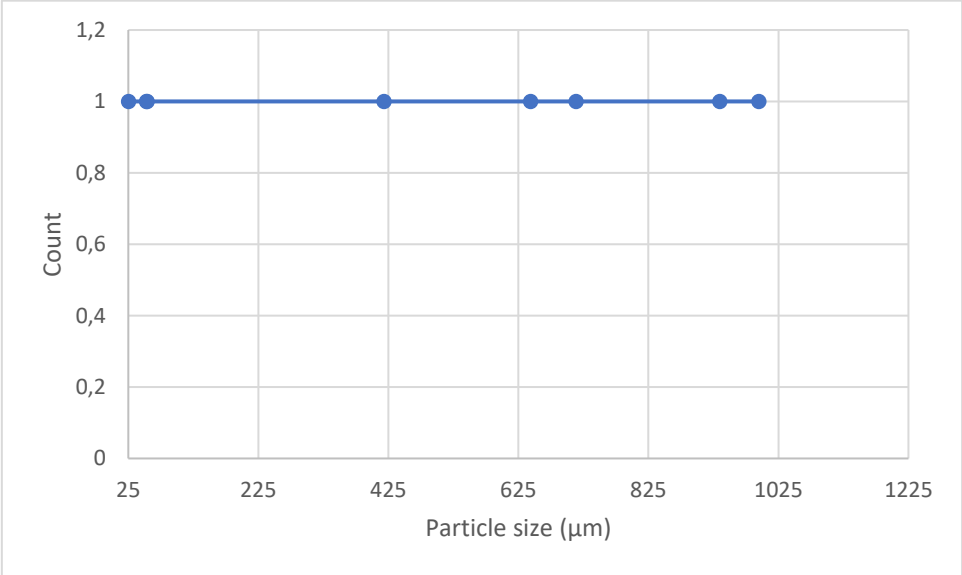

Figure 5.14 Particle size distribution of Na_2CO_3

5.5 CONCLUSIONS

i. $CaSO_4$ and $BaSO_4$ can be thermally reduced to CaS and BaS respectively, as demonstrated by both muffle furnace and the Pyrosim prediction simulation studies.

ii. BaS is more suitable than CaS for the production of Na_2S due to the low solubility of $BaSO_4$ and the lower ratio of coal needed per mol of $CaSO_4$ or $BaSO_4$.

iii. Less energy is needed to convert $BaSO_4$ to BaS than in the case of $CaSO_4$ to BaS

iv. $NaHCO_3$ and NaHS can be produced by contacting Na_2S and CO_2.

v. Na_2S can be used to produce $Mg(OH)_2$ by contacting it with $MgSO_4$.

vi. Freeze-crystallization can be used to separate (i) NaHS and Na_2SO_4, and (ii) $NaHCO_3$ and NaHS.

vii. The Fe^{2+} can be back oxidised to Fe^{3+} through chemical or biological oxidation.

viii. H_2S can be converted to S by contacting it with $Fe_2(SO_4)_3$ through OLI software.

ix. OLI software showed that O_2 can be used for oxidation of H_2S to S_8

CHAPTER 6: RECOVERY OF RARE EARTH METALS FROM WASTE STREAMS

Conny P Mokgohloa[1,2], Johannes P Maree[1,3], Malose P Mokhonoana[2]

Email addresses: connyputjie@gmail.com; johannes.maree@ul.ac.za; malose.mokhonoana@ul.ac.za

[1]Department of Water and Sanitation, University of Limpopo, Private Bag X1106, Sovenga, 0727, South Africa.

[2]Department of Chemistry, University of Limpopo, Private Bag X1106, Sovenga, 0727, South Africa.

[3]Institute for Nanotechnology and Water Sustainability (iNanoWS), College of Science, Engineering and Technology, University of South Africa, Private Bag X6, Florida Science Campus, Johannesburg 1709, South Africa.

ABSTRACT

REE recovery has become an attractive process due to its high cost and limited availability. Additionally, recovery of REEs has become necessary due to their high toxicity and negative impact on the environment. Growing demand for REEs is expected to be met by an increase in supply. PG is a secondary raw material of interest for REEss because it is abundant and contains significant amounts of REEs. Common processes for recovering REEs from waste streams include chemical precipitation, coagulation, flocculation, flotation, ion exchange, adsorption, and electrochemical processes. These processes are subject to lengthy purification processes, low extractability, and high wastewater flow.

The aim of this study was to quantify REEs in AMD collected from Kopseer mine and PG collected from waste gypsum dump of the fertilizer industry FOSKOR in Phalaborwa. Nitric acid was used to leach out REEs in PG because it is a strong oxidizing agent, forms soluble nitrates and has the advantage of selectively leaching REEs while leaving behind other unwanted minerals and impurities. Sodium hydroxide was used to adjust the pH of AMD to 3.5. The effectiveness of time on chemical precipitation was studied at this pH. It was noted that all the REEs chosen for this

study, namely, Ce, Dy, Gd, La, Nd, Pr, and Sm precipitated at time 60 min. Only Dy, Gd, Nd and Pr precipitated at time 0 and only Dy, La, and Pr precipitated at time 20.

The study also focused on the formation of $CaSO_4 \cdot ½H_2O$ from $CaSO_4 \cdot 2H_2O$. It was founded that $CaSO_4 \cdot ½H_2O$ formed when $CaSO_4 \cdot 2H_2O$ was heated to 180 °C for 120 min and 240 °C for 60 min. In the process, $CaSO_4 \cdot 2H_2O$ lost 1.5 molecules of water to form $CaSO_4 \cdot ½H_2O$. The hydration of $CaSO_4 \cdot ½H_2O$ leading to the crystallization of $CaSO_4 \cdot 2H_2O$ was also studied. The conditions needed to produce $CaSO_4 \cdot 2H_2O$ tiles were determined by doing a series of experiments where H_2O, $CaSO_4 \cdot 2H_2O$ and $CaSO_4 \cdot ½H_2O$ were varied. It was noted that hardness of hydrated $CaSO_4 \cdot ½H_2O$ is influenced by the H_2O/ $CaSO_4 \cdot ½H_2O$ ratio. This chapter further evaluated the following stages for the processing of gypsum to $CaCO_3$: (i) Reduction with carbon and (ii) $CaCO_3$ and $Ca(HS)_2$ formation by adding CO_2 and (iii) Behaviour of rare earth metals.

6.1 INTRODUCTION

Acid mine drainage has been an environmental problem for decades but has proven to be a viable source of rare earths. Rare earths are important raw materials for many technological and innovative applications. They are considered important in modern society. However, the current supply chain includes a relatively small number of major producers, and most of the ore production takes place in China (Bleiwas & Gambogi, 2013). The risks associated with REE supply have been reported in numerous studies over the last decade (Eggert, *et al*., 2016) This near monopoly creates a potential impairment for the USA and other countries where REEs are not readily produced. For example, during the 2010-2012 rare earth crisis, China reduced its export quotas during periods of increasing demand. This limited market has caused many REEs prices to rise 100 times or more, creating a shortage in downstream markets. (Jordens, *et al*., 2013).

Many industrial processes rely on REEs for their products including catalysts, metallurgy, petroleum refining, catalytic converters, ceramics, phosphors, magnets, and electronics. The USA consumes approximately 12,000 metric tons of REEs per year [U.S. Geological Survey (2018)]. Of that, the Department of Defence uses less than 5%, or approximately 600 metric tons (Humphries, 2010). Future demand for individual REEs is difficult to predict due to the number of elements involved and

variety of uses; however, given the increasing forecasted demand for green technologies and electronic devices, many researchers believe that demand for REEs will also increase (Campbell, 2014; Goodenough, *et a*l., 2018).

Calcium sulphate hemihydrate commonly known as plaster of Paris is manufactured from gypsum. It is given by the equation:

$$CaSO_4 \cdot 2H_2O \rightarrow CaSO_4 \cdot \frac{1}{2}H_2O + 1\frac{1}{2}H_2O \quad (6.1)$$

Calcium sulphate hemihydrate is extensively used in buildings, ceramics, and medical industries. Hydration of $CaSO_4 \cdot ½H_2O$ is a highly exothermic reaction and occurs as:

$$CaSO_4 \cdot \frac{1}{2}H_2O + 1\frac{1}{2}H_2O \rightarrow CaSO_4 \cdot 2H_2O \quad (6.2)$$

During hydration, crystallization of the gypsum takes place. When hydration occurs in the paste form, the plaster solidifies and develops strength. This framework includes physical and mechanical processes. The hardened mass is not a dense solid but a very porous material with a relatively large internal surface area consisting of interlocking crystals in the form of plates and needles.

The objectives of the study were the following:

i. Produce $CaSO_4$/C plates as feed to thermal treatment
ii. Thermal treatment of plates (Mass loss, Sulphide, Alk)
iii. REEs in AMD and PG
iv. REEs in $CaCO_3$ and $Ca(HS)_2$ fractions

6.2 LITERATURE

6.2.1 Introduction

The first element considered REE was discovered in 1788 in rocks excavated in Sweden. The element yttrium was considered "rare" because it had never been discovered before, and the geological term "Earth" at the time defined acid-soluble minerals. In 1794, the chemist Johann Gadolin named the yttrium "Earth", previously unknown, after the city where he had discovered it. Over time, the mines around Ytterby produced rocks that provided the city with four elements: yttrium, ytterbium,

terbium, and erbium. The discovery of new elements was an authoritative but controversial activity of nineteenth-century European chemists. Jones Jacob Berzelius isolated and named cerium in 1803 and thorium in 1828. In 1839, the Swedish chemist Carl Gustaf Mosander discovered and named lanthanum, erbium, and terbium, and began a systematic analysis of mixed rare earths. At the end of the 19th century, chemists Gustav Kirchhoff and Robert Bunsen developed spectroscopy as a method of determining elements by studying the spectrum of light. Rare Earth Elements (REEs) are a group of 17 chemical elements, 15 lanthanides, together with yttrium, and scandium in the periodic table, as defined by the International Union of Pure and Applied Chemistry (IUPAC). This group consists of lanthanides (Ln) and scandium (Sc) and yttrium (Y). The last two elements were introduced based on similarities of properties with REEs and are often found in the same ores (Balachandran, *et al*., 2014; Faris, *et al*., 2017). The first element to be considered an REE was in a rock excavated in Sweden in 1788.

Despite the name, rare earth elements are not uncommon. All metals, except the radioactive promethium, are more abundant in the earth's crust than silver, gold, and platinum. Because this metal has many similar properties, it is often found in geological sediments. These are also called "rare earth oxides" because most of them are commonly sold as oxide compounds. They are generally like silver-white metal and have a high electrical conductivity**. Figure 6.1** shows a list of REEs.

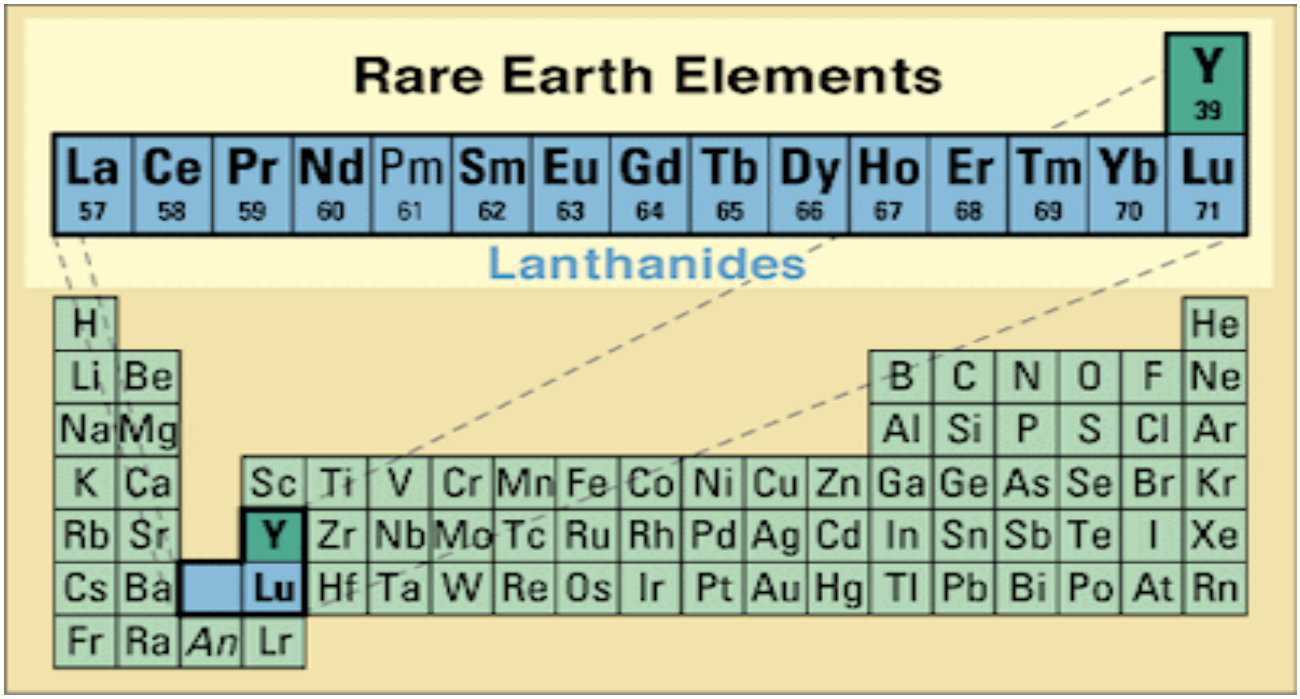

Figure 6.1 Rare earth metals (Ramos, *et al*., 2016).

Rare earth elements are a group of special metals with unique physical, chemical, and luminescent properties, whose demand is growing rapidly due to technological applications. The unique properties of REEs make them important materials for many emerging technologies that are widespread today. Data show that 110 million tonnes of REEs reserves are scattered around the globe, along with valuable deposits (Wübbeke, 2013). The 97% of the global REEs supply is produced by China (Massari & Ruberti, 2013), 1.73 percent by Russia, and 1.18 percent by the USA (some minimum other reserves in Brazil and the Democratic Republic of Congo). China is currently the largest producer of REEs (Chu & Majumdar, 2012). However, in 2008, China began to introduce rare-earth production quotas and limit the number of permitted exporting countries, which made the global rare earth market very volatile (Walters, *et al*., 2010). While many REEs are important for sustainable mobility and energy delivery, the production of REE itself is essential for the environment. (Schüler, *et al*., 2011; Ali, 2014). The widespread use of renewable energy sources in various industries can ultimately lead to serious pollution of the environment, agriculture, and soil, which in turn can seriously harm human health. Several studies have recently been conducted to evaluate the toxic effects of REEs on soil, water, model organisms and humans. (Laveuf & Cornu, 2009; Taunton, *et al*., 2000). Many research groups

are studying the toxicity effects of different REEs due to REEs' persistence in the environment over long times.

6.2.2 Chemistry of REEs

According to the REE group classification, there are 15 lanthanide elements: lanthanum (La), cerium (Ce), praseodymium (Pr), promethium (Pm, not found in nature), neodymium (Nd), samarium (Sm), Europium (Eu) , Gadolinium (Gd), Terbium (Tb), Dyslexia (Dy), Gomiu (Ho), Erbium (Er), Thulium (Tm), Iterbium (Yb) and Luteium (Lu). Lanthanide and lanthaniode are used interchangeably, but lanthanoide was chosen because the suffix -oid means the same or like REE, not -ide to indicate a functional group. The 14 lanthanides are f-block elements, and the 15^{th} element is lutetium, a d-block element, but they are considered lanthanides because their chemical properties are like those of the other 14. Lanthanides are divided into 2 or 3 subgroups, depending on the authors (Sadeghi, *et al*., 2013; Yanfei, *et al*., 2016). These are heavy, medium, and light REEs based on atomic weight. According to the United States Geological Survey (USGS), HREE contains elements Tb at Lu and Y, and LREE contains elements La at Nd. Other authors have assigned HRRE from Tb to Lu and Y, LREE from La to Nd, and MREE that contain elements from Sm to Gd (Jorjani & Shahbazi, 2016; Yanfei, *et al*., 2016). The HREEs group is referred as the yttrium group by other authors, whereas LREEs are called the cerium group (Jordens, *et al*., 2013). The terminologies, yttrium and cerium groups predominate.

6.2.3 Common Properties of Lanthanides

Common Properties of the Lanthanides (Atwood, 2013):

i. Silvery-white REE that changes colour and forms oxides when exposed to air.

ii. Relatively soft metal. The higher the number of atoms, the higher the hardness.

iii. The radius of each lanthanide 3^{+} ion decreases steadily as it moves from left to right across a period with (increase in atomic number). This is called "lanthanide contraction".

iv. High melting and boiling points.

v. Reacts with water to release hydrogen (H_2), slow when cold / fast when hot.

vi. Interacts with H_2 in exothermic reactions.

vii. Burns easily in air.

viii. Their compounds are primarily ionic.

ix. Many layers of rare-earths burn at high temperatures.

x. Most rare-earth compounds are extremely paramagnetic.

xi. Many rare-earth compounds are highly fluorescent in ultraviolet light.

xii. Lanthanide ions are pale in colour.

xiii. The magnetic moments of lanthanide and iron ions are opposites of each other.

xiv. Lanthanides react easily with many base metals and form binary systems with most base metals when heated.

xv. Large coordination is possible with lanthanides (more than 6, usually up to 8 or 9 or 12).

6.2.4 Electron configuration.

The chemical, metallurgical and physical behavior of rare earths is determined by the electronic composition of these elements. These elements are usually trivalent R^{3+}, but some have anomalous valences. The number of electrons 4f for each lanthanide is given in **Table 6.1** with the number of electrons 4f and the ionic radius of the ion R^{3+}. The energy of the 4f electron is less than the extreme trivalent electron and is located radially (*i.e.*, the 4f electron is "localized" and is part of the ionic nucleus), so it does not interact directly with other elements when the bond is formed. For lanthanides and lanthanum, the outermost electrons or valence electrons are the same, $5d^6s^2$; for scandium, $3d^4s^2$; and for yttrium, $4d^5s^2$. There are some changes in the chemical properties of lanthanides due to the reduction of lanthanides and the hybridization or mixing of 4f electrons and valence electrons. The typical electronic configuration of lanthanides is $4f^{0,\ 2\ to\ 14}\ 5d^{0,1}\ 6s^2$. The elements scandium and yttrium are d-block elements. However, due to their chemical properties and shape, these two elements are also members of rare-earth family.

Table 6.1 Electron configuration of rare earth.

Rare earth element electronic configuration		
Elements	Atomic number	Electronic configuration
Scandium (Sc)	21	[Ar] $3d^1$ $4s^2$
Yttrium (Y)	39	[Kr] $4d^1$ $5s^2$
Lanthanum (La)	57	[Xe] $4f^0$ $5d^1$ $6s^2$
Cerium (Ce)	58	[Xe] $4f^1$ $5d^1$ $6s^2$
Praseodymium (Pr)	59	[Xe] $4f^3$ $5d^0$ $6s^2$
Neodymium (Nd)	60	[Xe] $4f^4$ $5d^0$ $6s^2$
Promethium (Pm)	61	[Xe] $4f^5$ $5d^0$ $6s^2$
Samarium (Sm)	62	[Xe] $4f^6$ $5d^0$ $6s^2$
Europium (Eu)	63	[Xe] $4f^7$ $5d^0$ $6s^2$
Gadolinium (Gd)	64	[Xe] $4f^7$ $5d^1$ $6s^2$
Terbium (Tb)	65	[Xe] $4f^9$ $5d^0$ $6s^2$
Dysprosium (Dy)	66	[Xe] $4f^{10}$ $5d^0$ $6s^2$
Holmium (Ho)	67	[Xe] $4f^{11}$ $5d^0$ $6s^2$
Erbium (Er)	68	[Xe] $4f^{12}$ $5d^0$ $6s^2$
Thulium (Tm)	69	[Xe] $4f^{13}$ $5d^0$ $6s^2$
Ytterbium (Yb)	70	[Xe] $4f^{14}$ $5d^0$ $6s^2$
Lutetium (Lu)	71	[Xe] $4f^{14}$ $5d^1$ $6s^2$

6.2.5 Atomic mass

Lanthanides have an atomic number between 57 (lanthanum) and 71 (lutetium). The elements Yttrium (Y) and Scandium (Sc) are included due to their similar chemical properties. Lanthanides with smaller atomic numbers are more abundant in the earth's crust than lanthanides with larger atomic numbers (Castor & Hedrick, 2006). Despite their similarities in the chemical reactivity of elements in the lanthanide series, their abundances in Earth’s crust vary by two orders of magnitude.

6.2.6 Uses of REEs

REEs have widespread applications in various industries (Charalampides, *et al*., 2015). Some major applications of REEs are catalysts (20%) rare earth magnets (21%) alloys (18%), production of powder (12%) and in phosphorus (7%) (Bünzli & Eliseeva, 2010). The uses of REEs can be described as follows.

i. Lanthanum

Lanthanum has no commercial use. However, alloys have different uses. Lanthanum is used in equipment such as colour TVs, fluorescent lamps, energy-saving lamps, and eyeglasses. La_2O_2 is used to make special optical glasses (infrared absorbent glass, cameras, and telephoto lenses).

ii. Cerium

Cerium is the main component of non-metallic alloys (less than 50%). The most popular use of this alloy is "flint" for lighters. The only other thing that does this is iron.

iii. Praseodymium

Praseodymium is used in several alloys. A very strong magnesium alloy is used in aircraft engines. Mischmetal is an alloy containing about 5% praseodymium and is used to make flint for briquettes. Praseodymium is also used in permanent magnet alloys. Used in carbon arc electrodes along with other lanthanide elements to illuminate and design the studio.

iv. Neodymium

The main use of neodymium is to alloy iron and chalk to make very strong permanent magnets. These innovations in 1983 led to the decline of many electronic devices, including mobile phones, microphones, speakers, and electronic musical instruments. These magnets are also used in car vacuum cleaners and wind turbines.

v. Samarium

Samarium-cobalt magnets are much stronger than iron magnets. They remain magnetic at high temperatures, so they are used in microwave ovens. It has made possible the miniaturization of electronic devices such as headphones and the development of discrete stereo devices.

vi. Europium

Europium is used to print euro banknotes. It glows red under ultraviolet light and without this red light, fakes can be detected. Low energy light bulbs contain some europium, which balances the blue (cold) light with the slightly red (warm) light to provide natural light. Europium is useful for control rods in nuclear reactors because it absorbs neutrons well. Europium-made plastic was used as a laser material. It is also used in the manufacture of superconducting thin alloys.

vii. Gadolinium

Gadolinium has beneficial properties for alloys. Only 1% gadolinium can improve the machinability and resistance to high temperatures and oxidation of iron and chromium alloys. It is also used in alloys to make magnets, electronic components, and data storage disks.

viii. Terbium

Terbium is used to dope calcium fluoride, calcium tungstate and strontium molybdate, all used in solid-state devices. It is also used in energy saving lamps and mercury lamps. It has been used to improve the safety of medical X-rays by producing images of the same quality with much shorter exposure times.

ix. Dysprosium

It is rarely used as a pure metal because it reacts easily with water and air. Indigestion is mainly used in neodymium-based alloys for magnets. This is because it is resistant to demagnetization at high temperatures. This property is important for magnets used in motors or generators. These magnets are used in wind turbines and electric vehicles, leading to a rapidly growing demand for ovarian cysts.

x. Holmium

Because holmium can absorb neutrons, it is used to control chain reactions in nuclear reactors. Its alloys are used in some magnets.

xi. Erbium

Erbium is rarely used as a metal because it slowly fades in the air and attacks water. Erbium, when combined with metals such as vanadium, reduces its hardness and improves performance.

xii. Thulium

When irradiated in a nuclear reactor, the thulium forms isotopes that emit X-rays. This "button" of this isotope makes X-ray equipment light and portable for medical use. Thulium is used in surgical lasers.

xiii. Ytterbium

Ytterbium is beginning to find a variety of uses, such as in memory devices and tuneable lasers. It can also be used as an industrial catalyst and is increasingly being used to replace other catalysts considered to be too toxic and polluting.

xiv. Lutetium

Lutetium is little used outside research. One of its few commercial uses is as a catalyst for cracking hydrocarbons in oil refineries.

xv. Scandium

Scandium is mainly used for research purposes. However, the potential is high because it has a density as low as aluminium and has a much higher melting point.

xvi. Yttrium

Yttrium is often used as an additive in alloys. It increases the strength of aluminium and magnesium alloys. It is also used in the manufacture of radar microwave filters and as a catalyst for the polymerization of ethylene. Yttrium Aluminium Garnet (YAG) is used in metal cutting lasers. It is also used to illuminate white LEDs.

6.2.7 Production of REEs

The characteristics and concentration of impurities present in PG produced are mostly dependent on the quality and composition of phosphate ore used. PG is predominantly made of gypsum (>90%) in the form of calcium sulphate dehydrate, but also contains impurities such as trace metals (*e.g.*, Cr, Cu, Zn and Cd), residual acids, REEs and certain naturally occurring radionuclides. It has been reported that during the process of acidulation of Phalaborwa phosphorite with sulfuric acid, about 70-85 % of REEs end up in PG (Wang, *et al*., 2010). This makes PG a possible source of REEs and can be further utilized to recover sulphur and $CaCO_3$.

Until 1965, there was little demand for REEs. At that time, most of the supply in the world came from the placer deposits of India and Brazil. In the 1950s, South Africa became the largest producer of rare earths with monazite deposits.

The demand for REEs first exploded in the mid-1960s, when the first colour TVs appeared on the market. Europe was an important material for the creation of colourful images. China began producing significant amounts of rare earth oxides in the early 1980s and became the world's largest producer in the early 1990s. In the 1990s and early 2000s, China steadily strengthened its global rare earth market.

In addition, the fact that rare-earth products are produced in a variety of defence, aerospace, industrial and consumer electronics products has led to a sharp increase in global demand. China has used its dominance to cut exports and raise rare earth prices to historic levels (Chu & Majumdar, 2012). China is not only the world's largest producer of REEs, but also a major consumer. They mainly use REEs in the production of electronic products for domestic and export markets. Japan and the United States are the second and third largest consumers of rare materials.

In previous years, the importance of the REE industry has grown significantly, emerging from an industry that was widely ignored to one that is important to an important sector for an environmentally-friendly economy (Bourzac, 2010; Kara, *et al*., 2010; Binnemans, *et al*., 2013; Clapper, 2013; Adibi, *et al*., 2014). Although many REEs are critically important to sustainable mobility and energy supply, production of REEs itself incurs significant environmental damages (Schüler, *et al*., 2011).

Similarly, large-scale REE production in China has created serious environmental problems associated with the release of heavy metals and radioactive materials into groundwater, rivers, soil, plants, and the atmosphere around mines (He, *et al*., 2004; Liang, *et al*., 2014). According to the Chinese Society for Rare Earths, 1 tonne of RES produces 8.5 kg of fluorine and 13 kg of flue gas, and treatment with H_2SO_4 produces 9,600-12,000 m3 of gas together with smoke dust concentrate, HF, SO_2 and H_2SO_4 (Paul & Campbell, 2011; Sonich-Mullin, 2012). Other estimates indicate that 1 tonne of REES will produce 60,000 m^3 of mixed H_2SO_4 and HF gas, 200 m^3 of acid water and 1.4 tonnes of radioactive waste. (Blakely, *et al*., 2012). In addition, long-term mining dust inhalation can cause pneumoconiosis (black lung) (Hirano & Suzuki, 1996). Overall, production of REEs involves many process steps, out of which many

incur significant material/energy consumption and environmental release (Golev, *et al*., 2014).

Extraction of rare earths from ores requires a complex process designed according to the characteristics and mineralogy of each field. For selective leaching of REEs, in very rare cases, a leaching process (also called solution production) is injected into a well drilled in the ore to perform a leaching process that reduces the load on the environment. limited to a minimum. pollution (Li & Yang, 2014). By hydrometallurgy, REEs are extracted into alkalis and transformed into oxides, chlorides, or halogens of pure rare earths (Gupta & and Krishnamurthy, 2004).

Different methods have been proposed for separation and pre-concentration of REEs, such as:

i. co-precipitation,
ii. solvent extraction,
iii. ion-exchange,
iv. solid-phase extraction (Das & Das, 2013).

Solvent extraction and ion-exchange are the two most common methodologies for the pre-concentration and separation of REEs from various matrices.

Several ways of direct application and technologies have been developed in South Africa to utilize waste gypsum. These application/technologies include: (i) fertilizers and soil conditioner, (ii) cement and wallboard production, and (iii) filler for road construction. However, only 5% to 10% of the total gypsum produced finds utility for such applications and the rest is stockpiled in open spaces or dumped into sea.

6.3 MATERIAL AND METHODS

6.3.1 Feedstock

High purity reagents were used for the preparation of samples. All the dilutions and solutions were done with deionized water. The following chemicals were used: $CaSO_4 \cdot 2H_2O$ (Foskor), activated carbon (MCL), CO_2 gas (Air Liquide, South Africa), 1 N HCl, 5N HNO_3, 0.1 N I_2, 0.1 N $Na_2S_3O_4$, 1N NaOH, and starch solution.

6.3.2 Equipment

A muffle furnace was used for reduction of $CaSO_4 \cdot 2H_2O$ to CaS and $CaSO_4 \cdot 2H_2O$ to $CaSO_4 \cdot ½H_2O$. 30ml crucibles with lids were used to carry out samples for thermal studies. 500 mL beakers were used for reaction studies. A pH and conductivity meter were used to measure the pH of the samples.

6.3.3 Experimental and Procedure

6.3.3.1 *Thermal treatment*

Thermal studies were carried out by reacting mixtures of $CaSO_4 \cdot 2H_2O$ (18 g) and coal (4.52 g) at temperatures 1 000 ºC in the muffle furnace to produce CaS. The CaS produced was collected and analyzed for mass loss, sulphide content, and alkalinity. The retention times for all the reduction experiments was 30 min.

6.3.3.2 Hemihydrate production

A 100 g of $CaSO_4 \cdot 2H_2O$ was placed in a muffle furnace at various temperatures ranging from 140 to 240 ºC. the retention times for all the reduction experiments was 60 min. Another set of hemihydrates was produced by a placing 100 g of $CaSO_4 \cdot 2H_2O$ in a muffle furnace at temperature 180 ºC at various retention times ranging from 30 – 120 min.

6.3.3.3 Effect of H_2O/ $CaSO_4 \cdot ½H_2O$ ratio on the hardness of hydrated hemihydrate

An 18 g of $CaSO_4 \cdot 2H_2O$ was placed in a muffle furnace of 200 ºC. The temperature was dropped down to 170 ºC for 28 min to allow $CaSO_4 \cdot ½H_2O$ to form. The final mass was weighed, and mass loss was calculated. The product was mixed with various amount of water to determine the hardness of the tiles formed.

6.3.3.4 Effect of setting time on the hardness of hydrated hemihydrate when mixed with carbon.

An 18 g $CaSO_4 \cdot 2H_2O$ was placed at 200 ºC to 170 ºC with the retention time of 28 min. The product was allowed to cool to 50 ºC. The product was mixed with 11.16 g

C and 6.9 mL of water. The setting time on the hardness of the tiles was varied from 5 – 15 min.

6.3.3.5 Effect of C/Gypsum mole ratio on the CaS yield

A 15.17g of $CaSO_4 \cdot ½H_2O$ was mixed with C/$CaSO_4$ mol/mol ratio ranging from 2 to 8. The mixtures were placed in a muffle furnace of 1000 ºC at a retention time of 30 min. The products were allowed to cool. The sulphide and hardness of the products were determined.

6.3.3.6 Effect of temperature on the CaS yield

Another set of CaS production was done by mixing a 15.17 g $CaSO_4 \cdot ½H_2O$ with 4.52 g C and 9 ml water. The hard tiles were placed in a muffle furnace ranging from 800 to 1000 ºC for CaS production. The CaS produced was analysed for sulphide. Hardness of the tiles was also determined.

6.3.3.7 Gypsum processing

Calcium sulphide was produced by reacting 18 PG with 4.5 g activated carbon at 1000 °C in crucible with a lid on to maintain reducing conditions. Sulphide and Alkalinity analyses were carried out. Cooled CaS was put in 200 mL water and contacted with different portions of CO_2, up to pH 9, to convert CaS to $CaCO_3$ and $Ca(HS)_2$. Sulphide and alkalinity were determined on the solution phase and $CaCO_3$ and CaS were determined on the solid fraction. Excess CO_2 was added to 100 mL of the $Ca(HS)_2$ solution to convert unreacted CaS to $Ca(HS)_2$. Rare earth metals were analysed in the $CaCO_3$ solid fraction and in the $Ca(HS)_2$ solution.

6.3.3.8 Rare earth metals content in PG and AMD

A 1 g $CaSO_4 \cdot 2H_2O$ was dissolved in 100 mL 5N HNO_3. The mixture was stirred for 60 min. The mixture was then filtered and analysed with ICP-OES for REEs recovery.

A 100 mL Kopseer mine water was filtered and analysed with ICP-OES for REEs recovery.

6.3.4 Analysis

Sulphide was determined by standard iodometry (APHA, 2012) as reported in **section 5.4.3.**

6.4 RESULTS AND DISCUSSION

6.4.1 Rare earth metals in PG

Table 6.2 shows the concentrations of REEs in PG. High amounts of PG are generated in the production of phosphoric acid. Obtaining REEs from PG is a promising alternative to managing waste. In this study, a 5 N HNO_3 was used for leaching REE from PG (Error! Reference source not found.**)**. The values ranged from 1 .88 mg/g gypsum for Ce to 0.22 mg/g gypsum for Sm.

Table 6.2 Rare earth metals in PG

	PG
REEs	Conc (mg/g)
Ce	1.88
Nd	1.08
La	0.78
Pr	0.52
Sm	0.22
Total	4.48

6.4.2 Rare earth metals in AMD

Rare earth metals are present in lower concentrations in AMD (

Table 6.3). The concentrations ranged from 0.7 to 9.1 mg/L. Ma *et al* reported low concentrations of Ce (5.5 mg/L), La (0.854 mg/L), and Nd (1.310 mg/L) in AMD collected from Mpumalanga coal fields (Ma, *et al*., 2018). The AMD from Jaintia coal fields in India also contained low concentrations of Ce, La, Pr, Nd, Sm, Dy and Gd, ranging from 0.418 mg/L to 1.11 mg/L (Zhao, *et al*., 2007). The concentrations of Ce, La Pr, Dy, Sm and Nd in AMD collected from The Sitai coal fields in China ranged from 0.002 mg/L to 0.019 mg/L (Sahoo, *et al*., 2012).

Table 6.3 REEs content of Kopseer mine water

REEs in Kopseer mine water	Conc mg/L
Ce	9.1
Nd	2.5
Pr	1.6
La	1.0
Sm	0.7
Total	14.9

6.4.3 Gypsum reduction in the case of hemihydrate

6.4.3.1 Why hemihydrate?

The purpose of this section is to determine whether gypsum and the reductant should be processed as a powder or as a solid in the form of a brick or a tile. This possibility was studied by Joubert (Joubert & Pocock, 2013) and planned to investigate further by D S van Vuuren (personal communication, 2022). This will determine the type of kiln to be selected. The rate of heat transfer from the hot gas to the gypsum/reductant particle is determined by the distance heat neat to travel. In the case of a tile or brick a short distance is needed for heat to travel to reach the centre of the tile or brick, as it can be spaced in the hot space. If the hot space is filled with powder, heat needs to travel a long distance to the centre of the body, requiring a much longer reaction time.

A kiln needs to be used for reduction of $CaSO_4 \cdot 2H_2O$ to CaS at 900 °C to 1000 °C. The following options need to be considered:

- kiln type (rotary, fluidised-bed, shaft or tunnel kilns).
- Feed material (powder in the case of rotary and fluidised-bed kilns or pellets in the case of shaft or tunnel kilns).
- Material of construction (metal, ceramic). Due to the high corrosivity of sulphide at high temperatures, most alloys can handle sulphide compounds at high temperatures which make the selection of rotary kilns with steel tubes a risky option, leaving the shaft and tunnel kilns as attractive options.
- Rate of heat transfer. The rate of heat transfer is determined by the distance heat need to be travelled to the centre of the mass of material that needs to be

heated. In the case of powder, the distance is short, and the rate of heat transfer is rapid. In the case of a large mass in a container, the rate of heat transfer is slow, due to the large distance and low rate of heat transfer of non-metallic compounds. To order to avoid systems that need heat to travel a long distance to reach the centre of the mass that need to be heated, the raw material needs to be feed as pellets or tiles, so that hot air can be in contact with a large surface area.

- Binder (starch, gypsum anhydrite). Powders can be processed into pellets by adding a binder such a starch. Joubert suggested the use of gypsum hemihydrate is a suitable binder for a gypsum/coal mixture.

The conditions needed to produce gypsum tiles were determined by doing a series of experiments where water and gypsum hemihydrate were varied. The gypsum hemihydrate ($CaSO_4.2H_2O \rightarrow CaSO_4.½H_2O$) was formed when $CaSO_4 \cdot 2H_2O$ was heated at 170 °C.

Table 6.4 shows how hardness of hydrated hemihydrate is **influenced by the H_2O/Hemihydrate ratio**. It was noted that the more water added to hemihydrate, the harder is the gypsum product. **Table 6.5** shows the results when anhydrite was **contacted with both water (6.9 mol H_2O/ mole gypsum) and activated carbon (6 mole C / mole gypsum)**. It was noted that hard gypsum formed when anhydrite was contacted with water in the presence of activated carbon. The table indicated the rate at which the gypsum set. A setting time of 15 min was needed.

Table 6.4 Effect of H_2O/Hemihydrate ratio on the hardness of hydrated hemihydrate

No		1	2	3	4	5	6	7	8	9
Gypsum to anhydrate										
Glass beaker	mL	100	100	100	100	100	100	100	100	100
Tile thickness	Mm	10	10	10	10	10	10	10	10	10
$C/CaSO_4$	mol/mol	0	0	0	0	0	0	0	0	0
Formation of anhydrate:										
$CaSO_4 \cdot 2H_2O$		172	172	172	172	172	172	172	172	172
C		12	12	12	12	12	12	12	12	12
$CaSO_4 \cdot 2H_2O$	%	90	90	90	90	90	90	90	90	90
C	%	75	75	75	75	75	75	75	75	75
$CaSO_4 \cdot 2H_2O$	G	18	18	18	18	18	18	18	18	18
Furnace	°C	200	200	200	200	200	200	200	200	200
Heat to 170°C	°C	170	170	170	170	170	170	170	170	170

Time	Min	28	28	28	28	28	28	28	28	28
Cool outside to Temp	°C	50	50	50	50	50	50	50	50	50
Cooling time	Min	16	16	16	16	16	16	16	16	16
C	G	0.00	0.00	0.00	0.00	0.00	0.00	0.00	0.00	0.00
Final mass	G	16.20	15.86	15.71	15.38	15.54	15.91	15.14	15.11	15.90
Mass loss	G	1.80	2.14	2.29	2.62	2.46	2.09	2.86	2.89	2.10
Effect of H_2O on hardness:										
H_2O		**0.00**	**3.00**	**6.00**	**7.00**	**8.00**	**9.00**	**9.00**	**10.00**	**12.00**
Anhydrate+H_2O		16.20	18.86	21.71	22.38	23.54	24.91	24.14	25.11	27.90
Mix – spatula		Too little	Hard	Hard	Hard	hard	Hard	Hard	Soft	soft
Portion hard	%	0.00	20.00	50.00	70.00	90.00	100.00	100	Soft	soft
H_2O /Gypsum	mol/mol	0.00	1.59	3.19	3.72	4.25	**4.78**	**4.78**	5.31	6.37

Table 6.5 Effect of setting time on the hardness of hydrated hemihydrate when mixed with carbon

Parameter		**Setting time (min)**		
Time	**Min**	**5**	**10**	**15**
Beaker		Glass	Glass	Glass
Glass beaker	mL	100	100	100
Tile thickness	mm	10	10	10
C/CaSO4	mol/mol	6	6	6
$CaSO_4 \cdot 2H_2O$		172	172	172
C		12	12	12
$CaSO_4 \cdot 2H_2O$	%	90	90	90
C	%	75	75	75
$CaSO_4 \cdot 2H_2O$	g	**18**	**18**	**18**
Furnace	°C	200	200	200
Heat to 170°C	°C	170	170	170
Time	min	28	28	28
Cool outside to Temp	°C	50	50	50
Cooling time	min	16	16	16
C	g	**11.16**	**11.16**	**11.16**
Final mass		25.89	25.89	25.89
Mass loss		3.27	3.27	3.27
H_2O		**13.00**	13.00	13.00
H_2O/Gypsum ratio		**6.90**	6.90	6.90
Anhydrate+H_2O		38.89	38.89	38.89
Mix – spatula				
Hardness out of 10		2	9	10

Table 6.6 and **Figure 6.2** show the effect of temperature on the conversion of $CaSO_4 \cdot 2H_2O$ to $CaSO_4 \cdot ½H_2O$. It was noted that $CaSO_4 \cdot ½H_2O$ formed at a

temperature of 240 °C when 60 min reaction time was allowed. This was concluded from the correspondence in calculated and actual mass loss at 240°C. At lower temperatures the actual mass loss was less than the expected mass loss.

Table 6.7 and **Figure 6.3** show the effect of reaction time on the conversion of $CaSO_4 \cdot 2H_2O$ to $CaSO_4 \cdot ½H_2O$. It was noted that $CaSO_4 \cdot ½H_2O$ formed at a temperature of 180 °C when 120 min reaction time was allowed. This was concluded from the correspondence in calculated and actual mass loss at 120 min.

Table 6.6 Effect of temperature and time on the formation of $CaSO_4 \cdot ½H_2O$

Parameter	**Unit**	**Condition**					
$CaSO_4 \cdot 2H_2O$	g	100	100	100	100	100	100
Furnace temp	°C	140	160	180	200	220	240
Measured temp	°C	140	160	180	200	220	240
Time	min	60	60	60	60	60	60
Reactant	g	99.66	100.04	99.99	100.02	100.00	100.10
Product	g	97.91	94.15	91.65	89.40	86.90	84.40
Mass difference	g	1.75	5.89	8.34	10.62	13.10	15.70
Expected mass loss for $CaSO_4 \cdot ½H_2O$	Calc	15.64	15.70	15.70	15.70	15.70	15.71
Expected mass loss for $CaSO_4 \cdot 0H_2O$	Calc	20.86	20.94	20.93	20.93	20.93	20.95

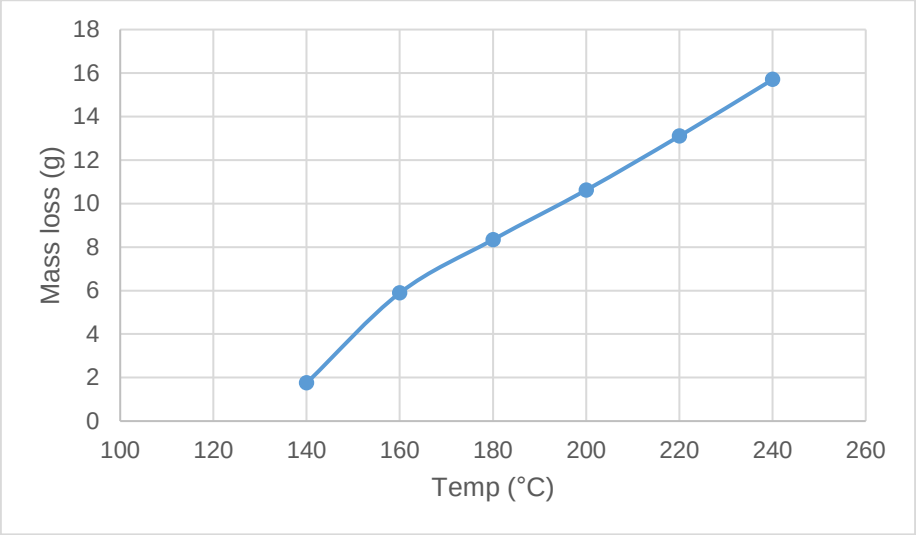

Figure 6.2 Effect of temperature on the formation of $CaSO_4 \cdot ½H_2O$

Table 6.7 Effect of reaction time on the formation of $CaSO_4 \cdot ½H_2O$

Parameter	Unit	Condition		
$CaSO_4 \cdot 2H_2O$	G	100	100	100
Furnace temp	°C	180	180	180
Measured temp	°C	180	180	180
Time	Min	30	60	120
Reactant	G	102.80	99.99	100.10
Product	G	94.40	91.65	84.40
Mass difference	G	8.40	8.34	15.70
Expected mass loss for $CaSO_4 \cdot ½H_2O$	Calc	16.14	15.70	15.71
Expected mass loss for $CaSO_4 \cdot 0H_2O$	Calc	21.52	20.93	20.95

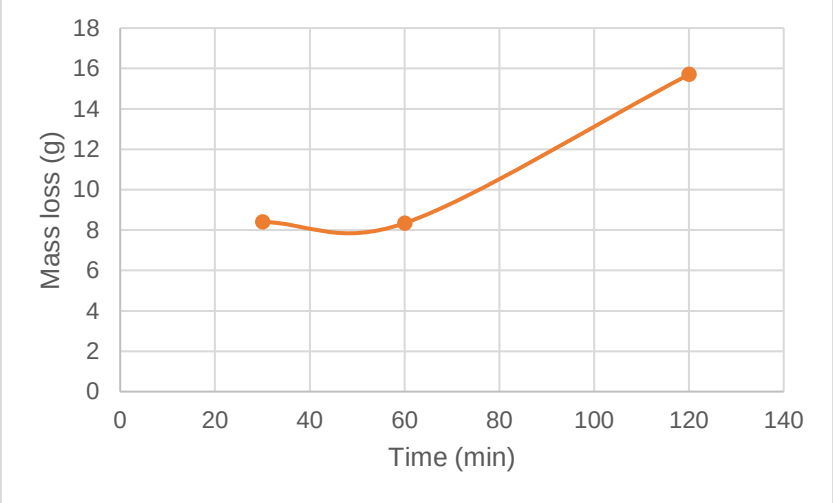

Figure 6.3 Effect of reaction time on the formation of $CaSO_4 \cdot ½H_2O$

6.4.3.2 *Gypsum reduction in the form of a tile*

6.4.3.2.1 Effect C/Gypsum ratio

Table 6.8 shows the effect when hemihydrate/activated carbon was contacted with water to form a hard tile of gypsum/activated carbon. The C/Hemihydrate mole ratio varied between 8 and 2. It was noted that:

- Pellets exploded when heated to 1 000°C for mole ratio's of 4.5 and higher. This can be ascribed to rapid conversion of crystal water in $CaSO_4 \cdot 2H_2O$ to gas.
- The yield of CaS increased from 38% to 97% as the mole ratio increased from 2.0 to 3.0.

Table 6.8 Effect of C/Gypsum mole ratio on the CaS yield

Parameter		**C/Anhydrite**					
Hemihydrate/Gypsum ratio		**1.00**	**1.00**	**1.00**	**1.00**	**1.00**	**1.00**
C/$CaSO_4$	mol/mol	8.00	4.50	3.00	3.00	2.50	2.00
C	%	75.00	75.00	75.00	75.00	75.00	75.00
Gypsum	g	0.00	0.00	0.00	0.00	0.00	0.00
Gypsum purity	%	90.00	90.00	90.00	90.00	90.00	90.00
Hemihydrate	g	15.17	15.17	15.17	15.17	15.17	15.17
Total	g	15.17	15.17	15.17	15.17	15.17	15.17
Total (as $CaSO_4 \cdot 2H_2O$)	g	18.00	18.00	18.00	18.00	18.00	18.00
C	g	12.06	6.78	4.52	4.52	3.77	3.01
H_2O/Hemihydrate	mol/mol	4.78	4.78	4.78	4.78	4.78	4.78
H_2O	mL	9.00	9.00	9.00	9.00	9.00	9.00
Temp	°C	1000	1000	1000	1000	1000	1000
Heat each to 1000°C		Fast	Fast	Fast	Fast	Fast	Fast
Time at Temp	min	30	30	30	30	30	30
Mass of reactants (Plan)				28.70	28.70	27.95	27.19
Mass of reactants (Meas.)	g			30.16	28.64	27.05	27.09
Mass of products	g			12.75	12.81	10.12	9.46
Mass loss	g			17.41	15.83	16.93	17.63
Sulphide in 0.05 g sample	mg			25.92	24.84	14.76	13.68
Sulphide as CaS in product	mg			6610	6364	2987	2588
Conversion	%			97.47	93.85	44.05	38.17
Explosion		Yes	Yes	No	No	No	No
Hardness	out of 10			6.00	6.00	6.00	6.00

6.4.3.2.2 Effect of temperature

Table 6.9 shows the effect when hemihydrate/activated carbon was contacted with water to form a hard tile of gypsum/activated carbon. The temperature was varied between 800 and 1000 °C. It was noted that the yield of CaS increased from 57% to 94% as the temperature increased from 800 to 1000 °C.

Table 6.9 Effect of temperature on the CaS yield

Parameter		**Temp**		
Hemihydrate/Gypsum ratio		**1.0**	**1.0**	**1.0**
C/$CaSO_4$	mol/mol	3	3	3
C	%	75	75	75
Gypsum	g	0	0	0
Gypsum purity	%	90	90	90
Hemihydrate	g	15.17	15.17	15.17
Total	g	15.17	15.17	15.17
Total (as $CaSO_4 \cdot 2H_2O$)	g	18	18	18
C	g	4.52	4.52	4.52

H_2O/Hemihydrate	mol/mol	4.78	4.78	4.78
H_2O	mL	9.00	9.00	9.00
Temp	°C	1000	900	800
Heat each to 1000°C		Fast	Fast	Fast
Time at Temp	Min	30	30	30
Mass of reactants (Plan)		28.70	28.70	28.70
Mass of reactants (Meas.)	g	28.64	28.47	28.66
Mass of products	g	12.81	14.38	18.62
Mass loss	g	15.83	14.09	10.04
Sulphide in 0.05 g sample	mg	24.84	15.12	10.44
Sulphide as CaS in product	mg	6364	4349	3888
Conversion	%	93.85	64.12	57.33
Explosion		No	No	No
Hardness	out of 10	6	5	4
Stick to crucible	out of 10			

It has been shown that solid gypsum /carbon tiles can be formed in tunnel kilns for conversion into CaS. In hard gypsum, the crystal water in a high C/gypsum ratio can cause an explosion. This is due to the phase conversion from solid to vapor at 290 °C when converting gypsum to anhydrite. In hemihydrate gypsum, water vapour in the solid structure caused an explosion due to the higher temperatures No explosion occurred in powdered gypsum because the water vapor could escape freely. Although there is much merit in the use of solid pellets in a tunnel kiln as described by Joubert (Joubert & Pocock, 2013) and planned by van Vuuren (personal communication, 2022), normal gypsum was used in this study for thermal treatment with the aim to recover $CaCO_3$ and to study the behaviour of rare earth metals.

6.4.4 Gypsum processing

6.4.4.1 $CaCO_3$ recovery

The purpose of this section was to evaluate the following stages for the processing of gypsum to $CaCO_3$: (i) Reduction with carbon and (ii) $CaCO_3$ and $Ca(HS)_2$ formation by adding CO_2 and (iii) Behaviour of rare earth metals. The results in **Table 6.10** was generated as follows:

i. CaS was produced by reacting 18 PG with 4.5 g activated carbon at 1000 °C in crucible with a lid on to maintain reducing conditions. Sulphide and Alkalinity analyses were carried out.

ii. Cooled CaS was put in 200 mL water and contacted with different portions of CO_2, up to pH9, to convert CaS to $CaCO_3$ and $Ca(HS)_2$. Sulphide and alkalinity were determined on the solution phase and $CaCO_3$ and CaS were determined on the solid fraction.

iii. Excess CO_2 was added to 100 mL of the $Ca(HS)_2$ solution to convert unreacted CaS to $Ca(HS)_2$.

iv. Rare earth metals were analysed in the $CaCO_3$ solid fraction.

Table 6.10 shows the results for the processing of: (i) $CaSO_4$ to CaS through reduction with activated carbon at 1000 °C, (ii) CaS to $CaCO_3$ and $Ca(HS)_2$ by contacting it with CO_2 and (iii) stripping of H_2S with CO_2. It was found that 72.86% of the gypsum was converted to CaS (**Eq 6.1**). Of the 68.6 mmol CaS that was produced, 82.0% was converted to $CaCO_3$ when CO_2 was added to reduce the pH from 12 to 9.0 The $Ca(HS)_2$ yield was determined as 71.1% (**Eq 6.2**). The sulphide left, was removed partially though H_2S-stripping by adding excess CO_2. Sulphide was reduced form 48.79 mmol in 200 mL to 19.83 mmol, representing a removal of 75.4%. The H_2S stripping was applied for only 5 min. The removal of H_2S can be improved by applying a longer reaction time. Only 5 min was used.

$$CaSO_4 + 4C \rightarrow CaS + 4CO \quad (6.1)$$

$$2CaS + CO_2 + H_2O \rightarrow CaCO_3 + Ca(HS)_2 \quad (6.2)$$

$$Ca(HS)_2 + 2CO_2 + 2H_2O \rightarrow Ca(HCO_3)_2 + 2H_2S \quad (6.3)$$

Table 6.10 Processing of gypsum via CaS to $CaCO_3$

Parameter	mol mass (g)	Unit	Feed	Thermal	CaS processing (CO_2 to pH 9)				H_2S-stripping
					Feed (200 mL)	Solid	Solution	Gas	
$CaSO_4 \cdot 2H_2O$ (90%)	172	g	18.00						
$CaSO_4$	136	g		3.48					
CaS	72	g		4.94					
Activated carbon		g	4.52	2.87					
Impurities (20% of C)		g		0.90					
$CaCO_3$	100	g				5.63			
$Ca(HS)_2$ (as CaS)	72	g			3.51				0.86
Reactants		g	22.46						
Products (measured)		g		10.48					

Products (calc)				12.19					
$CaSO_4 \cdot 2H_2O$	172	mmol	94.19						
$CaSO_4$	136	mmol		25.56					
CaS	72	mmol		68.62	68.62				
Activated carbon	12	mmol	376.67	239.42					
Impurities		mmol							
$CaCO_3$	100	mmol				56.27			
$Ca(HS)_2$ (as CaS)	72	mmol					48.79	19.83	12.00
C/Gypsum		mol/mol	4.00						
Conversion									
CaS from Gypsum		%		72.86					
$CaCO_3$ from CaS		%				82.00			
$Ca(HS)_2$ from CaS		%				71.10			
H_2S stripping		%							39.49

6.4.4.2 REE recovery

It is expected that REEs will stay with the solid $CaCO_3$ faction and not stay in solution with the $Ca(HS)_2$ solution. This was confirmed experimentally. The REEs in the solid $CaCO_3$ fraction was solubilized by dissolving 1 g $CaCO_3$, that was produced from CaS, in 100 mL 5 N HNO_3. The 1 g $CaCO_3$ was produced through the following steps: (i) 18 g phosphogypsum, in contact with 4.52 g activated carbon, was treated at 1 000°C, to form 10.48 g CaS/$CaSO_4$/unreacted carbon/impurities, (ii) 10 g of this product was dissolved in 200 mL of water, contacted with CO_2 to pH 9, to form $CaCO_3$, (iii) the $CaCO_3$ was filtered, dried and weighed (5.63 g $CaCO_3$), (iv) 1 g of the $CaCO_3$ was dissolved in 100 mL 5 N HNO_3, and analysed for REEs. From the previous figures it is calculated that the REEs was recovered from 3.051g phosphogypsum(18g x 10.00 / 10.48 x 1.00 / 5.63). **Table 6.11** shows that on average, 94.2% of the REEs were recovered with the crude $CaCO_3$. This indicates that should pure $CaCO_3$ be produced via $Ca(HS)_2$ (when CaS is contacted with H_2S and not CO_2), the REEs will be on the small coal impurity mass fraction.

Table 6.11 REE fraction recovered on crude $CaCO_3$

REE	REE leached from phosphogypsum	REE from 1 g $CaCO_3$ in 100 mL 5 $NHNO_3$	REEs collected together with $CaCO_3$	REEs collected together with $CaCO_3$
	mg/g gypsum	mg/L	mg/g gypsum	%
Ce	1.88	5.5	1.80	95.9
La	0.78	2.4	0.79	100.9
Nd	1.08	3.6	1.18	109.3
Pr	0.52	1.2	0.39	75.6
Sm	0.22	0.6	0.20	89.4
Average				94.2

Gasser reported that REEs from PG typically ranged from 0.04 to 1% (Gasser, *et al*., 2022). In their study a 3N HNO_3 was used to leach out REEs in PG. The concentrations detected were lower than the concentration range in REEs detected in this study. Table 6.12 shows that the phosphogypsum used in this study contained +4 480 mg REE/kg gypsum compared to 481 mg REE/kg gypsum in the samples used by Gasser.

Table 6.12 Comparison of REE concentrations in phosphogypsum samples

REE	REE (mg/kg gypsum)	
	This study	Gasser study
Ce	1 880.0	234.1
La	780.0	117.0
Nd	1 080.0	<0.1
Pr	520.0	27.1
Sm	220.0	2.0
Er		79.1
Y		21.6
Yb		<0.1
Total	4 480.0	480.9

6.4.5 Comparison of energy needed for direct conversion versus via hemihydrate.

$CaSO_4 \cdot 2H_2O$ can be converted to CaS by feeding it as (i) a tile produced from hemihydrate ($CaSO4 \cdot ½H_2O$) and (ii) a powder. **Table 6.13** and **Table 6.14** show the calculations to determine the energy needed in each case respectively. In the case of the hemihydrate route the coal usage amounted to 14.3 t/h compared to 11.7 t/h when powder gypsum is fed for the processing of 50 t/h gypsum with moisture content of 20%. The various thermodynamic values used were the same is reported in Section 5.4.1 (Thermodynamic values for $CaSO_4$, $BaSO_4$ and Na_2SO_4).

Table 6.13 Calculation of coal needed for the processing of 50 kg/h 80% $CaSO_4 \cdot 2H_2O$ to CaS via hemihydrate.

Parameter	**Input (Mass) (t/h)**	**Output (Mass) (t)**	**T1 (°K)**	**T2 (°K)**	**Cp (KJ/kg.K)**	**H_f (KJ/mol)**	**Hv (KJ/kg)**	**Enthalpy (MJ/h)**	**Hrxn (MJ/mol)**
Wet gypsum	**50.00**								
Moisture content (%)	**20.00**								
	Step 1. (Drying) -$H_2O_{(aq)}$ → $H_2O_{(g)}$								
Total inputs									
Input (Sensible)								426	
$CaSO_4.2H_2O$	40.0		298	303.0	1.08	-		216	
H_2O	10.0		298	303.0	4.19	-		209	
Combustion of Coal	1.1						27 000	28 984	
Total output									
Output (Sensible)								**29 409**	
$CaSO_4.2H_2O$	40.0		298	378.0	1.08	-		3 460	
H_2O	10.0		298	378.0	4.19	-		3 349	
H_2O to Steam	10.0						**2 260**	22 600	
Total output									
Output (Sensible)									
	Step 2. Gypsum to hemi hydrate $CaSO_4.2H_2O$ → $CaSO_4.0.5H_2O + 1.5H_2O$ (g)								
Total inputs								**32 827**	
Input (Sensible)								426	
$CaSO_4.2H_2O$	**40.00**		298	303.0	1.08	**-2 022.6**		216	-2 023
H_2O	10.00		298	303.0	4.19	-285.83		209	-0.29
Combustion of Coal	1.20						27 000	32 401	
Total output								**32 827**	
Output (Sensible)								18 636	
$CaSO_4.½H_2O$	33.72		298	463.0	2.57			14 299	-2 023
H_2O (Free)	6.28		298	463.0	4.19			4 337	-0.29
H_2O to Steam	6.28						2 260	14 191	
	Step 3. Hemihydrate + Water → $CaSO_4 .2H_2O$								
Total inputs								**2 816**	
Input (Sensible)								591	
$CaSO_4.½H_2O$	33.72		298	303.0	2.57			433	-2 023
H_2O (Free)	7.53		298	303.0	4.19			158	
Coal (for drying)	0.08						27 000	2 225	
Total outputs									
Output (Sensible)								**2 816**	0.00
$CaSO_4.2H_2O$	40.00		298	363.0	1.08			2 812	-2 023
Heat of reaction $CaSO_4.2H_2O$ [$CaSO4.½H_2O + 1.5H_2O$ → $CaSO4.2H_2O$]						18.86		4	
	Step 4. Gypsum to anhydrite → $CaSO_4$								
Total inputs								3 460	
$CaSO_4.2H_2O$	40.00		298	378.0	1.08			3 460	

Coal (for drying)	1.16						27 000	31 332	
Total outputs								**34 793**	
Outputs								34 793	
$CaSO_4$	31.63		303	673.0	0.73			8 519	-0.48
Water (H_2O) free	8.37		303	373.0	4.19			2 456	
	8.37		373	673.0	1.95			4 898	
Steam	8.37		303	673.0	1.95		2 260	18 921	-0.79
Coal for dehydration	1.29				1.26		27 000	0	
	Step 5. Reduction ($CaSO_4$ + 2C→ CaS + $2CO_2$)								
Total inputs								**8 681**	
Input (Sensible)								8 681	
$CaSO_4$	31.63		298	673.0	0.73			8 634	-0.48
Coal for reduction	7.44		298	303.0	1.26	-393.51		47	-0.79
Coal for combustion	2.05						27 000	55 250	
Total outputs								**63 931**	
Output (Sensible)									
CaS	16.7		298	1 273.0	0.66	-482.40		10 742	
CO_2	20.5		298	1 273.0	0.85			16 960	
Heat of reaction CaS	16.7	232.6				155.78		36 228	
Total coal usage (t/h)	**14.3**								
Total energy required	**5.6**						27 000	**150 192**	
Coal usage (t coal/t wet gypsum)	**0.11**								

Table 6.14 Calculation of coal needed for the processing of 50 ton/h $CaSO_4 \cdot 2H_2O$ (powder) to CaS

Parameter	**Input (Mass) (t/h)**	**Output (Mass) (t)**	**T1 (°K)**	**T2 (°K)**	**Cp (KJ/kg.K)**	**H_f (KJ/mol)**	**Hv (KJ/kg)**	**Enthalpy (MJ/h)**	**Hrxn (MJ/mol)**
Wet gypsum	**50.00**								
Moisture content (%)	20.0								
	Step 1. Drying H_2O (aq) → H_2O (g)								**0.00**
Total inputs								**29 409**	
Input (Sensible)								426	
$CaSO_4 \cdot 2H_2O$	**40.00**		298	303.0	1.08	**-2 023**		216	**-2.02**
H_2O	10.00		298	303.0	4.19	-285.8		209	-0.29
Combustion of Coal	1.07						27 000	28 984	
Total output								**29 409**	
Output (Sensible)								6 809	
$CaSO_4 \cdot 2H_2O$		40.00	298	378.0	1.08			3 460	**-2.02**
H_2O (Free)		10.00	298	378.0	4.19			3 349	**-0.29**
Steam		10.00	378	378.0	1.95	-285.83		0	**-0.24**
H_2O to Steam		10.00					2 260	22 600	

	Step 2. Gypsum to Anhydride $CaSO_4 \cdot 2H_2O$ → $CaSO_4$ + $2H_2O$								**0**
Total inputs								**35 083**	
Input (Sensible)								3 460	
$CaSO_4 \cdot 2H_2O$	40.00		298	378.0	1.08	-2 023		3 460	**-2.02**
Coal (for drying)	1.17						27 000	31 623	
Total outputs									
Output (Sensible)								**35 083**	**0.00**
$CaSO_4$		31.63	298	673.0	0.73	-1 425		8 634	**-1.43**
H_2O (Free)		8.37	298	373.0	4.19			2 631	
Steam		8.37	373	673.0	1.95			4 898	
Steam		8.37	373	673.0	1.95	-285.8	2 260	18 921	**-0.24**
									0.00
	Step 3. Reduction ($CaSO_4$ + 2C → CaS + $2CO_2$								
Total Inputs								**63 749**	
Input								8 681	
$CaSO_4$	31.63		298	673.0	0.73	-1 425		8 634	**-1.43**
Coal for reduction	7.44		298	303.0	1.26	0.00		47	
Coal for Step 3	2.04						27 000	55 068	**0.00**
Total outputs								**63 749**	
Outputs (Sensible)								27 521	
CaS		16.74	303	1 273.0	0.66	-482.4		10 687	**-0.48**
CO_2		20.47	303	1 273.0	0.85	-393.5		16 834	**-0.79**
Heat of reaction CaS		16.74				155.8		36 228	**0.16**
Total coal usage (t/h)	**11.7**						27 000	**86 900**	
Total Energy Required	**3.22**							115 675	
Coal usage (t coal/t wet gypsum)	**0.23**								
$CaSO_4$ (MJ/t $CaSO_4$)								2 748	
Coal (MJ/kg)								27	
Coal required (kg/t $CaSO_4$)								102	
Coal required (kg/h)								3 219	

6.4.6 REM behaviour

Rare earth elements in PG and in AMD needs to be concentrated as a first step, then it needs to be recovered as crude REEs sludge, followed by separation of the individual metals. In the case of gypsum, the 0.6% REEs can be concentrated through (i) thermal reduction of $CaSO_4$ to CaS, (ii) solubilization of the CaS by contacting it with H_2S, (iii) separation of the soluble $Ca(HS)_2$ fraction from the residue which contains coal impurities and crude REEs sludge in the form of metals sulphide and metals hydroxides. In the case of acid leachate from a waste coal dump, where the REEs concentration is low, it will be attractive to remove the REEs first from the water, rather than to precipitate it together with Fe^{3+} and Al^{3+} as hydroxides.

OLI simulations were used to predict the effect of various alkalis (CO_3^{2-}, OH^-, PO_4^{3-}, S^{2-} and oxalic acid) as a function of pH on its solubility. Focus was placed on the 5 most prominent REEs in PG and coal discard, namely: Ce, Pr, Nd, Sm and La. The behaviour of the various REEs were compared with Fe^{3+} and Al^{3+} when treated with various chemicals, namely Na_2HPO_4, Na_2S, Na_2CO_3, NaOH and NH_4OH. OLI simulation (**Figure 6.4** - **Figure 6.9**) showed the following:

- When treated with Na_2HPO_4, all REEs present in higher concentrations (Ce, Pr, Nd, La and Sm), as well as Fe^{3+}, precipitated as phosphates at pH 1 and higher (**Figure 6.4** - **Figure 6.9 and Table 6.15**). This means that REEs can be removed first as a mixed sludge. Since Fe^{3+} are often present in high concentration in AMD (coal discard leachate) it would be attractive if it can be removed separately so that REEs free of iron can be precipitated as REEs phosphates.
- When treated with NaOH (**Figure 6.9** and **Table 6.16**), La^{3+} was removed as $La(OH)_3$ at pH 7 and higher, Ce and Nd^{3+} at pH 7.7 and Pr^{3+} at pH 8.1. These pH values are significantly higher than the pH value of 3.0 where Fe^{3+} precipitates as $Fe(OH)_3$ or Al^{3+} as $Al(OH)_3$ at pH 3.6. This means that pH adjustment with and hydroxide (*e.g*. NaOH, NH_4OH, $Ca(OH)_2$) can be used for selective removal of Fe^{3+} and Al^{3+} prior to the removal of REEs. It will need to be investigated to see if the small differences in pH needed for precipitation of the various metals will allow selective recovery.
- When treated with Na_2S, only Ce^{3+} was removed as Ce_2S_3 between pH 6.6 and 7.9 (**Table 6.17**). Since Fe^{2+} also precipitates as FeS in the same pH range, it will be needed that Fe^{2+} be oxidised to Fe^{3+} and removed as $Fe(OH)^3$ prior to sulphide treatment. This could provide a possible way for the selective recovery of Ce, one of the prominent REEs in both mine water and PG.
- The other alkalis that were testes, NH_4OH and Na_2CO_3, resulted mainly in the precipitation of REEs as hydroxides, similar to when NaOH is used.

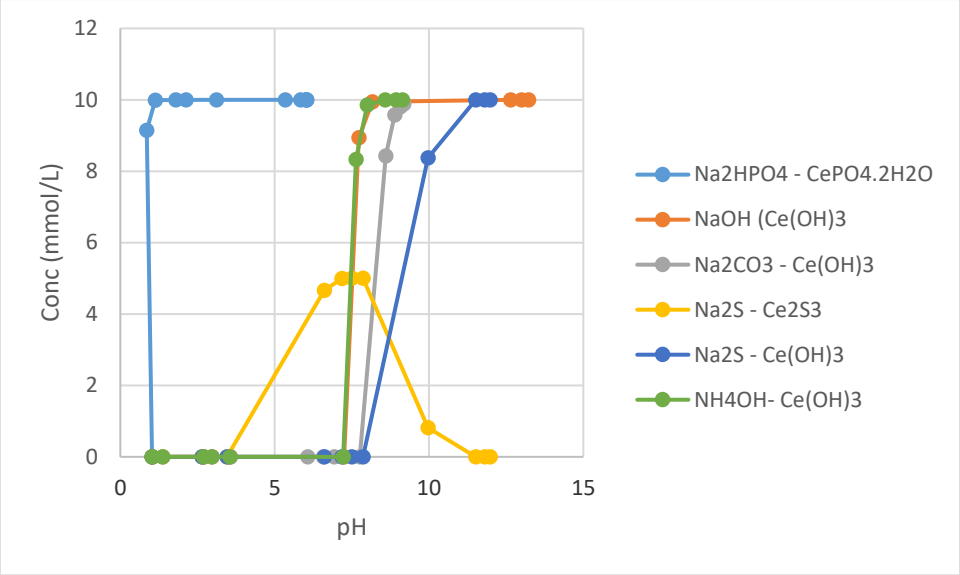

Figure 6.4 Removal of 10 mmol/L $CeCl_3$ with various chemicals

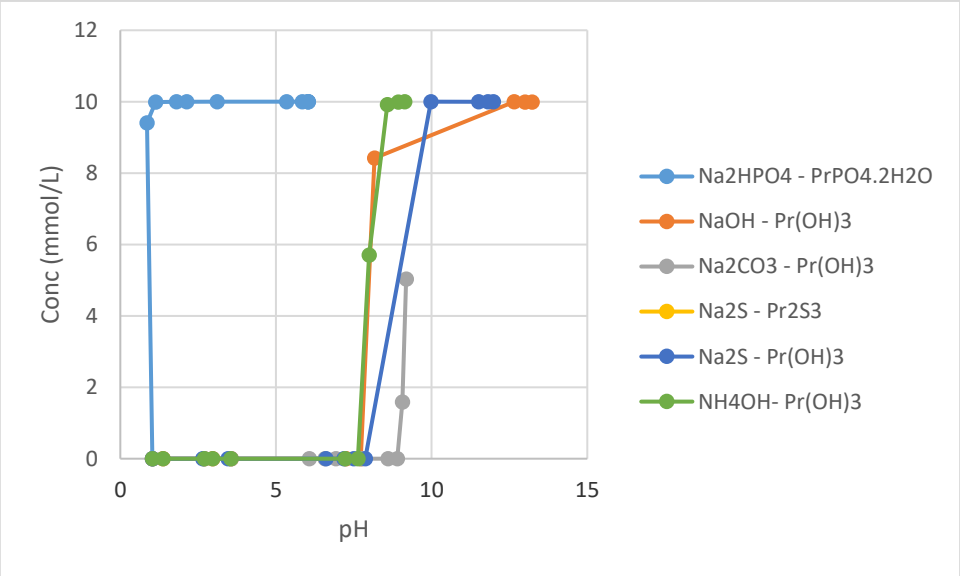

Figure 6.5 Removal of 10 mmol/L $PrCl_3$ with various chemicals

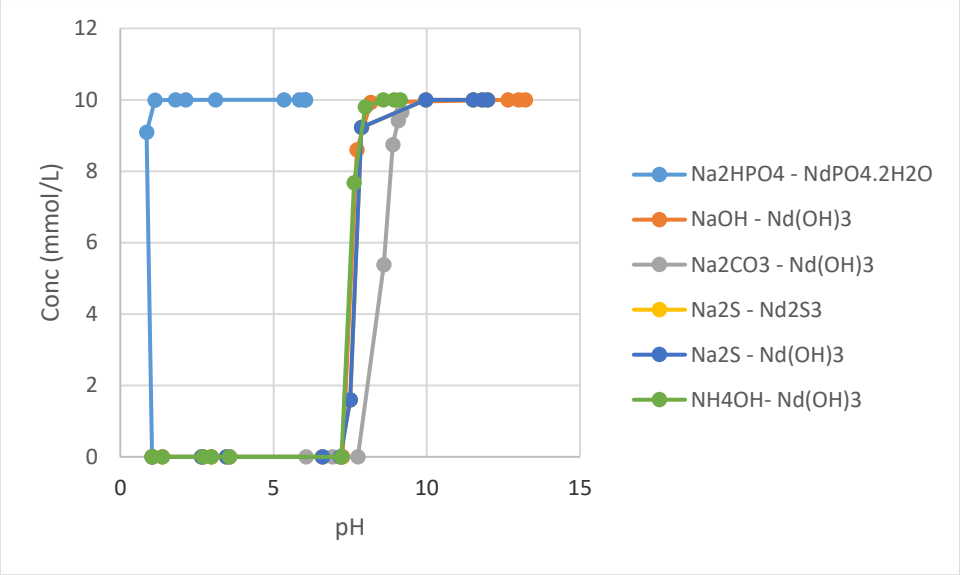

Figure 6.6 Removal of 10 mmol/L $NdCl_3$ with various chemicals

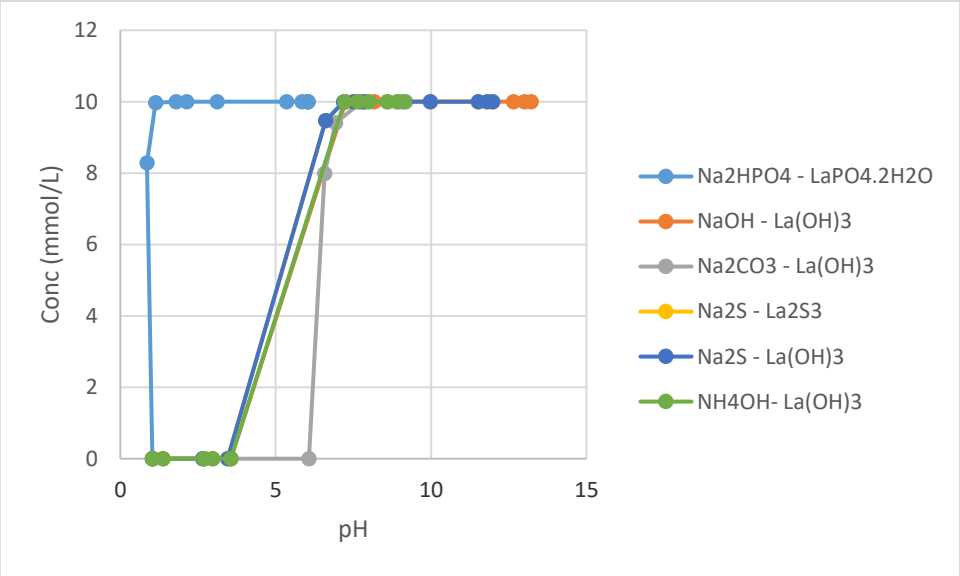

Figure 6.7 Removal of 10 mmol/L $LaCl_3$ with various chemicals

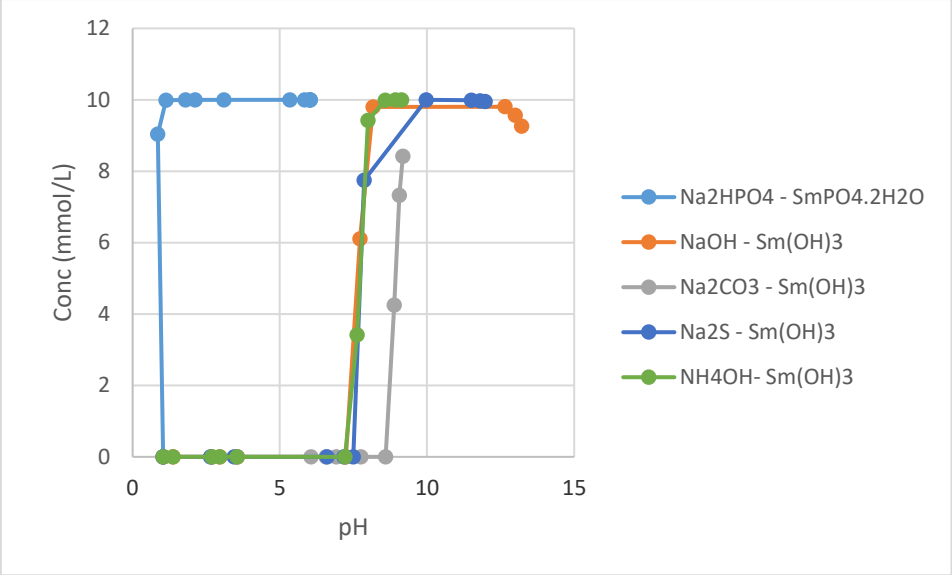

Figure 6.8 Removal of 10 mmol/L $SmCl_3$ with various chemicals

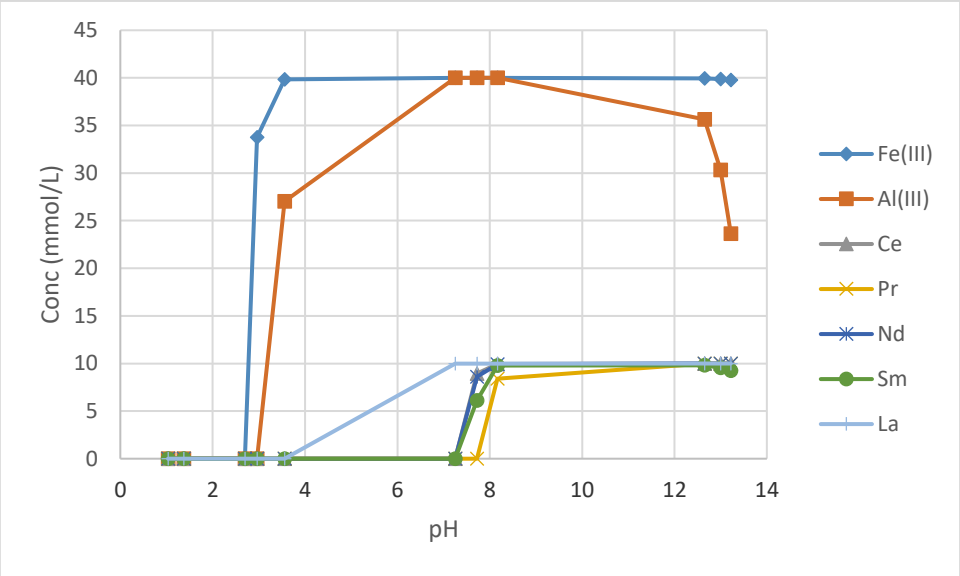

Figure 6.9 Removal of 10 mmol/L metals with NaOH

Table 6.15 Behaviour of various metals when treated with Na_2HPO_4

Na_2HPO_4 [mmol]	pH (Y2)	$CePO_4 \cdot 2H_2O$ [mmol] (Y2)	$PrPO_4 \cdot 2H_2O$ [mmol] (Y2)	$NdPO_4 \cdot 2H_2O$ [mmol] (Y2)	$LaPO_4.2H_2O$ [mmol] (Y2)	$SmPO_4.2H_2O$ [mmol] (Y2)	$FePO_4.2H_2O$ (Phosphosiderite) [mmol] (Y2)	$Fe_3(PO_4)_2 \cdot 8H_2O$ (Vivianite) [mmol] (Y2)	AlPO4 (Berlinite) - Sol [mmol] (Y2)
0.00	1.03	0.00	0.00	0.00	0.00	0.00	0.00	0.00	0.00
100.00	0.86	9.15	9.41	9.09	8.28	9.04	36.48	0.00	0.00
200.00	1.13	9.99	9.99	9.99	9.97	9.99	39.91	0.00	0.00
300.00	1.8	10.00	10.00	10.00	10.00	10.00	40.00	0.00	0.00
400.00	2.13	10.00	10.00	10.00	10.00	10.00	40.00	0.00	32.88
500.00	3.11	10.00	10.00	10.00	10.00	10.00	40.00	0.00	39.96
600.00	5.34	10.00	10.00	10.00	10.00	10.00	40.00	5.83	40.00
700.00	5.84	10.00	10.00	10.00	10.00	10.00	40.00	6.46	40.00
800.00	6.03	10.00	10.00	10.00	10.00	10.00	40.00	6.54	40.00
900.00	6.03	10.00	10.00	10.00	10.00	10.00	40.00	6.54	40.00
1000.00	6.02	10.00	10.00	10.00	10.00	10.00	40.00	6.54	40.00

Table 6.16 Behaviour of various metals when treated with NaOH

NaOH [mmol]	pH (Y2)	$Fe(OH)_3$ (Bernalite) - Sol [mmol] (Y2)	$Al(OH)_3$ (Gibbsite) - Sol [mmol] (Y2)	$Fe(OH)_2$ (Amakinite) - Sol [mmol] (Y2)	$Ce(OH)_3$ - Sol [mmol] (Y2)	$Pr(OH)_3$ - Sol [mmol] (Y2)	$Nd(OH)_3$ - Sol [mmol] (Y2)	$La(OH)_3$ - Sol [mmol] (Y2)	$Sm(OH)_3$ - Sol [mmol] (Y2)
0.00	1.03	0.00	0.00	0.00	0.00	0.00	0.00	0.00	0.00
100.00	1.37	0.00	0.00	0.00	0.00	0.00	0.00	0.00	0.00
200.00	2.70	0.00	0.00	0.00	0.00	0.00	0.00	0.00	0.00
300.00	2.96	33.74	0.00	0.00	0.00	0.00	0.00	0.00	0.00
400.00	3.56	39.84	27.02	0.00	0.00	0.00	0.00	0.00	0.00
500.00	7.25	40.00	40.00	0.00	0.00	0.00	0.00	9.99	0.00
600.00	7.72	40.00	40.00	0.00	8.94	0.00	8.60	10.00	6.10
700.00	8.17	40.00	40.00	13.74	9.94	8.42	9.93	10.00	9.80
800.00	12.65	39.94	35.66	20.00	10.00	10.00	10.00	10.00	9.81
900.00	12.99	39.87	30.31	20.00	10.00	9.99	10.00	10.00	9.56
1000.00	13.22	39.78	23.64	20.00	10.00	9.99	10.00	10.00	9.26

Table 6.17 Behaviour of various metals when treated with Na_2S

Na_2S [mmol]	pH (Y2)	Ce_2S3 - Sol [mmol] (Y2)	FeS (Pyrrhotite) - Sol [mmol] (Y2)
0.00	1.03	0.00	0.00
100.00	2.64	0.00	0.44
200.00	3.45	0.00	19.56
300.00	6.61	4.66	20.00
400.00	7.18	4.99	20.00
500.00	7.50	5.00	20.00
600.00	7.86	5.00	20.00
700.00	9.97	0.81	20.00
800.00	11.51	0.00	20.00
900.00	11.80	0.00	20.00
1000.00	11.98	0.00	20.00

The above information can be used as guidance how to approach the treatment of mine water and PG rich in REEs. In the case of AMD the following approach could be evaluated in the laboratory: (i) remove Fe^{2+} though biological oxidation to form Fe^{3+}, (ii) remove Fe^{3+} and Al^{3+} by raising the pH with $Ca(OH)_2$ or NaOH to 4.5 for removal as $Fe(OH)_3$ and $Al(OH)_3$ respectively, (iii) selective recovery of Ce^{3+} as Ca_2S_3 by dosing Na_2S at pH 6. The remaining REEs (Pr^{3+}, Nd^{3+}, La^{3+}, Sm^{3+}) can be removed as hydroxides by dosing $Ca(OH)_2$, Na_2CO_3 or NaOH. If $Ca(OH)_2$ is used, the REEs sludge will be mixed with gypsum which need to be avoided. An alternative approach will be to precipitate the REEs as phosphates by dosing Na_2HPO_4 after Fe^{3+} and Al^{3+} has been removed at pH 4.

In the case of PG , the REEs will be present as sulphides and hydroxides after reduction of $CaSO_4$ to CaS and solubilization of CaS with H_2S. The $Ca(HS)_2$ solution will be free of REEs, while the residue will contain Ce_2S_3 (**Figure 6.4**) and the remaining REEs present as REEs hydroxides (**Figure 6.9**). The REEs in the residue can be dissolved in a HNO_3 solution and further treated with conventional techniques for separation of the various REEs. Ce^{3+} can be selectively separated as Ce_2S_3 at pH 6.6 as the other REEs need pH 7.7 before it precipitates as hydroxides.

6.4.7 Morphological characteristics of hemihydrate

Figure 6.10 shows the crystal morphology and size distribution of were $CaSO_4 \cdot ½H_2O$ analyzed by SEM. The calcium sulphate hemihydrate was prepared from $Ca_2SO_4 \cdot 2H_2O$ in thermal conditions. **Figure 6.10** shows that the $CaSO_4 \cdot ½H_2O$ comprised of rhombohedral and mainly irregular plate particles with the broad particle size range of between 8.4 µm and 70.8 µm with the average particle size of 30.6 µm (**Figure 6.11**). The average height of the particles was found to be 2.6 µm. The small particles appear to be forming on top of the large particles. There is a slight difference in the morphology of the small and large particles. The images show a defined crack on the plates at higher magnification as compared to (**Figure 5.5**). The morphology of $Ca_2SO_4 \cdot 2H_2O$ (**Figure 5.5**) and $CaSO_4 \cdot ½H_2O$ (**Figure 6.10**) are somewhat similar. The difference is in the size and height of the particles. There is a decrease in the average particle size from 44.0 µm $Ca_2SO_4 \cdot 2H_2O$ to 30.6 µm $CaSO_4 \cdot ½H_2O$. The height of the particles also decreased from 4.6 µm of $Ca_2SO_4 \cdot 2H_2O$ to 2.6 µm $CaSO_4 \cdot ½H_2O$. Numerous researches have focused on the relationship between the properties of $CaSO_4 \cdot ½H_2O$ and its crystal morphology (Chen, *et al*., 2021), (Kutkut & Andreana, 2010) (Parikh, 2002).

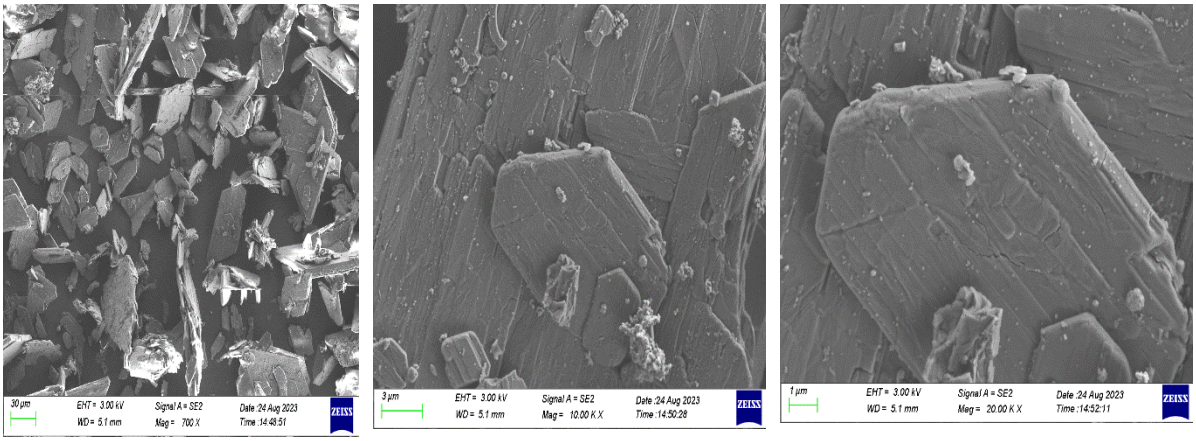

a. 1 k times magnification b. 10 k times magnification c. 20 k times magnification

Figure 6.10 SEM images of Calcium sulphate hemihydrate ($CaSO_4 \cdot ½H_2O$).

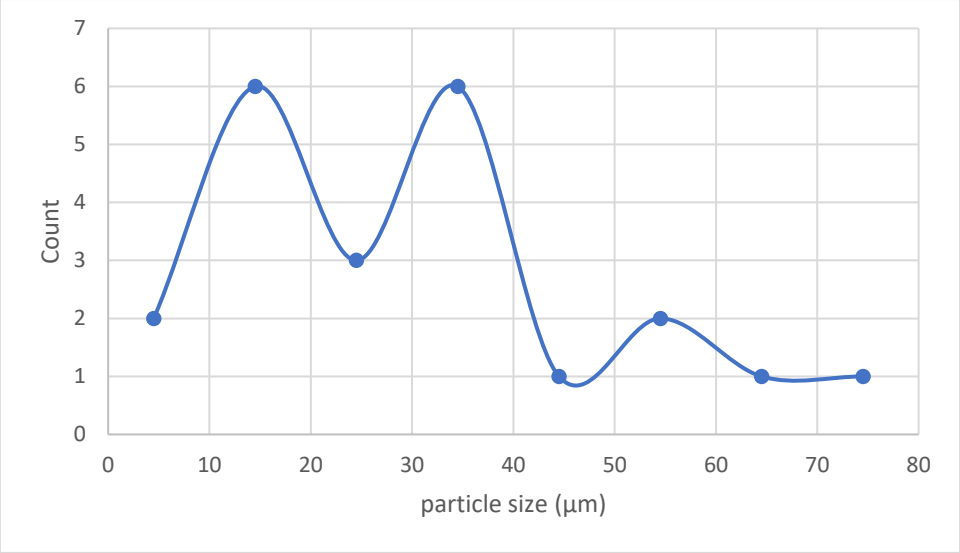

Figure 6.11 Particle size distribution of $CaSO_4 \cdot ½H_2O$

6.5 CONCLUSIONS

i. Rare earth metals in phosphogypsum amounted to 4.48 mg/g gypsum and can be collected with the crude $CaCO_3$ or solid impurities.

ii. Leachate from a waste coal dump contained 14.9 mg/L REE.

iii. Gypsum reduction in a kiln can be carried out by feeding a powder or as a solid when processed via hemihydrate ($CaSO_4 \cdot ½H_2O$).

iv. The yield of CaS produced from hemihydrate/carbon ratio increased from 57% to 94% as the temperature increased from 800 to 1000 °C.

v. CaS can be produced from $CaSO_4$ through reduction with activated carbon at 1000 °C.

vi. CaS can be converted to $CaCO_3$ and $Ca(HS)_2$ by contacting it with CO_2.

vii. H_2S can be stripped off by adding excess CO_2.

CHAPTER 7: CONCLUSIONS AND RECOMMENDATIONS

7.1 CONCLUSIONS

Mine waste is a potential source of environmental pollution due to the release of large amounts of heavy metals and acids. According to current legislation, hazardous waste disposed of in landfills must not contain more than 40% water. This is further motivation why waste streams in mining and other industries need to be processed into saleable products to minimize the need for waste disposal in toxic waste landfills. The zero-waste disposal is applied in this study to prevent the high disposal costs. If the solid waste cannot be treated to yield valuable products, they would have to be transported to a toxic waste disposal site. The transport and disposal costs normally amount to R1000/t and R1500/t, respectively. The value of saleable products, *e.g*., $CaCO_3$, Na_2CO_3 and REEs, will offset most of the capital redemption and running cost.

Gypsum waste from the fertilizer industry, brine rich in sodium and magnesium sulphates from mines and power plants can be used to obtain valuable products. First, waste gypsum is converted into CaS through thermal reduction at 1000 °C at a retention time of 60 min. Secondly, CaS is mixed with deionized H_2O and reacted with CO_2 to form $CaCO_3$ and $Ca(HS)_2$. The latter $Ca(HS)_2$ is further reacted with a solution of Na_2CO_3 to form nano $CaCO_3$. High-grade precipitated $CaCO_3$ can be produced by reacting CO_2 with a solution of $Ca(HS)_2$.

In this study, the process steps required for the processing of Na_2SO_4 to Na_2CO_3 and NaHS were evaluated. It was showed that Na_2SO_4 cannot be directly reduced with carbon due to the relatively low melting point of 890 °C of Na_2SO_4. Sodium sulphide can be produced indirectly from Na_2SO_4 by reaction with CaS or BaS. Barium sulphide was formed when $BaSO_4$ was mixed with carbon and reduced thermally at 1000 °C in a muffle furnace. The production of Na_2S via BaS was the preferred above Na_2S via CaS due to less $CaSO_4$ left in solution. The Na_2S produced can be further used as a reactant to produce to form $NaHCO_3$(aq) and NaHS(aq). The latter two compounds can be separated through freeze-crystallization, as $NaHCO_3$ has a lower solubility at 0 °C. Sodium bicarbonate can be converted into Na_2CO_3 though heating.

The principle of freeze crystallization shows the potential to be economical in terms of low energy demand, low by-product pollution, process flexibility, simplicity and

subsequent low temperature usage as a by-product of the process. $MgSO_4$ remains in solution due to its high solubility during freeze-crystallization. OLI simulation and beaker studies showed that $Mg(OH)_2$ successfully formed when $MgSO_4$ was contacted stepwise with Na_2S. The us of Na_2S to produce $Mg(OH)_2$ is an attractive route because the product, Na_2SO_4, was highly soluble. In contrast, the use of BaS was not attractive as $BaSO_4$ formed which has a low solubility. In the case of $MgSO_4$ and CaS, solid gypsum precipitated together with $Mg(OH)_2$. $Mg(OH)_2$(s) can be separated from the NaHS and the Na_2SO_4 through settling or filtration with a belt filter. Na_2SO_4 was successfully separated from the NaHS through cooling, as Na_2SO_4 has a solubility of only 45 g/L at 0 °C, compared to 400 g/L at room temperature. The $Na_2SO_4.10H_2O$ successfully crystallized from the Na_2SO_4 due to its decreased solubility at colder temperatures. NaHS remained in solution as it has a high solubility. NaHS can be concentrated through removal of water through freeze-crystallization.

It was founded in this study that H_2S was formed when CaS or Na_2S was contacted with CO_2. Hydrogen sulphide is highly flammable and highly toxic. It can be converted to S by using the Claus process. OLI software also showed that O_2 can be used for oxidation of H_2S to S_8.

The study determined whether gypsum and the reductant should be processed as a powder or as a solid in the form of a brick or a tile. Gypsum tiles were successfully produced by performing a series of experiments with varying water and hemihydrate gypsum ratio. The gypsum hemihydrate ($CaSO_4.2H_2O \rightarrow CaSO_4.½H_2O$) formed successfully when $CaSO_4 \cdot 2H_2O$ was heated at 170 °C.

With increasing global demand for REEs and limited supply due to government mining and export restrictions, there is an urgent need to find efficient ways to recover REEs from waste streams. Additionally, REEs are toxic and must be completely removed from wastewater. Therefore, the use of HNO_3 to recover REEs from PG is particularly important since it is a strong oxidizing agent, forms soluble nitrates, and removes rare earth elements. It may be a suitable solution as it has the advantage of leaching.

7.2 RECOMMENDATIONS

It is recommended that:

1. A tunnel kiln with a capacity of 10 kg/h be designed and constructed for the conversion to of $BaSO_4$ to BaS and the conversion of $CaSO_4$ to CaS
2. The BaS be used for the processing of Na_2SO_4 to Na_2S
3. The Na_2S be contacted with CO_2 for the production of Na_2CO_3 via $NaHCO_3$ and NaHS as the intermediate products.

REFERENCES

References

Abdel-Aal, H., Abdelkreem, M. & Zohdy, K., 2016. Dual-Purpose Solvay-Dow (Magnesium) Conceptual Process.. *Open Access Library Journal,* 3(11), pp. 1-5.

Abdel-Fattah, M. K., 2012. Role of gypsum and compost in reclaiming saline-sodic soils. *J. Agric. Vet. Sci,* 13(1), pp. 30-38.

Abdellatif, M. & Freeman, M., 2011. Mintek Thermal Magnesium Process: Status and Prospective. *the Advanced Metals Initiative*, 19 October.

Abreu, M. M., Santos, E. S., Ferreira, M. & Magalhães, M. C. F., 2012. Cistus salviifolius a promising species for mine wastes remediation. *Journal of Geochemical Exploration,* Volume 113, pp. 86-93.

ADB, 2002. *Report Prepared for Sustainable Development and Poverty Reduction Uni,* Côte dÍvoire: Solid Waste Management Options For Africa.

Adibi, N. et al., 2014. Introducing a multi-criteria indicator to better evaluate impacts of rare earth materials production and consumption in life cycle assessmen. *J. Rare Earths,* Volume 32, p. 288–292.

Adlem, C., Maree, J. P. & Du Plessis, P., 1991. *Treatment of sulphate-rich mining effluents with the barium hydroxide process and recovery of valuable by-products.* s.l., In Proc. 4th International Mine Water Assoc. Congress .

Akcil, A. & Koldas, S., 2006. Acid Mine Drainage (AMD): causes, treatment and case studies. *Journal of cleaner production,* Volume 14, pp. 1139-1145.

Ali, S., 2014. Social and environmental impact of the rare earth industries. *Resources,* Volume 3, p. 123–134.

Alvarado, E., Torres-Martinez, L., Fuentes, A. & Quintana, P., 2000. Preparation and characterization of MgO powders obtained from different magnesium salts and the mineral dolomite. *Polyhedron,* 19(22), pp. 2345-2351.

Amezketa, E., Aragüés, R. & Gazol, R., 2005. Efficiency of sulfuric acid, mined gypsum, and two gypsum by-products in soil crusting prevention and sodic soil reclamation. *Agronomy Journal,* 97(3), pp. 983-989.

Amran, N. et al., 2016. Parametric Study on the Performance of Progressive Cryoconcentration System. *Chemical engineering communications,* 203(7), pp. 957-975.

APHA, 2012. *Standard methods for the examination of water and wastewater, 12th ed.* Washington, DC: American Public health Association,.

Aphane, M., Van Der Merwe, E. & Strydom, C., 2009. Influence of hydration time on the hydration of MgO in water and in a magnesium acetate solution. *Journal of thermal analysis and calorimetry,* Volume 96, pp. 987-992.

Arai, S., 1975. Contact metamorphosed dunite-harzburgite complex in the Chugoku district, western Japan. *Contributions to Mineralogy and Petrology,* 52(1), pp. 1-16.

Argyle, M. D. & Bartholomew, C. H., 2015. Heterogeneous catalyst deactivation and regeneration: a review.. *Catalysts,* 5(1), pp. 145-269.

Ashok, A., Kennedy, L., Vijaya, J. & Aruldoss, U., 2018. Optimization of biodiesel production from waste cooking oil by magnesium oxide nanocatalyst synthesized using coprecipitation method. *Clean Technologies and Environmental Policy,* 20(6), pp. 1219-1231.

Atchudan, R., Perumal, S., Joo, J. & Lee, Y. R., 2022. Synthesis and Characterization of Monodispersed Spherical Calcium Oxide and Calcium Carbonate Nanoparticles via Simple Pyrolysis. *Nanomaterials,* 12(14), p. 2424.

Atwood, D. A., 2013. *The rare earth elements: fundamentals and applications.* USA: John Wiley & Sons.

Aube, B., 2004. *Sludge Disposal in Mine Workings at Cape Breton Development Corporation..* Sudbury, Ontario, Paper presented at the Sludge Management and Treatment of Weak Acid or Neutral pH Drainage.

Awadhwal, N. K. & Thierstein, G. E., 1985. Soil crust and its impact on crop establishment: a review. *Soil and Tillage Research,* 5(3), pp. 289-302.

Ayyıldız, Y. & Tarhan, L., 2013. Case study applications in chemistry lesson: gases, liquids, and solids. *Chemistry Education Research and Practice,* 14(4), pp. 408-420.

Babou-Kammoe, R., Hamoudi, S., Larachi, F. & Belkacemi, K., 2012. Synthesis of CaCO3 nanoparticles by controlled precipitation of saturated carbonate and calcium nitrate aqueous solutions. *The Canadian journal of chemical engineering,* 90(1), pp. 26-33.

Backus, R., 2007. *Focus on surfactants, synthetic soda ash vs natural soda,* s.l.: s.n.

Bafghi, M., Yarahmadi, A., Ahmadi & Mehrjoo, H., 2011. Effect of the type of carbon material on the reduction kinetics of barium sulfate. *Iranian Journal of Materials Science and Engineering,* 8(3), pp. 1-7.

Baig, S., Coulomb, I., Courant, P. & Liechti, P., 1999. Treatment of landfill leachates: Lapeyrouse and Satrod case studies.. *The Journal of the International Ozone Association,* Volume 21, pp. 1-22.

Balachandran, S., Thirumalai, K. & Swaminathan, M., 2014. Facile hydrothermal synthesis of a highly efficient solar active Pr 6 O 11–ZnO photocatalyst and its multiple applications. *RSC Advances,* Volume 53, pp. 27642-27653.

Barbosa, F., Barbosa, L., Jucá, M. & Cunha, R., 2010. Applications of magnesium sulfate in obstetrics and anesthesia. *Revista Brasileira de Anestesiologia,* Volume 60, pp. 104-110.

Batuecas, E. et al., 2021. Recycling CO2 from flue gas for CaCO3 nanoparticles production as cement filler: A Life Cycle Assessment.. *Journal of CO2 Utilization,* Volume 45, p. 101446.

Benalia, M. C. et al., 2022. Removal of heavy metals from industrial wastewater by chemical precipitation: mechanisms and sludge characterization. *Arabian Journal for Science and Engineering,* 47(5), pp. 5587-5599.

Benamor, Y., Bousselmi, L., Takenouti, H. & Triki, E., 2005. Influence of sulphate ions on corrosion mechanism of carbon steel in calcareous media. *Corrosion Engineering, Science and Technology,* Volume 40, pp. 129-136.

Berthelot, M., 1890. The reaction of materials with SiO2-derived at the temperature of sodium sulphate reduction. *Ann. chim. phys,* 21(6), p. 397.

Berthier, P., 1823. Sodium reduction using carbon as a reducing agent. *Ann. chim. phys.,* Volume 22, p. 229.

Beruto, D. & Giordan, M., 1993. Calcite and aragonite formation from aqueous calcium hydrogen carbonate solutions: effect of induced electromagnetic field on the activity of CaCO3 nuclei precursors. *J. Chem. Soc. Faraday Trans.,* Volume 89, p. 2457–2461..

Berzelius, J., 1822. Reduction of sodium sulphate using carbon. *Schweiggers Journ,* Volume 34, pp. 8-15.

Białowiec, A., 2011. Hazardous emissions from municipal solid waste landfills.. *Contemporary problems of management and environmental protection,* 9(9), pp. 7-28.

Billard, H., 2001. Waste disposal centers. Exploitation; Centres de stockage des dechets. Exploitation. *Techniques de l'Ingenieur. Environnement,* Volume 1.

Bini, C. & Wahsha, M., 2014. *Potentially harmful elements and human health. In PHEs, environment and human health.* Dordrecht: Springer.

Binnemans, K. et al., 2015. Towards zero-waste valorisation of rare-earth-containing industrial process residues: a critical review. *Journal of Cleaner Production,* Volume 99, pp. 17-38.

Binnemans, K. et al., 2013. Recycling of rare earths: a critical review. *J. Clean.Prod.,* Volume 51, p. 1–22.

Birchal, V., Rocha, S. & Ciminelli, V., 2000. The effect of magnesite calcination conditions on magnesia hydration. *Minerals engineering,* 13(14), pp. 1629-1633.

Blakely, C. et al., 2012. *Rare Earth Metals,* China: s.n.

Bleiwas, D. & Gambogi, J., 2013. *Preliminary estimates of the quantities of rare-earth elements contained in selected products and in imports of semimanufactured products to the United States,* s.l.: US Department of the Interior, US Geological.

Bodnarchuk, M. et al., 2014. Self-assembly of calcium carbonate nanoparticles in water and hydrophobic solvents. *The Journal of Physical Chemistry,* 118(36), pp. 21092-21103.

Bologo, V., Maree, J. P. & Carlsson, F., 2012. Application of magnesium hydroxide and barium hydroxide for the removal of metals and sulphate from mine water. *Water SA,* Volume 38, pp. 23-28.

Bonny, S. M. & Jones, B., 2008. Controls on the precipitation of barite (BaSO4) crystals in calcite travertine at Twitya Spring, a warm sulphur spring in Canada's Northwest Territories. *Sedimentary Geology,* 203(1), pp. 36-53.

Bourzac, K., 2010. Can the US rare earth industry rebound.. *Technol. Rev,* Volume 29.

Boyjoo, Y., Pareek, V. K. & Liu, J., 2014. Synthesis of micro and nano-sized calcium carbonate particles and their applications. *Journal of Materials Chemistry A,* 2(35), pp. 14270-14288.

Boyoo, Y., Pareek, V. K. & Liu, J., 2014. Synthesis of Micro and Nano-sized Calcium Carbonate Particles and their Applications. *Journal Material Chemistry A,* Volume 2, pp. 14270-14288.

Brahaita, I. et al., 2017. CARPATHIAN JOURNAL OF EARTH AND ENVIRONMENTAL SCIENCES,. *The efficiency of limestone in neutralizing acid mine drainage-A laboratory study.,* 12(2), pp. 347-356.

Budnikov, G. & Ulakhovich, N., 1980. Extraction polarography and its analytical applications.. *Russian Chemical Reviews,* 49(1), p. 74.

Bünzli, J. G. & Eliseeva, S. V., 2010. Lanthanide NIR luminescence for telecommunications, bioanalyses and solar energy conversion. *J. Rare Earth,* Volume 28, p. 824–842.

Camiletti, J., Soliman, A. & Nehdi, M., 2013. Effect of nanocalcium carbonate on early-age properties of ultra-highperformance concrete,. *Magazine of Concrete Research,* 65(5), p. 297–307.

Campbell, G., 2014. Rare earth metals: a strategic concern.. *Mineral Economics, ,* 27(1), pp. 21-31.

Castor, S. & Hedrick, J., 2006. Rare earth elements. *Industrial minerals and rocks,* pp. 769-792.

Chang, M., Lee, H., Wu, F. & Lai, C., 2004. Simultaneous removal of nitrogen oxide/nitrogen dioxide/sulfur dioxide from gas streams by combined plasma scrubbing technology. *Journal of the Air & Waste Management Association,* 54(8), pp. 941-949.

Chang, R., Choi, D., Kim, M. & Park, Y., 2017. Tuning crystal polymorphisms and structural investigation of precipitated calcium carbonates for CO2 mineralization. *ACS Sustain. Chem. Eng. ,* Volume 5, p. 1659–1667.

Charalampides, G., Vatalis, K., Apostoplos, B. & Ploutarch-Nikolas, B., 2015. Rare earth elements: industrial applications and economic dependency of Europe. *Procedia Economics and Finance,* Volume 24, pp. 126-135.

Chen, B. et al., 2009. Influence of nanoscale marble (calcium carbonate caco3) on properties of D600R surfacing electrode. *Welding Journal, Research Supplement,* Volume 88, pp. 99-103.

Chen, J. et al., 2021. Non-hazardous industrial waste in the United States: 100 Million tonnes of recoverable resources. *Resources, Conservation and Recycling,* Volume 167, p. 105369.

Chen, T. & Dutrizac, J., 2005. Mineralogical characterization of a copper anode and the anode slimes from the La Caridad copper refinery of Mexicana de Cobre. *Metallurgical and materials Transactions B,* Volume 36, pp. 229-240.

Chen, X., Wu, Q., Gao, J. & Tang, Y., 2021. Hydration characteristics and mechanism analysis of β-calcium sulfate hemihydrate. *Construction and Building Materials,* Volume 296, p. 123714.

Chian, E. & DeWalle, F., 1976. Sanitary landfill leachates and their treatment. *Journal of the Environmental Engineering Division,,* 102(2), pp. 411-431.

Chu, S. & Majumdar, A., 2012. Opportunities and challenges for a sustainable energy future.. *Nature,* Volume 488, p. 294–303.

Cipollina, A. et al., 2015. Reactive crystallisation process for magnesium recovery from concentrated brines. *Desalination and Water Treatment,* 55(9), pp. 2377-2388.

Clapper, J., 2013. *World wide Threat Assessment of the US Intelligence Community.,* Washington, DC: Senate Select Committee on Intelligence.

Clark, S., Poole, F. & Wang, Z., 2004. Comparison of some sediment-hosted, stratiform Barite deposits in China, the United States, and India. *Ore Geol. Rev.,* 24(1-2), p. 85−101.

Clement, F. & Desormes, J., 1801. Sodium reduction with carbon or carbon monoxide. *J. de Physique Hist. Nat,* Volume 89, p. 428.

Council, E. C. I., 2003. Process bref for soda ash. *European Soda Ash Producers Association,* pp. 1-70.

Curlin, L. C., Bommaraju, T. V. & Hansson, C. B., 1991. *Alkali and Chlorine Products.* s.l.:Encyclopedia of Chemical Technology.

Da Silva, E. F. et al., 2005. The effect of unconfined mine tailings on the geochemistry of soils, sediments and surface waters of the Lousal area (Iberian Pyrite Belt, Southern Portugal). *Land Degradation & Development,* 16(2), pp. 213-228..

Dalarsson, N., Dalarsson, M. & Golubovic, L., 2011. *Introductory statistical thermodynamics..* s.l.:Academic Press..

Das, N. & Das, D., 2013. Recovery of rare earth metals through biosorption: an overview. *Journal of rare earths,* 31(10), pp. 933-943.

de Beer, M., 2014. *The production of precipitated calcium carbonate from industrial gypsum wastes.* Potchefstroom: North West University, Ph.D. thesis.

de Beer, M., Doucet, F. J., Maree, J. P. & Liebenberg, L., 2015. Synthesis of high-purity precipitated calcium carbonate during the process of recovery of elemental sulphur from gypsum waste. *Waste Management,* Volume 46, pp. 617-627.

de Beer, M., Maree, J. P., Liebenberg, L. & Doucet, F. J., 2014. Conversion of calcium sulphide to calcium carbonate during the process of recovery of elemental sulphur from gypsum waste. *Waste Management,* 34(11), pp. 2373-2381.

de Beer, M. et al., 2010.. Acid mine water reclamation using the ABC process..

de Carvalho Pinto, P. C. et al., 2015. A cleaner production of sodium hydrogen carbonate: partial replacement of lime by steel slag milk in the ammonia recovery step of the Solvay process. *Clean Techn Environ Policy,* Volume 17, pp. 2311 - 2321.

Debrah, J., Vidal, D. & Dinis, M., 2021. Raising awareness on solid waste management through formal education for sustainability: A developing countries evidence review.. *Recycling,* 6(1), p. 6.

Department of Geology, 2015. *Carbonate Sediments and Chemistry.* [Online] Available at: http://www.geol.umd.edu/jmerck/geol342/lectures/14.html [Accessed 9 January 2015].

Desai, F., Prasad, J., Muthukumar, P. & Rahman, M., 2021. Thermochemical energy storage system for cooling and process heating applications. *A review. Energy Conversion and Management,* Volume 229, p. 113617.

Diz, H. R., 1997. *Chemical and biological treatment of acid mine drainage for the removal of heavy metals and acidity.* Virginia Tech: Doctoral dissertation.

Dold, B., 2008. Sustainability in metal mining: From exploration, over processing to mine waste management. *Rev. Environ. Sci. Bio/Technol,* Volume 7, p. 275–285.

Dragan, S. & Ozunu, A., 2012. Characterization of calcium carbonates used in wet flue gas desulphurization processes. *Open Chemistry,* 10(5), pp. 1556-1564.

DSI, 1995. *Technical Status; Industry, Technology in Indian Soda Ash,* india: s.n.

DWAF, 2008. *Bpgs water management for surface mining,* RSA: Department Of Water Affairs And Forestry, Best Practice Guidelines- A5.

Eggert, R. et al., 2016. Rare earths: market disruption, innovation, and global supply chains.. *Annu. Rev. Environ. Resour,,* 41(1), pp. 199-222.

Eggman, T., 2001. *Sodium Carbonate,* s.l.: Kirk-Othmer Encyclopedia of Chemical Technology.

Elsner, M., Menge, M., Müller, C. & Agar, D., 2003. The Claus process: teaching an old dog new tricks. *Catalysis Today,* Volume 79, pp. 487-494.

Engbrecht, D. & Hirschfeld, D., 2016. Thermal analysis of calcium sulfate dihydrate sources used to manufacture gypsum wallboard. *Thermochimica Acta,* Volume 639, pp. 173-185.

European, C., 2015. *Additional analysis to complement the impact assessment SWD (2014) 208 supporting the review of EU waste,* s.l.: Commission Staff Working Document.

Faris, N. et al., 2017. Application of ferrous pyrometallurgy to the beneficiation of rare earth bearing iron ores–a review.. *Minerals Engineering,* Volume 110, pp. 20-30.

Fashola, M. O., Ngole-Jeme, V. M. & Babalola, O. O., 2016. Heavy metal pollution from gold mines: environmental effects and bacterial strategies for resistance. *International journal of environmental research and public health,* 13(11), p. 1047.

Feldbaumer, E., Loquenz, H. & Sandri, A., 1980. *Reduction of sodium sulphate to sodium sulphide.* USA, Patent No. 4,198,385.

Ferronato, N. & Torretta, V., 2019. Waste mismanagement in developing countries: A review of global issues. *International journal of environmental research and public health,* Volume 16, p. 1060.

Finch, J., 1824. A Sketch of the Geology of the Country near Easton, Penn.; with a Catalogue of the Minerels, and a Map. *American Journal of Science and Arts,* 8(2), p. 236.

Fobil, J. N., 2000. *Municipal Solid Waste Characterization for Integrated Management in the Accra Metropoli,* Accra, Ghana.: University of Ghana.

Foo, T. S., 1997. Recycling of domestic waste: early experience in Singapore. *Habitat International,* Volume 21, pp. 277-289.

Frontera, P., Macario, A., Ferraro, M. & Antonucci, P., 2017. Supported catalysts for CO2 methanation: a review. *Catalysts,* 7(2), p. 59.

Frost, R. & Kloprogge, J., 1999. *Spectrochimica Acta Part A: Molecular and Biomolecular Spectroscopy,* 55(11), pp. 2195-2205.

Fu, J. & Sheng, G., 1999. A preliminary study of asphalt from a large sulphur deposit in China by the approach of molecular organic geochemistry. *J. Pet. Sci. Eng,* Volume 22, p. 95−102.

Gabasiane, T. S. et al., 2021. Environmental and Socioeconomic Impact of Copper Slag—A Review.. *Crystals,* Volume 11, p. 1504.

Gao, L. et al., 2007. Intrinsic peroxidase-like activity of ferromagnetic nanoparticles. *Nature nanotechnology,* 2(9), pp. 577-583.

Gasser, M. S. et al., 2022. Alkali treatment–acid leaching of rare earth elements from phosphogypsum fertilizer: insight for additional resource of valuable components. *BMC chemistry,* 16(1), pp. 1-10.

Gawaad, R. S., Sharma, S. K. & Sambi, S. S., 2011. Sodium sulphate recovery from industrial wastewater using nano-membranes: A review. *International Review of Chemical Engineering,* 3(3), pp. 392-398.

Gbadeyan, O. et al., 2020. Optimization of milling procedures for synthesizing nano-CaCO3 from Achatina fulica shell through mechanochemical techniques. *Journal of Nanomaterials,* pp. 1-9.

Genceli, F., 2008. *Scaling-up eutectic freeze crystallization. Ph.D. Thesis.,* s.l.: Delft University.

Genceli, F., Gartner, R. & Witkamp, G., 2005. Eutectic freeze crystallization in a 2nd generation cooled disk column crystallizer for the recovery of MgSO4.12H2O. *Journal of Crystal Growth,* Volume 275, pp. 1369-1372.

George, W., 2000. *Handbook of Filler, second ed.* Toronto: ChemTec Publishing.

Ghyselbrecht, K. et al., 2013. Desalination of an industrial saline water with conventional and bipolar membrane electrodialysis. *Desalination,* Volume 318, pp. 9-18.

Gleick, P. H., 1996. Basic water requirements for human activities: meeting basic needs. *Water international,* 21(2), pp. 83-92.

Golev, A. et al., 2014. Rare earths supply chains :current status, constraints and opportunities. *Resour.Policy ,* Volume 41, p. 52–59.

Goodenough, K., Wall, F. & Merriman, D., 2018. The rare earth elements: demand, global resources, and challenges for resourcing future generations.. *Natural Resources Research,,* 27(2), pp. 201-216..

Goodstein, D. L., 2002. *States of Matter (1975).* s.l.:Dover.

Gorakhki, M. H. & Bareither, C. A., 2015. Salinity effects on sedimentation behavior of kaolin, bentonite, and soda ash mine tailings. *Applied Clay Science,* Volume 114, pp. 593-602.

Greenlee, L. F. et al., 2009. Reverse osmosis desalination: water sources, technology, and today's challenges. *Water research,* Volume 43, pp. 2317-2348.

Guo, Y., Deng, W. & Wei, G., 2019. Kinetic effects during the experimental transition of aragonite to calcite in aqueous solution: Insights from clumped and oxygen isotope signatures. *Geochimica et Cosmochimica Acta,* Volume 248, pp. 210-230.

Gupta, C. & and Krishnamurthy, N., 2004. *Extractive Metallurgy of Rare Earths..* Boca Raton, CRC Press, FL..

Gutberlet, J., 2015. More inclusive and cleaner cities with waste management co-production: Insights from participatory epistemologies and methods. *Habitat International,* Volume 46, pp. 234-243.

Habashi, F., 1985. The recovery of the lanthanides from phosphate rock. *Journal of Chemical Technology and Biotechnology. Chemical Technology,* 35(1), pp. 1-47.

Halde, R., 1980. Concentration of impurities by progressive freezing.. *Water research,* 14(6), pp. 575-580..

Harmsen, J., 1983. Identification of organic compounds in leachate from a waste tip. *Water Research,* 17(6), pp. 699-705.

Harvey, E., 1957. A History of Luminescence: From the Earliest Times until 1990. In: J. H. Philadelphia, ed. *Memoirs of the American Physical Society,.* Baltimore, Maryland (USA): FURST Company,, pp. 11-43.

Hathorne, E. C., James, R. H., Savage, P. & Alard, O., 2008. Physical and chemical characteristics of particles produced by laser ablation of biogenic calcium carbonate. *Journal of Analytical Atomic Spectrometry,* 23(2), pp. 240-243.

Hay, E. R., Riemann, K., Van Zyl, G. & Thompson, I., 2012. Ensuring water supply for all towns and villages in the Eastern Cape and Western Cape Provinces of South Africa. *Water SA,* 38(3), pp. 437-444.

He, J. et al., 2004. Speciation and distribution characters of rare earth elements in the Baotou section of the Yellowriver.. *Environ. Sci.,* Volume 25, p. 61–66.

Hendrickson, H. & Moulton, R., 1956. *Research and development of processes for desalting water by freezing. R&D Report 10, US Dept. of Commerce,* s.l.: Office of Saline Water.

Heureuse, D., 1848. The reaction between sodium sulphate and carbon at elevated temperature. *Pegg. Ann.,* Volume 75, p. 255.

Hiligsmann, S. et al., 1996. Hiligsmann, S., Deswaef, S., Taillieu, X., Crine, M., MProduction of sulfur from gypsum as an industrial byproduct.. *In Seventeenth Symposium on Biotechnology for Fuels and Chemicals,* pp. 959-969.

Hilson, G. & Monhemius, A. J., 2006. Alternatives to cyanide in the gold mining industry: what prospects for the future?. *Journal of Cleaner production,* 14(12), pp. 1158-1167.

Hirano, S. & Suzuki, K., 1996. Exposure, metabolism, and toxicity of rare earth sand related compounds.. *Environ.Health Perspect.,* Volume 104, p. 85.

Hlabela, P., Maree, J. P. & Bruinsma, D., 2007. Barium Carbonate Process for Sulphate and Metal Removal from Mine Water. *Mine Water and the Environment,* 26(1), pp. 14-22.

Hopewell, J., Dvorak, R. & Kosior, E., 2009. Plastics recycling: challenges and opportunities. *hilosophical Transactions of the Royal Society B: Biological Sciences,* 364(1526), pp. 2115-2126.

Hornsby, P. & Watson, C., 1990. A study of the mechanism of flame retardance and smoke suppression in polymers filled with magnesium hydroxide. *Polymer Degradation and Stability,* 30(1), pp. 73-87.

Huang, F., Liang, Y. & He, Y., 2019. On the pickering emulsions stabilized by calcium carbonate particles with various morphologies. *Colloids Surf,* Volume 580, p. 123722.

Huang, H. & Wang, J., 2007. Improving polypropylene microcellular foaming through blending and the addition of nano-calcium carbonate.. *Journal of Applied Polymer Science,,* 106(1), pp. 505-513..

Hudson-Edwards, K. A., Jamieson, H. E. & Lottermoser, B. G., 2011. Mine wastes: past, present, future.. *Elements,* 7(6), pp. 375-380.

Huige, N., 1972. *Nucleation and growth of ice crystals from water and sugar solutions in continuous stirred tank crystallisers,,* Eindhoven:: Eindhoven University of Technology..

Humphries, M., 2010. *Rare earth elements: the global supply chain..* s.l.:Diane Publishing..

Hu, M. Z. C., Miller, G. A., Payzant, E. A. & Rawn, C. J., 2000. Homogeneous (co) precipitation of inorganic salts for synthesis of monodispersed barium titanate particles. *Journal of materials science,* Volume 35, pp. 2927-2936.

Hutson, A. M., Atmar, R. L. & Estes, M. K., 2004. Norovirus disease: changing epidemiology and host susceptibility factors. *Trends in microbiology,* 12(6), pp. .279-287.

Hutton, B., Kahan, I., Naidu, T. & Gunther, P., 2009. *Operating and maintenance experience at the eMalahleni water reclamation plant.* IMWA, http://www.imwa.info/docs/imwa_2009/IMWA2009_Hutton.pdf.

Jacob, C., Shehu, Z., Danbature, W. L. & Karu, E., 2016. Proximate analysis of the fruit Azanza garckeana (“Goron Tula”). *Bayero Journal of Pure and Applied Sciences,* 9(2), pp. 221-224.

Jagtap, S., Pande, A. & Gokarn, A., 1990. Effect of catalysts on the kinetics of reduction of Barite by carbon.. *Ind. Eng. Chem. Res,* 29(5), p. 795−799..

Jakubick, A. T., McKenna, G. & Robertson, A. M., 2003. *Slings deposits: International experience. Stabilization of tailings deposits.* Sudbury, In Mining and the Environment Conference, pp. 1-9.

Jambo, J. L. & Blowes, D. W., 1998. Theory and applications of mineralogy in environmental studies of sulphide bearing mine wastes. *Environmental mineralogy, mineral association of Canada,* Volume 27, pp. 367-401.

Jamshidi, E. & Ebrahim, H., 2008. A new clean process for barium carbonate preparation by Barite reduction with methane.. *Chem. Eng. Process.: Process Intensif,* 47(9), p. 1567−1577.

Jeong, S. B., Yang, Y. C., Chae, Y. B. & Kim, B. G., 2009. Characteristics of the treated ground calcium carbonate powder with stearic acid using the dry process coating system. *Materials Transactions,* 50(2), pp. 409-414.

Jimoh, O. A., Ariffin, K. S., Hussin, H. B. & Temitope, A. E., 2018. Synthesis of precipitated calcium carbonate: a review. *Carbonates and Evaporites,* Volume 33, pp. 331-346.

Ji, X., Li, G. & Huang, X., 2008. The synthesis of hollow CaCO3 microspheres in mixed solutions of surfactant and polymer. *Mater. Lett.,* Volume 62, p. 751–754.

Johnson, W., 1976. State-of-the-art of freezing processes, their potential and future.. *Desalination,* 19(1), pp. 349-358..

Jones, F. et al., 2002. Investigation into the effect of phosphonate inhibitors on barium sulfate precipitation. *Journal of Crystal Growth,* Volume 237, pp. 424-429.

Jordens, A., Cheng, Y. & Waters, K., 2013. A review of the beneficiation of rare earth element bearing minerals.. *Minerals Engineering,* Volume 41, pp. 97-114.

Jordens, A., Cheng, Y. & Waters, K., 2013. A review of the beneficiation of rare earth element bearing minerals.. *Minerals Engineering,* Volume 41, pp. 97-114.

Jorjani, E. & Shahbazi, M., 2016. The production of rare earth elements group via tributyl phosphate extraction and precipitation stripping using oxalic acid. *Arabian journal of chemistry,* Volume 9, pp. 1532-1539..

Joubert, J. & Pocock, G., 2013. *Preparation of of gypsum hemihydrate and then reduction to calcium sulphide,* Pretoria: Vitaone8.

Kara, H. et al., 2010. *Lanthanide Resources and Alternatives.,* s.l.: Aylesbury.

Karak, T., Bhagat, R. M. & Bhattacharyya, P., 2012. Municipal solid waste generation, composition, and management: the world scenario.. *Critical Reviews in Environmental Science and Technology,* 42(15), pp. 1509-1630.

Karani, P. & Jewasikiewitz, S., 2007. Waste management and sustainable development in South Africa. *Environment, Development and Sustainability,* Volume 9, pp. 163-185.

Karnofsky, G. & Steinhoff, P., 1960. *Saline water conversion by direct freezing with butane. R&D Report 40, US Dept. of Commerce:,* s.l.: Office of Saline Water.

Kaseva, M. E. & Mbuligwe, S. E., 2005. Appraisal of solid waste collection following private sector involvement in Dar es Salaam city, Tanzania. *Habitat international,* Volume 29, pp. 353-366.

Kasikowski, T., Buczkowski, R. & Lemanowska, E., 2004. Cleaner production in the ammonia–soda industry: an ecological and economic study. *Journal of environmental management,* 73(4), pp. 339-356.

Katsanoulas, C. et al., 2007. Severe barium sulphate aspiration: a report of two cases and review of the literature. Signa vitae. *journal for intesive care and emergency medicine,* 2(1), pp. 25-28.

Kawashima, S., Hou, P., Corr, D. & Shah, S., 2013. Modification of cement-based materials with nanoparticles. *Cement and Concrete Composites,* Volume 36, p. 8–15.

Khan, I. & Bhat, A. H., 2013. Micro and nano calcium carbonate filled natural rubber composites and nanocomposites. *RSC Polymer Chemistry Series No. 8 Natural Rubber Materials,* Volume 2, pp. 467-487.

Korayem, A. et al., 2017. A review of dispersion of nanoparticles in cementitious matrices: nanoparticle geometry perspective. *Construction and Building Materials,* Volume 153, p. 346–357.

Kralj, D. et al., 2008. *Comparison of Semicontinuous and Batch Precipitation of Calcium Carbonate.* Joachim, s.n.

Kucera, J., 2014. *Desalination: Water from water..* s.l.:Scrivener.

Kumar, R. et al., 2021. Impacts of plastic pollution on ecosystem services, sustainable development goals, and need to focus on circular economy and policy interventions. *Sustainability,* 13(17), p. 9963.

Kumar, S. S. S. F. G. V. C. K. S. et al., 2017. Challenges and opportunities associated with waste management in India. *Royal Society open science,* 4(3), p. 160764.

Kushwaha, A., Hans, N., Kumar, S. & Rani, R., 2018. A critical review on speciation, mobilization and toxicity of lead in soil-microbe-plant system and bioremediation strategies. *Ecotoxicology and environmental safety,* Volume 147, pp. 1035-1045.

Kushwaha, A., Rani, R. & Agarwal, V., 2016. Environmental fate and eco-toxicity of engineered nano-particles: current trends and future perspective. *Advanced nanomaterials for wastewater remediation,* pp. 387-404.

Kutkut, A. & Andreana, S., 2010. Medical-grade calcium sulfate hemihydrate in clinical implant dentistry: a review. *Journal of Long-Term Effects of Medical Implants,* Volume 20 , pp. 295-301.

Kutsovskaya M, L., Hepworth M, T. & McGaa J, R., 1996. Recovery of lime, sulfur, and iron from gypsum and pyrite waste,. *Industrial and engineering chemistry research,* Volume 35,, p. 1736–1746.

Kuzminchuk, A., Burmak, A., Litynska, M. & Dontsova, T., 2023. New diatomaceous earth and kaolinite ceramic membranes for turbidity reduction in water. *Applied Nanoscience,* pp. 1-9.

Lam, H., 2011. *Optimization with integration of renewable energy sources into energy supply chain. PhD thesis (Information Science and Technology),* Hungary: University of Pannonia.

Laveuf, C. & Cornu, S., 2009. A review on the potentiality of rare earth elements to trace pedogenetic processes.. *Geoderma,* Volume 154, p. 1–12.

Lazarides, H. & Katsanidis, E., 2003. Principles of reverse osmosis. In: C. B, ed. *Encyclopedia of Food Sciences and Nutrition, (Second edition).* s.l.:Academic press, pp. 3827-3833.

Leblanc, N., 1791. *Leblanc process for making soda ash (sodium carbonate).* France.

Lei, M., Li, P. G., Sun, Z. B. & Tang, W. H., 2006. Effects of organic additives on the morphology of calcium carbonate particles in the presence of CTAB. *Mater. Lett,* Volume 60, p. 1261–1264.

Lema, J., Mendez, R. & Blazquez, R., 1988. Characteristics of landfill leachates and alternatives for their treatment: a review.. *Water, air, and soil pollution,* 40(3), pp. 223-250.

Letjiane, S. L., Maree, J. P., Onyango, M. S. & Adeniyi, A., 2019. *Pre-treatment of coal dump leachate with MgO for pigment recovery.* Perm, Russia, International Mine Water Association, pp. 101-106.

Lewis, R. J., 2012. *Sax's Dangerous Properties of Industrial Materials..* 12 ed. Hoboken: Wiley-Interscience, Wiley & Sons, Inc.

Liang, T., Li, K. & Wang, L., 2014. State of rare earth elements in different environmental components in mining areas of China. *Environ. Monit. Assess,* Volume 186, p. 1499–1513.

Liang, X. et al., 2020. Hazardous waste disposal enterprise selection in China using hesitant Fuzzy PROMETHEE. *International Journal of Environmental Research and Public Health,* 17(12), p. 4309.

Li, L. Z. & Yang, X., 2014. *China's rare earth ore deposits and beneficiation techniques. Proceedings of the 1st European Rare Earth Resources Conference.* Milos, Greece,, s.n., p. 28–39.

Liu, B. et al., 2007. Preparation of Pt/MgO/CNT hybrid catalysts and their electrocatalytic properties for ethanol electrooxidation. *Energy & fuels,* 21(3), pp. 1365-1369.

Liu, D. et al., 2018. Co-treatment of flotation waste, neutralization sludge, and arsenic-containing gypsum sludge from copper smelting: solidification/stabilization of arsenic and

heavy metals with minimal cement clinker. *Environmental Science and Pollution Research,* Volume 25, pp. 7600-7607.

Liu, L., Miyawaki, O. & Nakamura, K., 1997. Progressive freeze concentration of model liquid food. *Food Sci. Technol. Int.,* Volume 3, p. 348–352.

Li, X., Yu, J., Jaroniec, M. & Chen, X., 2019. Cocatalysts for selective photoreduction of CO2 into solar fuels. *Chemical reviews,* 119(6), pp. 3962-4179.

Lorain, O., Thiebaud, P., Badorc, E. & Aurelle, Y., 2001. Potential of freezing in wastewater treatment: soluble pollutant applications.. *water research,* Volume 35, p. 541–547.

Lottermoser, B. G., 2010. Mine water. In: *In Mine Waste.* Heidelberg: Springer, pp. 119-203.

Lucas-Girot, A. et al., 2005. Gentamicin-loaded calcium carbonate materials: Comparison of two drug-loading modes. *Journal of Biomedical Materials Research Part B: Applied Biomaterials,* 73(1), pp. 164-170.

Lucko, G., 2003. *A statistical analysis and model of the residual value of different. PhD thesis (Civil Engineering), ,* USA: Virginia State University and Polytechnic.

Lung, C., Chen, S. & Wu, J., 1991. Study on the reducing conditions of the barite in Boyang. *J. Nanchang Univ,* 15(1), p. 1−6.

Lu, Z. & Cai, M., 2012. Disposal methods on solid wastes from mines in transition from open-pit to underground mining. *Procedia Environmental Sciences,* Volume 16, pp. 715-721.

Lu, Z. & Xu, L., 2010. *Freeze desalination processes,* s.l.: Incyclopedia of Desalination and Water Resources.

MacWilliams, D., 1978. *Kirk-Othmer: Encyclopedia of Chemical Technology.* New York: Wiley.

Makar, J. et al., 2012. Effect of n-CaCO3 and metakaolin on hydrated Portland cement. *Advances in Cement Research,* 24(4), p. 211–219.

Mamelkina, M. et al., 2017. Removal of sulfate from mining waters by electrocoagulation. *Separation and Purification Technology,* Volume 182, pp. 87-93.

Mansour, M. B., Soukaina, C. A., Benhamou, B. & Jabrallah, S. B., 2013. Thermal characterization of a Tunisian gypsum plaster as construction material. *Energy Procedia,* Volume 42, pp. 680-688.

Maree, J. & Du Plessis, P., 1990. *Sulphate Waste Processing.* Rustenburg, South Africa., Proceedings on Solid waste management.

Maree, J., Günther, P., Strobos, G. & and Waanders, F., 2004. Optimizing the Effluent Treatment at a Coal Mine by Process Modelling. *Mine Water and the Environment,* 23(2), pp. 87-90.

Maree, J. et al., 2013. Neutralisation treatment of AMD at affordable cost. *Water SA,* 39(2), pp. 245-250.

Maree, J. P., 1996. *Underground neutralisation of mine water with limestone,* Pretoria: WRC Report No 609/1/96.

Maree, J. P., 2013. *MBO (magnesium-barium-oxide) patent.* South Africa, USA, Austalia, Patent No. 8557124.

Maree, J. P. & du Plessis, P., 1994. Neutralisation of acid mine water with caclium carbonate. *Wat. Sci. Tech.,* 29(9), pp. 285-296.

Maree, J. P., Du Plessis, P. & Van der Walt, C. J., 1992. Treatment of acidic effluents with limestone instead of lime. *Water Science and Technology,* 26(1-2), pp. 345-355.

Maree, J. P. et al., 2004. *Integrated process for biological sulphate removal and sulphur recovery..* Cape Town,, In Proceedings of the Water Institute of Southern Africa (WISA) Biennial Conference, .

Maree, J. P. & Theron, D. J., 2005. *Conversion of a Sulphur-containing Waste Material into a Sulphur-containing Product.* South African, Patent No. 2005/3124.

Maree, J. P., van Tonder, G. J., Millard, P. & Erasmus, C., 1996. Pilot scale neutralisation of underground mine water. *Wat. Sci. Tech.,* 34(10), pp. 141 - 149.

Maree, J., Theron, D., Nengovhela, R. & Hlabela, P., 2005. Sulphur from smelter gases and sulphate-rich effluents. *Journal of the Southern African Institute of Mining and Metallurgy,* 105(9), pp. 641-644.

Marshall, J. W. & St. Armand, D., 1992. *The Chemistry and Technology of Magnesia.* , TAPPI:Proceedings Environmental Conference.

Mashigwana, L. et al., 2022. *Thermal processing of sodium sulphate to sodium carbonate.* Birchwood Hotel & OR Tambo Conference Centre, Johannesburg, 17-18 Mar, International Institute of Biological Chemical and Environmental Engineering (IICBEE).

Masindi, V., 2017. Recovery of drinking water and valuable minerals from acid mine drainage using an integration of magnesite, lime, soda ash, CO2 and reverse osmosis treatment processes. *Journal of environmental chemical engineering,* 5(4), pp. 3136-3142.

Masindi, V., Osman, M. S. & Abu-Mahfouz, A. M., 2017. Integrated treatment of acid mine drainage using BOF slag, lime/soda ash and reverse osmosis (RO): Implication for the production of drinking water. *Desalination,* Volume 424, pp. 45-52.

Massari, S. & Ruberti, M., 2013. Rare earth elements as critical raw materials: Focus on international markets and future strategies.. *Resour. Policy,* Volume 38, p. 36–43.

Masukume, M., Maree, J. P., Ruto, S. & Joubert, H., 2013. Processing of Barium Sulphide to Barium Carbonate and Sulphur. *J Chem Eng Process Technol,* 4(4), pp. doi:10.4172/2157-7048.1000157.

Matinde, E., Simate, G. & Ndlovu, S., 2018. Mining and metallurgical wastes: a review of recycling and re-use practices. *Journal of the Southern African Institute of Mining and Metallurgy,* Volume 118, pp. 825-844.

Ma, Y. et al., 2018. *Hydrometallurgical treatment of acid mine drainage (AMD) solution.* Serbia, 20th International YuCorr Conference.

Mbhele, N. R., van der Merwe, W., Maree, J. P. & Theron, D., 2009. *Recovery of Sulphur from Waste Gypsum.* Pretoria, South Africa, s.n., pp. 622-630.

Mekonnen, M. M. & Hoekstra, A. Y., 2016. Four billion people facing severe water scarcity. *Science advances,* 2(2), p. 1500323.

Meng, T., Yu, Y. & Wang, Z., 2017. Effect of nano-CaCO3 slurry on the mechanical properties and micro-structure of concrete with and without fly ash. *Composites Part B: Engineering,* Volume 117, p. 124–129.

Miyawaki, O., Kato, S. & Watabe, K., 2012. Yield improvement in progressive freeze-concentration by partial melting of ice. *Journal of Food Engineering,* 103(3), pp. 377-382.

Mogashane, T. M., Maree, J. P., Mujuru, M. & Mphahlele-Makgwane, M. M., 2020. Technologies that can be Used for the Treatment of Wastewater and Brine for the Recovery of Drinking Water and Saleable Products.. *Recovery of byproducts from acid mine drainage treatment,* pp. 97-156.

Mogashane, T. M. et al., 2023. Ferric Hydroxide Recovery from Iron-Rich Acid Mine Water with Calcium Carbonate and a Gypsum Scale Inhibitor. *Minerals,* 13(2), p. 167.

Mokgohloa, C. P., Maree, J. P., Motaung, M. P. & Mokhonoana, M. P., 2022. *Processing of Na2S to Na2CO3 and NaHS.* Johannesburg, InternationaL conference on chemical, biological, environmental engineering.

Mokgohloa, C. P. et al., 2022. Recovery of Na2CO3 and nano CaCO3 from Na2SO4 and CaSO4 wastes. In: *Nano Technology.* New York: Wiley Scrivener, pp. 1-2.

Moshtaghian, H., Bolton, K. & Rousta, K., 2021. Challenges for upcycled foods: definition, inclusion in the food waste management hierarchy and public acceptability. *Foods,* 11(10), p. 2874.

Msiza, J., 2013. World-class landfill cell at the Holfontein disposal site: environmental engineering. *Civil Engineering= Siviele Ingenieurswese,* Volume 21, pp. 20-22.

Mtombeni, T. & Maree, J. P., 2014. *Treatment of water – ROC process.* South Africa, Germany, France, Australia, USA, Patent No. 2014/04734Treatment of water – ROC process, ROC Water Technologies, RSA (No 2015/04639), Germany (No 3452414), France (No 3452414), Australia (No 2016405754 – Pending), USA No 16/099,009 – Pending).

Mtombeni, T., Maree, J. P., Zikalala, N. & S, F. C. J., 2016. *Desalination with a combined membrane filtration/freeze desalination process,* Durban: WISA Biennial Conference.

Mtombeni, T. et al., 2014. *Improved freeze desalination process for recovery of water and salts from brines.* Mbombela, 2014 WISA Biennial Conference, 25-29 May.

Mtombeni, T. et al., 2013. Evaluation of the performance of a new freeze desalination technology.. *International Journal of Environmental Science and Technology,* 10(3), pp. 545-550.

Muller, M. et al., 2009. Water security in South Africa. *Development Planning Division Working Paper Series,* Volume 12, pp. 1-10.

Naranjo, M., 2006. *Particle Development in a Fluidized Bed Black Liquor Steam Reformer,* University of Utah: Department of Chemical Engineering,.

Ndlovu, S., Simate, G. S. & Matinde, E., 2017. *Waste production and utilization in the metal extraction industry..* s.l.:CRC Press.

Nengovhela, R. N. et al., 2007. Recovery of sulphur and calcium carbonate from waste gypsum. *Water SA,* 33(5), pp. 741-748.

Neri, D. & Supuran, C. T., 2011. Interfering with pH regulation in tumours as a therapeutic strategy. *Nature reviews Drug discovery,* 10(10), pp. 767-777.

Nicholson, R. V., 1994. Iron Sulphide oxidation mechanisms. *Mineralogical association of Canada,* Volume 22, pp. 163-183.

Njegi, B. et al., 2009. Calcite crystal growth kinetics in the presence of charged synthetic polypeptides. *Crystal Growth Des,* p. 2425–2432.

Njoku, P., Edokpayi, J. & Odiyo, J., 2019. Health and environmental risks of residents living close to a landfill: A case study of Thohoyandou Landfill, Limpopo Province, South Africa. *International journal of environmental research and public health,* 16(12), p. 2125.

Nyman, C. J. & O'Brien, 1947. Catalytic reduction of sodium sulphate. *Industrial & Engineering Chemistry,* 39(8), pp. 1019-1021.

O'Brien, W. J., 2002. A study of lithopone. *The Journal of Physical Chemistry,* 19(2), pp. 113-144.

OECD, 2015. *Economic surveys,* South Africa: http://www. oecd.org/eco/surveys/South-Africa-OECD-economic-survey-overview.pdf.

Ogedengbe, A. et al., 2020. Valorization of sodium sulfate waste to potassium sulfate fertilizer: Experimental studies, process modeling, and optimization. *International Journal of Green Energy,* 17(8), pp. 521-528.

Okot-Okumu, J. & Nyenje, R., 2011. Municipal solid waste management under decentralisation in Uganda. *Habitat International,* Volume 35, pp. 537-543.

Okuno, T., Masumi, T. & M. Fukuyama, M., 1933. The reduction of the sodium sulphate solely by carbon monoxide. *J. Soc. Chea. Ind . Japan (Suppl. binding,* Volume 12, pp. 466-468.

OLI, 2015. *http://www.olisystems.com/..* [Online] [Accessed 2015].

Onwukwe, S. & Nwakaudu, M., 2012. Drilling wastes generation and management approach.. *International Journal of Environmental Science and Development,* 3(3), p. 252.

Örgül, S., 2003. *Evaluation of soda ash production parameters from Beypazari trona,* s.l.: The Middle East Technical University.

Palczynski, R. J., 2002. *Study on solid waste management options for Africa,* s.l.: Project Report for the African Development Bank – SustainableDevelopment & Poverty Reduction Unit. Abidjan, Cˆote d'Ivoire.

Palmqvist, N., Nedelec, J., Seisenbaeva, G. & Kessler, V., 2017. Controlling nucleation and growth of nano-CaCO3 via CO2 sequestration by a calcium alkoxide solution to produce nanocomposites for drug delivery applications. *Acta biomaterialia,* 57(15), pp. 426-434.

Parikh, S. N., 2002. Bone graft substitutes: past, present, future. *Journal of postgraduate medicine,* 48(2), p. 142.

Park, R. J. & Meldrum, F. C., 2002. Synthesis of single crystals of calcium carbonate with complex morphologies. *Adv. Mater,* Volume 14, p. 1167–1169.

Paul, J. & Campbell, G., 2011. *Investigating Rare Earth Element Mine Development in EPA Region 8 and Potential Environmental Impacts,* Washington: EPA Mining Reports.

Peng, H. & Guizhi, N., 2010. Discussion on China sulfur oreconcentrating area and the resource potential.. *Geol. Chem. Miner.,* 32(2), p. 95−104.

Phuntsho, S. et al., 2014. Membrane scaling and flux decline during fertiliser-drawn forward osmosis desalination of brackish groundwater. *Water Res,* Volume 57, pp. 172-182.

Pidwirny, M., 2012. *Carbon Cycle,.* [Online] Available at: http://www.eoearth.org/view/article/150923 [Accessed January 2015].

Pires, A. & Martinho, G., 2019. Waste hierarchy index for circular economy in waste managemen. *Waste Management,* Volume 95, pp. 298-305.

Poudyal, L. & Adhikari, K., 2021. Environmental sustainability in cement industry: An integrated approach for green and economical cement production.. *Resour. Environ. Sustain.,* Volume 4, p. 100024.

Pronk, P., 2006. *Fluidized bed heat exchangers to prevent fouling in ice slurry systems and industrial crystallizers. Ph.D. Thesis. ,* s.l.: Delft University of Technology..

Ragin, M. & Brooks D, R., 1990. *Recovery of sulfur from phosphogypsum: Conversion of calcium sulfate to calcium sulfide.* US: US Department of the Interior, Bureau of Mines..

Rahman, M., Ahmed, M. & Chen, M., 2006. Freezing-Melting Process and Desalination: I. Review of the State-of-the-Art. *Separation & Purification Reviews ,* p. 59–96.

Rameshni, M. & Santo, S., 2005. *Production of Elemental Sulphur from SO2 RSR (Rameshni SO2 Reduction),* s.l.: s.n.

Ramos, S. et al., 2016. Rare earth elements in the soil environment. *Current Pollution Reports,* Volume 2, pp. 28-50.

Randall, D. G., Nathoo, J. & Lewis, A. E., 2011. A case study for treating a reverse osmosis brine using Eutectic Freeze Crystallization-Approaching a zero waste process. *Desalination,* Volume 266, pp. 256-262.

Randall, D., Nathoo, J. & Lewis, A., 2009. *Seeding for selective salt recovery during eutectic freeze crystallization.* Pretoria, South Africa, International Mine Water Conference.

Ranjit, K., Krishnamoorthy, R., Varadarajan, T. & Viswanathan, B., 1995. Photocatalytic reduction of nitrite on CdS.. *Journal of Photochemistry and Photobiology A: Chemistry,* 86(1-3), pp. 185-189.

Rashmi, I. et al., 2018. Gypsum-an inexpensive, effective sulphur source with multitude impact on oilseed production and soil quality-A review. *Agricultural Reviews,* 39(3), pp. 218-225.

Razzaq, A. et al., 2021. Dynamic and causality interrelationships from municipal solid waste recycling to economic growth, carbon emissions and energy efficiency using a novel bootstrapping autoregressive distributed lag. *Resources, Conservation and Recycling,* Volume 166, p. 105372.

Read, A., Phillips, P. & Robinson, G., 1997. Landfill as a future waste management option in England: the view of landfill operators. *Resources, conservation and recycling,* 20(3), pp. 183-205.

Reddy, S. T. et al., 2010. Recovery of Na2SO4-10H2O from reverse osmosis retentate by euctetic freeze crystallization technology. *Chemical Engineering Research and Design,* Volume 88, pp. 1153-1157.

Regnault, H., 1836. Sodium sulphate reduction using carbon or carbon monoxide at 1000 deg C. *ibid,* 63(2), p. 374.

Reichl, C., Schatz, M. & Zsak, G., 2016. In Minerals Production; International Organizing Committee for the World Mining Congresses:. In: *World-Mining-Data.* Vienna, Austria: s.n.

Rice, D. A., Carter, O. C., Alexander, J. M. & Ragin, M. M., 1990. *Recovery of sulfur from phosphogypsum: Conversion of calcum sulfide to sulfur..* s.l., Buraeu of mines report of investigation..

Rich, A. et al., 2011. Freezing desalination of seawater in a static layer crystallizer. *Desalination,* Volume 269, p. 142–147.

Rizvi, S., Goswami, L. & Gupta, S., 2020. A holistic approach for melanoidin removal via Fe-impregnated activated carbon prepared from Mangifera indica leaves biomass. *Bioresource Technology Reports,* Volume 12, p. 100591.

Roberts, W. F., 1947. *The high temperature reactions between sodium sulphate and carbon monoxide,* Oklahoma: Oklahoma Agricultural and Mechanical College.

Robinson, P., 2015. Enzymes: principles and biotechnological applications. *Essays in biochemistry,* p. 1.

Rodriguez-Blanco, J. D., Shaw, S. & Benning, L. G., 2011. The kinetics and mechanisms of amorphous calcium carbonate (ACC) crystallization to calcite, via vaterite. *Nanoscale,* Volume 3, p. 265–271.

Rögener, F. et al., 2012. Metal recovery from spent stainless steel pickling solutions. *Resources, conservation and recycling,* Volume 60, pp. 72-77.

Roos, A. et al., 2003. Development of a Vacuum Crystallizer for the Freeze Concentration of Industrial Wastewater. *Chemical Engineering Research and Design,* 81(8), pp. 881-892.

Rotich, H. K., Yongsheng, Z. & Jun, D., 2006. Municipal solid waste managementchallenges in developing countries: Kenyan case study. *Waste Management,* Volume 26, pp. 92-100.

RoyChowdhury, A., Sarkar, D. & Datta, R., 2015. Remediation of acid mine drainage-impacted water. *Current Pollution Reports,* 3(1), pp. 131-141.

Ruto, S. J., Maree, J. P., Zvinowanda, C. M. & Louw, W. J., 2012. *Thermal studies on gypsum in a pilot- scale rotary kiln.* Cape Town, South Africa, Paper presented at the 2012 Water Institute of South Africa Biennial Conference and Exhibition, May 6-10.

Ruto, S. et al., 2011. *Thermal studies on barium sulphate in a pilot scale, rotary kiln.* Sheraton Santiago Hotel & Convention Center, Chile, 10 - 12 April, 9th International Conference on Clean Technologies for the Mining Industry.

Ruto, S. et al., 2011. *Thermal studies on gypsum in a pilot-scale, rotary kiln.* Ingwenyama Conference & Sport Resort, White River, 15 – 17 February, Water in the South African Minerals Industry Conference, The Southern African Institute of Mining and Metallurgy.

Sadeghi, M. et al., 2013. Rare earth element distribution and mineralization in Sweden: an application of principal component analysis to FOREGS soil geochemistry.. *Journal of geochemical exploration,* Volume 133, pp. 160-175.

Sahoo, P. K., Tripathy, S., Equeenuddin, S. M. & Panigrahi, M. K., 2012. Geochemical characteristics of coal mine discharge vis-à-vis behavior of rare earth elements at Jaintia Hills coalfield, northeastern India. *Journal of Geochemical Exploration,* Volume 112, pp. 235-243.

Sakorn, P., Rakariyatham, N., Niamsup, H. & Nongkunsarn, P., 2002. Rapid detection of myrosinase-producing fungi: a plate method based on opaque barium sulphate formation. *World Journal of Microbiology and Biotechnology,* Volume 18, pp. 73-74.

San Marchi, C., Somerday, B. & Robinson, S., 2007. Permeability, solubility and diffusivity of hydrogen isotopes in stainless steels at high gas pressures. *International Journal of Hydrogen Energy,* 32(1), pp. 100-116.

Saracho, A. C. et al., 2021. Controlling the calcium carbonate microstructure of engineered living building materials.. *Journal of Materials Chemistry A,* 9(43), pp. 24438-24451.

Sarma, S. et al., 2014. Application of magnesium sulfate and its nanoparticles for enhanced lipid production by mixotrophic cultivation of algae using biodiesel waste. *Energy,* Volume 78, pp. 16-22.

Sasowsky, I., Foos, A. & Miller, C., 2000. Lithic controls on the removal of iron and remediation of acidic mine drainage. *Water Research,* 34(10), pp. 2742-2746.

Sathe, S., Goswami, L., Mahanta, C. & Devi, L., 2020. Integrated factors controlling arsenic mobilization in an alluvial floodplain. *Environmental Technology & Innovation,* Volume 17, p. 100525.

Sawyer, D. et al., 1994. Episodic caldera volcanism in the Miocene southwestern Nevada volcanic field: Revised stratigraphic framework, 40Ar/39Ar geochronology, and implications for magmatism and extension.. *Geological Society of America Bulletin,* 106(10), pp. 1304-1318.

Scherzbert, H., Schmitz, R. & Wöhlk, W., 1991. New process and apparatus concept for the production of potassium sulphate from sodium sulphate. *Chemical technology,* 20(6), pp. 41-48.

Schiller, J., Tallman, D. & Khalafalla, S., 1984. Mineral processing water treatment using magnesium oxide.. *Environmental progress,* 3(2), pp. 136-141.

Schrotter, J. et al., 2010. Current and emerging developments in desilanation with reverse osmosis membrane systems.. In: E. Drioli & L. Giorno, eds. *Comprehensive memebrane science and enginnering..* s.l.:Elsevier, pp. 35-65.

Schüler, D. et al., 2011. *Study on Rare Earths and Their Recycling.,* Darmstadt: Öko-Institut .

Schulz-Stübner, S., Wettmann, G., Reyle-Hahn, S. & Rossaint, R., 2001. Magnesium as part of balanced general anaesthesia with propofol, remifentanil and mivacurium: a double-blind, randomized prospective study in 50 patients. *European journal of anaesthesiology,* 18(11), pp. 723-729.

Seckler, M., Verdoes, D. & Witkamp, G., 2002. *Application of eutectic freeze to process streams and wastewater purification. ,* s.l.: Economy, Ecology and Technology of the Ministry of Economic Affairs.

Serge-Kubanza, N. & Simatele, M. D., 2020. Sustainable solid waste management in developing countries: a study of institutional strengthening for solid waste management in Johannesburg, South Africa. *Journal of Environmental Planning and Management,* 63(2), pp. 175-188.

Shaikh F, U. & Supit, S., 2014. Mechanical and durability properties of high volume fly ash (HVFA) concrete containing calcium carbonate (CaCO3) nanoparticles. *Construction and Building Materials,* Volume 70, p. 309–321.

Shaikh, F. & Supit, S., 2015. Chloride induced corrosion durability of high volume fly ash concretes containing nano particles. *Construction and Building Materials,* Volume 99, p. 208–225.

Shainberg, I. et al., 1989. *Use of gypsum on soils: A review.* Springer, New York: In Advances in soil science.

Shakhtakhtinskii, G., Yusubov, R. & Samedova, A., 1972. Reduction of a granulated Barite concentrate by converted natural gas in a fluidized bed.. *Khim. Zh,* Volume 4, p. 114−116.

Shamshuddin, J. et al., 2010. Temporal changes in chemical properties of acid soil profiles treated with magnesium limestone and gypsum. *Pertanika Journal of Tropical Agricultural Science,* 33(2), pp. 277-295.

Shimpi, N., Mali, A., Hansora, D. & Mishra, S., 2015. Synthesis and surface modification of calcium carbonate nanoparticles using ultrasound cavitation technique.. *Nanoscience and Nanoengineering.,* 3(1), pp. 8-12.

Silakhori, M. et al., 2021. Effects of steam on the kinetics of calcium carbonate calcination. *Chemical Engineering Science,* Volume 246, p. 116987.

Singer, D. A., 1995. World class base and precious metal deposits; a quantitative analysis. *Economic Geology,* 90(1), pp. 88-104.

Singh, M., 2002. Treating waste phosphogypsum for cement and plaster manufactur. *Cement and Concrete Research,* 32(7), pp. 1033-1038.

Singh, M. & Garg, M., 2020. Making of anhydrite cement from waste gypsum. *Cement and Concrete Research,* 30(4), pp. 571-577.

Sisinno, C. et al., 2000. *Toxicity evaluation of a municipal dump leachate using zebrafish acute tests.,* s.l.: s.n.

Skårman, T., Danielsson, H., Mawdsley, I. & Hansson, K., 2019. *Evaluation of thresholds for capacities and pollutants according to the protocol on PRTR,* Nordic countries.: s.n.

Slater, R. & Frederickson, J., 2001. Composting municipal waste in the UK: some lessons from Europe.. *Resources, Conservation and Recycling,* 32(3-4), pp. 359-374.

Sliger, A. & The M, W., 1986. *Kellogg company Kel-S process..* s.l., Proceedings of the international symposium. Phosphogypsum, p. 83.

Smet, P., Moreels, I., Hens, Z. & Poelman, D., 2010. Luminescence in Sulfides: A Rich History and a Bright Future. *Materials,* 3(4), p. 2834–2883.

Snigdha, C. & Sarkhel, P., 2003. *Economics of solid waste management: a survey of existing literature.,* XXXX: Economic Research Unit Indian Statistical Institute.

Sohn, H., 2003. Thermodynamics of a new cyclic reaction system involving BaS and BaSO4 for converting sulfur dioxide to elemental sulfur.. *Ind. Eng. Chem. Res,* 42(23), p. 5946−5948.

Sohn, H., Savic, M., Padilla, R. & Han, G., 2006. A novel reaction system involving BaS and for converting to elemental sulfur without generatingpollutants: Part II. Kinetics of the hydrogen reduction of to BaS. *Chem. Eng. Sci,* 61(15), p. 5088−5093.

Sohn, H., Savic, M., Padilla, R. & Han, G., 2006. A novel reaction systeminvolving BaS and for converting to elemental sulfur without generating pollutants: Part I. Feasibility and kinetics of reduction with BaS. *Chem. Eng. Sci.,* 61(15), p. 5082−5087..

Sonawane, S. G. S. et al., 2009. Combined effect of surfactant and ultrasound on nano calcium carbonate synthesized by crystallization process.. *International Journal of Chemical Reactor Engineering,* 7(1).

Sonich-Mullin, C., 2012. *Rare Earth Elements: A Review of Production, Processing, Recycling, and Associated Environmental Issues,* Cincinnati: United States Environmental Protection Agency..

Speight, J., 2017. Industrial organic chemistry. *Environmental Organic Chemistry for Engineers,* pp. 87-151.

Steinhauser, G., 2008. Cleaner production in the Solvay Process: general strategies and recent developments. *Journal of cleaner production,* 16(7), pp. 833-841.

Stenger, V., 1996. Solubilities of various alkali metal and alkaline earth metal compounds in methanol. *Journal of Chemical & Engineering Data,* 41(5), pp. 1111-1113.

Stepakoff, G., Siegelmann, D., Johnson, R. & Gibson, W., 1974. Development of a eutectic freezing process for brine disposal.. *Desalination,* Volume 14, pp. 25-38..

Stromayer, A., 1858. Sodium sulphate reduction to identify polysulfides and carbonates among the reaction product. *Ann.,* Volume 107, p. 372.

Strydom, C. A., Groenewald, E. M. & Potgieter, J. H., 1997. Thermogravimetric studies on the synthesis of CaS from gypsum, CaSO4.2H2O, and phosphogypsum. *Thermal Analysis,* Volume 49, pp. 1501-1507.

Sun, H., Wu, J., Yu, P. & Li, J., 1998. Geology, geochemistry and sulfur isotope composition of the Late Proterozoic Jingtieshan (Superior-type) hematite-jasper-Barite iron ore deposits associated with stratabound Cu mineralization in the Gansu Province, China.. *Miner. Deposita,* 34(1), p. 102−112.

Suwanthai, W., Punsuvon, V. & Vaithanomsat, P., 2016. Optimization of biodiesel production from a calcium methoxide catalyst using a statistical model.. *Korean Journal of Chemical Engineering,* 33(1), pp. 90-98.

Taherzadeh, M., Bolton, K., Wong, J. & Pandey, A., 2019. *Sustainable resource recovery and zero waste approaches.* Sweden: Elsevier.

Tao, D., Chen, S., Parekh B, K. & Hepworth M, T., 2001. An investigation of a thermochemical process for conversion of gypsum and pyrite wastes into useful products. *Advances in environmental research,* Volume 5, p. 277–284.

Tathavadkar, V., Jha, A. & Antony, M., 2003. The effect of salt-phase composition on the rate of soda-ash roasting of chromite ores. *Metallurgical and Materials transactions,* Volume 34, pp. 555-563.

Taunton, A., Welch, S. & Banfield, J., 2000. Microbial controls on phosphate and lanthanide distributions during granite weathering and soil formation. *Chem. Geol.,* Volume 169, p. 371–382.

Tavakoli, A., Sohrabi, M. & Kargari, A., 2007. A review of methods for synthesis of nanostructured metals with emphasis on iron compounds. *chemical papers,* 61(3), pp. 151-170.

Teir, S., Eloneva, S. & Zevenhoven, R., 2005. Production of precipitated calcium carbonate from calcium silicates and carbon dioxide. *Energy Conversion and Management,* 46(18), pp. .2954-2979.

Telci, L. et al., 2002. Evaluation of effects of magnesium sulphate in reducing intraoperative anaesthetic requirements. *British journal of anaesthesia,* 89(4), pp. 594-598..

Teringo, J., 1987. *With Mg(OH)2, metals can be removed from solution at one pH unit lower than when NaOH is used.* s.l.:Pollution Engineering Magazine,.

Tewo, R. K. 2., 2014. *Processing of Waste Gypsum to Calcium Carbonate and Hydrogen Sulphide Gas,* Pretoria: s.n.

Tewo, R. K. et al., 2014. *The effect of hydrogen sulphide gas on the dissolution of calcium sulphide in the production of calcium carbonate and elemental sulphur.* Mbombela, 2014 WISA Biennial Conference, May 25-29.

Tewo, R. K. et al., 2017. The gypsum reduction process and its validation using the Mintek Pyrosim model. *Chemical Engineering Communications,* 204(12), pp. 1412-1419.

Thai, N., 2009. Hazardous industrial waste management in Vietnam: current status and future direction.. *Journal of material cycles and waste management,* 11(3), pp. 258-262.

Thammakarn, C. et al., 2014. Inactivation of avian influenza virus, newcastle disease virus and goose parvovirus using solution of nano-sized scallop shell powder. *Journal of Veterinary Medical Science,* 76(9), pp. 1277-1280..

Tong, S. I. et al., 2004. Distribution characteristics of rare earth metals in children's scalp hair from a rare earth mining are in Southern China. *Journal of Environmental Science and Health Part A Toxic/Hazardous Substances and Enviromental Engineering,* Volume 39, pp. 2517-2532.

Trikkel, A. & Kuusik, R., 1994. *Tallinna Tehnikaulik..* s.l.:Toim.

Trusler, G. E., Edwards, R. I., Brouckaert, C. J. & Buckley, C. A., 1988. *The chemical removal of sulfates.* Pretoria, s.n., pp. W3-0-W3-11.

Trypuć, M. & Łyjak, G., 2001. Application of NaVO3 for the utilization of the after-filtration liquor from Solvay's process. *Industrial & engineering chemistry research,* 40(9), pp. 2188-2191.

Tsuzuki, T. & McCormick, P., 2004. Mechanochemical synthesis of nanoparticles.. *Journal of materials science.,* 39(1), pp. 16-17.

Tun, C. & Groth, A., 2011. Sustainable integrated membrane contactor process for water reclamation, sodium sulfate salt and energy recovery from industrial effluent. *Desalination,* Volume 283, pp. 187-192.

Tuovinen, T., Tynjälä, P., Vielma, T. & Lassi, U., 2021. Utilization of waste sodium sulfate from battery chemical production in neutral electrolytic pickling. *Journal of Cleaner Production,* Volume 324, p. 129237.

Turkdogan, E. & Vinters J, V., 1976. Reduction of calcium sulphate by carbon..

Turner, A. & Filella, M., 2020. The influence of additives on the fate of plastics in the marine environment, exemplified with barium sulphate. *Marine pollution bulletin,* Volume 158, p. 111352.

Unger, F., 1847. Proposal of an actual equation for the reaction of sodium sulphate and carbon. *Ann,* Volume 63, p. 240.

USGS, 2009. *Soda Ash. ,* U.S: Mineral Industry Surveys, Annual Review,.

Vadapalli, V., Zvimba, J., Mulopo, J. & Motaung, S., 2013. Sulphate removal from sodium sulphate-rich brine and recovery of barium as a barium salt mixture.. *Journal of Environmental Science and Health,* 48(8), pp. 933-938.

Vallero, D., 2006. Dropping acid and heavy metal reactions. In: V. DA, ed. *Paradigms lost.* s.l.:Butterworth-Heinemann, pp. 339-365.

Vallero, D. A., 2005. *Paradigms lost: learning from environmental mistakes, mishaps and misdeeds.* s.l.:Elsevier.

Van der Ham, F., 1999. *Eutectic Freeze Crystallisation, ,* Netherlands: TU Delft.

van Vuuren, D. S. & Maree, J. P., 2020. *Production of sodium carbonate from sodium sulphate.* South Africa, Patent No. 2020/07178.

van Vuuren, D. S. & Maree, J. P., 2020. *Production of sodium carbonate from sodium sulphate.* PCT, Patent No. Provisional Patent Appl. No 2020/07178.

Vergaro, G. et al., 2015. Galectin-3 and myocardial fibrosis in nonischemic dilated cardiomyopathy. *International journal of cardiology,* Volume 184, pp. 96-100..

Viljoen, J. et al., 2021. Household waste management practices and challenges in a rural remote town in the Hantam Municipality in the Northern Cape, South Africa. *Sustainability,* 13(11), p. 5903.

Voigt, W., 2015. What we know and still not know about oceanic salts.. *Pure applied chemistry,* Volume 87, p. 1099–1126 .

Wagialla, K. M., Al-Mutaz, I. S. & El-Dahshan, M. E., 1992. The manufacture of soda ash in the Arabian Gulf. *International journal of production economics,* 27(2), pp. 145-153.

Wahlström, M. et al., 2016. *Hazardous waste classification: Amendments to the European Waste Classification regulation-what do they mean and what are the consequences?,* Europe: Nordic Council of Ministers.

Walters, A., Lusty, P., Chetwyn, C. & Hill, A., 2010. *Rare Earth Elements,* Keyworth: British Geological Survey (BGS)..

Wang, B. et al., 2016. Facile preparation of CaCO3 with diversified patterns modulated by N-[(2-hydroxyl)-propyl-3-trimethylammonium] chitosan chloride. *Powder Technol,* Volume 299, p. 51–61.

Wang, C., Sheng, Y. Z. X., Pan, Y. & Wang, Z., 2006. Synthesis of hydrophobic CaCO3 nanoparticles. *Materials Letters,* 60(6), pp. 854-857.

Wang, F., Smith, D. & El-Din, M., 2003. Application of advanced oxidation methods for landfill leachate treatment–A review.. *Journal of Environmental Engineering and Science,* 2(6), pp. 413-427.

Wang, H., Bua, P. & Capodice, J., 2014. A comparative study of calcium absorption following a single serving administration of calcium carbonate powder versus calcium citrate tablets in healthy premenopausal women. *Food & nutrition research,* 58(1), p. 23229.

Wang, L., Hung, Y., Lo, H. & Yapijakis, C., 2006. *Hazardous industrial waste treatment.,* s.l.: CRC Press.

Wang, P. & Chung, T., 2012. A conceptual demonstration of freeze desalination-membrane distillation (FD-MD) hybrid desalination process utilizing liquefied natural gas (LNG) cold energy,. *water research,* Volume 46, pp. 4037-4052.

Wang, P., Hu, Y. & Cheng, H., 2019. Municipal solid waste (MSW) incineration fly ash as an important source of heavy metal pollution in China.. *Environmental pollution,* Volume 252, pp. 461-475.

Wang, Q. et al., 2010. Discovery of the REE minerals and its geological significance in the Quyang bauxite deposit, West Guangxi, China. *Journal of Asian Earth Sciences,* 39(6), pp. 701-712.

Watten, B., Sibrella, P. & Schwartz, M., 2005. Acid neutralization within limestone sand reactors receiving coal mine drainage. *Environmental Pollution,* Volume 137, pp. 295-304.

Watts, D. B. & Dick, W. A., 2014. Sustainable uses of FGD gypsum in agricultural systems: Introduction. *Journal of Environmental Quality,* 43(1), pp. 246-252.

Weber, R. J. & Reisman, D. J. .., 2012. *Rare earth elements,* Kansas City: A review of production, processing, recycling, and associated environmental issues. US EPA Region.

Weiss, C. et al., 2014. Influence of temperature on calcium carbonate polymorph formed from ammonium carbonate and calcium acetate.. *J Nanotech Smart Mater,* pp. 1-6.

Welander, U., Henrysson, T. & Welander, T., 1997. Nitrification of landfill leachate using suspended-carrier biofilm technology.. *Water research,* 31(9), pp. 2351-2355.

White, E., 1955. The chemistry of the N-alkyl-N-nitrosoamides. I. Methods of preparation.. *Journal of the American Chemical Society,* 77(22), pp. 6008-6010.

Wiegandt, H., Harriott, P. & Leinroth J, P., 1968. *Desalting of seawater by freezing. R&D Report 376, US Dept. Of Commerce:,* US: Office of Saline Water.

Williams, P., Ahmad, M., Connolly, B. & Radcliffe, D., 2015. Technology for freeze concentration in the desalination industry. *Desalination,* Volume 356, p. 314–327..

Wolfe, J., 1984. Non-Metals. In: *In Mineral Resources a World Review.* Springer Netherlands: Dordrecht, pp. 193-269.

Wolkersdorfer, C., 2008. *Water management at abandoned flooded underground mines: fundamentals, tracer tests, modelling, water treatment.* s.l.:Springer Science & Business Media..

Wray, J. & Daniels, F., 1957. Precipitation of calcite and aragonite. *Journal of the american chemical society,* 79(9), pp. 2031-2034.

Wübbeke, J., 2013. Rare earth elements in china: Policies and narratives of reinventing an industry.. *Resour. Policy,,* Volume 38, p. 384–394.

Wu, Y. et al., 2019. Soda ash production with low energy consumption using proton cycled membrane electrolysis. *Industrial & Engineering Chemistry Research,* 58(8), pp. 3450-3458.

Xiong, F. et al., 2020. Synthesis of ortho-phenolic sulfilimines via an intermolecular sulfur atom transfer cascade reaction. *Organic Letters,* 22(10), pp. 3799-3803.

Xu, Y. et al., 2008. Flexible graphene films via the filtration of water-soluble noncovalent functionalized graphene sheets. *Journal of the American Chemical Society,,* 130(18), pp. 5856-5857.

Yanfei, X. et al., 2016. Adsorption ability of rare earth elements on clay minerals and its practical performance.. *Journal of Rare Earths,* 34(5), pp. 543-548.

Yang, H., Che, Y. & Zhang, M., 2016. Effect of nano-CaCO3/ limestone powder composite on the early age cement hydration products. *Key Engineering Materials,* Volume 703, p. 354–359.

Yang, R. et al., 2008. Discovery of hydrothermal venting community at the base of Cambrian Barite in Guizhou Province, Western China: Implication for the Cambrian biological explosion. *Prog. Nat. Sci.,* 18(1), p. 65−70.

Yuan, Y. et al., 2022. Mixing efficiency affects the morphology and compactness of chitosan/tripolyphosphate nanoparticles. *Carbohydrate Polymers,* Volume 287, p. 119331.

Yu, F. J. & Wang, Z. H., 2010. Study on the synthesis of high quality nanometer calcium Carbonate using ultrasonic technology. *In Advanced Materials Research,* Volume 92, pp. 235-240.

Zhang, C. et al., 2022. An overview of the waste hierarchy framework for analyzing the circularity in construction and demolition waste management in Europe. *Science of the Total Environment,* Volume 803, p. 149892.

Zhang, S. et al., 2016. Pressure retarded osmosis. *Sustainable Energy from Salinity Gradients,* p. 19–53.

Zhang, T., Klapper, I. & 2010, 2010. Mathematical model of biofilm induced calcite precipitation. *Water Science and Technology,* 61(11), pp. 2957-2964.

Zhang, X., Baruch, S. & Chris, H., 1998. Sulphur sources of sulphides from the lannigou and getang sedimenthosted gold deposits, SW Guizhou, China.. *Chin. Sci. Bull.,* Volume 43, p. 158−158.

Zhang, Y., 2021. *Geochemical kinetics.* 1 ed. Michigan: Princeton University Press..

Zhao, D. et al., 2011. Structural heterogeneity in the megathrust zone and mechanism of the 2011 Tohoku-oki earthquake. *Geophysical Research Letters,* 38(7).

Zhao, F., Cong, Z., Sun, H. & Ren, D., 2007. The geochemistry of rare earth elements (REE) in acid mine drainage from the Sitai coal mine, Shanxi Province, North China. *International Journal of Coal Geology,* 70(1), pp. 184-192.

Zhao, H., Park, Y., Lee, D. & Park, A., 2013. Tuning the dissolution kinetics of wollastonite via chelating agents for CO2 sequestration with integrated synthesis of precipitated calcium carbonates. *Phys. Chem. Chem. Phys.,* p. 15185–15192.

Zhao, S. et al., 2022. Skarn classification and element mobility in the Yeshan Iron Deposit, Eastern China: Insight from lithogeochemistry. *Ore Geology Reviews,* Volume 145, p. 104909.

Zoca, S. M. & Penn, C., 2017. An important tool with no instruction manual: a review of gypsum use in agriculture.. *Advances in Agronomy,* Volume 144, pp. 1-44.